



**HAL**  
open science

# Neuronal activity patterns during oscillatory events underlying the consolidation of hippocampus dependent memories

Ralitsa Todorova

► **To cite this version:**

Ralitsa Todorova. Neuronal activity patterns during oscillatory events underlying the consolidation of hippocampus dependent memories. *Neurons and Cognition [q-bio.NC]*. Université Paris sciences et lettres, 2018. English. NNT : 2018PSLET043 . tel-03091987

**HAL Id: tel-03091987**

**<https://theses.hal.science/tel-03091987v1>**

Submitted on 1 Jan 2021

**HAL** is a multi-disciplinary open access archive for the deposit and dissemination of scientific research documents, whether they are published or not. The documents may come from teaching and research institutions in France or abroad, or from public or private research centers.

L'archive ouverte pluridisciplinaire **HAL**, est destinée au dépôt et à la diffusion de documents scientifiques de niveau recherche, publiés ou non, émanant des établissements d'enseignement et de recherche français ou étrangers, des laboratoires publics ou privés.

# THÈSE DE DOCTORAT

de l'Université de recherche Paris Sciences et Lettres  
PSL Research University

Préparée à **Collège de France**  
**CIRB**

Neuronal activity patterns during oscillatory events underlying  
the consolidation of hippocampus dependent memories

**Ecole doctorale n°158**

École Doctorale Cerveau-Cognition-Comportement (ED3C)

**Spécialité** Neurosciences

**Soutenue par Ralitsa TODOROVA**  
**le 21 septembre 2018**

Dirigée par **Michaël ZUGARO**

## COMPOSITION DU JURY :

M. DESTEXHE Alain  
UNIC, Président du jury

M. SIROTA Anton  
LMU München, Rapporteur

M. BATTAGLIA Francesco  
Radboud University, Rapporteur

M. BEHCENANE Karim  
ESPCI, Membre du jury

Mme. QUILICHINI Pascale  
Aix-Marseille Université, Membre du jury

M. Michaël Zugaro  
Collège de France, Directeur de thèse



COLLÈGE  
DE FRANCE  
—1530—

PSL   
RESEARCH UNIVERSITY PARIS



---

## Abstract

Long term storage of episodic memories requires memory formation during awake experience as well as memory consolidation, a process strengthening the memory taking place during sleep. The rapid encoding of memory traces takes place in the hippocampus during awake behaviour. In sleep, hippocampal memory traces are ‘replayed’ during sharp wave-ripples – brief (50-150 ms) high-frequency oscillatory patterns of high synchronous activity. The synchronous bursting of hippocampal neurons during ripples makes them a key player in systems memory consolidation – the process of communicating memories to the neocortex for long-term storage.

Cortical activity in sleep is dominated by the slow oscillation – the synchronous alternation of cortical neurons between a depolarized (UP) state associated with high levels of endogenous activity, and a brief ( $\sim 200$  ms) hyperpolarized (DOWN) state when neurons remain silent. DOWN states are accompanied by large deflections of the local field potential – delta waves, while UP states bring elevated activity and thalamocortical spindles, both of which can drive synaptic plasticity. Systems memory consolidation is thought to involve the coordination between hippocampal and cortical rhythms – notably, hippocampal ripples precede ( $\sim 130$  ms) cortical delta waves, which are then followed by thalamocortical spindles.

To test if this temporal coupling drives memory consolidation, we triggered cortical delta waves following ripples to enhance the co-occurrence of coupled ripple-delta events. This boosted memory consolidation and rat performance on a spatial memory task, and resulted in a reorganization of prefrontal cortical networks following induced delta waves as well as increased prefrontal responsivity to the task on the next day. Crucially, these enhancements were not observed when a small delay (160-240 ms) was introduced in addition to the endogenous coupling, indicating the stabilization of memory traces requires a very fine-tuned interaction between ripples and delta waves.

How can the ‘interruption’ of cortical activity by generalized periods of silence during delta waves underlie memory consolidation when it occurs precisely between information transfer (hippocampal replay) and network plasticity (UP state)? Contrary to a generally accepted tenet, we found that delta waves are not periods of complete silence, and that the residual activity is not mere neuronal noise. Instead, cortical cells fired ‘delta spikes’ during delta waves in response to transient reactivation of hippocampal ensembles during ripples, and this occurred selectively during endogenous or induced memory consolidation. This suggests a new role for delta waves – namely, that the synchronized silence of the large majority of cells isolates the network from competing inputs, while a

---

select subpopulation of neurons remain active in response to hippocampal replay, bridging information between UP states and coordinating memory consolidation.

---

## Résumé

Le stockage à long terme des souvenirs épisodiques requiert la formation de la mémoire pendant l'expérience d'éveil ainsi que la consolidation de la mémoire, un processus de renforcement de la mémoire qui a lieu pendant le sommeil. L'encodage rapide des traces mnésiques a lieu dans l'hippocampe pendant l'éveil. Pendant le sommeil, les traces mnésiques de l'hippocampe sont « rejouées » pendant les ondulations – de brefs motifs oscillatoires hippocampiques (50-150 ms) à haute fréquence associés à une activité synchrone élevée. Les bouffées d'activité synchrone des neurones de l'hippocampe pendant les ondulations font d'eux des acteurs clés dans la consolidation de la mémoire des systèmes – le processus de communication des mémoires vers le néocortex pour un stockage à long terme.

L'activité corticale dans le sommeil est dominée par l'oscillation lente – l'alternance synchrone des neurones corticaux entre un état dépolarisé (état HAUT) associé à des niveaux élevés d'activité endogène, et un état bref ( $\sim 200$  ms) hyperpolarisé (état BAS) lorsque les neurones restent silencieux. Les états BAS sont accompagnés de grandes déviations du potentiel de champ local – ondes delta, tandis que les états HAUTS sont associés à une activité élevée et des fuseaux thalamocorticaux, deux processus pouvant entraîner une plasticité synaptique. On pense que la consolidation de la mémoire des systèmes implique une coordination entre les rythmes hippocampiques et corticaux – notamment, les ondulations hippocampiques précèdent ( $\sim 130$  ms) les ondes delta corticales, qui sont ensuite suivies par des fuseaux thalamocorticaux.

Pour vérifier si ce couplage temporel entraîne une consolidation de la mémoire, nous avons déclenché des ondes delta corticales suite à des ondulations hippocampiques afin d'améliorer la cooccurrence d'événements ondulation-delta couplés. Cela a augmenté la consolidation de la mémoire et la performance du rat sur une tâche de mémoire spatiale, et a entraîné une réorganisation des réseaux corticaux préfrontaux suite à des ondes delta induites ainsi qu'une réponse accrue du cortex préfrontal à la tâche le lendemain. De manière cruciale, ces améliorations n'ont pas été observées lorsqu'un retard (160-240 ms) a été introduit en plus du couplage endogène, indiquant que la stabilisation des traces mnésiques nécessite une interaction très fine entre les ondulations et les ondes delta.

Comment l'interruption de l'activité corticale par des périodes de silence généralisées pendant les ondes delta peut-elle sous-tendre la consolidation de la mémoire lorsqu'elle se produit précisément entre le transfert d'informations (réactivation hippocampique) et la plasticité du réseau (état HAUT) ? Contrairement à un principe généralement accepté, nous avons constaté que les

---

ondes delta ne sont pas des périodes de silence complet, et que l'activité résiduelle n'est pas un simple bruit neuronal. Au lieu de cela, nous avons montré que les cellules corticales émettent des « delta spikes » pendant les ondes delta en réponse à la réactivation transitoire d'ensembles hippocampiques pendant les ondulations, et que cela se produit sélectivement pendant la consolidation endogène ou induite de la mémoire. Ces résultats suggèrent un nouveau rôle pour les ondes delta, à savoir que le silence synchronisé de la grande majorité des cellules isole le réseau des entrées concurrentes, tandis qu'une sous-population sélectionnée de neurones reste active en réponse aux réactivations de l'hippocampe, faisant le pont entre les états HAUTs et coordonnant la consolidation de la mémoire.

---

## Résumé détaillé des chapitres

### *Chapitre 1 : Consolidation de la mémoire et ondulations hippocampiques*

L'hippocampe est une structure cérébrale qui joue un rôle central dans la mémoire épisodique. L'activité hippocampique dans les états « déconnectés » comme le sommeil et le repos est caractérisé par les « ondulations » – des brefs motifs oscillatoires hippocampiques (50–150 ms) à haute fréquence (110–200 Hz) associés à une activité synchrone élevée. Les poussées de potentiels d'action qui se suivent à une courte échelle de temps créent des conditions favorables qui lient les ondulations hippocampiques à la plasticité synaptique. Les ondulations qui ont lieu pendant le sommeil sont associés à la réactivation des séquences neuronales potentiées pendant l'apprentissage et des études causales ont démontré que ces ondulations sont essentielles à la consolidation de la mémoire spatiale chez le rat. Les ondulations qui ont lieu pendant l'éveil servent des fonctions différentes – notamment, elles ont été impliquées dans la mémoire de travail, la planification de la navigation ainsi que la stabilisation de la carte cognitive.

### *Chapitre 2 : Réactivations extra-hippocampiques de concert avec des ondulations*

Au-delà de leur impact local, les sorties synchrones de l'hippocampe au cours d'ondulations entraînent une forte dépolarisation des régions cibles de CA1, y compris le subiculum, les couches profondes du cortex entorhinal et de multiples zones néocorticales et sous-corticales. Des effets directs et indirects des ondulations hippocampiques ont été rapportés : la réactivation de l'hippocampe souvent précédant, mais parfois suivant, la réactivation neuronale dans d'autres zones du cerveau.

Ainsi, les ondulations ne sont pas des événements isolés de l'hippocampe, mais un élément essentiel d'un processus couvrant plusieurs régions du cerveau. Les ondulations de l'éveil sont suivies de réponses dans l'aire tegmentaire ventrale, le striatum ventral, le cortex préfrontal, mais pas dans le cortex entorhinal (sauf pendant des périodes d'immobilité prolongées). Les ondulations du sommeil, éventuellement biaisées par les entrées corticales, peuvent initier la réactivation d'ensembles corticaux et même des réactivations inter-structurelles impliquant d'autres zones, notamment les couches profondes du cortex entorhinal, le cortex préfrontal, le striatum ventral et l'amygdale, qui fournissent un contexte spatial, appétitif et aversif pour compléter les signaux de l'hippocampe.

---

### *Chapitre 3 : Rythmes corticaux du sommeil*

Sur la base des enregistrements EEG, le sommeil a été divisé en sommeil à mouvement rapide (REM) et sommeil non-REM, également appelé sommeil lent. Le sommeil lent est associé à l'oscillation lente, aux fuseaux du sommeil dans le cortex et aux ondulations dans l'hippocampe.

L'oscillation lente est l'alternance généralisée entre un état dépolarisé (HAUT) et un état hyperpolarisé (BAS) de neurones corticaux synchronisés. En revanche, les fuseaux du sommeil sont des événements thalamocorticaux oscillatoires (10–15 Hz) qui se produisent enchâssés dans l'oscillation lente corticale. Comme les ondulations de l'hippocampe, les rythmes du sommeil lent sont étroitement associés à la consolidation de la mémoire. En particulier, l'entrée du calcium pendant les fuseaux du sommeil ainsi que l'activité élevée et les séquences de décharge lors de la transition BAS-HAUT permettent d'obtenir des fenêtres optimales pour la plasticité synaptique.

### *Chapitre 4 : Couplage hippocampo-corticale*

L'efficacité du dialogue hippocampo-cortical dans la consolidation de la mémoire reposerait sur la coordination temporelle de l'activité de ces régions. La synchronisation des ondulations est influencée par l'oscillation lente du néocortex et par les fuseaux du sommeil thalamocortical, éventuellement grâce aux entrées dans l'hippocampe qui peuvent faire avancer ou retarder l'apparition d'ondulations à venir. À son tour, l'activité des ondulations peut influencer sur la synchronisation de ces deux rythmes du sommeil. Le couplage des rythmes hippocampo-corticaux serait impliqué dans la consolidation de la mémoire des systèmes.

Les ondes delta ont tendance à suivre les ondulations de l'hippocampe, ce qui suggère que ces ondulations pourraient faciliter une transition HAUT–BAS à venir. On signale également des ondulations immédiatement après les ondes delta; cela est probablement lié à l'augmentation de l'activité corticale pendant la transition BAS–HAUT. Par rapport aux fuseaux thalamo-corticaux, les rapports de couplage avec les ondulations s'étendent sur plusieurs échelles de temps. À l'échelle des secondes, les fuseaux ont tendance à suivre les ondulations de l'hippocampe. À l'échelle de temps plus fine, les ondulations sont verrouillées en phase sur les cycles individuels des fuseaux.

Par conséquent, la consolidation de la mémoire pendant le sommeil s'accompagne d'un dialogue hippocampo-cortical orchestré par un couplage ondulation–onde delta–fuseau affiné. Les ondulations du sommeil peuvent précéder les ondes

---

delta, les suivre, précéder les fuseaux ou se produire pendant les fuseaux, en phase verrouillée à des cycles individuels. Le rôle de l'association des rythmes hippocampo-corticaux pour la consolidation de la mémoire a été au centre des travaux de cette thèse.

### ***Chapitre 5 : Rôle du couplage ondulation-delta dans la consolidation de la mémoire***

Pour vérifier si le couplage temporel entre les ondulations hippocampiques et les ondes delta entraîne une consolidation de la mémoire, nous avons déclenché des ondes delta corticales suite à des ondulations hippocampiques afin d'améliorer la cooccurrence d'événements ondulation-delta couplés. Cela a augmenté la consolidation de la mémoire et la performance du rat sur une tâche de mémoire spatiale, et a entraîné une réorganisation des réseaux corticaux préfrontaux suite à des ondes delta induites ainsi qu'une réponse accrue du cortex préfrontal à la tâche le lendemain. De manière cruciale, ces améliorations n'ont pas été observées lorsqu'un retard (160–240 ms) a été introduit en plus du couplage endogène, indiquant que la stabilisation des traces mnésiques nécessite une interaction très fine entre les ondulations et les ondes delta.

### ***Chapitre 6 : Rôle des discharges pendant les ondes delta dans la consolidation de la mémoire***

Comment l'interruption de l'activité corticale par des périodes de silence généralisées pendant les ondes delta peut-elle sous-tendre la consolidation de la mémoire lorsqu'elle se produit précisément entre le transfert d'informations (réactivation hippocampique) et la plasticité du réseau (état HAUT) ? Contrairement à un principe généralement accepté, nous avons constaté que les ondes delta ne sont pas des périodes de silence complet, et que l'activité résiduelle n'est pas un simple bruit neuronal. Au lieu de cela, nous avons montré que les cellules corticales émettent des « décharges delta » pendant les ondes delta en réponse à la réactivation transitoire d'ensembles hippocampiques pendant les ondulations, et que cela se produit sélectivement pendant la consolidation endogène ou induite de la mémoire. Ces résultats suggèrent un nouveau rôle pour les ondes delta, à savoir que le silence synchronisé de la grande majorité des cellules isole le réseau des entrées concurrentes, tandis qu'une sous-population sélectionnée de neurones reste active en réponse aux réactivations de l'hippocampe, faisant le pont entre les états HAUTs et coordonnant la consolidation de la mémoire.

---

## ***Chapitre 7 : Ondes delta***

Les ondes delta sont souvent précédées par la réponse corticale substantielle aux ondulations de l'hippocampe. Le contenu de ces ondulations pourrait donc entraîner l'activité corticale qui suit, y compris les décharges émises dans les ondes delta suivantes. Dans cette vue, les décharges delta peuvent refléter les entrées arrivant juste avant la fin de l'état HAUT. Cela correspond souvent à des entrées fortes telles que des ondulations, car elles peuvent déclencher une transition HAUT-BAS.

De cette manière, les décharges delta peuvent servir de pont entre l'activité à la fin d'un état HAUT (reflétant les entrées à la fin de l'état HAUT) et le début de l'état HAUT suivant, où la plasticité a lieu. Selon cette hypothèse, les pics delta lors des ondes delta précédées d'ondulations devraient refléter le contenu de l'hippocampe, mais les décharges delta lors d'autres ondes delta devraient refléter l'activité d'autres zones partenaires en dehors de l'hippocampe. Ceci soulève l'idée des décharges delta en tant que mécanisme général permettant de relier les informations entre les états HAUTs impliqués dans la communication avec de multiples zones partenaires corticales.

## ***Chapitre 8 : Mécanismes alternatifs pour le dialogue hippocampo-cortical***

Il existe des formes de couplage hippocampo-corticaux au-delà du couplage ondulation-delta qui a été au centre de cette thèse. Notamment cela inclut le couplage delta-ondulation et le couplage ondulation-fuseaux. Ces autres formes de couplage ne peuvent expliquer les effets du couplage ondulation-delta sur la consolidation de la mémoire, car ils ne différaient pas entre les conditions de stimulation couplée et retardée. Bien que ces formes de communication n'aient pas été affectées par le couplage ondulation-delta, elles ne sont nullement hors de propos pour le dialogue hippocampo-cortical. Une consolidation réussie de la mémoire peut nécessiter l'intégration de tous ces facteurs. Comprendre le rôle de chaque phénomène nécessiterait des recherches supplémentaires.

## ***Chapitre 9 : Rôle des séquences thêta dans la formation de la mémoire***

Pendant l'exploration, les séquences thêta permettent la compression des trajectoires de l'animal à une échelle de temps compatible avec des processus de plasticité. Par conséquent, ces séquences thêta pourraient soutenir l'apprentissage

---

séquentiel pendant l'exploration, et pourraient sous-tendre le codage initial des traces mnésiques. Toutefois, des preuves directes en faveur de ce scénario n'ont pas été fournies. Dans cette étude causale, nous avons sélectivement perturbé les séquences thêta tout en préservant les séquences de champs d'activité. Nos résultats montrent que les séquences thêta des assemblées cellulaires hippocampiques pendant l'exploration sous-tendent les réactivations ultérieures pendant le sommeil, et font valoir l'idée que les séquences thêta sont à la base de la formation initiale des traces mnésiques consolidées ultérieurement pendant le sommeil.

---

## Remerciements

I would like to sincerely thank the members of my jury for reading and assessing my thesis: Anton Sirota, Alain Destexhe, Pascale Quilichini, Francesco Battaglia, and Karim Benchenane. Thank you for your warm words, your questions, and your discussion of my work.

Thank you to everyone who devised and carried out the experiments, building the backbone that made the projects in this thesis possible: Nicolas Maingret, Gabrielle Girardeau, Marie Goutierre, Céline Drieu and Michaël Zugaro. I thank the whole BR&NCM team for their input and scientific discussions.

But it takes more than science to support a PhD student, so thank you everyone for making me feel like I belong. Thank you, Michaël, for welcoming me so warmly to the team. You have always made me feel that my opinion is valued. Thank you for truly caring about the students and always having our best interest in mind.

Thank you to the past members of the team. Nico, I'm still recovering from your graduating and leaving the lab. Thank you for being my voice of reason and for making me speak French. Tu es un flot incessant de soutien (et des blagues). Ta créativité est contagieuse. Merci d'avoir été si incroyable ! Céline, c'est toujours difficile de croire que tu ne reviendras pas au labo demain (mais à Noël, c'est loin !) Ton énergie et ta joie sont une inspiration et tu fais ressortir le meilleur des gens. J'ai adoré nos plans d'attaque et nos réflexions tardives qui ont coloré ma thèse. Merci aux meilleures anciens stagiaires : Romain, Anna, Gabriel. Virginie, tu n'es pas un ancien membre, tu reviens, hein ? Merci pour la bonne humeur et tous les bons moments.

Merci aux membres de l'équipe actuelle. On s'amusera ! Nadia, Céline, Ariane, Ombeline, Diane et Eulalie, merci pour l'ambiance super positive. Marco, merci d'être si proactif, attentionné et fiable. Merci, Sid et Susan, pour votre orientation et conseil.

Merci à tous de m'avoir donné envie de rester.

Quand je suis arrivée en France en 2013, je ne connaissais personne ici. Au fil des années, j'ai rencontré beaucoup de gens incroyables qui m'ont aidé à chaque étape du chemin. Je remercie l'ENP de m'avoir donné l'occasion de venir. Je tiens particulièrement à remercier Yvette Hénin pour tout ce qu'elle a fait pour moi ; Laura Peeters, Laëtitia Fillaudeau, merci pour votre aide !

Les gens formidables que j'ai rencontrés au Cogmaster, j'espère que vous savez à quel point je vous apprécie. Vlad, Hippo, merci pour tous nos débats, trips,

---

moments spéciaux ! Arnaud et Audrey, merci de m'avoir accueillie plusieurs fois à Bruxelles ! Anna, Maxime, Raphaëlle, Clara, Chris, Ignacio, Mehdi, merci de m'avoir fait me sentir chez moi ici. Ceux d'entre vous qui ont déménagé à l'étranger, j'espère que je pourrai être votre port d'attache où vous pourrez continuer à revenir. Merci pour tous les bons moments que nous avons passés ensemble !

Merci à tous mes amis français qui sont venus en Bulgarie - Nico, Jeanne, Céline, Hippo, Mehdi, Gnuts ! Merci de vous être laissés entraîner dans mon pays étranger. Vous êtes toujours les bienvenus à Feta-land.

Merci à mon équipe de joueurs de jeux de société - Rémi, Virginie, Richard, Anabelle, Marco. Merci de m'avoir donné de la nourriture et des divertissements quand j'en avais besoin.

I want to thank my awesome flatmates, Fanny, Ani, and Marco, for cooking such delicious meals and for helping me expand my interests and discover new things. And all my other friends for helping in that endeavour.

And of course, I would like to thank my family. Благодаря ви за безкрайната ви подкрепа и обич. Чувствам се обгърната с любов всеки ден.

Thank you all for making my life wonderful and for always being there for me.

---

# Contents

<b>I</b>	<b>Introduction</b>	<b>1</b>
<b>1</b>	<b>Memory consolidation and hippocampal ripples</b>	<b>3</b>
1.1	Theoretical framework . . . . .	5
1.1.1	Systems consolidation theories . . . . .	5
1.1.2	Ripples and synaptic plasticity . . . . .	6
1.2	Hippocampal activity during ripples . . . . .	8
1.2.1	Sleep ripples . . . . .	8
1.2.2	Awake ripples . . . . .	15
<b>2</b>	<b>Extrahippocampal reactivations in concert with ripples</b>	<b>21</b>
2.1	Entorhinal cortex . . . . .	21
2.2	Associative cortices . . . . .	23
2.3	Sensory cortices . . . . .	24
2.4	Subcortical areas . . . . .	25
<b>3</b>	<b>Cortical sleep rhythms</b>	<b>29</b>
3.1	Slow oscillation . . . . .	29
3.1.1	UP/DOWN state initiation . . . . .	31

## CONTENTS

---

3.1.2	Extent of silence in delta waves . . . . .	32
3.1.3	Delta waves and synaptic plasticity . . . . .	34
3.1.4	Delta waves and memory consolidation . . . . .	35
3.2	Sleep spindles . . . . .	36
3.2.1	Spindles and synaptic plasticity . . . . .	37
3.2.2	Spindles and memory consolidation . . . . .	37
<b>4</b>	<b>Hippocampo-cortical coupling</b>	<b>39</b>
4.1	Slow oscillation . . . . .	39
4.1.1	Ripples preceding delta waves . . . . .	40
4.1.2	Ripples following delta waves . . . . .	41
4.2	Sleep spindles . . . . .	42
4.2.1	Ripples preceding spindles . . . . .	42
4.2.2	Ripples nested in spindle cycles . . . . .	43
<b>II</b>	<b>Results</b>	<b>45</b>
<b>5</b>	<b>Role of ripple-delta coupling in memory consolidation</b>	<b>49</b>
<b>6</b>	<b>Role of delta spikes in memory consolidation</b>	<b>71</b>
<b>III</b>	<b>Discussion</b>	<b>97</b>
<b>7</b>	<b>Delta waves</b>	<b>99</b>
7.1	Ripple-delta coupling . . . . .	99
7.2	Delta spikes . . . . .	100
7.2.1	Influence on delta spikes . . . . .	101

7.2.2	Influence of delta spikes . . . . .	102
<b>8</b>	<b>Alternative mechanisms for the hippocampo-cortical dialogue</b>	<b>103</b>
8.1	Delta-ripple coupling . . . . .	103
8.2	Ripple-spindle coupling . . . . .	106
8.3	Perspectives . . . . .	108
<b>IV</b>	<b>Appendix</b>	<b>111</b>
<b>9</b>	<b>Role of awake theta sequences in memory formation</b>	<b>113</b>

---

# **Part I**

## **Introduction**



# Chapter 1

## Memory consolidation and hippocampal ripples

Early clinical work and animal studies have established the hippocampus as a key structure in the formation and consolidation of episodic and spatial memory (Scoville and Milner, 1957; Morris et al., 1982). Investigations into the neurophysiological mechanisms underlying these functions are largely based on the discovery of place cells, hippocampal pyramidal cells that fire selectively in a specific locations as a rat freely explores an environment (O’Keefe and Dostrovsky, 1971; O’Keefe and Nadel, 1978).

While the theta rhythm (7–14 Hz) dominates rodent hippocampal local field potentials (LFPs) during exploration, in moments of consummatory behaviour, awake immobility, and slow-wave sleep, the network switches to a mode of large irregular activity, in which sharp wave-ripples occur (Figure 1.1). Sharp wave-ripples are brief (50–150 ms) events with two components: a large amplitude negative polarity deflection (sharp wave) in the stratum radiatum (Buzsáki et al., 1983; Buzsáki, 1986), and a high frequency (110–200 Hz) oscillation (ripple) originating in the CA1 pyramidal layer (Buzsáki et al., 1992).

Sharp waves are immediately preceded by extensive bursts of activity in CA3, with up to 10%–20% of CA3 neurons participating in a single sharp wave event (Csicsvari et al., 2000). These bursts result in massive excitation of CA1 neurons through CA3 Schaffer collaterals, recruiting CA1 pyramidal cells and interneurons that fire synchronously. The interplay of interconnected interneuronal networks and widespread excitatory activity results in an oscillatory event – a ripple.

While the heavily interconnected CA3 region has long been considered the source of ripple events, a subpopulation of CA2 cells play an important role in triggering ripples (Oliva et al., 2016). In CA3, recent data suggests that the

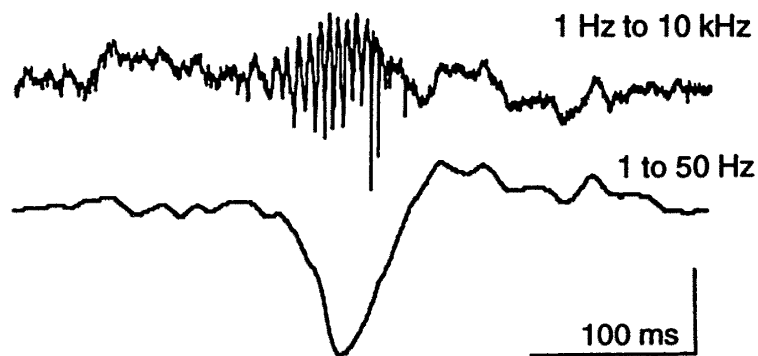


**Figure 1.1:** A hippocampal ripple recorded in CA1 in the dorsal hippocampus. LFP from the pyramidal layer (top) and the stratum radiatum (bottom) of CA1 of the dorsal hippocampus. Reproduced from Buzsáki et al. (1992).

bursting of a subpopulation of deep-layer stratum radiatum cells with distinct morphology (‘athorny’, as they have no mossy-fiber synapses which appear as thorny excrescences) may trigger ripples (Hunt et al., 2018). The particular spiking sequences observed in CA1 during ripples appears to result mainly from local circuit dynamics (Stark et al., 2015), although this activity may be biased by upstream activity (Ellender et al., 2010; Rothschild et al., 2017). Ripple timing may also be influenced by extra-hippocampal inputs (discussed in chapter 4), including neuromodulatory tone<sup>1</sup>.

Ripples can be either local, or propagate in diverse patterns along the septo-temporal axis of the hippocampus, although the ventral pole seems independent from the dorsal and intermediate poles (Csicsvari et al., 2000; Patel et al., 2013).

This chapter presents research into the function of these highly synchronous events, with a special focus on studies testing the causal role of ripple-related activity in cognitive processes. First, I briefly present the theoretical framework that forms the basis for studies of ripple function. I then review seminal work and more recent studies on the functional content of ripple activity in slow-wave sleep and its relation to experience and memory. Finally, I discuss the properties and function of ripples in the awake state.

---

<sup>1</sup>While dopamine can promote ripple generation (Miyawaki et al., 2014), activation of the cholinergic (Vandecasteele et al., 2014), serotonergic (Wang et al., 2015a), and noradrenergic (Novitskaya et al., 2016; Ul Haq et al., 2012) pathways has been shown to suppress ripples. These pathways may promote wakefulness and memory encoding, rather than memory consolidation during slow-wave sleep.

## 1.1 Theoretical framework

Since ripples have been shown to play a critical role in memory consolidation, this section provides a brief overview of the most prominent theories of systems memory consolidation, as well as the relation between ripples and plasticity processes likely to underlie learning and memory.

### 1.1.1 Systems consolidation theories

Marr (1971) first proposed that information could be cleared from temporary hippocampal storage as it is stored in more permanent neocortical representations; moreover, he put forth the notion that this process should take place during sleep, free from sensory interference. This hypothesis is the base of the standard theory of systems consolidation, which holds that memory traces are initially formed in the hippocampus, then gradually transferred to the neocortex, and ultimately become independent of the hippocampus (Squire and Alvarez, 1995).

Alternatively, the multiple trace theory posits that each time an episodic memory is recalled, it generates an additional trace in the hippocampus, each with a spatio-temporal context, while the neocortex stores context-free, semantic features; retrieval of episodic memories would always require the hippocampus (Nadel and Moscovitch, 1997). This led to the transformation hypothesis, which states that context-bound hippocampal memory traces support the development of a schematic neocortical trace (Winocur et al., 2010).

While these theories might disagree about the nature of the memories stored in the hippocampus and the neocortex, the underlying mechanisms for memory consolidation are the same – that an interplay between the hippocampus and the cortex results in connectivity changes in cortical networks. Buzsáki (1989) proposed that ripple-associated hippocampal outputs would communicate information to a stabilized neocortical memory trace. Synapses would be weakly potentiated during exploration, when the hippocampus oscillates at the theta frequency. In the subsequent consolidation stage, the strong excitatory drive occurring during ripples would induce the long-term synaptic modifications required to induce long-lasting memories, both in the hippocampus and its target areas. (Buzsáki, 1989)

### 1.1.2 Ripples and synaptic plasticity

There is a vast literature on general plasticity mechanisms at intra-hippocampal synapses. At the CA3-CA1 synapse, long-term potentiation (LTP) can be induced by tetanic stimulation of Schaffer collaterals at 200 Hz (Buzsáki, 1984), as well as by pharmacological induction of CA3 bursting *in vitro* (Buzsáki et al., 1987). Stimulating CA1 cells during spontaneous ripples detected on-line (by micro-stimulation adjacent to the cell body) increases the probability that the selected neurons participate in future ripples without affecting overall cell excitability, indicating potentiation of the synaptic inputs to CA1 (King et al., 1999). This potentiation of the CA3-CA1 synapse by stimulating the post-synaptic cell is likely to reflect the Hebbian mechanism of spike-timing dependent plasticity (STDP), in which the temporal order and precise timing of pre- and postsynaptic spikes determine the extent and polarity of synaptic plasticity (Magee and Johnston, 1997; Markram et al., 1997). The classical STDP learning rule states that pre-then-post paired excitation induces LTP, while post-then-pre pairings result in long term depression (LTD).

Modelling work based on this classical rule has suggested that synchronous firing during ripples could result in decoupling of coactive neurons in CA3 (Lubenov and Siapas, 2008), consistent with the theory that hippocampal memory traces could be erased upon transfer to the neocortex (Squire and Alvarez, 1995). However, a variety of factors can influence the learning rule. Wittenberg and Wang (2006) showed that in hippocampal slices, a few pairings of CA3 presynaptic spikes and CA1 postsynaptic bursts cause LTP even when the postsynaptic burst precedes the presynaptic spike. Conversely, prolonged synaptic pairings involving CA1 single spikes, rather than bursts, led to LTD (Wittenberg and Wang, 2006). Moreover, the learning rule for isolated pairs of spikes cannot be extrapolated for spike trains composed of multiple spikes (Froemke and Dan, 2002). Besides local circuit dynamics, STDP also depends on neuromodulatory tone. For instance, in hippocampal slices noradrenaline can widen the time window between a pre-post pairing that can still successfully induce LTP (Lin et al., 2003). In hippocampal cultured neurons and slices, dopamine can also widen this window, and alter the STDP learning rule such that a post-then-pre stimulation protocol induces LTP rather than LTD (Zhang et al., 2009; Brzosko et al., 2015). This indicates that the potential synaptic plasticity mechanisms triggered by ripples may depend on ongoing neuromodulatory activity, which in turn would vary with the behavioural context.

What learning rule is promoted by the timing of spikes during hippocampal ripples? In rat hippocampal slices, Sadowski et al. (2016) stimulated CA3 presynaptic and CA1 postsynaptic cells to replicate activity patterns recorded *in vivo*. This was not sufficient to reliably evoke LTP. However, when the same

protocol was complemented by stimulation of the Schaffer collateral pathway at 100 Hz, mimicking ripple activity recorded *in vivo*, LTP could be reliably induced. The dendritic depolarization associated with sharp-wave ripples was concluded to be crucial for the induction of synaptic plasticity (Sadowski et al., 2016). Moreover, the change in synaptic strength was well correlated with the number of pairings of CA3 spikes followed by CA1 spikes, indicating that pairs of single spikes are sufficient to bring about LTP during a ripple. The reverse order, CA3 spikes following CA1 spikes, resulted in neither LTP nor LTD. This argues for a modified learning rule during ripples, involving a potentiation component resembling classical STDP but with no depression component.

In a recent study, Norimoto et al. (2018) suggested that ripple activity can lead to synaptic depression of neurons that are not active during the ripple. In mouse hippocampal oblique slices (in which ripples occur spontaneously), they observed that the network response (in the form of field excitatory postsynaptic potentials) to Shaffer collateral stimulation decreased over time in an NMDA receptor-dependent mechanism, indicative of synaptic plasticity. A closed-loop optogenetic stimulation of somatostatin neurons upon ripple detection blocked ripples and prevented this spontaneous synaptic depression, whereas control stimulation with a delay of 100 ms, leaving ripples intact, had no effect. Two-photon imaging of dendritic spines revealed that while the majority of spines (‘thin’ and ‘stubby’ type spines) shrank in size, some dendritic spines (‘mushroom’ type spines) remained unaffected by this net synaptic depression. The authors suggested that ripples cause net depression through the removal of unused synapses, while synapses active during ripples are spared and potentiated.

In addition to modifying local hippocampal circuitry, ripples are also expected to yield plasticity in output structures. Although studies reproducing the physiological conditions during ripples are lacking, high frequency stimulation protocols (200 Hz) typically used to induce LTP are reminiscent of hippocampal ripple activity. Such protocols have been demonstrated to induce synaptic potentiation at the CA1-prefrontal cortical synapse (Laroche et al., 1990) and at the CA1-subiculum synapse (O’Mara et al., 2000) *in vitro*. It has been hypothesized that the physiological role of the population bursts associated with hippocampal ripples might be to modify synaptic connectivity at downstream targets (Chrobak and Buzsaki, 1994) – changes that the relatively low firing rates of hippocampal neurons during awake behaviour would be insufficient to trigger.

Hippocampal activity patterns during ripples appear well suited to promote synaptic potentiation in downstream structures, which would support the theory that ripples play a role in consolidating labile memory traces. The results of Norimoto et al. (2018) argue for a role for ripples in erasing inactive hippocampal

memories leading to the gradual hippocampal disengagement posited by the standard theory of memory consolidation. On the other hand, neurons active together during hippocampal ripples would strengthen their synaptic connections. To address the question of what information is consolidated, the next section examines the neuronal activity during ripples and its behavioural correlates.

## 1.2 Hippocampal activity during ripples

Given that ripples occur in both sleep and waking states, a discussion of the function of ripples must take brain state into account. While both sleep and awake ripples have been shown to be involved in memory processes, evidence suggests that they might have distinct roles in addition to potentiating previously activated synapses. In sleep, free from interference, ripples are well suited for communicating a memory trace to be consolidated into a framework of existing memories possibly involving multiple regions (Frankland and Bontempi, 2005; Tse et al., 2007; Girardeau et al., 2009; Ego-Stengel and Wilson, 2010), while awake ripples may be involved in processes immediately relevant to ongoing behaviour, such as navigational planning (Carr et al., 2011; Jadhav et al., 2012; Roumis and Frank, 2015).

### 1.2.1 Sleep ripples

#### Coactivation of cell pairs

Early studies provided the first evidence that activity in CA1 during sleep reflects activity during behaviour. More specifically, cofiring patterns established in awake behaviour are reinstated during sleep. Pavlides and Winson (1989) showed that place cells active during behaviour subsequently fired at higher rates during sleep. Building on this work, Wilson and McNaughton (1994) provided the first large-scale recordings of hippocampal neurons, allowing them to quantify the tendency of multiple cell pairs to fire together (within 100 ms of each other). They showed that pairs of place cells coactive during exploration (i.e. with overlapping place fields) retained an increased tendency to coactivate in sleep after the task, compared to sleep before the task. This increase was strongest in sleep immediately following the task and decayed over time. Importantly, this reactivation took place preferentially during ripples.

Given that hippocampal place cells together form a cognitive map of the environment, the question arises whether this reinstatement of correlated activity reflects the reactivation of the spatial representation of the most recently visited

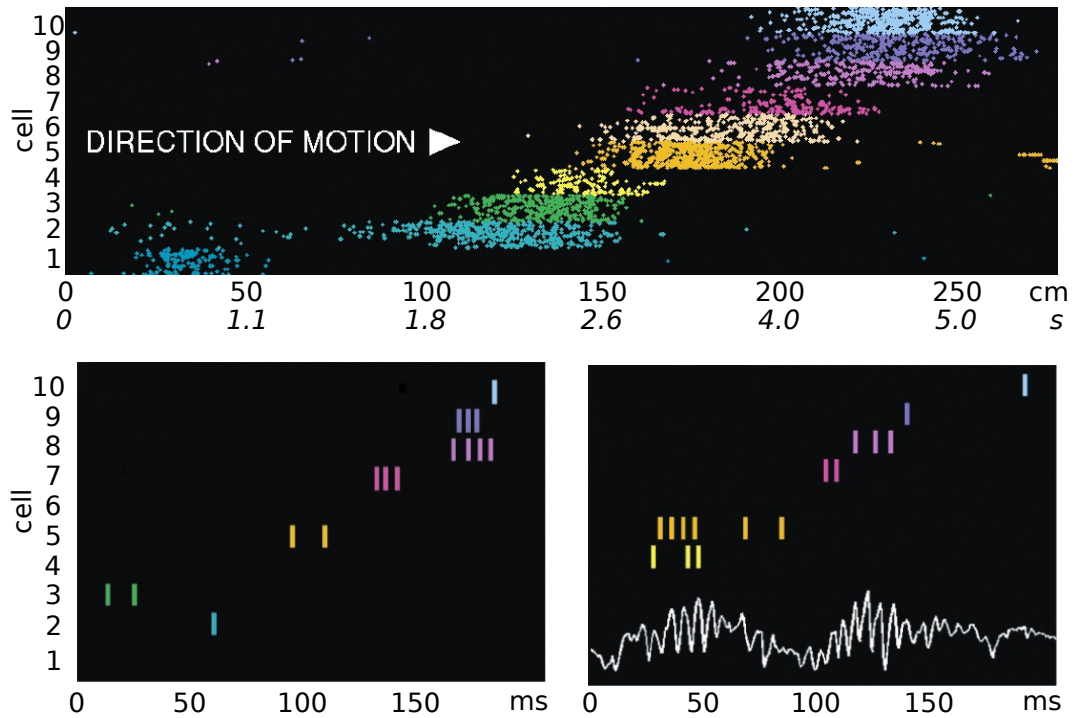


**Figure 1.2:** Replay in sleep ripples. Top: Raster plot of place cell activity for 30 laps on the track. Each color corresponds to a different cell, and responses for the respective laps are stacked for each cell. Nonuniform time axis below shows time within average lap. Bottom: examples of compressed replay during sleep. Note the CA1 pyramidal layer LFP trace displayed on the right panel, indicating that replay events coincide with ripples. Adapted from Lee and Wilson (2002).

environment (semantic memories), or of specific trajectories and behaviours experienced in this environment (episodic-like memories). O'Neill et al. (2008) provided compelling evidence that the coactivation of cell pairs during sleep is a direct consequence of their coactivation in awake behaviour. They showed that the number of times two place cells fired together during exploration predicted the increase of the pair's cofiring during sleep ripples after the task, compared to sleep before (conversely, the number of times the pair fired independently resulted in the opposite trend). This suggests that an associative learning process takes place during behaviour, leading to future reactivations. Conditions leading to increased ripple incidence is further discussed below.

## Replay of neuronal sequences

Beyond coactivation of cell pairs, further studies have investigated replay of entire sequences of activity observed during behaviour. Skaggs and McNaughton (1996) trained rats to run on a triangular track repeatedly in the same direction, so that pairs of place cells would always be activated in the same order. This temporal bias during awake behaviour was reinstated during subsequent sleep, but was absent in sleep before the task. Nádasdy et al. (1999) extended these findings from cell pairs to cell triplets and to spiking sequences of multiple neurons ('templates'). They found that such sequences were overrepresented during active behaviour (as rats ran on a running wheel) and also during sleep, when they were replayed on a faster timescale during ripples. To investigate replay of spatial trajectories, Lee and Wilson (2002) recorded place fields of many neurons covering a linear track. They defined the order of the place fields on the track as a template, and found population bursts that matched the template during sleep, coinciding with ripples (Figure 1.2). These replay events were compressed by a factor of 10–20 relative to behaviour, a timescale compatible with synaptic plasticity. The authors suggested that replay sequences could broadcast learned information to target structures, reinstating and strengthening the memory trace.

One caveat of these studies is that they investigated the network mechanisms of memory consolidation in rats performing stereotypical and over-trained behaviours in familiar environments, rather than performing elaborate learning tasks (with the exception of one of the three rats in Lee and Wilson, 2002). In order to probe the potential role of hippocampal ripples in memory processes, the next step was to study replay in the context of encoding novel experiences.

## Novelty increases replay

Kudrimoti et al. (1999) compared reactivation during sleep following exploration of familiar vs novel zones of an environment (based on simple firing rate correlations between CA1 cell pairs). In both the familiar and the novel zones, reactivation increased after exploration, was most pronounced during ripples, and declined quickly over the first hour of sleep. Unlike previous studies, the correlations in sleep before exploration of the familiar area already resembled those observed during the actual exploration episode. Notably, this was not the case for exploration of the novel area, indicating that a novel experience can introduce new correlation patterns in the hippocampal network. Consistent with this view, O'Neill et al. (2008) directly compared reactivation quality following exploration of a novel vs familiar environment, and reported that reactivation of coactivity patterns was more pronounced during ripples following exploration of the novel environment. This may be due to increased synaptic plasticity in the

novel environment, an effect dependent on dopamine (discussed in section 2.4).

In addition, Hirase et al. (2001) reported that exploration of a novel environment altered the firing rates of single CA1 neurons during behaviour and subsequent sleep, compared to sleep preceding exploration. Because the global firing rate remained stable between the two sleep sessions, the authors hypothesized that a subset of neurons increase their firing rates in the novel environment, compensated by a commensurate decrease of the remaining neurons, by a homeostatic mechanism. This may have implications on the structure of correlations described by Kudrimoti et al. (1999), since correlations can be biased by firing rates (de la Rocha et al., 2007).

These studies indicate that awake exploration, especially in novel environments, reshapes the structure of spontaneous activity during subsequent sleep. However, this notion was challenged by reports of hippocampal sequences representing spatial trajectories in an environment that the animal had never experienced before, but was about to explore – as if anticipating the future exploration (Dragoi and Tonegawa, 2011, 2013). Such sequences were termed ‘preplay’ (not to be confused with awake preplay, discussed in section 1.2.2). Hence, hippocampal sequences be would selected from a pre-existing, pre-wired repertoire, rather than formed *de novo* during experience.

This remains debated. On the one hand, preplay was confirmed by Grosmark and Buzsáki (2016), who further documented a distinction between subsets of cells, ‘plastic’ or ‘rigid’, based on their relative contributions to preplayed vs (novel) replayed sequences. According to these authors, ‘plastic’ cells have lower firing rates and higher spatial specificity during exploration, as well as increased firing in ripples in post-task sleep, suggesting that a memory trace would involve a specific subset of plastic neurons preferentially reactivated in ripples in subsequent sleep. On the other hand, Ólafsdóttir et al. (2015) reported that preplay of previously unexplored zones occurred only under very specific conditions – the unexplored zones were visible through a barrier, and baited with food. The authors hypothesized that preplay may be formed only when the anticipated experience is relevant to the motivation of the animal. Further, using much larger numbers of neurons in multiple environments, Silva et al. (2015) found that preplay sequences do not occur more often than chance, and that the formation of replay sequences during the first exploration of a novel environment required NMDA receptor-dependent synaptic plasticity. Settling this question will require additional experiments (Dragoi et al., 2017).

## Learning increases ripple incidence

An ideal protocol to evaluate the role of ripples and associated replay in memory consolidation should include a reasonably elaborate learning task. Whereas mere exposure to a novel environment does not affect the ripple rate during subsequent sleep (Kudrimoti et al., 1999; Hirase et al., 2001), training on memory tasks does induce an increase in ripple incidence (Eschenko et al., 2008; Ramadan et al., 2009). Eschenko et al. (2008) trained rats in an odor discrimination task and found that the ripple incidence, duration and amplitude increased for 2 hours after the learning session; this increase correlated with behavioural performance, as it was more pronounced in rats that improved during the session. Ramadan et al. (2009) trained rats on an eight-arm radial maze task, and reported that ripple incidence in sleep increased on the day when rats started to perform above chance.

Ripple facilitation may be a direct consequence of learning-related synaptic changes. *In vitro*, stimulation protocols that induce LTP in CA3 also lead to increased ripple incidence (Behrens et al., 2005). Although a similar effect was not observed for LTP induction *in vivo* (Dragoi et al., 2003), endogenous plasticity mechanisms do appear to regulate ripple incidence, and this could be a part of a regulatory process related to ongoing consolidation. During rest following training on a memory task, Girardeau et al. (2014) interfered with ripple activity using a closed-loop single-pulse electrical stimulation protocol. Ripple disruption triggered a dynamic compensatory increase in subsequent ripple incidence. Blocking NMDA receptors during training, but not after, abolished this response, indicating that NMDA receptor-dependent plasticity processes taking place during learning regulate ripple dynamics and enhance ripple rate in subsequent sleep. Such a process would ensure that memory consolidation is enhanced in sleep after an episode of learning, when there would be more to consolidate than after routine behaviour.

Memory performance is not only related to ripple incidence, but also to the reactivation of specific place cells during ripples. Dupret et al. (2010) trained rats to visit three goal locations on a ‘cheeseboard’ maze, and reported that hippocampal activity during sleep ripples often represented one of the goal locations. Importantly, subsequent memory performance for a given goal was correlated with the proportion of sleep ripples in which the goal location had been reactivated. This argues for a role of ripple-associated reactivations in strengthening neuronal representations of memories.

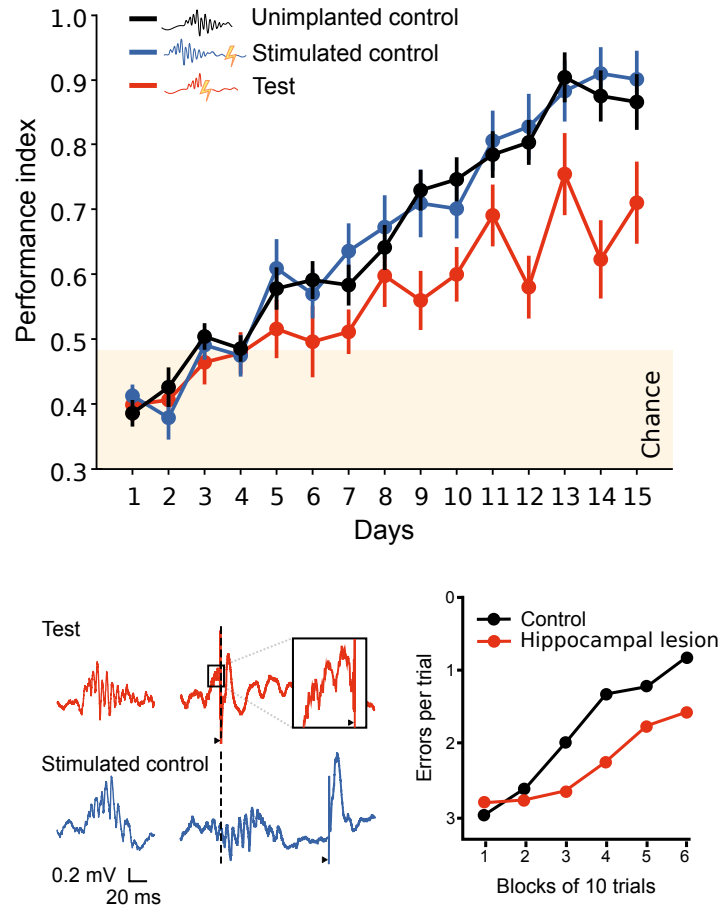


**Figure 1.3:** Suppression of sleep ripples interferes with memory consolidation. Top: Test rats (red) were significantly impaired in the radial maze task compared with control rats (blue, stimulated; black, unimplanted). Bottom left: in the test condition (red), ripples were immediately disrupted upon detection; in the control condition (blue), a random delay was introduced before stimulation. Unperturbed ripples are shown to the left, example stimulations to the right. Dashed vertical lines, ripple detection; black triangles, stimulation; box inset shows magnified trace. Bottom right: the effect of complete hippocampal lesion on radial maze (Jarrard, 1995). Note that the y-axis (number of events) is reversed to allow for the comparison with Girardeau et al. (2009)'s results. Adapted from Girardeau et al. (2009) and Jarrard (1995).

### **A causal role for sleep ripples in memory consolidation**

Overall, there is abundant evidence that neuronal activity of past experiences is replayed during sleep ripples. Crucially, the causal relationship between ripples and memory consolidation was demonstrated in two independent studies where sleep ripples were perturbed by precisely timed electrical stimulation of the ventral hippocampal commissure (Girardeau et al., 2009; Ego-Stengel and Wilson, 2010). In both studies, the rats were trained on a spatial memory task where they learned across days to preferentially visit the baited arms of a maze. In the first hour of sleep following training, ripples were detected on-line and interrupted by precisely timed single pulse stimulation, briefly suppressing ongoing neuronal activity and preventing further development of the ripple (Figure 1.3). This closed-loop protocol impaired subsequent performance on the task (Girardeau et al., 2009; Ego-Stengel and Wilson, 2010) to levels comparable to complete hippocampal lesions (Jarrard, 1995). Importantly, non-specific effects of the stimulation were ruled out as no impairment was observed in a group of control animals that underwent the same stimulation protocol, but with a random delay between ripple detection and the stimulation, thus leaving ripples intact (Girardeau et al., 2009). This established that ripple activity is critical for memory consolidation.

On the other hand, Kovács et al. (2016) provided evidence that that CA1 activity during sleep ripples is not essential for place field stability. In this study, mice explored a novel environment, then underwent a sleep session where pyramidal cells in CA1 were optogenetically silenced during ripples (or outside ripples in the control condition). During the second exploration session, firing maps remained stable, indicating that CA1 pyramidal activity in sleep ripples is not essential for the formation of a stable spatial representation of a novel environment. The authors suggested that this function might be carried out during awake ripples (see section 1.2.2), while the main role of sleep ripples would be the communication of information to extra-hippocampal areas.

Furthermore, Kovács et al. (2016) found that pairwise firing rate correlations of CA1 pyramidal cells were unaffected by ripple suppression. This is at odds with the results of van de Ven et al. (2016), who reported that neuronal coactivation patterns (cell assemblies detected using independent component analysis of the binned multiunit spiking activity) were considerably less reactivated upon re-exposure to the environment when CA1 pyramidal cells were optogenetically silenced upon ripple detection during intervening sleep epochs. Interestingly, the authors reported two different kinds of encoding dynamics during the first exploration of a novel open field. While some assemblies stabilized in the first few minutes of exposure, after which their activity plateaued, other assemblies gradually strengthened – their activity continually increased throughout the

first exploration<sup>2</sup>. Ripple suppression selectively altered the reactivation of the gradually stabilized assemblies. The authors suggested that early stabilized patterns might provide a ‘ready to use’ representation of space needed for navigation, while the gradually strengthened assemblies might reflect the memory trace of the experience.

While experiments suppressing sleep ripples have provided invaluable information about the functional role of ripples, to gain further insight about the specific role of different replay events, either with respect to network changes or on the level of memory consolidation, it will be necessary to selectively enhance or suppress specific ripples based on their associated patterns of activity. It is possible that not all ripples participate equally in this function, since in most cases the associated activity patterns do not match identified patterns of wake activity and appear ‘noisy’. Alternatively, all ripples do participate in valuable information exchanges, although we are simply unable to recognize the underlying patterns of activity. Further experiments will be required to address these open questions.

### 1.2.2 Awake ripples

Awake ripples occur during prolonged periods of immobility, but also during brief pauses in exploration, while the rat is engaged in the task. Several studies have reported differences between these two types of ripples, suggesting that ripples during prolonged immobility may resemble sleep ripples, while exploration ripples tend to encode representations relevant to the ongoing (O’Neill et al., 2006; Csicsvari et al., 2007; Dupret et al., 2010; Ólafsdóttir et al., 2017). Notably, there are reports of replayed trajectories both in the forward and in the reverse direction (Figure 1.4).

#### Reverse replay

Foster and Wilson (2006) reported replay events in CA1 when rats stopped to consume food at the end of a linear track. Interestingly, hippocampal sequences replayed the preceding trajectory in reverse order, from the reward zone to the starting point. Such reverse sequences were more prevalent in novel environments, suggesting a potential role in learning. The authors proposed that reverse replay, accompanied by a reward signal such as dopamine, could retroactively assign value to behaviourally relevant locations.

---

<sup>2</sup>One can perhaps relate the early stabilized and gradually strengthened assemblies to the rigid and plastic cells in Groszmar and Buzsáki (2016), although van de Ven et al. (2016) did not report a difference in firing rates and spatial information between the two populations.

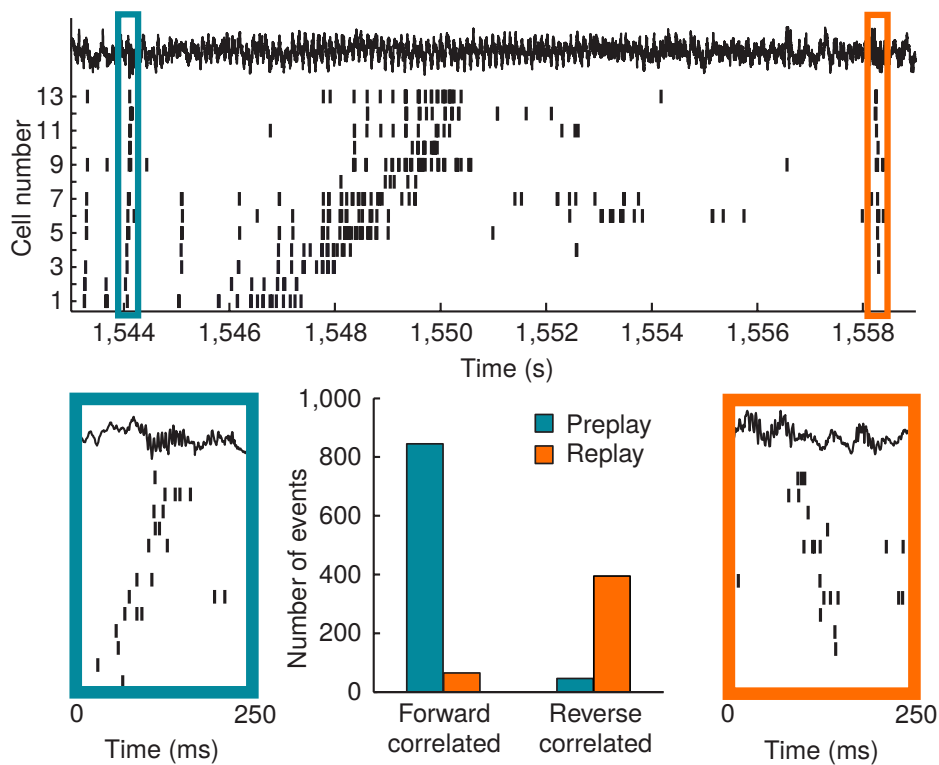


**Figure 1.4:** Forward and reverse replay. CA1 LFP and CA3 place cell spiking activity before, during, and after a single lap on a linear track. Ripple sequences are highlighted before (blue) and after (orange) the lap and are magnified at the bottom. Note that forward replay tends to occur immediately before a lap ('preplay'), while reverse replay takes place after a lap. Reproduced from Diba and Buzsáki (2007).

What is the mechanism of reverse replay? Buzsáki (1989) had predicted reverse sequences during awake ripples, hypothesizing that the activity would sweep from the most excitable neurons (those receiving spatially tuned inputs for the current location of the animal) backwards to previously activated neurons, whose excitability slowly decays. Consistent with this prediction, O'Neill et al. (2006) reported that ripples occurring during brief pauses in exploration (but not during prolonged periods of immobility) were often accompanied by replay of trajectories involving the current location of the rat. Extending these findings, Csicsvari et al. (2007) reported that, in addition to cells with nearby place fields, more recently activated neurons tended to fire earlier in ripples, again during brief pauses but not prolonged immobility. This effect of recent firing history may favor participation of neurons carrying relevant information about the most recent events. However, decreasing excitability cannot account for reverse replay of remote experiences, i.e. replay in one environment of trajectories experienced long before in a different environment (Karlsson and Frank, 2009).

Further studies have linked reverse replay with rewarding experiences. Singer and Frank (2009) trained rats on a maze where reward sites could be baited or not depending on an ongoing rule. Most reactivations when rewards were available (68%) included reverse replay. Ripple incidence and participation of CA3 neurons in replay increased in rewarded trials. Moreover, rule changes induced increases in ripple activity at reward sites. This is consistent with the notion that reverse replay at reward sites may bind memories of actions with the resulting reward outcomes, since the need for binding would decrease with familiarity.

Ambrose et al. (2016) further investigated the link between replay and reward by varying the amount of reward. The number of ripples increased with increased reward and decreased when reward was removed. Interestingly, this effect was entirely driven by ripples containing reverse replay, as forward replay was unaffected by changes in reward. This further supports the idea that reverse replay plays a role in encoding advantageous experiences.

### **Forward preplay**

Diba and Buzsáki (2007) recorded CA3 place cell activity as rats ran on a linear track. In addition to reverse replay at reward sites, they also observed sequences proceeding in the forward direction, describing the future trajectory. Such forward preplay occurred as rats were facing the track, just before initiating the next lap.

Forward preplay has also been linked with future behaviour in spatial navigation tasks. In the early learning phases of a spatial alternation task, forward preplay

preceded correct trials (Singer et al., 2013). In particular, the proportion of cell pairs that fired together predicted performance on a trial-by-trial basis. Pfeiffer and Foster (2013) trained rats to retrieve food rewards on a cheeseboard maze and compared replay during pauses when rats foraged for food (random walk), and before they returned to their home cage (goal-based navigation). Forward preplay selectively occurred during goal-based navigation. Recently, Wu et al. (2017) placed rats on a track where a restricted zone was associated with mild electric foot shocks. They described reactivation of place cells representing the shock zone in ripples occurring as the animal stopped on its way towards the shock zone, and turned back to avoid it. Collectively, these results suggest a potential role of hippocampal ripples in memory retrieval, working memory, and navigational planning.

### **Extended, remote, and ‘noisy’ replay**

In larger environments, replay can span multiple ripples (‘extended replay’, Davidson et al., 2009). In addition to sequences extending (in the forward or reverse direction) from the current position of the rat, a considerable proportion of replay events involve distant trajectories on the track, which do not appear to be related to the ongoing behaviour (Davidson et al., 2009; Gupta et al., 2010). In more elaborate environments, sequences can code for never-experienced ‘shortcut’ trajectories, indicating that awake replay does not simply reflect recent experience, but instead may serve to maintain a complete representation of the environment (a cognitive map) and possibly retrieve information from this representation to support goal-driven behaviour (Gupta et al., 2010).

It is important to note that a substantial proportion of ripple activity cannot be matched to known trajectories. As mentioned earlier, Karlsson and Frank (2009) documented replay of remote experiences (trajectories). This suggests that at least some of the ‘noisy’, non-decodable sequences in ripples, correspond to replay of past experiences, possibly unknown to the experimenter.

### **Ripples during prolonged immobility**

In addition to brief pauses in task-related behaviour, ripples can occur during longer periods of immobility. Their content is no longer biased to include the current position of the animal or recently activated neurons (O’Neill et al., 2006; Csicsvari et al., 2007). Ólafsdóttir et al. (2017) confirmed and extended these results, providing evidence that cortical responses to CA1 ripples occurring during prolonged periods of immobility (‘disengaged’) were followed by cortical responses similar to immobility and sleep ripples, contrary to ripples occurring within 5 s

before or after movement ('engaged'). The authors suggested that 'disengaged' replay resembles sleep replay and might also be involved in memory consolidation.

### **Manipulating awake ripples**

While studies describing hippocampal activity during awake ripples point to potential functional roles for these events, manipulation of awake ripples and the ongoing activity is required to conclusively determine which processes they are critical for. In a spatial alternation working memory task, Jadhav et al. (2012) interrupted awake ripples via electrical pulses triggered upon ripple detection. This impaired performance on the task, indicating that awake ripples play a role in navigational decision making, which requires integrating immediate past experience with a known rule. Consistently, perturbation of awake replay increases vicarious trial and error (Papale et al., 2016), an exploratory behaviour related to decision making (Tolman, 1938). Future studies will need to determine whether awake ripples at trial onset (mostly forward replay) vs at reward consumption (mostly reverse replay) contribute equally to navigational planning. On the other hand, Wang et al. (2016) reported that muscimol inactivation of the medial septum resulted in impaired performance, although awake replay was not affected by the pharmacological treatment. Thus, while awake replay contributes to navigational planning, additional mechanisms appear to be required. Incidentally, perturbation of awake replay did not seem to affect post-task reactivation (Jadhav et al., 2012), which also argues for complementary mechanisms to bridge the gap between awake and sleep processes (see chapter 9).

Recently, Roux et al. (2017) directly tested another proposed role of awake replay, namely in constructing and stabilizing the cognitive map of the environment (Gupta et al., 2010). In rats performing a spatial memory task, they optogenetically inhibited hippocampal neurons during awake ripples occurring at goal locations. During subsequent exploration, the place fields of the inhibited neurons were destabilized, while the place fields of the remaining neurons remained stable. Intriguingly, optogenetic inhibition during sleep ripples does not trigger a similar perturbation of place fields (Kovács et al., 2016), suggesting a specific role of awake ripples in the immediate stabilization of hippocampal spatial representations.

## **Conclusion**

Hippocampal sharp wave-ripple complexes are transient events of highly synchronous neuronal activity that typically occur during 'offline' brain states.

This endogenous surge of activity consists in behaviourally relevant spiking patterns, describing spatial trajectories. They have been shown to play a critical role in memory consolidation during sleep and in navigational planning during awake behaviour. These processes may require the involvement of multiple brain areas beyond the hippocampus. In the next chapter, I discuss the direct and indirect effects ripples exert on target cortical and subcortical areas, which are thought to play a key role in information processing and semantic network reconfiguration.

# Chapter 2

## Extrahippocampal reactivations in concert with ripples

Beyond their local impact within the hippocampal formation, synchronous hippocampal outputs during ripples strongly depolarize CA1 target regions, including the subiculum, deep layers of the entorhinal cortex, and multiple neocortical and subcortical areas. Both direct and indirect effects of hippocampal ripples have been reported, with hippocampal replay often leading, but in some cases following, neuronal reactivations in other brain areas. This chapter presents the evidence for a functional interplay between hippocampal ripples and patterns of cortical and subcortical activity.

### 2.1 Entorhinal cortex

The subiculum and the deep layers of the entorhinal cortex are prominent targets of CA1 outputs. In awake rats, Chrobak and Buzsáki (1994) recorded increased activity in response to ripples in the subiculum and deep (V/VI) but not superficial (II/III) layers of the entorhinal cortex. Chrobak and Buzsáki (1996) extended these findings in awake and sleeping rats, showing that the highly synchronous resultant activity, in both the subiculum and the deep layers of the entorhinal cortex, led to local ripples which followed hippocampal CA1 ripples with a 5–30 ms lag. The authors suggested that this strong depolarization might represent a physiological mechanism for relaying memory traces from the hippocampus to other brain areas such as the neocortex.

Recently, two studies have addressed a possible coupling between entorhinal and hippocampal neuronal activities during replay of memory traces. Ólafsdóttir

et al. (2016) simultaneously recorded hippocampal place cells and grid cells from deep layers of the medial entorhinal cortex (MEC). While the number of simultaneously recorded grid cells was limited (in many cases three at a time) due to the challenging nature of the recordings, using clever analyses the authors were able to quantify cross-structural replay. They first detected hippocampal reactivation events and decoded neuronal activity as a spatial trajectory. They then showed that the grid cell representation was spatially coherent with the hippocampal template. The position encoded by the entorhinal cortex lagged behind hippocampal replay by  $\sim 11$  ms, which is consistent with monosynaptic propagation delays from CA1. This suggests that hippocampal replay is translated into replay in deep layers of the MEC, possibly relaying spatial information to the neocortex. Interestingly, in a follow-up study, Ólafsdóttir et al. (2017) reported that a similar coordination takes place in awake ripples during prolonged ( $>10$  s) but not brief periods of immobility (although the number of recorded replay events was small: prolonged  $<400$ ; brief  $<150$ ). They concluded that awake ripples during rest periods might contribute to systems memory consolidation by communicating information to downstream targets through the deep layers of the MEC. On the other hand, ‘engaged’ ripples (during brief periods of immobility) may play a role in navigational planning through a pathway independent of the MEC; this pathway is likely to involve the prefrontal cortex (see section 2.2).

In a complementary study, O’Neill et al. (2017) compared reactivations between the hippocampus and the superficial layers of the MEC. While they did report replay in both regions, these were not temporally coupled. Moreover, the decoded spatial representations of the two regions did not overlap. These findings indicate that, unlike cells in deep layers of the entorhinal cortex, neurons in superficial layers replay task-related trajectories independently of the hippocampus. Surprisingly, superficial MEC replay events were not more likely than chance to be preceded or followed by hippocampal ripples. This is puzzling given that the superficial MEC is the main input area of the hippocampus, suggesting that ripples should at least be biased by strong synchronous inputs. Similarly, some of the areas projecting to the MEC respond to hippocampal ripples, so one might expect increased ripple probability preceding MEC events. Neither of these expected relationships was observed, and the authors proposed that superficial MEC replay may represent a parallel reactivation system with a role different from that of hippocampal ripples. Given the extensive multi-regional effects of hippocampal ripples, it is unclear how such a system may remain independent of hippocampal ripples. Investigating the timing of superficial MEC replay relative to prominent field events in its input areas, notably delta waves or spindles, may provide informative cues. Crucially, determining the potential behavioural impairments resulting from blockade of superficial MEC replay may give insight into the possible functions of this

hypothesized system.

In summary, while the deep layers of the MEC may relay hippocampal information to the neocortex, the role of reactivations in superficial layers remains unknown. In both cases, experiments manipulating neuronal activity in the respective layers will be required to shed light on the functional roles of these reactivation patterns.

## 2.2 Associative cortices

The medial prefrontal cortex (mPFC) receives direct projections from the intermediate and ventral CA1 regions, as well indirect hippocampal projections through the subiculum, the entorhinal cortex, and multiple subcortical areas (Cenquizca and Swanson, 2007). In sleeping rats, Siapas and Wilson (1998) showed increased activity in the mPFC up to a second after the onset of hippocampal ripples. Wierzynski et al. (2009) found that during sleep a subset of mPFC cells reliably respond to hippocampal firing with a short latency of 11-18 ms, consistent with known monosynaptic delays (Tierney et al., 2004) while a larger population response follows  $\sim 100$  ms later. Both responses were most prominent for hippocampal spikes during ripples, supporting the notion that ripple activity communicates information to the prefrontal cortex during sleep.

Peyrache et al. (2009) recorded neuronal activity from the mPFC and the hippocampus of rats trained on a set-shifting task, and provided the first evidence for a temporal coupling between hippocampal ripples and reactivation of task-related mPFC assemblies. In the mPFC, reactivation strength of task-related co-activity patterns increased around hippocampal sleep ripples, reaching a peak 40 ms after the ripple peak. One can speculate that this is indicative of a polysynaptic response, either within the local prefrontal network, or (this is not mutually exclusive) through the entorhinal cortex or the thalamic nucleus reuniens. The finding that mPFC reactivation closely follows hippocampal ripples lends support to the notion that ripples can trigger reinstatement of neocortical assemblies in a process that would underlie the reorganization and stabilization of neocortical memory traces (Frankland and Bontempi, 2005).

A substantial fraction ( $\sim 35\%$ , excitatory and inhibitory) of mPFC neurons also respond to awake hippocampal ripples (Jadhav et al., 2016). This coordination might contribute to decision-making and deliberation dependent on awake ripples (Jadhav et al., 2012). In this view, ripples during brief pauses in exploration would select prefrontal representations that are relevant to ongoing behaviour, including

working memory retrieval and navigational planning. Interestingly, Tang et al. (2017) showed that responses of a prefrontal neuron to awake and to sleep ripples are not correlated, and thus awake and sleep ripples appear to modulate distinct neuronal populations. In light of the results of Ólafsdóttir et al. (2017) presented above (section 2.1), one could speculate that the responses to sleep and awake ripples may reach the prefrontal cortex through different pathways. Sleep and prolonged immobility ripples might modulate the prefrontal cortex directly or via the deep layers of the entorhinal cortex, whereas awake ripples might modulate prefrontal neurons through a different pathway, either via direct projections or a relay area such as the nucleus reuniens.

The parietal cortex, although it receives no direct projections from the hippocampus, has also been shown to reactivate task-related activity following sleep ripples. Wilber et al. (2017) recorded in multiple sites (300  $\mu\text{m}$  apart) in the parietal cortex, and found that the multiunit activity on a given site encoded movements as the animals were performing a navigation task. Treating each parietal recording site as a unit, they found reactivation of compressed (4–10 fold) sequences of activity that followed hippocampal ripples by  $\sim 100$  ms. Their functional role in memory consolidation remains unknown.

Another cortical area that has received limited attention in its relation to the hippocampus is the retrosplenial cortex, where place cells have been recorded. These have been shown to reflect direct hippocampal inputs (Mao et al., 2017), and are therefore likely to reactivate during ripples, although to my knowledge no studies have yet investigated this.

## 2.3 Sensory cortices

While many regions that receive direct CA1 projections respond to hippocampal ripples with brief delays, the temporal relationship between ripples and activity in sensory cortices appears more variable. In the somatosensory cortex, neuronal activity peaks  $\sim 100$  ms before hippocampal ripples (Sirota et al., 2003). DOWN-UP transitions in the visual cortex lead hippocampal periods of elevated activity (‘frames’) by  $\sim 50$  ms, and reactivation can be observed simultaneously in the hippocampus and visual cortex (Ji and Wilson, 2007), consistent with the idea that that replay-rich periods are initiated by the neocortex, which would provide context and thus bias hippocampal activity; hippocampal replay, via some intermediary region, would then bias cortical activity towards a matching cortical replay, resulting in systems consolidation.

Bi-directional information flow was also documented between the hippocampus and the auditory cortex (Rothschild et al., 2017). Not only did CA1 activity

during sleep ripples predict subsequent cortical activity, but in addition, a subpopulation of cortical neurons elevated their firing rates prior to ripple onset, effectively predicting ripple occurrence and even replay content. To probe this potential cortico-hippocampal communication, task-related sounds were played during sleep. The sounds biased neuronal activity in the auditory cortex as well as subsequent hippocampal ripple activity, supporting the notion that during ripples information can flow from the cortex to the hippocampus. This extends previous results by Bendor and Wilson (2012), who trained rats to retrieve food rewards on the left or right side of a track, depending on instructing sounds. Playing the same instructing sounds during slow-wave sleep biased subsequent reactivation events – for at least 10 s following sound presentation, replay was  $\sim 10\%$  more likely to involve the trajectory associated with the respective sound. Together, these studies provide evidence that cortico-hippocampal communication can affect ripple activity.

While the above studies did not include behavioural readouts of effective memory consolidation, they provide a plausible mechanism for the intriguing phenomenon of targeted memory consolidation. A body of work in humans has established that after a task involving the presentation of cues such as odors (Rasch et al., 2007) or sounds (Rudoy et al., 2009), re-exposing subjects to the cues during slow-wave sleep can selectively strengthen cue-associated memories and improve recall performance. Evidence from rodent studies suggests that targeted memory consolidation is related to the ability of sensory cortices to bias hippocampal replay during sleep ripples. Causal studies blocking or enhancing cortical activity assumed to bias ripple content will be required to provide conclusive support for this hypothesis.

## 2.4 Subcortical areas

A number of studies have addressed how hedonic values (representations of rewarding versus aversive stimuli) are integrated into memory traces, and how activity in relevant subcortical areas is related to hippocampal replay during ripples.

### Ventral tegmental area

The ventral tegmental area (VTA) has long been known to be involved in reward associations. During awake behaviour, ripples are more prevalent at reward sites (Singer and Frank, 2009), and reward-responding neurons in the VTA fire in coordination with hippocampal ripples, especially during replay of rewarded

locations (Gomperts et al., 2015). Could such coupling be instrumental in forming reward-place associations? De Lavilléon et al. (2015) used a closed-loop protocol that paired the activity of one place cell with stimulation of the medial forebrain bundle, known to elicit reward signals, in particular via the VTA. During the subsequent test session, mice headed directly toward the place field of the paired neuron, attesting that a memory trace had been formed during sleep. This indicates that VTA activation during hippocampal ripples is sufficient to establish new associations, most likely involving multiple brain areas<sup>1</sup>. But does such associative memory consolidation actually take place during natural sleep? While the VTA does reactivate reward-related firing patterns in post-task sleep (Valdés et al., 2015), there is no evidence that such reactivations are coordinated with hippocampal ripples. On the contrary, Gomperts et al. (2015) reported that the coordination between VTA firing and ripples observed in the awake state is greatly diminished during sleep. Instead, they suggested that VTA activity during awake ripples may serve to link reward representations across brain regions, setting the stage for subsequent consolidation.

## Ventral striatum

The ventral striatum is a candidate region for such a process. Pennartz et al. (2004) showed that activation patterns observed in the ventral striatum during behaviour are reactivated in post-task sleep and also that reactivated neurons fire more around sleep ripples. In a follow-up study, Lansink et al. (2009) reported cross-structural replay on a compressed (10-fold) timescale, where hippocampal place cells fire in sequence, replaying the trajectory leading up to a goal zone, followed by reward-responding cells in the ventral striatum. Such joint reactivation of hippocampal and ventral striatal neurons may underlie the off-line consolidation of memories associating a place with a reward. Awake ripples may play a role in the initial formation of such memories – recently, Sosa et al. (2017) reported neurons in the ventral striatum that respond to awake ripples. These studies are consistent with the hypothesized VTA-dependent mechanism described above. In this proposed scenario, the associative memory is formed as neurons from the hippocampus and the striatum are active together during awake ripples in reward zones, memory-trace formation is facilitated by the concurrent dopaminergic drive from the VTA, and the linked hippocampo-striatal representations are consolidated in cross-structural replay during sleep ripples. Validating this hypothesis will require testing whether joint VTA–hippocampus–striatum activity during awake ripples is required for cross-structural replay in sleep ripples and whether such cross-structural replay

---

<sup>1</sup>In addition, this study was the first to show that a place cell’s activity during sleep conveys the same spatial information as during behaviour.

is crucial for memory consolidation and thus future retrieval.

## **Locus coeruleus**

In addition to memory of reward associations, dopamine mediates the facilitation of synaptic plasticity induced by novelty (Li et al., 2003). This is expected to have an impact on memory consolidation, as optogenetic stimulation of VTA dopaminergic terminals enhances hippocampal ripple reactivations and memory performance (McNamara et al., 2014). Indeed, mere exposure to a novel environment can promote the retention of recent memories preceding the novel experience (Ballarini et al., 2009). While the VTA has long been thought to mediate the effects of novelty, recently Takeuchi et al. (2016) reported that memory enhancement is instead induced by dopamine co-released from noradrenergic terminals of the locus coeruleus (LC). It is not yet known how this activity is related to awake ripples.

## **Basolateral amygdala**

The interactions between hippocampal ripples and activity patterns in the basolateral amygdala (BLA) were investigated by Girardeau et al. (2017), who studied the consolidation of aversive associations. They trained rats on a place-threat association task, in which an aversive air puff was delivered at a specific location on a linear track, in one running direction only, resulting in one ‘air puff’ and one ‘safe’ trajectory per complete lap. The location of the air puff was changed every day, and thus the rats had to learn a new location in each recording session. The authors documented hippocampo-amygdalar co-activation patterns during subsequent sleep, coinciding with sleep ripples. Notably, only patterns observed in the ‘air puff’ direction were enhanced relative to pre-task sleep. These results suggest that the hippocampus reactivates contextual information while the amygdala reactivates the emotional value of the memory, and that these two components are integrated during ripples to consolidate aversive memories.

## **Conclusion**

Ripples are not isolated hippocampal events, but a vital component of a process spanning multiple brain regions. Awake ripples are followed by responses in the VTA, the ventral striatum, the prefrontal cortex, but not in the entorhinal cortex (except during prolonged periods of immobility). Sleep ripples, possibly

## CHAPTER 2. EXTRAHIPPOCAMPAL REACTIVATIONS IN CONCERT WITH RIPPLES

---

biased by cortical inputs, may initiate reactivations of cortical ensembles and even cross-structural reactivations, involving other areas including the deep layers of the entorhinal cortex, the prefrontal cortex, the ventral striatum, and the amygdala that provide spatial, appetitive, and aversive context to complement hippocampal signals. How are these reactivations temporally organized? The next chapter discusses the cortical sleep rhythms which are believed to orchestrate brain communication during slow wave sleep.

# Chapter 3

## Cortical sleep rhythms

On the basis of EEG patterns, sleep has been divided into rapid eye movement (REM) sleep and non-REM sleep, also termed slow wave sleep (SWS)<sup>1</sup>. The electrophysiological patterns in REM sleep are markedly similar to waking patterns, namely low amplitude, high frequency signal in the cortex, and theta oscillations in the hippocampus. On the other hand, SWS is associated with the slow oscillation and sleep spindles in the cortex and with ripples in the hippocampus. SWS and REM stages alternate in cycles and the roles of these two sleep periods and their underlying mechanisms are likely to be complementary (Diekelmann and Born, 2010). In this chapter, I describe the rhythms that are the hallmarks of slow wave sleep, namely, the slow oscillation and sleep spindles.

### 3.1 Slow oscillation

Perhaps the most prominent sleep rhythm is the cortical slow oscillation (Figure 3.1) – the generalized alternation between a depolarized (UP) state and a hyperpolarized (DOWN) state of synchronized cortical neurons (Steriade et al., 1993c). The DOWN state is characterized by a transient cessation of firing and a positive deflection of the local field potential in deep cortical layers, known as a delta wave (Sirota and Buzsáki, 2005). This is because the large neurons in cortical layer V contribute most to the measurable extracellular currents – when these cells become hyperpolarized during a DOWN state, current is drawn from the superficial layers, where delta waves have reversed polarity (Figure 3.1A).

---

<sup>1</sup>While the term ‘SWS’ is often used to denote exclusively the deep stages of non-REM sleep, where the slow wave amplitude is highest, in this manuscript, SWS refers to all stages of non-REM sleep.

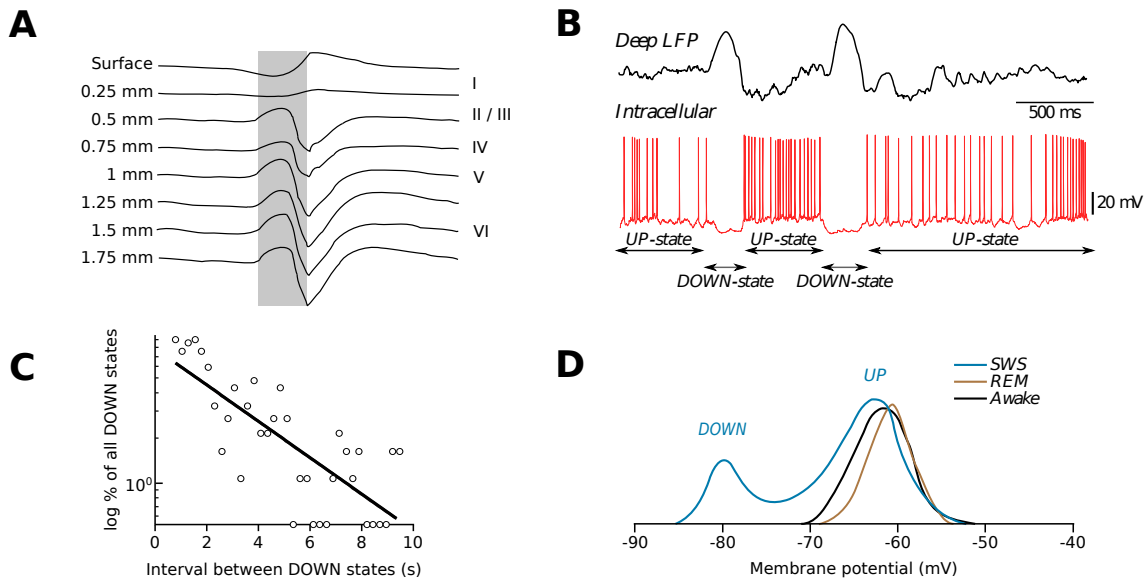


**Figure 3.1:** The cortical slow oscillation. **A.** Laminar distribution of delta waves recorded in sleeping cats (average of  $n=50$  events). Note the potential reversal at 0.3 mm depth. **B.** Example of simultaneous LFP and intracellular recordings of a layer V neocortical neuron in a sleeping cat. Note the hyperpolarized cell membrane potential (DOWN state) and the accompanying positive wave at the LFP level (delta wave). **C.** In SWS recorded in the rat, the distribution of intervals between DOWN states is approximately exponential, indicating that in natural sleep DOWN state occurrence is not periodic, but rather a random process, and does not reflect a true oscillation. **D.** Distribution of membrane potential values of a cortical neuron across behavioural states. Note the bimodality and in particular, that the DOWN state is only present in SWS. **A, B, C,** and **D** are adapted from Amzica and Steriade (1997), Johnson et al. (2010), Steriade et al. (2001), and Timofeev and Bazhenov (2005), respectively.

In natural slow wave sleep, the DOWN state lasts for  $\sim 200$  ms and is followed by a much longer UP state (up to several seconds). In contrast with natural sleep, ketamine-xylazine anaesthesia dramatically increases the duration of the DOWN state and decreases that of the UP state; the slow oscillation also becomes more rhythmic (Chauvette et al., 2011). However, in natural sleep, the term ‘slow oscillation’ can be considered a misnomer given that DOWN state occurrence is stochastic rather than rhythmic (Figure 3.1C).

The slow oscillation is generated in the cortex – it is absent in the thalamus of decorticated cats (Timofeev and Steriade, 1996) and it persists in deafferented cortical slabs (Timofeev et al., 2000) and cortical slices *in vitro* (Sanchez-Vives and McCormick, 2000), albeit with a prolonged DOWN state lasting for tens of seconds. The DOWN state is not caused by inhibition – interneurons are also silent during DOWN states, and reversing the action of  $GABA_A$  channels<sup>2</sup> does not abolish the slow oscillation (Timofeev et al., 2001b). Rather, the DOWN state is a period of disfacilitation, a reduction of cortical synaptic excitation, and requires leak potassium current, which reduces the resting membrane potential of cortical neurons (Timofeev et al., 2001b). This is why DOWN states only occur in slow wave sleep – in the awake brain and in REM sleep, increased cholinergic activity blocks potassium conductance, preventing DOWN states from taking place (Steriade et al., 1993a). Indeed, all brain states other than SWS can be thought of as persistent UP states (Shu et al., 2003).

### 3.1.1 UP/DOWN state initiation

In isolated cortical slabs (Timofeev et al., 2000) and slices (Sanchez-Vives and McCormick, 2000), DOWN states are prolonged, lasting up to a minute, and UP state terminations are less synchronous than in the intact brain (Volgushev et al., 2006). This indicates that although the slow oscillation can be sustained by a cortical network, in natural conditions extra-cortical inputs help trigger DOWN-UP and UP-DOWN transitions. Indeed, Shu et al. (2003) showed that local electrical stimulation (within layer V, within layers II/III, or in the white matter below the recording site) can terminate the current state, be it an UP state or a DOWN state, and trigger a state change. Therefore strong synchronous inputs to the cortex can help drive the slow oscillation.

There is strong evidence that inputs from the thalamus trigger DOWN-UP

---

<sup>2</sup>Timofeev et al. (2001b) recorded cortical neurons with intracellular pipettes filled with KCl, which changes the chloride reversal potential of  $GABA_A$  receptors and transforms the membrane response to  $GABA_A$  receptors from hyperpolarizing to depolarizing. While this increased the neuronal firing rate during UP states, it did not affect DOWN state occurrence, indicating that the DOWN state is not maintained by  $GABA_A$ -mediated inhibition.

transitions, and that the timing of thalamic activity leads to the short duration of DOWN states (Destexhe et al., 2007). Thalamic neurons are highly synchronous with the ongoing slow oscillation, and thalamocortical projection cells burst at the end of the DOWN state, typically preceding the first cortical spikes in the UP state (Contreras and Steriade, 1995). In cortical slices, Rigas and Castro-Alamancos (2007) showed that stimulating the thalamus reliably triggered cortical UP states, whereas cutting the connections between thalamus and cortex reduced UP state incidence.

With respect to UP-DOWN transitions, progressive synaptic depression and disfacilitation have been proposed to bring the network to a silent state (Timofeev et al., 2001b; Bazhenov et al., 2002). However, Volgushev et al. (2006) showed that UP-DOWN transitions occur very synchronously in a cortical network, even more so than DOWN-UP transitions. The authors proposed the existence of a subpopulation of inhibitory cells that fire synchronously at the end of UP-states, triggering the DOWN state in all neurons including themselves. This idea was supported by Chen et al. (2012), who found that increasing interneuronal excitability lead to an enhanced UP-DOWN transition synchrony. They also developed a detailed computational model which reproduced these findings and predicted that interneuron-pyramidal connections could account for the high synchrony of the DOWN-UP transition. Supporting this, Lemieux et al. (2015) found increased inhibition preceding the UP-DOWN transition in sleeping cats.

Such increased inhibition is also a candidate mechanism for the synchrony of DOWN-UP transitions in response to inputs. Shu et al. (2003) reported that electrical stimulation during the UP state (triggering an UP-DOWN transition) resulted in a larger response of inhibitory cells as compared to the same stimulation during the DOWN state (triggering an DOWN-UP transition). Jercog et al. (2017) developed a rate model which indicated that stimulation during the DOWN state serves as a bump of activity that triggers a DOWN-UP transition, whereas stimulation during an UP state results in excess inhibition, triggering an UP-DOWN transition. Indeed, DOWN states can be brought about by electrical stimulation (Amzica and Steriade, 1997; Vyazovskiy et al., 2009). In natural conditions, DOWN states would be triggered by strong input from cortical afferent areas. Indeed, UP-DOWN transitions are less synchronous in deafferented cortical slabs (Lemieux et al., 2015), suggesting that inputs to the cortex play a role in triggering UP-DOWN transitions (see section 4.1.1).

### 3.1.2 Extent of silence in delta waves

While delta waves represent periods of synchronized silence, as perhaps it may be expected in a biological system, there are limits and exceptions to this synchrony.

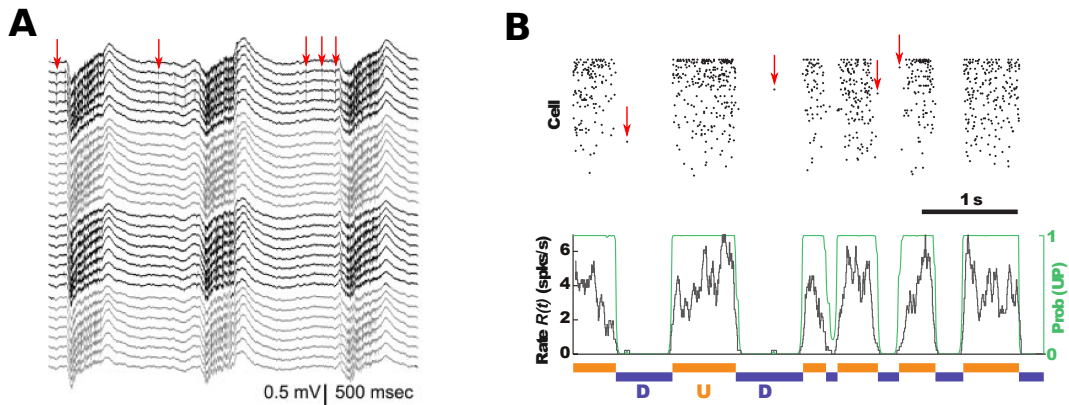


**Figure 3.2:** Examples of spikes recorded during delta waves in rats under urethane anaesthesia. **A.** Wideband multichannel recording of layer V of the somatosensory cortex. Note the spikes occurring while the rest of the network is silent (red arrows). **B.** Top: population raster of 92 simultaneously recorded single units (sorted by firing rate) in the deep layers of the somatosensory cortex. Note the spikes during the synchronized DOWN state (red arrows). Bottom: instantaneous population rate and the detected UP states (U, orange) and DOWN states (D, purple). **A** and **B** are adapted from Csicsvari et al. (2003) and Jercog et al. (2017), respectively.

There are two temporal scales for considering the extent of the neuronal silence.

On the macro-scale, delta waves do not occur in the whole cortex at once. Rather, they propagate across the cortex at 1-7 mm/ms typically in the anterioposterior direction (Massimini et al., 2004), most likely through long-range connections (Compte et al., 2003). While some delta waves may travel through the whole cortex, others remain localized events (Massimini et al., 2004). In such cases, a DOWN state may occur in one cortical area, resulting in neuronal silence and a delta wave, but not take place in a nearby area only 1 mm away, where neurons continue to fire and there is no delta wave (Sirota and Buzsáki, 2005).

On a smaller scale, there have been cases of ‘rogue neurons’ continuing to fire despite the ongoing DOWN state of the rest of the population (Figure 3.2). These have often been overlooked, and attention has been brought instead of the relative silence of the network. Note that while Hahn et al. (2012) reported medial entorhinal cortex (MEC) neurons remaining active during certain DOWN states, the network DOWN states were estimated from the LFP in the medial prefrontal cortex, and it is therefore possible that these delta waves have simply failed to propagate to the MEC.

### 3.1.3 Delta waves and synaptic plasticity

The slow oscillation has been shown to induce synaptic plasticity. In an elegant study, Chauvette et al. (2012) recorded the spikes of a cortical neuron and the accompanying LFP signal from a sleeping cat, and then used this SWS pattern as a stimulation protocol *in vitro* – stimulation pulses were matched to replicate the pre-recorded spike train, thus mimicking realistic input to the target cell. In the absence of the slow oscillation, this stimulation protocol only resulted in transient facilitation of synaptic activity but no long-term potentiation (LTP). In the slow oscillation condition, the protocol was accompanied by introducing the slow oscillation in the target neuron by hyperpolarizing it with an intracellular current pattern emulating DOWN states in time with the delta waves in the pre-recorded SWS pattern. This ‘full sleep-like protocol’ with a realistic stimulation pattern delivered in UP states interleaved by hyperpolarized DOWN states resulted in long-lasting synaptic plasticity in a calcium-dependent mechanism. (Chauvette et al., 2012)

This suggests that while the cortex is largely unresponsive to outside inputs during DOWN states (Timofeev et al., 1996), the DOWN state is required to bring cortical neurons to a more receptive state for synaptic plasticity during the UP state, where neuronal activity occurs, including the reactivation of awake-related neuronal patterns (Euston et al. 2007; Ji and Wilson 2007; Johnson et al. 2010; Peyrache et al. 2011, see chapter 2) and gamma oscillations (Mukovski et al., 2007), possibly due to coincident cholinergic inputs (Mena-Segovia et al., 2008). In particular, cortical neuronal activity peaks just after UP-DOWN transitions (Destexhe et al., 1999). Destexhe et al. (2007) proposed that this synchronous activity might represent a window of synaptic plasticity. Moreover, it has been suggested that the thresholds for triggering synaptic plasticity might change with the level of background activity in a network; in such a case, the silence preceding the DOWN-UP transition might further enhance the efficacy of synaptic plasticity as the first spikes in an UP state would occur in a context of minimal background activity (El Boustani et al., 2012). Such a mechanism may help explain the results of Chauvette et al. (2012) in the paragraph above.

What happens at the UP state onset? In thalamocortical slices, MacLean et al. (2005) reported that cortical neurons fire in reproducible sequences after DOWN-UP transitions. Importantly, the thalamocortical bursts that initiate UP states (see section 3.1.1) would not bias the UP state activity, which is determined by local dynamics alone (MacLean et al., 2005). Luczak et al. (2007) first reported these sequences *in vivo* and showed that the average latency of the activation of a given neuron at the UP state onset did not correlate with cell excitability, and that sequential activations were preserved regardless of the direction of the travelling delta wave. These sequences do not reflect delta wave

propagation, but rather possibly synaptic weights brought about by experience in behaviour (Buzsáki 2006<sup>3</sup>, also see chapter 5). Such sequential activity also has consequences: neurons firing in repeated sequences facilitate the emergence of LTP at the UP state onset (Levenstein et al., 2017; Kruskal et al., 2013).

Recently, Khodagholy et al. (2017) recorded neural activity from the surface of the brain in sleeping rats and reported cortical oscillations in the ripple band at UP state onsets in association cortices, including parietal, retrosplenial, anterior cingulate, and medial prefrontal cortex. The relation between these oscillatory events and cortical sequences, synaptic plasticity, and memory consolidation remain to be explored, but the similarities with hippocampal ripples (sequential activity, ripple-band oscillations) make them worthy of further investigation.

### 3.1.4 Delta waves and memory consolidation

Whether the effects of the slow oscillation on synaptic plasticity are direct (e.g. sequences at UP state onset) or indirect (e.g. through orchestrating other rhythms, including sleep spindles), there is ample evidence for a role of the slow oscillation in memory consolidation. After humans learn a declarative memory task, slow oscillation amplitude and UP state duration have been shown to correlate with subsequent performance after sleep (Heib et al., 2013). In an elegant study, Huber et al. (2004) showed that learning a motor skill selectively enhanced slow oscillation amplitude in the cortical area associated with the task, and further, the degree of enhancement predicted performance improvement.

Beyond correlational studies, other works have addressed the causality of the relation between the slow oscillation and memory consolidation. In sleeping humans and rats, transcranial stimulation in sleep at the frequency of the slow oscillation was reported to enhance memory consolidation of declarative memory (Marshall et al., 2006; Binder et al., 2014). However, more recent studies have failed to replicate this effect (Eggert et al., 2013; Sahlem et al., 2015) and questioned whether transcranial stimulation can entrain the slow oscillation (Lafon et al., 2017). Still, a different technique – closed-loop auditory stimulation in phase with the ongoing slow oscillation – reliably boosts the slow oscillation and enhances declarative memory retention (Ngo et al., 2013), confirming that the slow oscillation plays a critical role in memory consolidation. The authors have suggested that this could be mediated by increased slow wave amplitude as well as temporal alignment of sleep spindles, although an alternative interpretation based on the temporal coupling between the slow oscillation and hippocampal

---

<sup>3</sup>Although “Rhythms of the Brain” was published before the article of Luczak et al. (2007), György Buzsáki, as one of the authors of the article, was aware of the work and discussed it in Buzsáki (2006) on page 194.

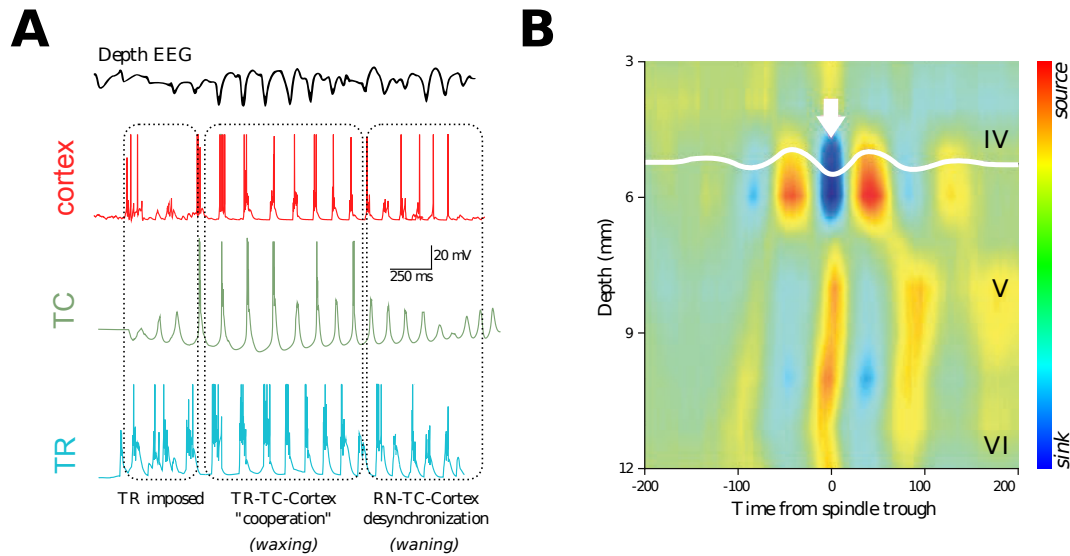


**Figure 3.3:** Sleep spindles. **A.** *In vivo* intracellular recordings of a cortical neuron, a thalamocortical cell (TC), and a thalamic reticular neuron (TR) throughout a spindle sequence. **B.** Average neocortical current source density (CSD) centred on spindles, highlighting deep neocortical sink-source pairs. Approximate positions of neocortical layers are indicated on the right. **A, B** are adapted from Timofeev and Bazhenov (2005) and Sirota et al. (2003), respectively.

ripples is possible (see section 7.1).

## 3.2 Sleep spindles

Sleep spindles are thalamocortical waxing-and-waning oscillatory events (10–15 Hz) (Berger, 1933; Steriade et al., 1993b) which occur mostly in the light stages of NREM sleep. Spindles are embedded in the cortical slow oscillation, closely following delta waves, triggered by the upsurge of activity of cortical cells after a DOWN-UP transition (Amzica and Steriade, 1997; Peyrache et al., 2011), although some occur spontaneously in isolation (Sirota and Buzsáki, 2005; Peyrache et al., 2011).

Spindles are thalamocortical events involving three populations of neurons: thalamic reticular neurons, thalamocortical cells and cortical neurons (Figure 3.3). Thalamic reticular neurons, which are densely interconnected by gap junctions, synchronously burst and inhibit thalamocortical neurons. This hyperpolarization de-inactivates a low-threshold  $\text{Ca}^{2+}$  current, which leads to low-threshold calcium spikes and induces bursts of action potentials. Thalamocortical bursts excite thalamic reticular neurons via a feedback mechanism and also

project to neocortical dendrites. The neocortical afferents to both thalamocortical cells and thalamic reticular cells synchronizes sleep spindles (Contreras et al., 1996; Destexhe et al., 1998). Spindle termination proceeds through the waning phase, where the network becomes desynchronized, possibly due to out-of-phase cortical feedback (Timofeev et al., 2001a; Gardner et al., 2013).

### 3.2.1 Spindles and synaptic plasticity

Spindles are known to promote synaptic plasticity (Sejnowski and Destexhe, 2000; Steriade and Timofeev, 2003). The thalamocortical inputs to cortical dendrites result in massive calcium entry in neocortical neurons (Contreras et al., 1997; Seibt et al., 2017). Applying spindle-like stimulation patterns *in vitro* induces long-term potentiation in cortical synapses via an NMDA receptor-dependent process (Rosanova and Ulrich, 2005).

In a recent calcium imaging study, Seibt et al. (2017) showed that spindles are associated with calcium entry into cortical dendrites, but not into the cell bodies of the same neocortical cells. This decoupling of dendritic and somatic activity might be due to increased inhibitory drive during sleep spindles (Contreras et al., 1997; Peyrache et al., 2011). This dissociation implies that dendritic synaptic plasticity could take place in the absence of any resulting spiking activity through a non-Hebbian mechanism, which could make it difficult to interpret the spiking patterns recorded during sleep spindles (Seibt et al., 2017).

### 3.2.2 Spindles and memory consolidation

Spindle activity has been shown to play a role in memory consolidation. The rate of spindle occurrence increases in sleep after learning a declarative memory tasks in both humans (Gais et al., 2002) and rats (Eschenko et al., 2006). Moreover, pharmacologically enhancing sleep spindle occurrence improves declarative memory performance in healthy humans (Mednick et al., 2013).

## Conclusion

During SWS, neocortical neurons alternate between silent DOWN states and active UP states. Like hippocampal ripples, SWS rhythms are closely associated with memory consolidation. In particular, the calcium entry during sleep spindles and the elevated activity and spiking sequences at the DOWN-UP transition result in optimal windows for synaptic plasticity. The efficacy of

the hippocampo-cortical dialogue in the consolidation of memory would rely on temporal coordination between these events. In the next chapter, I discuss the coupling between ripples and these prominent sleep rhythms.

# Chapter 4

## Hippocampo-cortical coupling

Ripple occurrence is irregular, yet it is coupled with other recurrent brain rhythms. Most notably, ripple timing is influenced by the neocortical slow oscillation and by thalamocortical sleep spindles (Figure 4.1), possibly because inputs to the hippocampus may advance or delay the occurrence of forthcoming ripples (Buzsáki, 2006). In turn, ripple activity may influence the timing of these two sleep rhythms. This chapter describes the coupling of hippocampo-cortical rhythms and its role in systems memory consolidation.

### 4.1 Slow oscillation

Because both ripples and delta waves are recurring events, it is difficult to infer causal relationships between the two activity patterns based on their relative timing. Delta waves tend to follow hippocampal ripples, suggesting that ripples might facilitate a forthcoming UP-DOWN transition. There are also reports of ripples immediately following delta waves; this is likely related to the surge of cortical activity during the DOWN-UP transition, as discussed below.<sup>1</sup>

---

<sup>1</sup>Due to the traveling nature of cortical delta waves (with a tendency to propagate from anterior to posterior areas), the precise timing between delta waves and hippocampal ripples may vary between regions. However, given the estimated speeds of delta wave propagation (1.2–7 m/s) (Massimini et al., 2004) and the duration of a typical delta wave ( $\sim 200$ ms), the order of events (ripple-delta versus delta-ripple) is not expected to be affected by delta propagation.

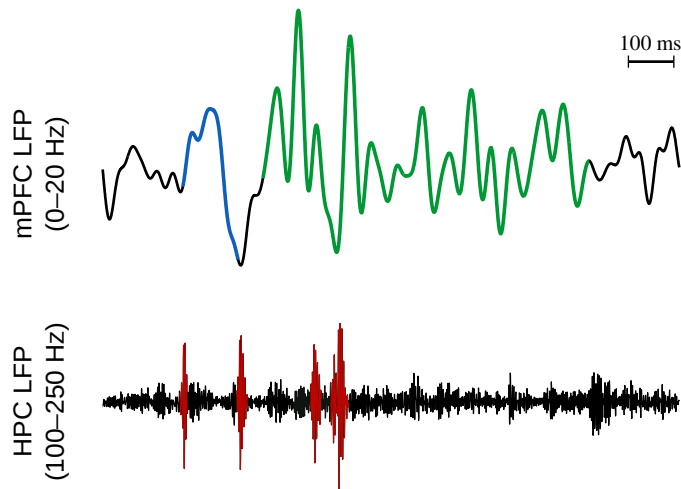


**Figure 4.1:** A representative example of hippocampo-cortical coupling, showing low-pass filtered (0–20 Hz) prefrontal LFP and simultaneously recorded hippocampal LFP filtered in the ripple band (100–250 Hz, ripples are highlighted in red). Note the first ripple preceding the delta wave (blue), the second ripple following the delta wave while preceding the spindle (green), and the last two ripples embedded in the spindle oscillation.

#### 4.1.1 Ripples preceding delta waves

The first systematic study of a temporal coupling between delta waves and ripples was provided by Sirota et al. (2003), who showed that while ripples follow periods of elevated activity in the somatosensory cortex, they precede somatosensory delta waves by 50–150 ms. The authors suggested that this coupling could mediate coordinated information transfer between the hippocampus and the neocortex.

A possible mechanism for ripple-delta coupling is that the surge of excitatory activity serves as a ‘kick’ that destabilizes the UP state and thus biases the transition from an UP to a DOWN state (Jercog et al., 2017). Consistently, hypersynchronous recruitment of hippocampal neurons through strong electrical stimulation of the ventral hippocampal commissure leads to a decrease in prefrontal activity lasting  $\sim 200$  ms (Girardeau et al., 2009), comparable to the duration of a DOWN state, as well as to an increase in delta power (Gelinias et al., 2016), consistent with a contribution of ripples in facilitating the emergence of delta waves.

Evidence for a possible role of ripple-delta coupling in memory consolidation was provided by Peyrache et al. (2009), who performed simultaneous recordings in the hippocampus and the prefrontal cortex of rats trained on a set-shifting task. The authors detected prefrontal coactivation patterns during the task

and measured their reactivation in post-task sleep. Both the hippocampal ripple incidence and the reactivation strength of prefrontal ensembles peaked before delta waves. Moreover, prefrontal reactivation tended to closely follow (by  $\sim 40$  ms) hippocampal ripples. This suggests that a hippocampo-cortical information transfer might be preferentially initiated briefly before delta waves. A possible role for the delta wave (neural silence) might be to avoid interference with other, unrelated inputs (see chapter 6).

### 4.1.2 Ripples following delta waves

Battaglia et al. (2004) reported a higher ripple rate around DOWN-UP transitions in multiple cortical areas. A fine timescale analysis further revealed that cortical firing rates decreased 400-200 ms before sharp wave ripples; the authors attributed this decrease to a consistent occurrence of delta waves before ripples. In recordings of the prefrontal electroencephalogram (EEG) of sleeping rats, Mölle et al. (2006) showed ripples following delta waves by 140-480 ms and suggested that the cortical UP state following the delta wave may promote hippocampal ripples via efferent pathways.

A thorough assessment of the influence of neocortical slow oscillations on hippocampal activity in anesthetized and sleeping rats was provided by Isomura et al. (2006), who reported that prefrontal DOWN-UP transitions were closely followed by entorhinal DOWN-UP transitions and increased activity in the dentate gyrus and CA1<sup>2</sup>. Most ripples occurred  $\sim 100$  ms after entorhinal DOWN-UP transitions and  $\sim 200$  ms after prefrontal DOWN-UP transitions. The authors proposed that the upsurge of activity in the dentate gyrus associated with the entorhinal UP state may activate selected populations of CA3 and suppress the rest by feedforward inhibition, thus biasing hippocampal ripple occurrence as well as the identity of the participating neurons.

Recently, Khodagholy et al. (2017) recorded neural activity from the surface of the brain in sleeping rats and reported cortical oscillations in the ripple band in association cortices, including parietal, retrosplenial, anterior cingulate, and medial prefrontal cortex. These events took place at the DOWN-UP transition, preceding spindles, and occurred synchronously with hippocampal ripples. The coupling between cortical and hippocampal ripples increased in

---

<sup>2</sup>Surprisingly, Isomura et al. (2006) reported increased activity in CA3 during entorhinal DOWN states (possibly due to feedforward disinhibition from the dentate gyrus) that did not result in an increased ripple rate, which remained at its lowest. On the other hand, during periods of reduced activity in the dentate gyrus associated with entorhinal DOWN states Sullivan et al. (2011) reported a small decrease of CA3 activity, which would be consistent with the concurrent low ripple rate.

sleep following training on a cheeseboard maze task, suggesting a potential role in memory consolidation. The authors hypothesized that such joint events might be a substrate of communication in the hippocampo-cortical dialogue, although it remains to be investigated in which direction information might flow. Alternatively, this concurrence might result from a common drive orchestrated by the cortical slow oscillation, and the ripple event in each region might consolidate relevant information locally.

## 4.2 Sleep spindles

Reports of ripple-spindle coupling span multiple timescales. On the timescale of seconds, spindles tend to follow hippocampal ripples. On a finer timescale, ripples are phase-locked to individual spindle cycles. The implications of these coupling relations on memory consolidation are discussed below.

### 4.2.1 Ripples preceding spindles

Siapas and Wilson (1998) first documented the tendency of hippocampal ripples to precede spindles in the prefrontal cortex. Later studies have shown that the ripple rate tends to peak  $\sim 0.5$  s before prefrontal spindles (Mölle et al., 2006; Peyrache et al., 2009).

Sirota and Buzsáki (2005) proposed that the slow oscillation might orchestrate both hippocampal ripples and thalamocortical spindles — ripples tend to precede (or closely follow) cortical delta waves, which are in turn followed by spindles. It is therefore plausible that the slow oscillation may explain the coupling of these events on this long timescale.

When do neocortical reactivations take place with respect to ripple-spindle events? Peyrache et al. (2009) showed that the highest spiking probability of prefrontal units occurred during the second half of spindles. However, prefrontal reactivation of task-related patterns peaked much earlier, before spindle onset (almost coinciding with ripple activity). Memory-related cell assemblies would therefore be reinstated a few hundred milliseconds before the high spiking activity associated with spindles.

In freely moving rats trained on a spatial memory task, Novitskaya et al. (2016) applied a closed-loop stimulation protocol in post-task sleep, where the locus coeruleus (LC) was electrically stimulated upon ripple detection. While stimulation did not affect the ongoing ripple, ripple-spindle coupling was reduced and memory consolidation was impaired. Although one cannot rule out that

the noradrenergic release following LC stimulation had widespread uncontrolled effects beyond disrupting hippocampo-thalamic coupling, this remains consistent with a potential role of ripple-spindle coupling in memory consolidation.

A classical account of how a hippocampo-cortical dialogue involving ripple-spindle events can lead to memory consolidation is therefore the following: ripple-related activity facilitates the resurgence of cortical cell assemblies relevant to a given memory trace; this is then followed by the strong synchronized spindle activity that induces synaptic plasticity. However, a caveat in this scenario is that these events typically take place hundreds of milliseconds apart, which is not consistent with classical forms of long term potentiation<sup>3</sup>. A recent study reported a long timescale form of synaptic plasticity, where a calcium plateau potential in CA1 dendrites can potentiate inputs offset by seconds (Bittner et al., 2017). While it is not yet known whether a similar mechanism might take place during sleep in the neocortex, one could speculate that during spindles, the bursting of neocortical pyramidal cells combined with the massive calcium influx may retroactively potentiate synapses activated  $\sim 0.5$  s earlier, and that as a result ripple-triggered reactivated cortical traces are consolidated during the following sleep spindles.

### 4.2.2 Ripples nested in spindle cycles

Ripples can also occur phase locked to individual spindle cycles, both in rats (somatosensory cortex, Sirota et al., 2003) and mice (prefrontal cortex, Phillips et al., 2012). Ripples are also phase locked to parietal spindles in humans (Clemens et al., 2011).

Coordination on such a fine timescale indicates a thalamocortical influence on the timing of hippocampal ripples, possibly via the entorhinal cortex (Sullivan et al., 2014) or via the nucleus reuniens (Varela et al., 2014). It is possible that the mechanism which promotes ripple nesting might also bias which specific neuronal populations participate in the ripple, although this remains to be investigated.

There is causal evidence confirming that thalamocortical activity can entrain hippocampal ripples and that this plays a role in memory consolidation. In a recent study in mice, Latchoumane et al. (2017) manipulated thalamic activity in sleep after contextual fear conditioning, a classical hippocampus-dependent task. In this closed-loop stimulation protocol, detection of frontal delta waves triggered optogenetic stimulation in the thalamic reticular nucleus simulating spindle activity. The stimulation entrained cortical networks in the UP state, resulted in hippocampal ripples phase-locked to the stimulation, and improved

---

<sup>3</sup>A further complication is that ripple-spindle sequences are often interrupted by delta waves (see chapter 6).

memory performance relative to non-stimulated mice. A control version of the protocol involved stimulating during the DOWN state, when cortical networks are silent. Memory performance was not improved, although ripples were still locked to the stimulation. The authors concluded that the co-occurrence of hippocampal ripples with neocortical UP state activity during sleep spindles is instrumental to memory consolidation. One caveat however is that light pulses were delivered at 8 Hz, rather than at spindle frequency (10–20 Hz), making mechanistic interpretations in terms of underlying brain rhythms more challenging.

How would spindle-nested ripples participate in memory consolidation? In one view, this coupling could be a substrate for unidirectional cortico-hippocampal communication. Because ripple-associated cortical reactivation is high before but not during spindles, spindles could correspond to a period of reorganization and plasticity at the level of cortico-cortical synapses. Ripples embedded in spindles might then integrate this newly reconfigured information into the hippocampal network, while the cortical network would remain dominated by local interactions (Peyrache et al., 2011).

Alternatively, it is possible that this phenomenon allows for a bidirectional information transfer, where in addition to cortical inputs biasing replay activity in ripples nested in spindles, hippocampal outputs in turn modulate cortical activity during spindles. Indeed, while hippocampal inputs would have to compete with local inhibition to discharge prefrontal neurons during spindles (Peyrache et al., 2011), they may nevertheless bias activity at the population level (Wierzynski et al., 2009). Because during spindles calcium entry into the dendrites can be decoupled from somatic firing (Seibt et al., 2017), the absence of cortical spikes should not be interpreted as evidence that cortical networks are unaffected by hippocampal ripples occurring during spindles.

## Conclusion

In summary, memory consolidation during sleep is accompanied by a hippocampo-cortical dialogue orchestrated by fine-tuned ripple-delta-spindle coupling. Sleep ripples precede delta waves, follow delta waves, precede spindles, and occur during spindles, phase-locked to individual cycles. The role of the coupling of hippocampo-cortical rhythms for memory consolidation has been the central focus of the work in this thesis.

# Part II

# Results



---

According to the two-stage model of memory consolidation, memories are initially encoded in the hippocampus and are later transferred to the cortex during slow wave sleep (Buzsáki, 1989). Hippocampal communication to the cortex is believed to take place during ripples (Buzsáki, 1989). This is supported by the finding that ripple activity in post-task sleep is critical for spatial memory consolidation (Girardeau et al., 2009). Given the tendency of delta waves to follow hippocampal ripples and the associated cortical reactivations (Sirota et al. 2003; Peyrache et al. 2009, see section 4.1), we were interested in the role of this ripple-delta coupling for memory consolidation.

The central focus of my thesis has been to address the question of how ripple-delta coupling causes memory consolidation. A review (Todorova and Zugaro, 2018) as well as the two articles presented in the following chapters have been the direct result of this work.

---

# Chapter 5

## Role of ripple-delta coupling in memory consolidation

To address the possible causality of ripple-delta coupling in memory consolidation, we (Maingret et al., 2016) tested whether memory consolidation critically depended on the temporal coordination between ripples and delta waves, rather than on the prevalence or strength of each of these oscillations independently.

To then demonstrate a causal link, a stimulation protocol was designed to induce delta-spindle sequences timed on the online detection of hippocampal ripples, i.e. to boost the coordination between these rhythms. The memory consolidation task employed to determine whether this could potentially improve memory consolidation was a modified version (Ballarini et al., 2009) of a classical spatial memory task: rats were first placed in a rectangular arena with two identical objects in adjacent corners (sampling); on the following day (recall), they were returned to the arena, where one of the two objects had been displaced; the critical modification compared to the classical version of the task was that the sampling period was much briefer, actually too brief for the animals to memorize the configuration of the objects and notice the change during recall. Yet, following a period of stimulation enhancing hippocampo-cortical coupling during sleep, the rats reacted to the altered arrangement of the objects, demonstrating that the transient memory traces formed during sampling had now been consolidated.

All the experiments were performed by Nicolas Maingret. Gabrielle Girardeau was involved in the conception of the project and the pilot experiment with non-implanted control rats. Marie Goutierre was involved in some of the experiments and early stages of data analysis. My contribution to the project was to use the collected datasets to probe for possible neuronal mechanisms that could account for the striking behavioural effect.

In addition to the numerous alternative hypotheses that we tested (some of which are discussed in chapter 8), we investigated the sequences of cortical neurons following the DOWN-UP transition. The latency of a neuron to the UP state does not depend on its excitability or the direction of the travelling delta wave, but it remains stable across a sleep session (Luczak et al., 2007). We reasoned that if sequential firing reflects network connectivity, sequences might change with memory consolidation.

We therefore estimated the stability of each cell’s activity profile following UP-DOWN transitions in the synchronized and delayed control stimulation conditions. In the control condition, activity profiles following induced delta waves remained stable, echoing Luczak et al. (2007)’s results. In contrast, a subpopulation of cells changed their activity profiles following the delta waves induced to follow ripples with the endogenous delay of  $\sim 130$  ms, reflecting a selective functional reorganization of prefrontal subnetworks.

Further, to estimate the encoding of the task by the cortical network<sup>1</sup>, we divided the arena into four quadrants and we measured the firing rate of cortical cells in the quadrants containing the objects relative to the firing rate in empty quadrants. While cortical cells did not respond to objects in the encoding phase of the task, prefrontal cells responded selectively to the displaced object on the test day. This effect was exclusive to the synchronized stimulation condition and was not observed in the delayed stimulation condition, paralleling memory consolidation.

Our results indicate that ripple-delta coupling is sufficient to induce reorganization of the cortical network as reflected by cortical firing in the UP state onset<sup>2</sup>. After ripple-delta coupling, the reorganized cortical network is more engaged in the task and memory performance is improved, demonstrating a direct link between the fine-timescale ripple-delta coupling and memory consolidation.

---

<sup>1</sup>Although the spatial object recognition task can be performed by animals with prefrontal cortex lesions (Barker and Warburton, 2011), this does not exclude the possibility that cells in the prefrontal cortex of healthy non-lesioned animal encode and respond to ongoing experience including the task.

<sup>2</sup>In addition to reflecting network connectivity, the sequential firing at the UP state onset is a possible driving force of the ripple-delta coupling effect on memory consolidation, as the firing at that period is considered to be a likely window for synaptic plasticity

# Hippocampo-cortical coupling mediates memory consolidation during sleep

Nicolas Maingret<sup>1-4</sup>, Gabrielle Girardeau<sup>1-6</sup>, Ralitsa Todorova<sup>1-4,6</sup>, Marie Goutierre<sup>1-4</sup> & Michaël Zugaro<sup>1-4</sup>

Memory consolidation is thought to involve a hippocampo-cortical dialog during sleep to stabilize labile memory traces for long-term storage. However, direct evidence supporting this hypothesis is lacking. We dynamically manipulated the temporal coordination between the two structures during sleep following training on a spatial memory task specifically designed to trigger encoding, but not memory consolidation. Reinforcing the endogenous coordination between hippocampal sharp wave-ripples, cortical delta waves and spindles by timed electrical stimulation resulted in a reorganization of prefrontal cortical networks, along with subsequent increased prefrontal responsivity to the task and high recall performance on the next day, contrary to control rats, which performed at chance levels. Our results provide, to the best of our knowledge, the first direct evidence for a causal role of a hippocampo-cortical dialog during sleep in memory consolidation, and indicate that the underlying mechanism involves a fine-tuned coordination between sharp wave-ripples, delta waves and spindles.

The 'two-stage' theory of memory posits that memory consolidation involves a dialog during sleep between the hippocampus, where traces are initially formed, and the neocortex, where they are stored for long-term retention<sup>1,2</sup>. Candidate target neocortical areas include the medial prefrontal cortex (mPFC), which receives monosynaptic input from the hippocampus<sup>3</sup>. Over the course of days, the mPFC becomes progressively involved in spatial memory recall, concomitantly with a gradual hippocampal disengagement<sup>4,5</sup>. Consistent with the hypothesized dialog during sleep, task-related neural activity patterns are replayed during sleep, both in the hippocampus<sup>6,7</sup> and mPFC<sup>8,9</sup>. Coordination between the two structures could involve various oscillations that are known to have a causal role in memory consolidation. These include hippocampal sharp wave-ripples (SPW-Rs)<sup>10,11</sup> (150–200 Hz), cortical slow oscillations<sup>12,13</sup> and delta waves<sup>14</sup> (0.1–4 Hz), and thalamo-cortical spindles<sup>15</sup> (10–20 Hz), which are often observed in temporal proximity<sup>16–20</sup>. However, the causal role of a hippocampo-cortical dialog in memory consolidation has remained speculative.

To provide direct evidence for this hypothesis, we first characterized the endogenous temporal coordination between brain oscillations in the hippocampus and mPFC during slow-wave sleep (SWS). The observed coupling selectively increased following training on a task leading to memory consolidation, but not following time-limited training on the same task that did not result in memory consolidation. We then boosted this coupling during sleep following time-limited training by applying SPW-R-triggered stimulation to the neocortex, which induced propagating delta waves and spindles. This resulted in the reorganization of activity profiles in selected mPFC neurons, as well as a subsequent increase in prefrontal responsivity to the task and high recall performance on the next day, in contrast with control rats, which performed at chance levels.

## RESULTS

### Hippocampo-cortical oscillatory coupling

The hippocampal network is most active during SPW-Rs<sup>2</sup>. We therefore examined the temporal correlation between SPW-Rs in the hippocampus and cortical delta waves and spindles in the mPFC during unperturbed SWS in rats. Delta waves reflect the down states of the slow oscillation<sup>21,22</sup>, when cortical neurons stop firing (Fig. 1a). Consistent with previous reports<sup>16–18</sup>, delta waves were prevalent in close temporal proximity to hippocampal SPW-Rs, with probability peaking at ~130 ms after SPW-Rs (Fig. 1b and Supplementary Fig. 1a), indicating that delta waves generally followed SPW-Rs. A lower and broader peak ~140 ms before SPW-Rs further indicated that delta waves were, in turn, often followed by SPW-Rs, although this pattern was more temporally diffuse. In most cases, spindles closely followed a delta wave<sup>18,23</sup> (Supplementary Fig. 1b). Consistently, delta-spindle sequences were most probable ~140 ms after SPW-Rs (Fig. 1b). Thus, we hypothesized that the fine temporal relation between SPW-Rs and delta-spindle sequences is instrumental for communication between the hippocampus and neocortex.

### Consolidation-associated increase in oscillatory coupling

A straightforward consequence of our hypothesis is that this coupling should increase when learning leads to memory consolidation. We therefore measured the incidence of coupled SPW-Rs and delta-spindle sequences following training on a hippocampus-dependent memory task<sup>24</sup> (Fig. 1c). In the encoding phase, rats were exposed to two identical objects that were located in adjacent corners of a rectangular box for either 3 min (time-limited training) or 20 min (complete training). In the recall phase on the following day, one of the objects was moved to a different corner before the rats were allowed to visit the rectangular box. As previously reported<sup>25</sup>, only complete training yielded memory

<sup>1</sup>Collège de France, Center for Interdisciplinary Research in Biology (CIRB), Paris, France. <sup>2</sup>CNRS UMR 7241, Paris, France. <sup>3</sup>INSERM U1050, Paris, France.

<sup>4</sup>PSL Research University, Paris, France. <sup>5</sup>Present address: Neuroscience Institute, New York University Medical Center, New York, New York, USA. <sup>6</sup>These authors contributed equally to this work. Correspondence should be addressed to M.Z. (michael.zugaro@college-de-france.fr).

Received 18 December 2015; accepted 14 April 2016; published online 16 May 2016; doi:10.1038/nn.4304

**Figure 1** Increased hippocampo-cortical oscillatory coupling correlates with memory consolidation. (a) Example traces of LFPs recorded in the mPFC (top trace, low-pass filtered) and hippocampus (center trace, low-pass filtered; bottom trace, filtered in the ripple band) during a typical sleep session. Raster plots show action potentials (colored vertical ticks) emitted by individual prefrontal units. SPW-Rs (blue traces and asterisks), delta waves (brown traces and asterisk) and spindles (red traces and asterisk) are highlighted for clarity. Note the mPFC neuronal silence during delta waves (down states, gray shading).

(b) Temporal cross-correlation between SPW-Rs and delta waves (top) or delta-spindle sequences (bottom) during SWS preceding a behavioral task (pre-sleep,  $n = 7$  animals). Note the temporal proximity between these patterns.

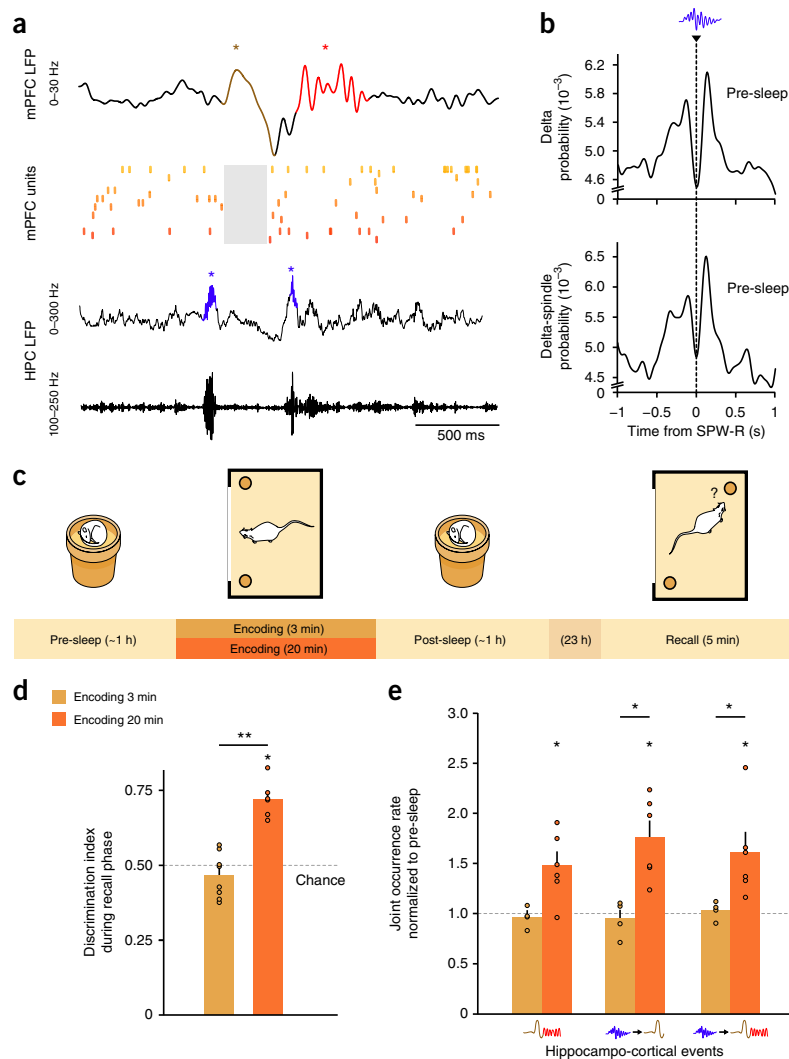
(c) The rats were allowed to explore the arena and encode the locations of the two objects for either 3 or 20 min. Pre- and post-encoding sleep recordings were carried out in both conditions.

(d) Discrimination indices during the recall phase, computed during the first 2 min of exploration. The rats discriminated between the stable and displaced objects only after the 20-min encoding phase (3 versus 20 min encoding, Wilcoxon rank-sum test,  $n = 8$ ,  $n = 6$ ,  $Z = 3.00$ ,  $**P = 0.002$ ; 3 min versus chance, Wilcoxon signed-rank test,  $n = 8$ ,  $Z = 1.40$ ,  $P = 0.161$ ; 20 min versus chance, Wilcoxon signed-rank test,  $n = 6$ ,  $Z = 2.20$ ,  $*P = 0.028$ ).

(e) Incidence of hippocampo-cortical events during SWS following either 3- (ochre) or 20-min (orange) encoding (left, delta spindle; center: SPW-R-delta; right, SPW-R-delta spindle), normalized to corresponding pre-sleep epochs. Note the increase in hippocampo-cortical event rate following the 20-min, but not 3-min, exposure to the objects. Delta-spindle incidence, 3 min versus 20 min encoding, Wilcoxon rank-sum test,  $n = 4$ ,  $n = 6$ ,  $Z = 1.81$ ,  $P = 0.067$ ; 3 min versus chance, Wilcoxon signed-rank test,  $n = 4$ ,  $Z = 0.73$ ,  $P = 0.465$ ; 20 min versus chance, Wilcoxon signed-rank test,  $n = 6$ ,  $Z = 1.99$ ,  $*P = 0.046$ .

SPW-R-delta incidence, 3 min versus 20 min encoding, Wilcoxon rank-sum test,  $n = 4$ ,  $n = 6$ ,  $Z = 0.36$ ,  $P = 0.715$ ; 20 min versus chance, Wilcoxon signed-rank test,  $n = 6$ ,  $Z = 2.20$ ,  $*P = 0.028$ . SPW-R-delta-spindle incidence, 3 min versus 20 min encoding, Wilcoxon rank-sum test,  $n = 4$ ,  $n = 6$ ,  $Z = 2.45$ ,  $*P = 0.014$ ; 3 min versus chance, Wilcoxon signed-rank test,  $n = 4$ ,  $Z = 0.73$ ,  $P = 0.465$ ; 20 min versus chance, Wilcoxon signed-rank test,  $n = 6$ ,  $Z = 2.20$ ,  $*P = 0.028$ .

Error bars represent s.e.m.



consolidation 24 h later, as measured by preferential exploration of the displaced object (discrimination indices: time-limited training,  $0.45 \pm 0.04$ ; complete training,  $0.72 \pm 0.03$ ; **Fig. 1d** and **Supplementary Table 1**). Consistent with our prediction, enhanced hippocampo-cortical coupling co-occurred with memory consolidation, as joint occurrence of hippocampal and cortical rhythms selectively increased after complete, but not time-limited, training (**Fig. 1e**).

### Causal role of the hippocampo-cortical dialog

To establish a causal link between increased hippocampo-cortical coupling and memory consolidation, we designed a closed-loop stimulation protocol to dynamically and selectively enhance the temporal coupling between SPW-Rs and delta spindles during SWS. SPW-Rs were detected online by band-pass filtering (100–250 Hz) and thresholding the hippocampal local field potential (LFP)<sup>10</sup>. Threshold

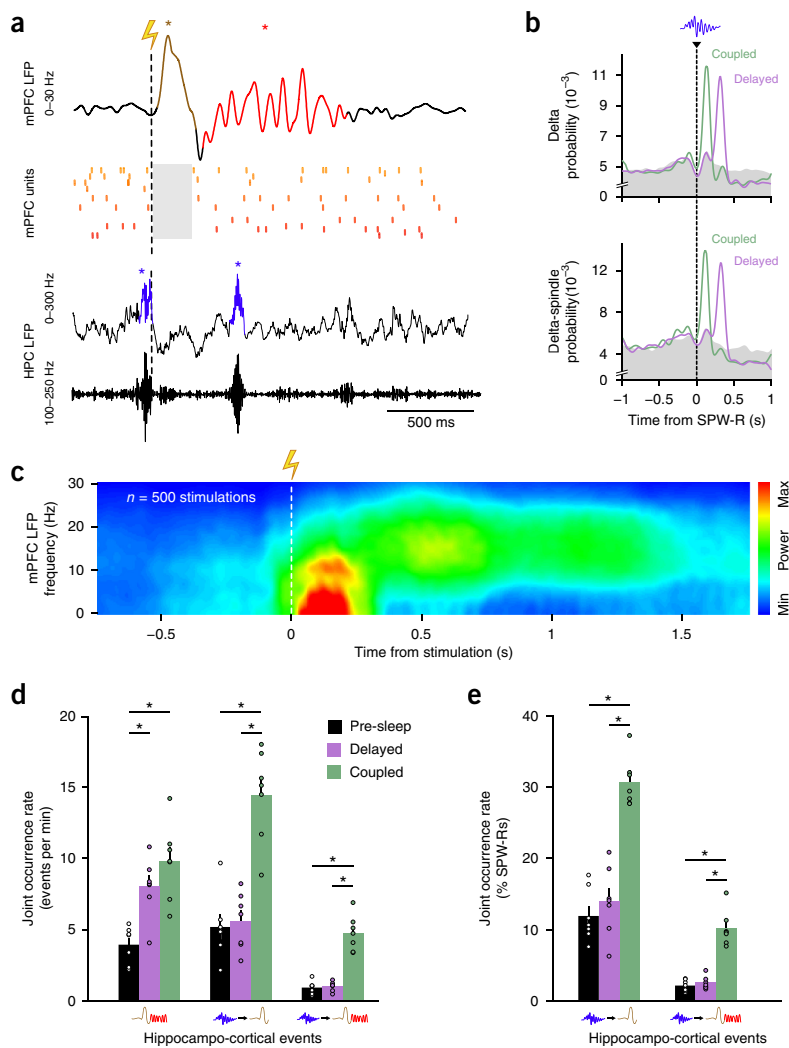
crossing automatically triggered brief (0.1 ms, 20 V) single-pulse stimulation of the neocortex, evoking propagating delta waves followed by spindles<sup>26</sup>. To avoid hyper-synchronous recruitment of the mPFC network by direct current injection and to ensure that delta waves and spindles would be elicited at the optimal delay, emulating endogenous events in the mPFC, we targeted the stimulation to the deep layers of the motor cortex. Delta waves would subsequently propagate across the cortical mantle<sup>26</sup>, including the mPFC. This protocol resulted in a dynamic, temporally specific reinforcement of the endogenous coupling between SPW-Rs and delta spindles (**Fig. 2a–c**).

To test the effect of increased coupling between SPW-Rs and delta spindles on memory consolidation, we trained rats ( $n = 9$ ) on the time-limited (3 min) version of the task. Our goal was to potentiate the consolidation of the weak memory traces by reinforcing the hippocampo-cortical oscillatory interactions during SWS following

**Figure 2** SPW-R-triggered stimulation of neocortical deep layers enhances the temporal coupling between hippocampal and cortical events. **(a)** Example SPW-R-triggered stimulation of neocortical deep layers (lightning icon and vertical dotted line), which induced a delta wave followed by a spindle in the mPFC, similar to the endogenous pattern observed in **Figure 1a**.

**(b)** Data presented as in **Figure 1b**, but during SWS periods when stimulation was triggered following SPW-R detection (green curves) or following a brief (160–240 ms) pseudo-random delay (purple curves). Pre-sleep values from **Figure 1b** are shown in gray ( $n = 7$  animals).

**(c)** Stimulation-triggered average spectrogram of mPFC LFPs for a coupled stimulation session in one rat. Note the marked increase in delta power (0–6 Hz), followed by spindle activity (10–20 Hz). **(d)** Incidence of hippocampocortical events (left, delta spindle; center, SPW-R-delta; right, SPW-R-delta spindle) during pre-sleep (black) and stimulation periods (purple, delayed stimulation; green, coupled stimulation). Delta-spindle incidence, Friedman test,  $\chi^2 = 10.57$ ,  $n = 7$ ,  $d.f. = 2$ ,  $P = 0.005$ ; Wilcoxon matched pairs test,  $n = 7$ , pre-sleep versus coupled:  $Z = 2.36$ ,  $*P = 0.018$ ; pre-sleep versus delayed:  $Z = 2.36$ ,  $*P = 0.018$ ; coupled versus delayed:  $Z = 1.18$ ,  $P = 0.237$ . SPW-R-delta incidence, Friedman test,  $\chi^2 = 10.57$ ,  $n = 7$ ,  $d.f. = 2$ ,  $P = 0.005$ ; Wilcoxon matched pairs test,  $n = 7$ , pre-sleep versus coupled:  $Z = 2.36$ ,  $*P = 0.018$ ; pre-sleep versus delayed:  $Z = 0.68$ ,  $P = 0.499$ ; coupled versus delayed:  $Z = 2.36$ ,  $*P = 0.018$ . SPW-R-delta-spindle incidence, Friedman test,  $\chi^2 = 11.14$ ,  $n = 7$ ,  $d.f. = 2$ ,  $P = 0.004$ ; Wilcoxon matched pairs test,  $n = 7$ , pre-sleep versus coupled:  $Z = 2.36$ ,  $*P = 0.018$ ; pre-sleep versus delayed:  $Z = 1.69$ ,  $P = 0.091$ ; coupled versus delayed:  $Z = 2.36$ ,  $*P = 0.018$ . **(e)** Data presented as in **d**, but expressed as a proportion of SPW-Rs. SPW-R-delta percentage, Friedman test,  $\chi^2 = 11.14$ ,  $n = 7$ ,  $d.f. = 2$ ,  $P = 0.004$ ; Wilcoxon matched pairs test,  $n = 7$ , pre-sleep versus coupled:  $Z = 2.36$ ,  $*P = 0.018$ ; pre-sleep versus delayed:  $Z = 1.86$ ,  $P = 0.063$ ; coupled versus delayed:  $Z = 2.36$ ,  $*P = 0.018$ . SPW-R-delta spindle percentage, Friedman test,  $\chi^2 = 11.14$ ,  $n = 7$ ,  $d.f. = 2$ ,  $P = 0.004$ ; Wilcoxon matched pairs test,  $n = 7$ , pre-sleep versus coupled:  $Z = 2.36$ ,  $*P = 0.018$ ; pre-sleep versus delayed:  $Z = 1.69$ ,  $P = 0.091$ ; coupled versus delayed:  $Z = 2.36$ ,  $*P = 0.018$ . Error bars represent s.e.m.



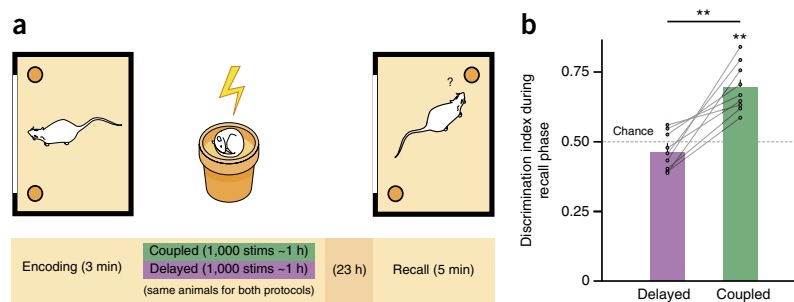
encoding. In the coupled stimulation condition, stimulations ( $n = 1,000$ ) were triggered following SPW-R detection to reinforce the coordination between SPW-Rs and delta spindles. In the delayed stimulation condition, the stimulations ( $n = 1,000$ ) were delayed by a random interval (160–240 ms) to probe the functional specificity of a fine-tuned temporal sequence between hippocampal and neocortical events. The same animals were used in both conditions: each rat performed the task twice (using different object pairs), once for each stimulation protocol (coupled and delayed), in a pseudo-randomized order. In both cases, the period of stimulation corresponded to the first ~4,000 s of SWS following the encoding phase, when most hippocampal replay events were expected to occur<sup>27</sup>.

Stimulations reliably induced delta waves (stimulation efficacy: coupled,  $66.5 \pm 3.3\%$ ; delayed,  $65.2 \pm 4.8\%$ ) and spindles (stimulation efficacy: coupled,  $39.8 \pm 4.0\%$ ; delayed,  $41.0 \pm 4.2\%$ ). Notably, stimulation efficacy was identical in the two stimulation protocols (**Supplementary Fig. 2a**). As a result, although the incidence of SPW-Rs

was not affected by the stimulation (**Supplementary Fig. 2b**), the overall occurrence rates of both delta waves and spindles were higher during stimulation periods than during baseline sleep, but were identical in the two stimulation protocols (**Supplementary Fig. 2b**). Moreover, delta waves and spindles had unaltered peak power across conditions (**Supplementary Fig. 2c,d**). Induced delta waves were associated with a near-complete cessation of mPFC spiking activity (down state; **Fig. 2a** and **Supplementary Fig. 2e**) and did not differentially affect hippocampal firing rates (**Supplementary Fig. 2f**). Stimulations did not directly drive spiking activity in the mPFC (**Supplementary Fig. 3**), nor did the two stimulation conditions differentially alter the global sleep architecture (**Supplementary Fig. 4**).

As expected, coupled stimulations strongly enhanced the temporal correlation between hippocampal and cortical oscillations (**Fig. 2b,c** and Online Methods). Delta-spindle sequences were elicited ~120 ms after SPW-Rs, emulating endogenous patterns observed in baseline sleep, but the incidence of SPW-R-delta-spindle sequences was

**Figure 3** Enhancing the fine-tuned coupling of hippocampal SPW-Rs and cortical delta waves and spindles boosts next day performance in a spatial memory task. **(a)** Rats ( $n = 9$ ) were exposed for 3 min to two identical objects located in two adjacent corners of a familiar arena (encoding phase) and then underwent SPW-R-triggered cortical stimulation ( $n = 1,000$ ) during SWS following the task (~1 h). Each animal performed the task twice (with different object pairs), in pseudo-random order. In the coupled condition, stimulation was delivered following SPW-R detection. In the delayed condition, stimulation occurred after a random delay (160–240 ms) following SPW-R detection. Twenty-four hours after the encoding phase, one of the objects was displaced to the opposite corner, and the animals were allowed to explore the arena for 5 min (recall phase). Memory recall was reflected in a preferential exploration of the displaced object. Note that in the absence of stimulation following the encoding phase, non-implanted control animals performed at chance level the following day ( $n = 8$ ; **Fig. 1d**). **(b)** Discrimination index for the displaced object during the recall phase, computed during the first 2 min of exploration. Memory recall was observed only following coupled stimulation (coupled versus delayed, Wilcoxon matched pairs test,  $n = 9$ ,  $Z = 2.67$ ,  $**P = 0.008$ ; coupled versus chance, Wilcoxon signed-rank test,  $n = 9$ ,  $Z = 2.67$ ,  $**P = 0.008$ ; delayed versus chance, Wilcoxon signed-rank test,  $n = 9$ ,  $Z = 1.48$ ,  $P = 0.139$ ). Error bars represent s.e.m.



increased fivefold (**Fig. 2d**). The proportion of SPW-Rs followed by cortical patterns increased by a similar magnitude (**Fig. 2e**). In contrast, delayed stimulation evoked cortical delta waves at latencies of ~320 ms following hippocampal SPW-Rs (**Fig. 2b**), far exceeding the timing of endogenous SPW-R-delta pairs (~130 ms). As a result, joint hippocampo-cortical patterns were unchanged compared with baseline, both in incidence (**Fig. 2d**) and in proportion of SPW-Rs (**Fig. 2e**). Notably, the proportion of induced delta waves followed by SPW-Rs in the two conditions was unchanged compared with endogenous events (**Supplementary Fig. 5**).

How did this selective enhancement of hippocampo-cortical coupling during sleep affect memory consolidation? In the absence of stimulation, performance was not significantly different from chance, that is, the animals spent as much time exploring the stable object as the displaced object (**Fig. 1d**). However, following coupled stimulation, the rats preferentially explored the displaced object (discrimination index,  $0.69 \pm 0.03$ ; **Fig. 3** and **Supplementary Table 1**), indicating that timed enhancement of the hippocampo-cortical dialog resulted in successful consolidation of the weak memory traces. This bias persisted after 3 or 5 min of exploration (**Supplementary Fig. 6**). Conversely, delayed stimulations did not improve performance above chance level (discrimination index,  $0.46 \pm 0.04$ ; **Fig. 3** and **Supplementary Table 1**), indicating that fine-tuned temporal coordination between the two structures is required to promote memory consolidation, and ruling out the possibility that the improved performance following coupled stimulation could be accounted for by a mere increase in delta and spindle rates alone. This was further supported by the complementary finding that randomly timed stimulation, unrelated to (that is, uniformly distributed relative to) SPW-R times, also resulted in subsequent chance performance (random stimulation group, discrimination index,  $0.48 \pm 0.03$ ; **Supplementary Fig. 7** and **Supplementary Table 1**).

### Reorganization of the mPFC network

Systems consolidation has been hypothesized to involve reorganization of functional cortical networks<sup>28</sup>. We carried out large-scale unit recordings in stimulated rats and compared spatio-temporal spiking patterns of mPFC pyramidal neurons following coupled versus delayed induced delta waves. First, to examine potential changes in the sequential spread of activity in local cortical networks, we measured cell-specific activation latencies following up-state transitions<sup>29</sup>, when cortical activity resumes following silencing during the delta

wave. Because latencies are independent of single-cell or global properties, such as excitability or traveling wave direction, and instead appear to reflect local functional connectivity<sup>29</sup>, changes in latencies would reflect non-trivial network alterations that are possibly related to consolidation processes. Thus, for each cell, we computed the difference in latency following induced versus endogenous delta waves. Comparison of coupled and delayed stimulation revealed that the latencies of mPFC neurons changed following SPW-R-coupled, but not delayed, delta waves (**Fig. 4a**), suggesting that specific reorganization processes result from hippocampo-cortical interactions. To further investigate selective reshaping of network activity, we then assessed changes in spike train profiles after up state onsets, reflected in the peri-event time histograms (PETHs) of mPFC pyramidal neurons. PETHs were computed for each neuron (**Fig. 4b,c**) and compared between coupled and delayed stimulation using a similarity index (uniqueness)<sup>29</sup>. PETHs remained unchanged following delayed stimulation, indicating that mere stimulation did not alter cell-specific features of mPFC spike trains. However, induced delta waves, when coupled to SPW-Rs, gave way to two clearly distinct responses, including stable and varying PETHs (**Fig. 4b,c**). This suggests that a specific subpopulation of mPFC cells selectively changed their activity profiles following induced hippocampo-cortical coupling. This was further supported by the finding that, in contrast with the rest of the population, these cells changed the order in which they activated following SPW-R-coupled delta waves (**Fig. 4c**). Finally, to test whether activity changes during sleep were subsequently reflected during recall, we computed an object responsivity index for each mPFC cell and compared the distributions of responsivity indices for each object following coupled versus delayed stimulation sleep sessions. Although mPFC cells did not respond to either object following delayed stimulation sessions, responsivity to the displaced object selectively increased following coupled stimulation sessions, paralleling the improvement in memory recall (**Fig. 4d** and **Supplementary Fig. 8**).

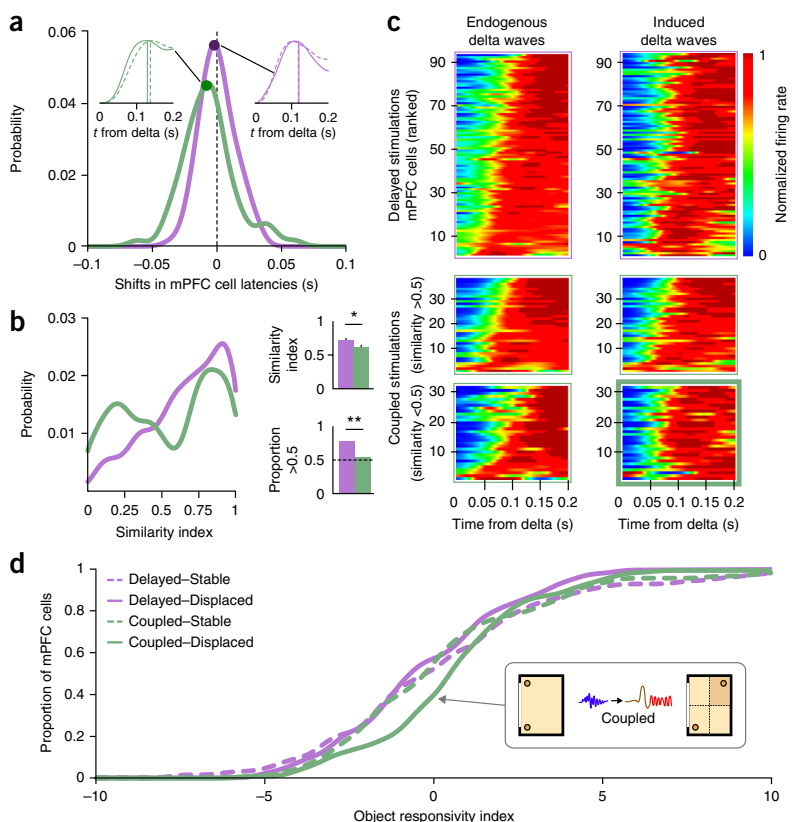
### DISCUSSION

Dynamically enhancing the coupling between hippocampal SPW-Rs and cortical delta waves and spindles during SWS resulted in the consolidation of a labile memory trace. Furthermore, this coupling required very fine temporal precision, as introducing a random delay as brief as 200 ms between hippocampal and cortical events was sufficient to cancel the induction of memory consolidation. Our results

**Figure 4** Changes in spatio-temporal spiking profiles of mPFC neurons parallel memory consolidation and recall improvements.

(a) Distribution of shifts in mPFC cell latencies in stimulation-induced delta waves relative to endogenous, non-SPW-R-coupled delta waves in the coupled (green) and delayed stimulation (purple) sessions. The latencies shifted to more negative values in the coupled condition, indicating changes in the spread of activity in local cortical networks (coupled versus delayed, Wilcoxon rank-sum test,  $n = 70$ ,  $n = 93$ ,  $Z = 3.00$ ,  $P = 0.003$ ; coupled versus zero, Wilcoxon matched pairs test,  $n = 70$ ,  $Z = 2.85$ ,  $P = 0.004$ ; delayed versus zero, Wilcoxon matched pairs test,  $n = 93$ ,  $Z = 0.20$ ,  $P = 0.845$ ). Insets show the PETHs of two typical mPFC cells and the location of their latency differences on the distribution curves.

Continuous curves and lines indicate induced up states. Dashed curves and lines indicate endogenous up states. Vertical lines represent mean latencies. (b) Distribution of PETH similarity indices (Online Methods) in both stimulation conditions. Bar plots on the right show median similarity indices (coupled versus delayed, Wilcoxon rank-sum test,  $n = 70$ ,  $n = 93$ ,  $Z = 2.12$ ,  $*P = 0.034$ ) and proportion of cells with a similarity index  $> 0.5$  (two-proportion Z-test,  $Z = 3.12$ ,  $**P = 0.001$ ). The PETH similarity index distribution was bimodal in the coupled condition (Hartigan's dip test,  $\text{dip} = 0.025$ ,  $P = 0.0002$ ), but not in the delayed condition (Hartigan's dip test,  $\text{dip} = 0.006$ ,  $P = 0.999$ ), indicating that a specific subpopulation of mPFC cells selectively changed their activity profiles following induced SPW-R-delta sequences. (c) Up state-triggered PETHs for all cells following endogenous (left) and induced (right) delta waves (top, delayed condition; bottom, coupled condition). Individual PETHs are ordered according to their mean latency following endogenous events. Top, delayed condition; note the consistency of cell organization in endogenous and induced events (Spearman's rank correlation,  $\rho = 0.668$ ,  $P < 0.001$ ). Bottom, PETHs are shown separately for mPFC cells in the two subpopulations forming the bimodal distribution in (b) (green). Note the reorganization in the subpopulation with low ( $< 0.5$ ) (Spearman's rank correlation,  $\rho = 0.001$ ,  $P = 0.995$ ), but not high ( $> 0.5$ ), PETH similarity (Spearman's rank correlation,  $\rho = 0.854$ ,  $P < 0.001$ ). (d) Cumulative distributions of mPFC responsivity indices for each object during the recall phase of the task following both stimulation protocols. Medial prefrontal cortical cells selectively became responsive to the displaced object following coupled stimulations (displaced object: coupled versus delayed, Wilcoxon rank-sum test,  $n = 99$ ,  $n = 61$ ,  $Z = 2.41$ ,  $P = 0.016$ ; coupled versus zero, Wilcoxon signed-rank test,  $n = 99$ ,  $Z = 2.32$ ,  $P = 0.020$ ; delayed versus zero, Wilcoxon signed-rank test,  $n = 61$ ,  $Z = 1.21$ ,  $P = 0.226$ ; stable object: coupled versus delayed, Wilcoxon rank-sum test,  $n = 99$ ,  $n = 61$ ,  $Z = 0.21$ ,  $P = 0.838$ ; coupled versus zero, Wilcoxon signed-rank test,  $n = 99$ ,  $Z = 0.45$ ,  $P = 0.655$ ; delayed versus zero, Wilcoxon signed-rank test,  $n = 61$ ,  $Z = 0.31$ ,  $P = 0.755$ ). Error bars represent s.e.m.



show that long-term stabilization of memory traces is promoted by timed functional interactions between the hippocampus and cortex during offline states.

The underlying mechanism is a fine-tuned coupling between hippocampal SPW-Rs and cortical delta waves and spindles, orchestrating local network reorganizations in selected subpopulations of mPFC neurons<sup>2,30</sup>. Given that delta waves and spindles are propagating patterns that affect the entire neocortex<sup>26</sup>, other cortical areas, including rhinal cortices, may undergo similar reorganization processes.

Following SPW-R-associated replay<sup>6,7,27</sup>, cell assemblies would be reactivated in the mPFC<sup>9</sup>. The following cortical delta wave would then isolate target synapses from competing inputs, allowing selective reorganization of the network during the ensuing up state transition and strengthening by subsequent spindles<sup>31</sup>. Depending on learning requirements, cortical patterns could in turn regulate hippocampal SPW-Rs<sup>32</sup>.

## METHODS

Methods and any associated references are available in the [online version of the paper](#).

Note: Any Supplementary Information and Source Data files are available in the [online version of the paper](#).

## ACKNOWLEDGMENTS

We thank C. Driev, V. Obereto, H.-Y. Gao, A. Cei, S. Sara, S.I. Wiener and K. Benchenane for advice and comments on the manuscript, and S. Dautremer, M.A. Thomas and Y. Dupraz for technical support. This work was supported by the French Ministry of Research (N.M.), a grant from the Fondation pour la Recherche Médicale (grant no. FDT20150532568) (N.M.), and a joint grant from École des Neurosciences de Paris Île-de-France and LabEx MemoLife (ANR-10-LABX-54 MEMO LIFE, ANR-10-IDEX-0001-02 PSL\*) (R.T.).

## AUTHOR CONTRIBUTIONS

N.M., G.G. and M.Z. designed the study. N.M., G.G. and M.G. performed the experiments. N.M., R.T. and M.Z. designed the analyses. N.M. and R.T. performed the analyses. N.M. and M.Z. wrote the manuscript with input from all authors.

## COMPETING FINANCIAL INTERESTS

The authors declare no competing financial interests.

Reprints and permissions information is available online at <http://www.nature.com/reprints/index.html>.

## ARTICLES

1. Marr, D. Simple memory: a theory for archicortex. *Philos. Trans. R. Soc. Lond. B Biol. Sci.* **262**, 23–81 (1971).
2. Buzsáki, G. Two-stage model of memory trace formation: a role for “noisy” brain states. *Neuroscience* **31**, 551–570 (1989).
3. Ferino, F., Thierry, A.M. & Glowinski, J. Anatomical and electrophysiological evidence for a direct projection from Ammon’s horn to the medial prefrontal cortex in the rat. *Exp. Brain Res.* **65**, 421–426 (1987).
4. Maviel, T., Durkin, T.P., Menzaghi, F. & Bontempi, B. Sites of neocortical reorganization critical for remote spatial memory. *Science* **305**, 96–99 (2004).
5. Bontempi, B., Laurent-Demir, C., Destrade, C. & Jaffard, R. Time-dependent reorganization of brain circuitry underlying long-term memory storage. *Nature* **400**, 671–675 (1999).
6. Wilson, M.A. & McNaughton, B.L. Reactivation of hippocampal ensemble memories during sleep. *Science* **265**, 676–679 (1994).
7. Lee, A.K. & Wilson, M.A. Memory of sequential experience in the hippocampus during slow-wave sleep. *Neuron* **36**, 1183–1194 (2002).
8. Euston, D.R., Tatsuno, M. & McNaughton, B.L. Fast-forward playback of recent memory sequences in prefrontal cortex during sleep. *Science* **318**, 1147–1150 (2007).
9. Peyrache, A., Khamassi, M., Benchenane, K., Wiener, S.I. & Battaglia, F.P. Replay of rule-learning related neural patterns in the prefrontal cortex during sleep. *Nat. Neurosci.* **12**, 919–926 (2009).
10. Girardeau, G., Benchenane, K., Wiener, S.I., Buzsáki, G. & Zugaro, M.B. Selective suppression of hippocampal ripples impairs spatial memory. *Nat. Neurosci.* **12**, 1222–1223 (2009).
11. Ego-Stengel, V. & Wilson, M.A. Disruption of ripple-associated hippocampal activity during rest impairs spatial learning in the rat. *Hippocampus* **20**, 1–10 (2010).
12. Marshall, L., Helgadóttir, H., Mölle, M. & Born, J. Boosting slow oscillations during sleep potentiates memory. *Nature* **444**, 610–613 (2006).
13. Ngo, H.-V.V., Martinetz, T., Born, J. & Mölle, M. Auditory closed-loop stimulation of the sleep slow oscillation enhances memory. *Neuron* **78**, 545–553 (2013).
14. Johnson, L.A., Euston, D.R., Tatsuno, M. & McNaughton, B.L. Stored-trace reactivation in rat prefrontal cortex is correlated with down-to-up state fluctuation density. *J. Neurosci.* **30**, 2650–2661 (2010).
15. Mednick, S.C. *et al.* The critical role of sleep spindles in hippocampal-dependent memory: a pharmacology study. *J. Neurosci.* **33**, 4494–4504 (2013).
16. Sirota, A., Csicsvari, J., Buhl, D. & Buzsáki, G. Communication between neocortex and hippocampus during sleep in rodents. *Proc. Natl. Acad. Sci. USA* **100**, 2065–2069 (2003).
17. Battaglia, F.P., Sutherland, G.R. & McNaughton, B.L. Hippocampal sharp wave bursts coincide with neocortical “up-state” transitions. *Learn. Mem.* **11**, 697–704 (2004).
18. Peyrache, A., Battaglia, F.P. & Destexhe, A. Inhibition recruitment in prefrontal cortex during sleep spindles and gating of hippocampal inputs. *Proc. Natl. Acad. Sci. USA* **108**, 17207–17212 (2011).
19. Phillips, K.G. *et al.* Decoupling of sleep-dependent cortical and hippocampal interactions in a neurodevelopmental model of schizophrenia. *Neuron* **76**, 526–533 (2012).
20. Staresina, B.P. *et al.* Hierarchical nesting of slow oscillations, spindles and ripples in the human hippocampus during sleep. *Nat. Neurosci.* **18**, 1679–1686 (2015).
21. Steriade, M., Nuñez, A. & Amzica, F. A novel slow (<1 Hz) oscillation of neocortical neurons *in vivo*: depolarizing and hyperpolarizing components. *J. Neurosci.* **13**, 3252–3265 (1993).
22. Sirota, A. & Buzsáki, G. Interaction between neocortical and hippocampal networks via slow oscillations. *Thalamus Relat. Syst.* **3**, 245–259 (2005).
23. Amzica, F. & Steriade, M. Cellular substrates and laminar profile of sleep K-complex. *Neuroscience* **82**, 671–686 (1998).
24. Barker, G.R.I. & Warburton, E.C. When is the hippocampus involved in recognition memory? *J. Neurosci.* **31**, 10721–10731 (2011).
25. Ballarini, F., Moncada, D., Martínez, M.C., Alen, N. & Viola, H. Behavioral tagging is a general mechanism of long-term memory formation. *Proc. Natl. Acad. Sci. USA* **106**, 14599–14604 (2009).
26. Vyazovskiy, V.V., Faraguna, U., Cirelli, C. & Tononi, G. Triggering slow waves during NREM sleep in the rat by intracortical electrical stimulation: effects of sleep/wake history and background activity. *J. Neurophysiol.* **101**, 1921–1931 (2009).
27. Kudrimoti, H.S., Barnes, C.A. & McNaughton, B.L. Reactivation of hippocampal cell assemblies: effects of behavioral state, experience, and EEG dynamics. *J. Neurosci.* **19**, 4090–4101 (1999).
28. Frankland, P.W. & Bontempi, B. The organization of recent and remote memories. *Nat. Rev. Neurosci.* **6**, 119–130 (2005).
29. Luczak, A., Barthó, P., Marguet, S.L., Buzsáki, G. & Harris, K.D. Sequential structure of neocortical spontaneous activity *in vivo*. *Proc. Natl. Acad. Sci. USA* **104**, 347–352 (2007).
30. Womelsdorf, T. *et al.* Modulation of neuronal interactions through neuronal synchronization. *Science* **316**, 1609–1612 (2007).
31. Rosanova, M. & Ulrich, D. Pattern-specific associative long-term potentiation induced by a sleep spindle-related spike train. *J. Neurosci.* **25**, 9398–9405 (2005).
32. Girardeau, G., Cei, A. & Zugaro, M. Learning-induced plasticity regulates hippocampal sharp wave-ripple drive. *J. Neurosci.* **34**, 5176–5183 (2014).



## ONLINE METHODS

**Animals.** All experiments were carried out in accordance with institutional (CNRS Comité Opérationnel pour l'Éthique dans les Sciences de la Vie) and international (US National Institutes of Health guidelines) standards, legal regulations (Certificat no. B751756), and ethical requirements (Ethics Committee approval #2012-0048) regarding the use and care of animals.

A total of 23 male Long Evans rats (René Janvier; weight, 280–350 g) were maintained on a 12-h:12-h light-dark cycle (lights on at 07:00 a.m.). Training and experiments took place during the day. Rats were group-housed until 1 week before surgery.

**Surgery.** Electrophysiological signals were acquired using tetrodes (groups of four twisted 12- $\mu$ m tungsten wires, gold-plated to  $\sim$ 200 k $\Omega$ ). The rats ( $n = 15$ ) were deeply anesthetized (xylazine, 0.1 ml intramuscular; pentobarbital, 40 mg per kg of body weight, intraperitoneal; 0.1 ml pentobarbital supplemented every hour) and implanted with a custom-built microdrive allowing for the adjustment of up to 16 individual tetrodes. Rats were implanted with 6 ( $n = 3$  rats, **Fig. 1d,e**;  $n = 3$  rats, **Supplementary Fig. 7**) or 16 ( $n = 9$  rats, **Figs. 2 and 3**) tetrodes targeted at the prelimbic and infralimbic regions of the right mPFC (AP: +2.7 mm from bregma; ML: +1.5 mm, angled at 10° from the sagittal plane) and the CA1 subfield of the right hippocampus (AP: -3.5 to -5.5 mm; ML: +2.5 to +5 mm). For the animals that underwent stimulation, a custom-built bipolar electrode consisting of two stainless steel wires (total length, 1.5 mm; inter-wire interval, 0.5 mm; wire diameter, 70  $\mu$ m) was implanted in the contralateral neocortex (AP: +2 mm; ML: -2 mm; DV: -1.5 mm from the dura (motor area);  $n = 9$  rats for coupled and delayed stimulation,  $n = 3$  rats for random stimulation). Miniature stainless steel screws (reference and ground) were implanted above the cerebellum. During recovery from surgery (minimum 3 d), the rats received food and water *ad libitum*. The recording electrodes were then progressively lowered until they reached their targets and then adjusted every day to optimize yield and stability.

**Recording and stimulation.** All training and recording sessions took place in the same dimly lit room, enclosed by black curtains. Behavior was monitored using an overhead video camera. One red light-emitting diode was fixed on the front of the microdrive to track the position of the animal. For rest and sleep sessions, rats were secluded in a familiar flower pot in the center of the recording arena. All analyses were conducted offline. Brain signals were preamplified (unity-gain headstage, Noted Bt), amplified 500 $\times$  (Neuralynx L8), acquired and digitized with two synchronized Power1401 systems (CED). During stimulation periods, threshold crossing on the ripple band-filtered hippocampal signal automatically triggered a monophasic single-pulse (0.1 ms) stimulation of the deep layers of the motor cortex, delivered by a constant current stimulator (SD9 square pulse stimulator, Grass Technologies). This induced the initiation and propagation of a delta wave across neocortical areas<sup>26</sup>. For each animal, the optimal stimulation voltage was defined as the minimum voltage necessary to reliably induce propagating delta waves, and was determined before training (range: 17.5–22.5 V). In the test condition (coupled), stimulation was used to emulate the endogenous fine-tuned coordination between hippocampal and cortical rhythms, and were therefore triggered 20 ms after SPW-R detection. In the control condition (delayed), an additional random delay ranging from 160–240 ms was introduced between SPW-R detection and stimulation onset. In both coupled and delayed conditions, the number of stimulations was limited to one every 2 s to ensure that a stimulation would not be triggered before the end of the previous elicited spindle (see **Fig. 2c**), and the total number of stimulations was set to 1,000, yielding a stimulation period of  $\sim$ 4,000 s during which most replay events were expected to occur<sup>27</sup>.

**Behavioral protocol.** All experiments (behavior and sleep sessions) took place in a dimly lit area enclosed by dark curtains. A 70-cm  $\times$  50-cm arena with 50-cm-high black plastic walls (**Fig. 1c**) was used for the behavioral task. A white card (20  $\times$  30 cm) on one wall served as a visual reference cue. During the habituation phase, the rats were allowed to freely explore the empty arena for 20 min once a day for 3 consecutive days. The spatial object recognition task consisted of an encoding and a recall phase, separated by a  $\sim$ 24-h interval. Both phases took place at the same time of the day. During the encoding phase, two identical objects were placed in two adjacent corners. The rats were released in the center of the arena and allowed to explore for either 3 min (time-limited training) or 20 min

(complete training). Time-limited training was intended to foil recall of the spatial configuration of the objects on the next day<sup>25</sup> (**Fig. 1d**; if the rats expressed a preference for one of the two objects during the encoding phase, the trial was aborted, and the rats were tested again 48 h later with different objects). The rats were then placed in a flower pot for sleep sessions, which lasted until 1,000 stimulations had been delivered ( $\sim$ 4,000 s of SWS), then returned to their home cage. The recall phase took place the following day. One of the objects was displaced to the opposite corner and the animals were allowed to freely explore the arena for 5 min. The same rats ( $n = 9$ ) underwent coupled and delayed stimulation: they performed the task twice (with different objects), in a pseudo-random order, at an interval of at least two days. Rats used for the random stimulation protocol ( $n = 3$ ) and unimplanted rats used for the complete training protocol ( $n = 3$ ) also performed the task twice. Data collection and analysis were not performed blind to the conditions of the experiments.

The discrimination index was defined as the time spent exploring the displaced object divided by the total time of exploration of both objects. The rats were considered to be exploring an object whenever their head was oriented toward and located within 2 cm of the object. Exploration time was measured from video files, both automatically and manually by two independent experimenters. All three measures yielded equivalent results (Friedman test,  $\chi^2 = 1.56$ ,  $n = 9$ , d.f. = 2,  $P = 0.459$ ), and the data presented here were derived with the automatic detection algorithm.

**Data processing and spike sorting.** A red LED was used to track the instantaneous position of animals (recorded at 25 Hz, resampled at 39.0625 Hz). For off-line spike sorting, the wide-band signals were converted, digitally high-pass filtered (nonlinear median-based filter) and thresholded, and waveforms were extracted and projected to a PCA subspace using NDManager (L. Hazan and M.Z., <http://neurosuite.sourceforge.net>)<sup>33</sup>. Spike sorting used a semi-automatic cluster cutting procedure combining KlustaKwik (K.D. Harris, <http://klustakwik.sourceforge.net>) and Klusters (L. Hazan, <http://neurosuite.sourceforge.net>)<sup>33</sup>. Putative interneurons and pyramidal cells were discriminated based on spike width<sup>34</sup>. Neurophysiological and behavioral data were explored using NeuroScope (L. Hazan, <http://neurosuite.sourceforge.net>)<sup>33</sup>. LFPs were derived from wide-band signals by downsampling all channels to 1,250 Hz.

**Data analysis Statistics.** Data were analyzed using Matlab (Statistical Toolbox; FMatToolbox, M.Z., <http://fmattoolbox.sourceforge.net>). Spectrograms were constructed using Chronux (<http://chronux.org>). No statistical methods were used to pre-determine sample sizes, but our sample sizes are similar to those generally employed in the field. All statistical tests were non-parametric and two-tailed. In accordance with standard procedures, proportional data were transformed as  $P' = \arcsin(\sqrt{P})$ , before performing non-parametric (for example, Wilcoxon matched pairs or Friedman) tests.

**SPW-Rs, delta waves and spindles.** For offline SPW-R detection, the LFP recorded in CA1 pyramidal layer was band-pass filtered (150–250 Hz), squared, low-pass filtered (8.8 ms running average) and normalized, yielding a transformed signal  $R(t)$ . SPW-Rs were defined as events where  $R(t)$  remained above 2 for 30 ms to 100 ms, and peaked at  $>5$ .

To detect delta waves, the LFP recorded in the mPFC was filtered (0–6 Hz) and z-scored, yielding  $D(t)$ . We extracted sequences ( $t_{\text{beginning}}$ ,  $t_{\text{peak}}$ ,  $t_{\text{end}}$ ) of upward-downward-upward zero-crossings of  $D'(t)$ , corresponding to the putative beginning, peak and end of delta waves, respectively. Sequences lasting less than 150 ms or more than 500 ms were discarded. Delta waves corresponded to epochs where  $D(t_{\text{peak}}) > 2$ , or  $D(t_{\text{peak}}) > 1$  and  $D(t_{\text{end}}) < -1.5$ .

For spindle detection, the LFP recorded in the mPFC was band-pass filtered (9–17 Hz) and z-scored. The squared magnitude of its Hilbert transform was smoothed using a 100-ms Gaussian window, yielding  $S(t)$ . Spindles corresponded to epochs where  $S(t)$  remained above 2.5 for more than 0.5 s, and peaked at  $>5$ . Events separated by less than 0.4 s were merged, and combined events lasting more than 3 s were discarded.

Delta-spindle sequences were defined as epochs where spindle peaks occurred between 100 ms and 1.3 s following delta peaks. SPW-R–delta sequences corresponded to epochs where delta peaks occurred between 50 ms and 250 ms following ripple peaks. SPW-R–delta-spindle sequences corresponded to the conjunction of these events. Delta–SPW-R sequences corresponded to occurrences of ripple peaks between 50 ms and 400 ms following delta peaks.



Only sleep epochs preceding the encoding phase and lasting more than 1,200 s were used for these analyses.

**Sleep scoring.** Sleep stages (SWS/rapid eye movement) were determined by automatic K-means clustering of the theta/delta ratio extracted from the power spectrograms during the episodes where the animal was immobile (linear velocity  $< 3 \text{ cm s}^{-1}$  for at least 30 s, with brief movements  $< 0.5 \text{ s}$ ).

**Down states.** Down states were defined as delta-wave centered epochs lasting 100–300 ms containing a maximum of three spikes. Only sessions with  $n_{\text{mPFC neurons}} > 7$  (average number of mPFC cells = 19, range 7–31) were used for down state detection and subsequent cross-correlation with delta waves.

**Network activity during up-state transitions.** For each cell, the activation latency was measured as its mean spike time within 200 ms of up state onset<sup>29</sup>. To compare PETHs triggered by up state transitions following induced versus endogenous, non-ripple-coupled delta waves, we computed the similarity index (PETH uniqueness) for each neuron as described previously<sup>29</sup>. Briefly, for each pair of neurons  $i$  and  $j$ , we computed the Euclidean distance  $d_{ij}$  between the PETH of  $i$  in endogenous up states, and the PETH of  $j$  in induced up states. The similarity index of neuron  $i$  is the proportion of neurons  $j$  for which  $d_{ii} < d_{ij}$ . Thus, a neuron with a similarity index greater than 0.5 has PETH features remaining consistent across endogenous and induced up states that can differentiate it from more than half of the other neurons. Bimodality in similarity index distributions was assessed using Hartigan's dip test on smoothed bootstrapped ( $n = 10,000$ ) similarity indices<sup>35</sup>.

**Object responsivity.** The arena was divided into four quadrants, two of which contained the objects. Distributions of firing rates in the empty quadrants were first estimated for each cell. Briefly, a random number of non-overlapping epochs of random durations were selected, adding up to 50% of the total time spent in the empty quadrants. This constituted one 'sample' over which the firing rate was computed. The procedure was repeated 1,000 times, yielding an estimated

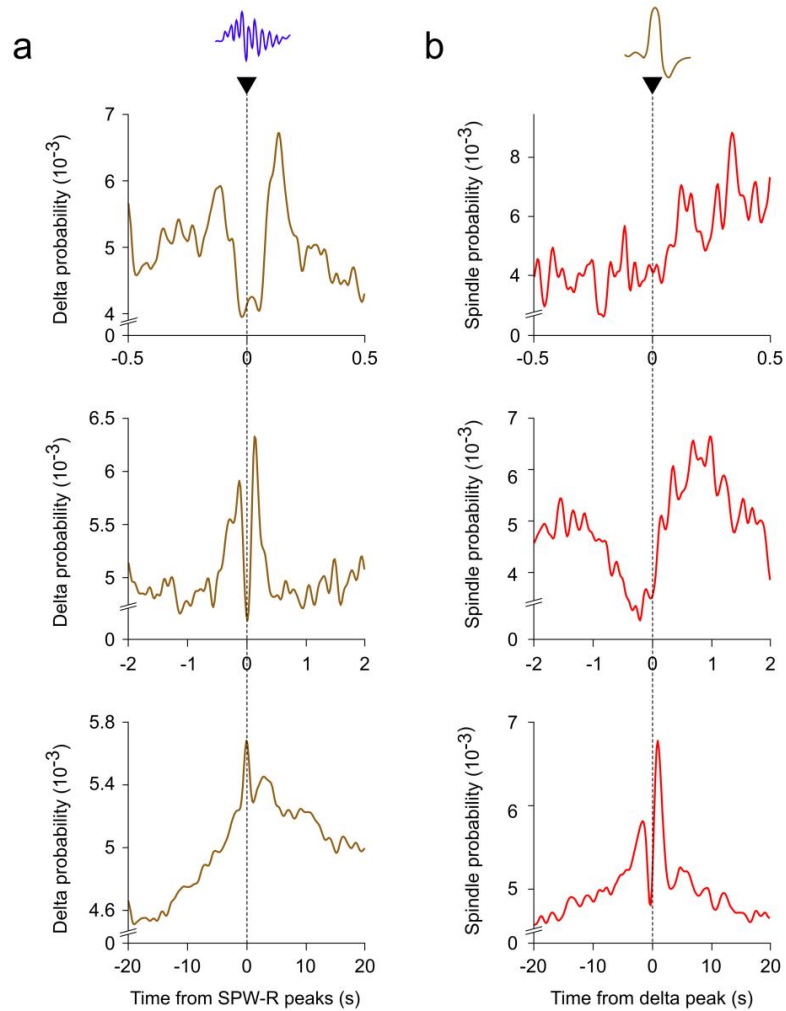
distribution  $F$  of firing rates in the empty quadrants. The responsivity index  $R$  to a given object was defined as the mean firing rate  $r$  over the corresponding quadrant,  $z$ -scored relative to  $F$ ; that is,  $R = (r - \mu)/\sigma$  where  $\mu$  and  $\sigma$  are the mean and s.d. of  $F$ . Thus, the object responsivity index  $R$  measured by how much, relative to its baseline variability, a cell increased its firing rate around the object. Because inevitable micro-movements of the independently movable electrodes precluded reliable tracking of single cells over successive days, comparisons between the encoding and recall phases were performed at the population level.

**Histology.** At the end of the experiments, electrolytic lesions were made at the tip of the electrodes to verify their precise location (CA1 pyramidal layer and deep layers of the prelimbic mPFC). Rats were deeply anesthetized with a lethal dose of pentobarbital, and intracardially perfused with saline (0.9%, wt/vol) followed by 400 ml of paraformaldehyde (10%, wt/vol). Brains were then sliced into coronal sections (40  $\mu\text{m}$ ) and stained with cresyl-violet.

**Data availability.** The data that support the findings of this study are available from the corresponding author upon request.

A **Supplementary Methods Checklist** is available.

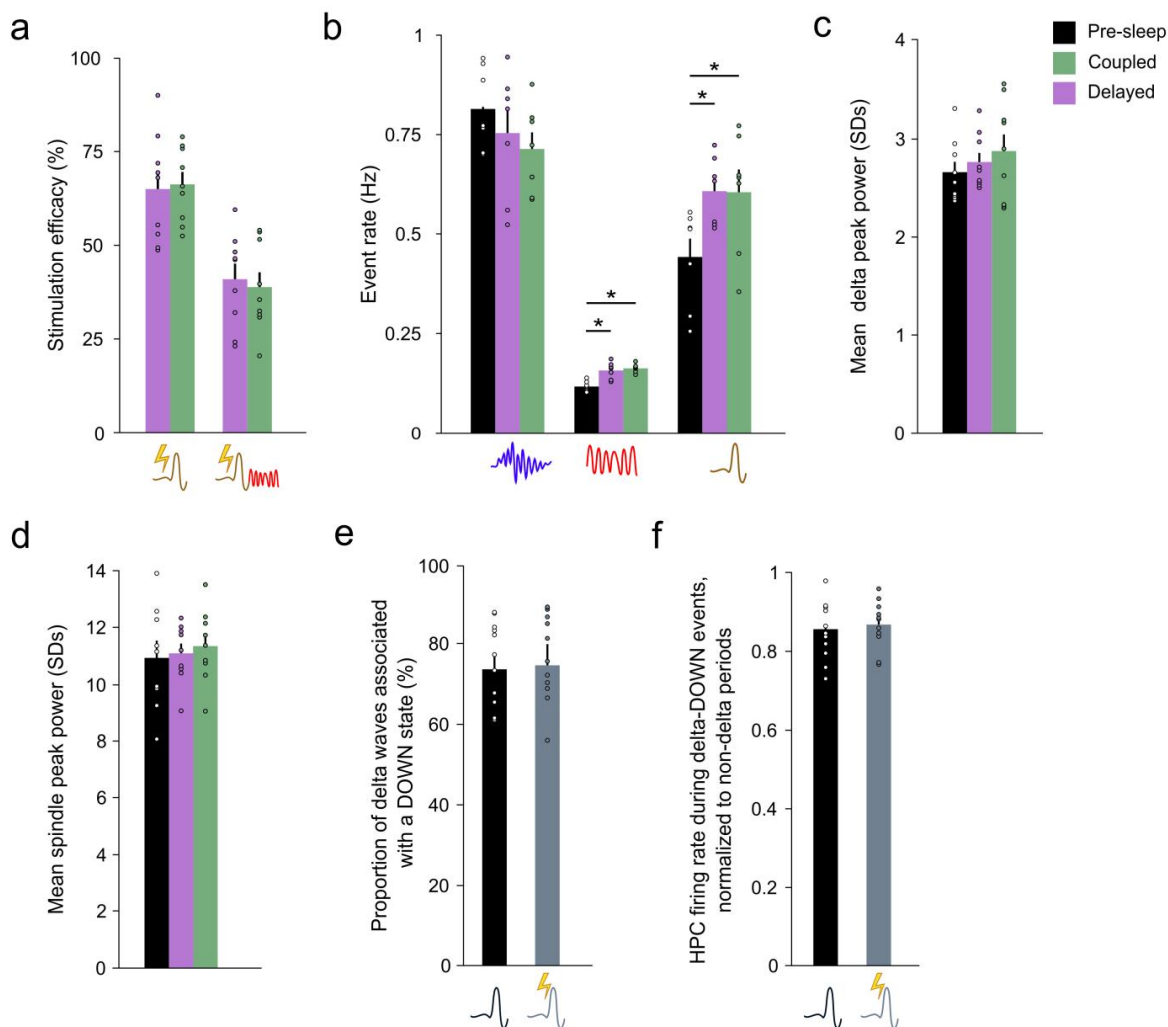
33. Hazan, L., Zugaro, M. & Buzsáki, G. Klusters, NeuroScope, NDManager: a free software suite for neurophysiological data processing and visualization. *J. Neurosci. Methods* **155**, 207–216 (2006).
34. Barthó, P. *et al.* Characterization of neocortical principal cells and interneurons by network interactions and extracellular features. *J. Neurophysiol.* **92**, 600–608 (2004).
35. Hartigan, J. & Hartigan, P. The dip test of unimodality. *Ann. Stat.* **13**, 70–84 (1985).



Supplementary Figure 1

**Hippocampo-cortical oscillatory interactions during unperturbed SWS.**

**a.** Temporal cross-correlation between SPW-Rs and delta waves at different timescales. The two peaks around SPW-R times indicate that SPW-Rs are both preceded and followed by delta waves. **b.** Temporal cross-correlation between delta waves and spindles. Note the increased spindle probability immediately following delta waves.

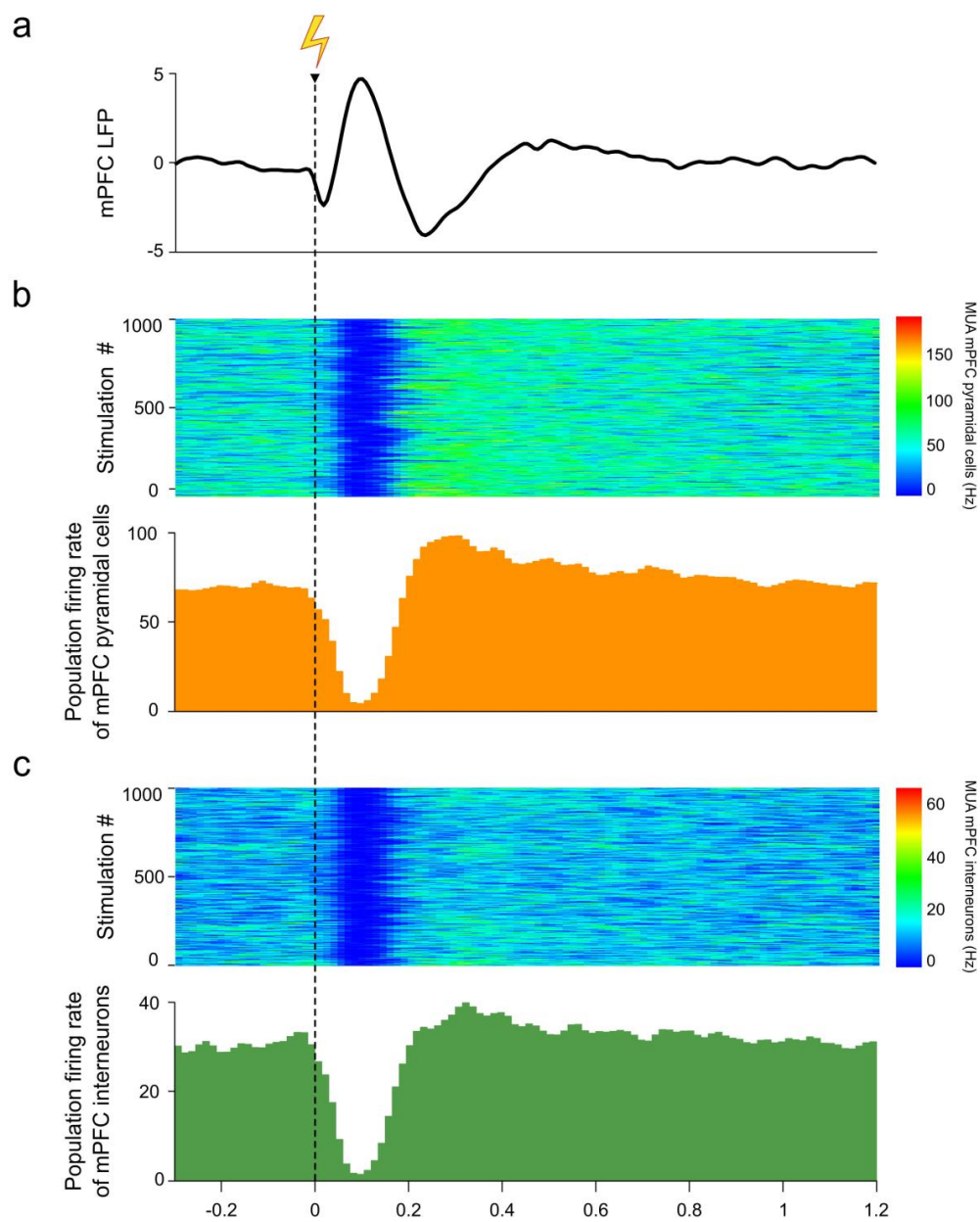


## Supplementary Figure 2

### Incidence of hippocampo-cortical rhythms is unchanged between coupled and delayed stimulation epochs.

**a.** A large fraction of the applied stimulations efficiently triggered delta waves (left) or delta-spindle sequences (right) in both delayed (purple bars) and coupled (green bars) conditions. Stimulation efficacy was identical across conditions (delta waves efficacy, coupled vs delayed, Wilcoxon matched pairs test,  $n = 9$ ,  $Z = 0.18$ ,  $P = 0.859$ ; delta-spindle efficacy, coupled vs delayed, Wilcoxon matched pairs test,  $n = 9$ ,  $Z = 0.06$ ,  $P = 0.953$ ). **b.** SPW-R, delta wave and spindle occurrence rates during Pre-sleep (black bars) and during stimulation epochs (purple and green bars). As expected, delta waves and spindles were more frequent during stimulation than Pre-sleep epochs, but their occurrence rates were identical between stimulation conditions. SPW-R incidence, Friedman test,  $\chi^2 = 2.57$ ,  $n = 7$ ,  $d.f. = 2$ ,  $P = 0.277$ . Spindle incidence, Friedman test,  $\chi^2 = 10.57$ ,  $n = 7$ ,  $d.f. = 2$ ,  $P = 0.005$ ; Wilcoxon matched pairs test,  $n = 7$ , Pre-sleep vs. coupled:  $Z = 2.36$ ,  $*P = 0.018$ ; Pre-sleep vs. delayed:  $Z = 2.36$ ,  $*P = 0.018$ ; coupled vs. delayed:  $Z = 0.17$ ,  $P = 0.866$ .

Delta incidence, Friedman test,  $\chi^2 = 10.57$ ,  $n = 7$ ,  $d.f. = 2$ ,  $P = 0.005$ ; Wilcoxon matched pairs test,  $n = 7$ , Pre-sleep vs. coupled:  $Z = 2.36$ ,  $*P = 0.018$ ; Pre-sleep vs. delayed:  $Z = 2.36$ ,  $*P = 0.018$ ; coupled vs. delayed:  $Z = 0.34$ ,  $P = 0.735$ . **c.** Delta power was similar between naturally occurring and induced events (black, Pre-sleep; green, coupled stimulation; purple, delayed stimulation) Friedman test,  $\chi^2 = 0.89$ ,  $n = 9$ ,  $d.f. = 2$ ,  $P = 0.641$ . **d.** Same as in **c** for spindle peaks. Friedman test,  $\chi^2 = 0.67$ ,  $n = 9$ ,  $d.f. = 2$ ,  $P = 0.716$ . **e.** Proportion of endogenous (black) and induced (gray) delta waves associated with a down state revealing a strong correlation between these events (Wilcoxon matched pairs test,  $n = 11$  sessions with  $n_{\text{PFC neurons}} > 7$ ,  $Z = 0.27$ ,  $P = 0.790$ ). **f.** Mean HPC population activity during delta-down events identified in **e**, relative to the firing rate outside of these events during SWS (Wilcoxon matched pairs test,  $n = 11$  sessions with  $n_{\text{PFC neurons}} \& n_{\text{HPC neurons}} > 7$ ,  $Z = 0.27$ ,  $P = 0.790$ ). Error bars represent s.e.m.

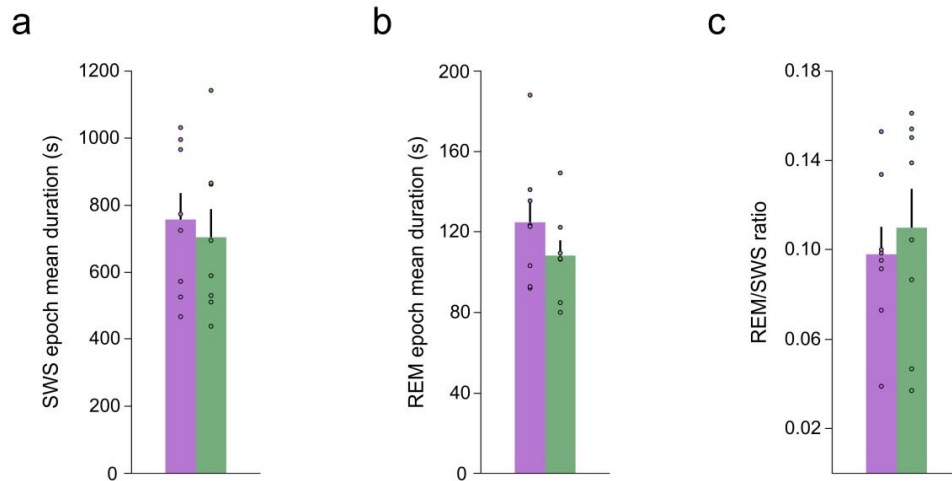


**Supplementary Figure 3**

**Stimulation did not trigger direct, hyper-synchronous activation of mPFC neurons.**

**a.** Average local field potential recorded in the mPFC (top trace, low-pass filtered) around stimulations ( $n = 1,000$ ) in one example session. **b.** Top, Multiunit activity of mPFC pyramidal cells. Bottom, average population firing rate across stimulations. **c.** Same as in **b**

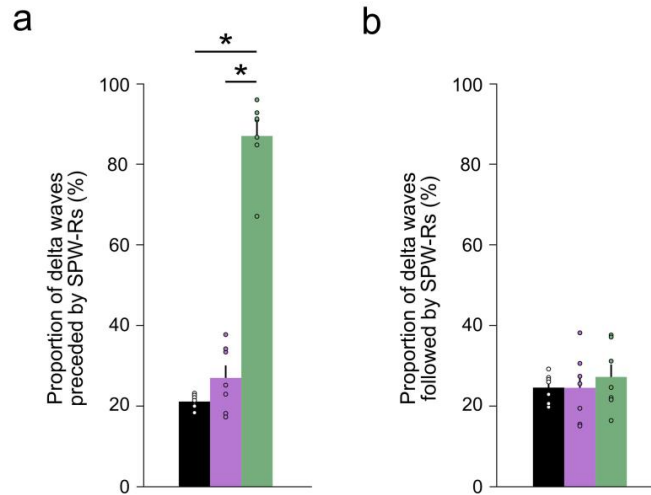
for mPFC interneurons. While stimulation-induced delta waves are accompanied by neuronal silence characteristic of endogenous down states, neither pyramidal cells nor interneurons dramatically increase their firing rates at the time of stimulation.



#### Supplementary Figure 4

##### Stimulation conditions and global sleep architecture.

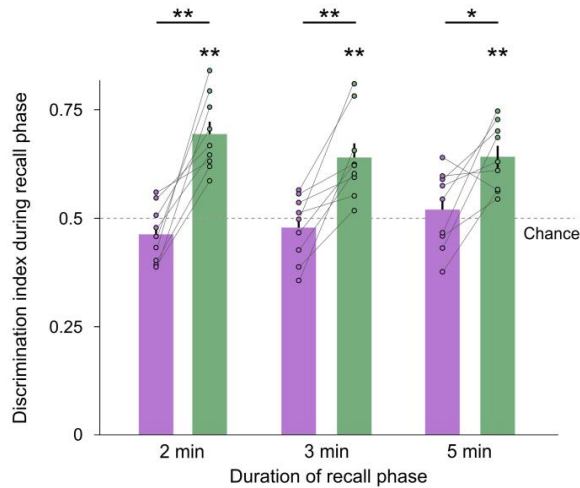
**a.** The duration of uninterrupted SWS epochs was similar during delayed (purple) and coupled (green) stimulation sessions (coupled vs delayed, Wilcoxon matched pairs test,  $n = 9$ ,  $Z = 0.56$ ,  $P = 0.575$ ). **b.** Same as in **a**, for REM epochs (coupled vs delayed, Wilcoxon matched pairs test,  $n = 9$ ,  $Z = 0.98$ ,  $P = 0.327$ ). **c.** Average REM/SWS ratios were similar across stimulation conditions (coupled vs delayed, Wilcoxon matched pairs test,  $n = 9$ ,  $Z = 0.70$ ,  $P = 0.484$ ). Error bars represent s.e.m.



**Supplementary Figure 5**

**Stimulation-induced delta waves did not alter subsequent SPW-R occurrence rates.**

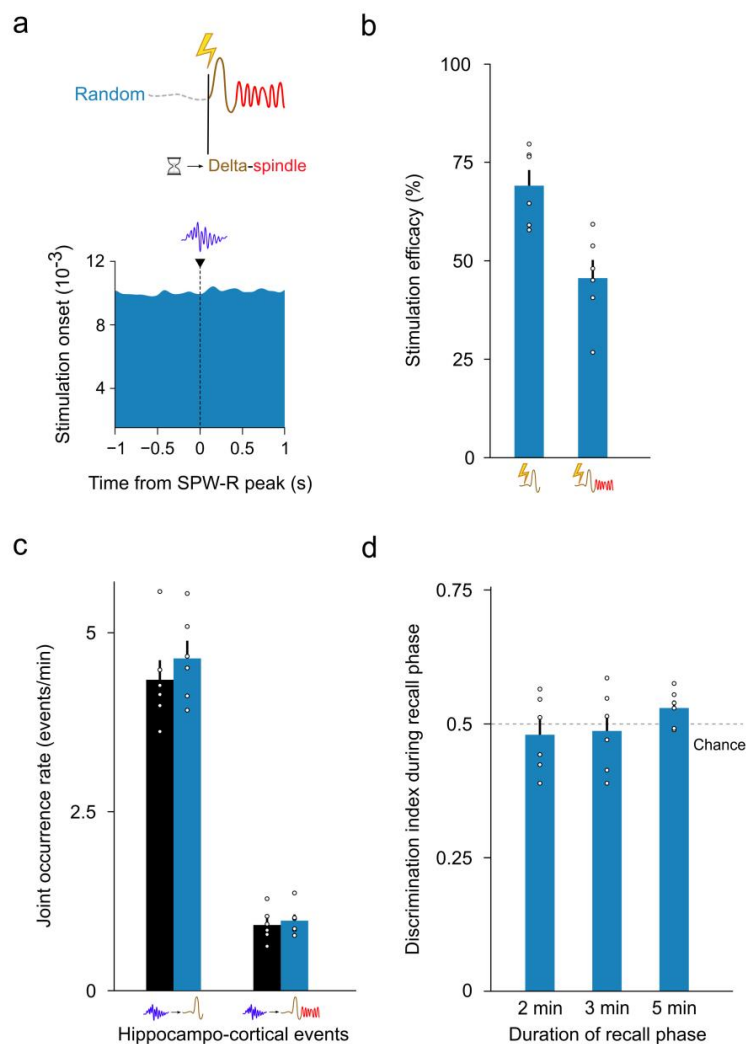
**a.** Proportion of delta waves preceded by SPW-Rs during Pre-sleep (black) and coupled (green bars) and delayed (purple bars) stimulation periods (only stimulation-evoked delta waves were counted in post-exploration sleep sessions). Friedman test,  $\chi^2 = 11.14$ ,  $n = 7$ ,  $d.f. = 2$ ,  $P = 0.004$ ; Wilcoxon matched pairs test,  $n = 7$ , Pre-sleep vs. coupled:  $Z = 2.36$ ,  $*P = 0.018$ ; Pre-sleep vs. delayed:  $Z = 1.18$ ,  $P = 0.237$ ; coupled vs. delayed:  $Z = 2.36$ ,  $*P = 0.018$ . **b.** The proportion of delta waves followed by SPW-Rs was similar across conditions (only stimulation-evoked delta waves were counted in post-exploration sleep sessions). Friedman test,  $\chi^2 = 0.29$ ,  $n = 7$ ,  $d.f. = 2$ ,  $P = 0.867$ . Error bars represent s.e.m.



**Supplementary Figure 6**

**Coupling hippocampal and cortical oscillations enhances recall above chance level and induces preferential exploration of the displaced object.**

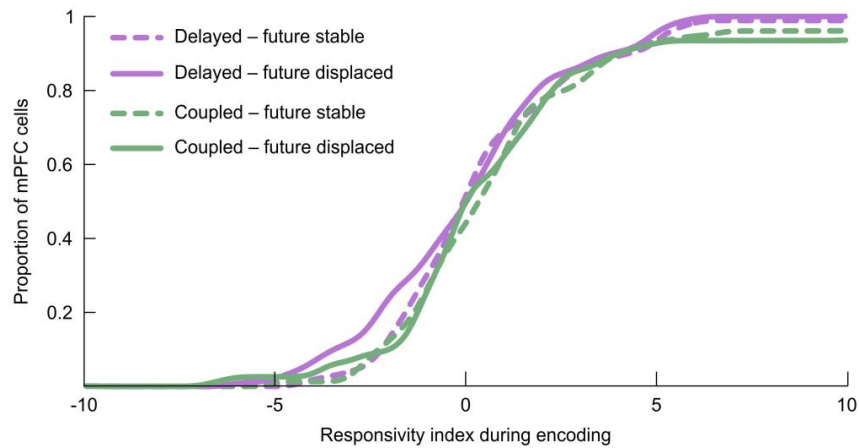
Memory performance remained significantly above chance level in the coupled condition for the whole duration (5 minutes) of the recall phase, whereas in the delayed condition, performance did not differ from chance (2 min coupled vs delayed, Wilcoxon matched pairs test,  $n = 9$ ,  $Z = 2.66$ ,  $**P = 0.008$ ; 2 min coupled vs chance, Wilcoxon signed-rank test,  $n = 9$ ,  $Z = 2.66$ ,  $**P = 0.008$ ; 2 min delayed vs chance, Wilcoxon signed-rank test,  $n = 9$ ,  $Z = 1.48$ ,  $P = 0.139$ . 3 min coupled vs delayed, Wilcoxon matched pairs test,  $n = 9$ ,  $Z = 2.66$ ,  $**P = 0.008$ ; 3 min coupled vs chance, Wilcoxon signed-rank test,  $n = 9$ ,  $Z = 2.66$ ,  $**P = 0.008$ ; 3 min delayed vs chance, Wilcoxon signed-rank test,  $n = 9$ ,  $Z = 0.65$ ,  $P = 0.515$ . 5 min coupled vs delayed, Wilcoxon matched pairs test,  $n = 9$ ,  $Z = 2.31$ ,  $*P = 0.021$ ; 5 min coupled vs chance, Wilcoxon signed-rank test,  $n = 9$ ,  $Z = 2.66$ ,  $**P = 0.008$ ; 5 min delayed vs chance, Wilcoxon signed-rank test,  $n = 9$ ,  $Z = 0.889$ ,  $P = 0.374$ ). Error bars represent s.e.m.



### Supplementary Figure 7

#### Random, non SPW-R-triggered stimulation does not lead to memory consolidation on the spatial object recognition task.

**a.** Random stimulation protocol (top) and temporal cross-correlation between SPW-Rs and stimulation onset (bottom). **b.** Stimulation efficacy for the random stimulation protocol. **c.** Incidence of hippocampo-cortical events (left: SPW-R-delta, right: SPW-R-delta-spindle) during Pre-sleep (black) and random stimulation periods (blue). SPW-R-delta incidence, Wilcoxon matched pairs test,  $n=6$ ,  $Z=1.57$ ,  $P=0.116$ ; SPW-R-delta-spindle incidence, Wilcoxon matched pairs test,  $n=6$ ,  $Z=1.36$ ,  $P=0.173$ . **d.** Performance did not differ from chance during recall following the random stimulation protocol (2 min random vs chance, Wilcoxon signed-rank test,  $n=6$ ,  $Z=0.73$ ,  $P=0.463$ ; 3 min random vs chance, Wilcoxon signed-rank test,  $n=6$ ,  $Z=0.52$ ,  $P=0.600$ ; 5 min random vs chance, Wilcoxon signed-rank test,  $n=6$ ,  $Z=1.57$ ,  $P=0.116$ ) Error bars represent s.e.m.



**Supplementary Figure 8**

**Medial prefrontal cortical cells were not responsive to the objects during the encoding phase.**

Cumulative distributions of mPFC responsivity indices to each object during the encoding phase of the task preceding each stimulation condition. mPFC cells were not responsive to any object in any condition (displaced object: coupled vs delayed, Wilcoxon rank-sum test,  $n = 77$ ,  $n = 93$ ,  $Z = 1.14$ ,  $P = 0.255$ ; coupled vs zero, Wilcoxon matched pairs test,  $n = 77$ ,  $Z = 1.32$ ,  $P = 0.188$ ; delayed vs zero, Wilcoxon matched pairs test,  $n = 93$ ,  $Z = 0.14$ ,  $P = 0.890$ ; stable object: coupled vs delayed, Wilcoxon rank-sum test,  $n = 77$ ,  $n = 93$ ,  $Z = 0.79$ ,  $P = 0.432$ ; coupled vs zero, Wilcoxon matched pairs test,  $n = 77$ ,  $Z = 1.65$ ,  $P = 0.099$ ; delayed vs zero, Wilcoxon matched pairs test,  $n = 93$ ,  $Z = 0.65$ ,  $P = 0.516$ ).

Condition	<i>n</i>	Displaced object (s)	Stable object (s)	Discrimination index
Naive (3 min encoding)	8	9,57 ± 0,99	11,73 ± 1,35	0,45 ± 0,04
Trained (20 min encoding)	6	13,74 ± 2,04	5,22 ± 0,81	0,72 ± 0,03
Coupled stimulation (3 min encoding)	9	14,77 ± 1,55	6,67 ± 1,19	0,69 ± 0,03
Delayed stimulation (3 min encoding)	9	9,94 ± 1,48	11,75 ± 1,98	0,46 ± 0,04
Random stimulation (3 min encoding)	6	10,17 ± 2,00	10,00 ± 1,25	0,48 ± 0,03

**Supplementary Table 1 | Object exploration times.** Time spent exploring the objects during the recall phase for each condition, and corresponding discrimination index. Errors are s.e.m.

CHAPTER 5. ROLE OF RIPPLE-DELTA COUPLING IN MEMORY  
CONSOLIDATION

---

# Chapter 6

## Role of delta spikes in memory consolidation

In Maingret et al. (2016), we demonstrated the causal link between ripple-delta coupling and memory consolidation. The acute cortical response to hippocampal ripples in the form of ripple-triggered reactivations takes place before the delta wave (Peyrache et al., 2009). Yet cortical synaptic plasticity is believed to take place after the delta wave, in the surge of activity at the UP state onset (Destexhe et al., 2007; Kruskal et al., 2013; Levenstein et al., 2017) and in sleep spindles (Sejnowski and Destexhe, 2000; Rosanova and Ulrich, 2005) that closely follow delta waves. How does the hippocampal information persist in the network during the synchronized silence of the network during the delta wave? We considered the possibility that the occasional “rogue spikes” we observed in the literature (see section 3.1.2) and in our recordings may represent a residual signal that retains information about the previous UP state.

First, we addressed whether spiking during delta waves is a robust phenomenon. In  $\sim 10\%$  of delta waves, we detected spikes on the same electrode as the delta wave. We probed if these events might be distinct from classical delta waves associated with complete silence, but silent and non-silent delta waves had the same characteristics (waveform, coupling with ripples, spindles and gamma oscillations). We then considered that all delta waves may have some spiking activity, which may or may not be detected depending on the recording range. Consistent with this, we detected less non-silent delta waves in experiments with fewer recorded cortical neurons.

We then investigated if this neuronal activity in delta waves could represent a signal rather than noise. In particular, we addressed if delta wave neuronal activity could be a part of the hippocampal-cortical dialogue. Supporting this

hypothesis, hippocampal ripple activity preceding the delta wave could predict the delta spikes. Strikingly, the cortical cells that were predicted by the hippocampal ripple content were the ones that had responded more to the objects during the task, further supporting a possible role of delta spikes in memory consolidation.

In the rare cases when we detected spikes from more than one cell, we found that the neurons remaining active in the same delta wave were not independent, but formed correlated cell assemblies. This suggests that while the rest of the network is silent, select subpopulations of neurons may perform cortical computations in isolation from interfering inputs.

Finally, we asked if this spiking in delta waves may explain the results in Maingret et al. (2016). If delta spikes represent a cortical signal that reflects the preceding hippocampal ripple activity and retains the information for synaptic plasticity, we should see a breakdown of the hippocampal bias of delta spikes in the delayed delta wave condition. Indeed, while hippocampal activity preceding delta waves coupled to ripples could predict delta spikes in the synchronized condition, delta spikes of delayed delta waves were no longer correlated with hippocampal activity.

In conclusion, hippocampal ripple activity can bias cortical activity at the optimal window of delta waves following ripples. In the absence of a delta wave to isolate the computation from ongoing cortical inputs, interference occurs and information is lost before the delayed delta wave, preventing memory consolidation. In contrast, when a delta wave follows the hippocampal ripple, a synchronized DOWN state of the majority of neurons isolates the cortical network while a selected subpopulation of cells remain active, retaining the information throughout the delta wave and resulting in memory consolidation.

# Isolated cortical computations during delta waves

Ralitsa Todorova,<sup>1</sup> Michaël Zugaro,<sup>1\*</sup>

<sup>1</sup>Center for Interdisciplinary Research in Biology (CIRB),  
Collège de France, CNRS, INSERM, PSL Research University, Paris, France

\*Corresponding author. E-mail: michael.zugaro@college-de-france.fr

Delta waves have been described as periods of generalized silence across the cortex, and their alternation with periods of endogenous activity results in the slow oscillations of slow wave sleep. Despite clear evidence that delta waves are instrumental for memory consolidation, the specific role for neuronal silence in reshaping cortical functional circuits remains puzzling. Here, we report that contrary to a generally accepted tenet, delta waves are not periods of complete silence, and the residual activity is not mere neuronal noise. Instead, cortical cells involved in learning a spatial memory task subsequently formed cell assemblies during delta waves in response to transient reactivation of hippocampal ensembles during ripples, and this occurred selectively during endogenous or induced memory consolidation. Thus, delta waves represent isolated cortical computations tightly related to ongoing information processing underlying memory consolidation.

Most of our time spent asleep is dominated by the slow oscillation (0.1–1 Hz), when cortical neurons synchronously alternate between a depolarized (UP) state associated with high levels of endogenous activity, and a hyperpolarized (DOWN) state when neurons remain silent (1). Delta waves are large deflections of the local field potential (LFP) which correspond to the DOWN states of the slow oscillation, and are thus considered periods of generalized cortical silence. The slow oscillation plays a causal role in memory consolidation (2–5) possibly by orchestrating an information transfer between the hippocampus and the neocortex (6). Indeed, recent research suggests that hippocampal replay (7) initiates reactivation of cortical cell assemblies (8) just before the occurrence of a delta wave (9), and that synaptic plasticity subsequently takes place during network reorganization early in the following UP state (10, 11) and during massive calcium entry accompanying the ensuing sleep spindle (12, 13). This hippocampo-cortical dialogue (14, 15) is instrumental for memory consolidation (5).

While recent investigation has progressively unravelled these delicate network mechanisms and their temporal relations, the incursion of generalized silence (delta wave) precisely between information transfer and network plasticity remains puzzling. Here, we report that contrary to a generally accepted tenet (1, 6, 16), spiking activity does take place during delta waves, and that this overlooked activity underlies cortical computation involved in the hippocampo-cortical dialogue.

We recorded prefrontal cortical activity in 9 rats during slow wave sleep (5). Neuronal activity occurred consistently in a substantial fraction of delta waves ( $9.2 \pm 2.7$  %), with one or a few neurons remaining active while the rest of the population became silent (Fig. 1A,B). This activity (‘delta spikes’) was not restricted to a particular subset of neurons, as persisting firing during delta waves involved all recorded neurons (Fig. 1C, Suppl. Fig. S1).

Conversely, to test whether delta spikes were restricted to a subset of delta waves

with distinct characteristics, we compared delta waves in which we did or did not detect cortical spikes, and found no significant difference between the two groups in terms of LFP waveform (Fig. 1D), decreased gamma power, coupling with thalamocortical spindles, and coupling with hippocampal ripples (Suppl. Fig. S2). It is therefore conceivable that spikes could take place during virtually all delta waves, but remain undetected given the limited number of recorded neurons relative to the entire population of cells. To test this hypothesis, we first compared sessions with different numbers of recorded neurons. The proportion of non-silent delta waves increased with greater numbers of recorded neurons (Suppl. Fig. S3A). To confirm this trend, we used a Monte-Carlo approach to generate progressively larger populations of neurons by iteratively subsampling greater fractions of the recorded population and estimating the resulting proportion of non-silent delta waves. Again, this proportion increased with the number of neurons (Suppl. Fig. S3B). We therefore propose that firing during delta waves is an overlooked phenomenon manifested in possibly all delta waves.

This suggests that during any given delta wave, the cortical network becomes silent, except for a small but ever-changing minority of cells. The most parsimonious explanation would be that delta spikes constitute random activity reflecting imperfections in the cortical alternation between UP and DOWN states. Yet, an alternative intriguing possibility is that this persistent activity actually serves a well-defined computational function. A hallmark of cortical computation is the emergence of cell assemblies. We thus tested for the presence of recurring co-active cell ensembles. Using independent component analysis (ICA), we found multiple significant assemblies active during delta waves (Fig. 2). This shows that delta spikes do form assemblies ('delta assemblies') and suggests that they are not random activity but genuine computations.

We then asked if delta spikes were involved in the hippocampo-cortical dialogue underlying memory consolidation. This would have two implications: 1) hippocampal activity

during ripples should predict which neurons (ideally, which assemblies) fire during the following delta wave, and 2) predictable cortical cells should be involved in the reactivation of previous wake experience.

The rats were trained on a spatial memory task, and hippocampal and cortical activity was recorded both during behavior and subsequent memory consolidation during sleep (5).

Hippocampal spiking activity during ripples was significantly correlated with cortical spikes emitted during immediately (50–200 ms) following delta waves (Fig. 3A). This was due to a large proportion of positively correlated inter-regional pairs of neurons (Fig. 3B). Further, a generalized linear model (GLM) analysis showed that delta spikes could be significantly predicted from the spike counts of the ensemble of individual hippocampal units (Fig. 3C). In contrast, delta spikes could not be predicted from the combined spike count of all units (multiunit activity) that ignored cell identity (Fig. 3C), ruling out that delta spikes merely reflect the overall level of hippocampal activity during ripples. Finally, the same GLM analysis applied to hippocampal and cortical ensembles showed that hippocampal activity could even predict delta assemblies (Fig. 3D). Thus, delta spikes and assemblies reflect the specific information content of the ripple preceding the delta wave.

Our second prediction concerned the behavioral correlates of the prefrontal units whose delta spikes were significantly predicted by hippocampal ripple activity. Strikingly, these cortical cells displayed higher levels of task-relevant firing during behavior immediately preceding sleep (Fig. 3E; we failed to find a similar effect for delta assemblies, possibly because of low statistical power due to their limited number:  $n = 14$  assemblies,  $n = 9$  predicted).

These observations suggest that in addition to triggering the reorganization of cortical subnetworks during the transition to the UP state (5), a critical role of the delta wave may be to isolate from interference specific cortical computations taking place in response

to hippocampal replay. This yields two predictions that we test below: 1) in natural sleep, hippocampal activity during ripples should predict cortical activity at the time of the delta wave ( $\sim 130$  ms later) whether the delta wave does in fact occur or not, but the occurrence of the delta wave (isolation) should be critical for memory consolidation, and 2) isolating cortical assemblies by experimental induction of delta waves should trigger memory consolidation, but only if the isolated activity is relevant to the hippocampo-cortical dialogue. Note that if verified, prediction 1 would provide correlative support, and prediction 2 complementary causal evidence, for our hypothesis that isolation of delta assemblies is instrumental for memory consolidation.

We first assessed the correlation between hippocampal activity during ripples and cortical activity at the expected time of delta waves ( $\sim 130$  ms later). This correlation remained significant even in the absence of a delta wave (Suppl. Fig. S4). On the other hand, we have previously shown (using the same data set) that memory consolidation took place only if delta waves repeatedly occurred  $\sim 130$  ms after ripples (5). This suggests that the critical difference between experimental conditions that do or do not lead to memory consolidation is not the hippocampo-cortical correlation (which is maintained in both conditions), but their isolation from competing inputs by delta waves.

Providing causal evidence requires experimentally isolating cortical computation, i.e. triggering delta waves, at times when endogenous mechanisms fail to do so (Fig. 4A). We have already shown that triggering timed delta waves does boost memory consolidation (5). We thus tested whether delta spikes did occur during experimentally induced delta waves, and whether they were predicted by hippocampal activity. Similar to our observations in natural sleep (above), stimulation-induced delta waves did feature spiking activity, and these delta spikes were predicted by preceding hippocampal activity coinciding with the time of ripple (Fig. 4B-D). In contrast, slightly delaying the induction of delta waves (by  $\sim 200$  ms, see Suppl. Fig. S4) so that delta spikes were no longer predicted

by hippocampal ripple activity (Fig. 4B-D) failed to induce memory consolidation (5), suggesting that isolation of cortical activity unrelated to the hippocampo-cortical dialogue did not favor memory consolidation processes.

In summary, our results challenge the generally accepted tenet that delta waves, reflecting the DOWN states of the sleep slow oscillation, are periods of complete cortical silence (1, 6, 17) — to the point that they have sometimes been defined as such (18, 19), and that occasional spikes have been routinely ignored when detected (20, 21). Here, we focused on delta spikes and showed that they are not exceptional, that they are not neuronal noise due to imperfect silencing of the cortical mantle, but on the contrary that they constitute a common phenomenon potentially implicating all neurons and all delta waves, and that they reflect genuine processing involved in memory consolidation. This also provides a mechanism for the documented but puzzling role of delta waves in memory consolidation: synchronized silence across most of the cortex isolates the network from competing inputs, while a select subpopulation of neurons maintains relevant spike patterns active between epochs of hippocampo-cortical information transfer (7, 8, 22), and epochs of cortical plasticity (10, 11) and network reorganization (5, 12, 13). It seems likely that delta spikes and assemblies also constitute a more general mechanism of isolated cortical computations during slow wave sleep, as many cortical neurons active during delta waves could not be predicted from hippocampal ripple activity and may have been prompted by other input areas.

## Acknowledgments

We thank Nicolas Maingret for performing the experiments that provided the dataset for this study. Romain Fayat for help with the delta wave detection algorithm. This work was supported by the Agence Nationale de la Recherche (ANR-15-CE16-0001-02), Collège de France (R.T.), and a joint grant from École des Neurosciences de Paris Île-de-

France and LabEx MemoLife (ANR-10-LABX-54 MEMO LIFE, ANR-10-IDEX-0001-02 PSL\*) (R.T.). The authors declare no competing interests. M.Z. designed the study. R.T. and M.Z. designed the analyses. R.T. performed the analyses. R.T. and M.Z. wrote the manuscript. Data of this study were stored and curated in servers of the Collège de France, Paris, France.

## References

1. M. Steriade, A. Nunez, F. Amzica, *Journal of Neuroscience* **13**, 3252 (1993).
2. H.-V. V. Ngo, T. Martinetz, J. Born, M. Mölle, *Neuron* **78**, 545 (2013).
3. L. Marshall, H. Helgadottir, M. Molle, J. Born, *Nature* **444**, 610 (2006).
4. S. Chauvette, J. Seigneur, I. Timofeev, *Neuron* **75**, 1105 (2012).
5. N. Maingret, G. Girardeau, R. Todorova, M. Goutierre, M. Zugaro, *Nature Neuroscience* **19**, 959 (2016).
6. A. Sirota, G. Buzsáki, *Thalamus and Related Systems* **3**, 245 (2005).
7. A. K. Lee, M. A. Wilson, *Neuron* **36**, 1183 (2002).
8. A. Peyrache, M. Khamassi, K. Benchenane, S. I. Wiener, F. P. Battaglia, *Nature Neuroscience* **12**, 919 (2009).
9. A. Sirota, J. Csicsvari, D. Buhl, G. Buzsáki, *Proceedings of the National Academy of Sciences* **100**, 2065 (2003).
10. P. B. Kruskal, L. Li, J. N. MacLean, *Nature Communications* **4**, 2574 (2013).
11. T. Gulati, L. Guo, D. S. Ramanathan, A. Bodepudi, K. Ganguly, *Nature Neuroscience* **20**, 1277 (2017).

12. M. Rosanova, D. Ulrich, *The Journal of Neuroscience* **25**, 9398 (2005).
13. J. Seibt, *et al.*, *Nature Communications* **8**, 684 (2017).
14. G. Buzsáki, *Neuroscience* **31**, 551 (1989).
15. P. W. Frankland, B. Bontempi, *Nature Reviews Neuroscience* **6**, 119 (2005).
16. M. Steriade, *Frontiers in Bioscience: A Journal and Virtual Library* **8**, d878 (2003).
17. M. Steriade, I. Timofeev, *Neuron* **37**, 563 (2003).
18. A. Luczak, P. Barthó, S. L. Marguet, G. Buzsáki, K. D. Harris, *Proceedings of the National Academy of Sciences of the United States of America* **104**, 347 (2007).
19. L. Johnson, D. Euston, M. Tatsuno, B. McNaughton, *The Journal of neuroscience : the official journal of the Society for Neuroscience* **30**, 2650 (2010).
20. J. Csicsvari, *et al.*, *Journal of Neurophysiology* **90**, 1314 (2003).
21. D. Jercog, *et al.*, *eLife* **6**, e22425 (2017).
22. G. Rothschild, E. Eban, L. M. Frank, *Nature Neuroscience* **20**, 251 (2017).
23. L. Hazan, M. Zugaro, G. Buzsáki, *J Neurosci Methods* pp. 207–216 (2006).
24. P. Barthó, *et al.*, *J Neurophysiol* **92**, 600 (2004).
25. G. M. van de Ven, S. Trouche, C. G. McNamara, K. Allen, D. Dupret, *Neuron* **92**, 968 (2016).

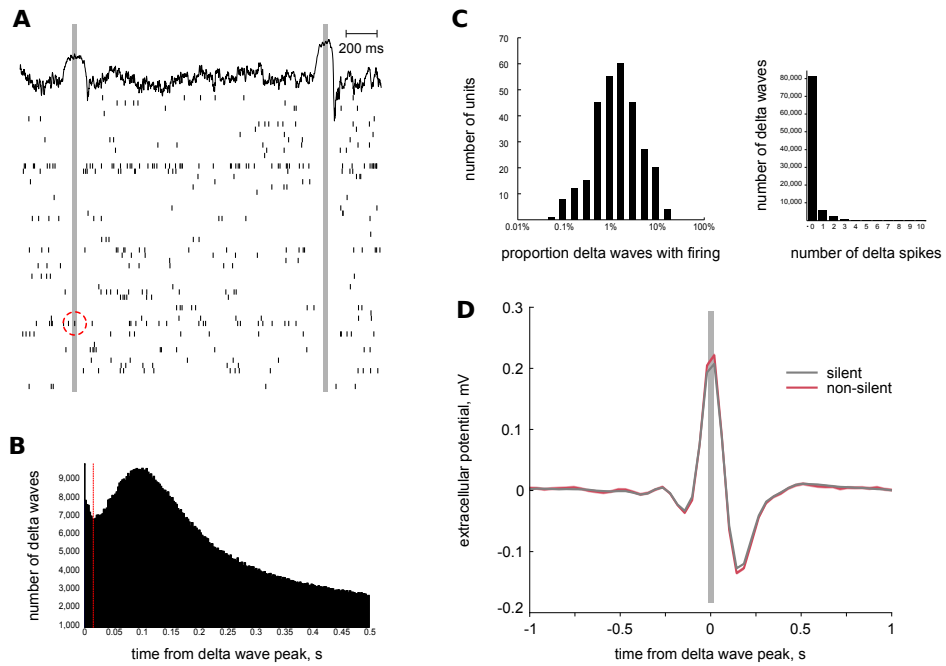


**Fig. 1. Firing during delta waves.** **(A)** An example recording of a non-silent and a silent delta wave. Above: local field potential (black trace) recorded in the deep layers of the medial prefrontal cortex. Below: raster plot of the activity of the simultaneously recorded prefrontal units. Grey bars mark the 30 ms window centered around delta waves. Note the delta spike (red circle) during the first delta wave. **(B)** Distribution of the closest spike emitted by each prefrontal neuron to each delta wave. Note that beside the large peak at  $\sim 100$  ms due to activity in the UP state, there is a smaller peak of spikes occurring during delta waves with a temporal distance below our threshold of 15 ms (red line). **(C)** Left: distribution of the number of delta waves in which each unit emitted delta spikes was log-normal. Right: distribution of the number of delta spikes detected in each delta wave. **(D)** Waveform of silent (black,  $n=101,161$ ) and non-silent (red,  $n=12,205$ ) delta waves were not different (Monte-Carlo test,  $p>0.05$ ).

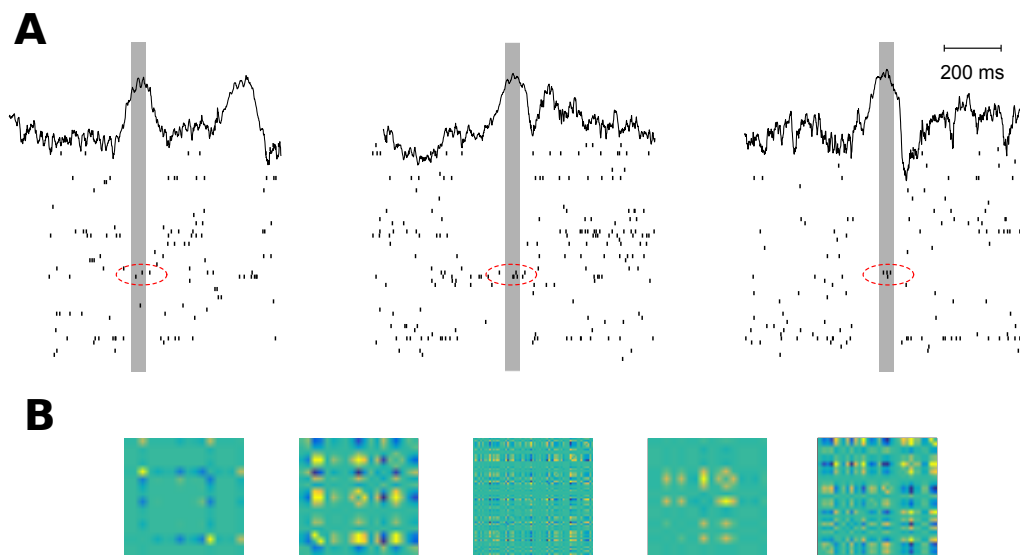


**Fig. 2. Activity components during delta waves.** (A) Examples of correlated firing of multiple units during delta waves (red circles). (B) Examples of significant templates representing cell assemblies identified using independent component analysis (ICA).

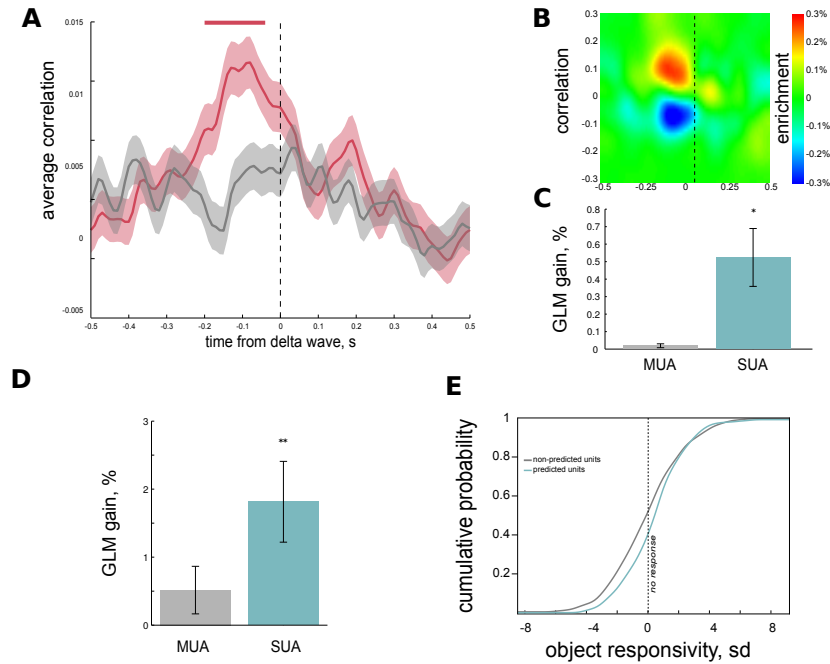


**Fig. 3. Hippocampal ripple activity predicts delta spikes.** **(A)** Cross-structural correlations between hippocampal ripple activity (sliding window) and delta spikes (fixed, 0 s). Real cross-correlations (red) were significantly different from a shifted control (grey) for hippocampal ripple activity preceding delta waves (red line). **(B)** Enrichment (see *Methods*) comparing the distributions in (A). Relative to the distribution of shifted cross-correlation values, in the original non-shifted data there was an enrichment of positively correlated pairs of neurons when the hippocampal activity preceding the delta wave was correlated to delta spikes of prefrontal units. **(C)** Predictive performance of a GLM trained to predict delta spikes based on multiunit (grey,  $p=0.2597$ , Wilcoxon signed rank test) and single-unit (blue,  $p=0.0403$ , Wilcoxon signed rank test) hippocampal ripple activity within a 200 ms window preceding delta waves measured as percent improvement relative to a shuffled control (see *Methods*). **(D)** Predictive performance of a GLM trained to predict template activation during delta waves based on multiunit (grey,  $p=0.1638$ , Wilcoxon signed rank test) and single-unit (blue,  $p=0.0092$ , Wilcoxon signed rank test) hippocampal ripple activity within a 200 ms window preceding delta waves. **(E)** Cumulative distribution of the responsivity index of prefrontal units either significantly predicted (red) or not significantly predicted (grey) by the preceding hippocampal ripple activity. Only predicted prefrontal units showed positive object responsivity (predicted units,  $p=0.0162$ ; non-predicted units,  $p=0.5967$ , Wilcoxon signed rank test).

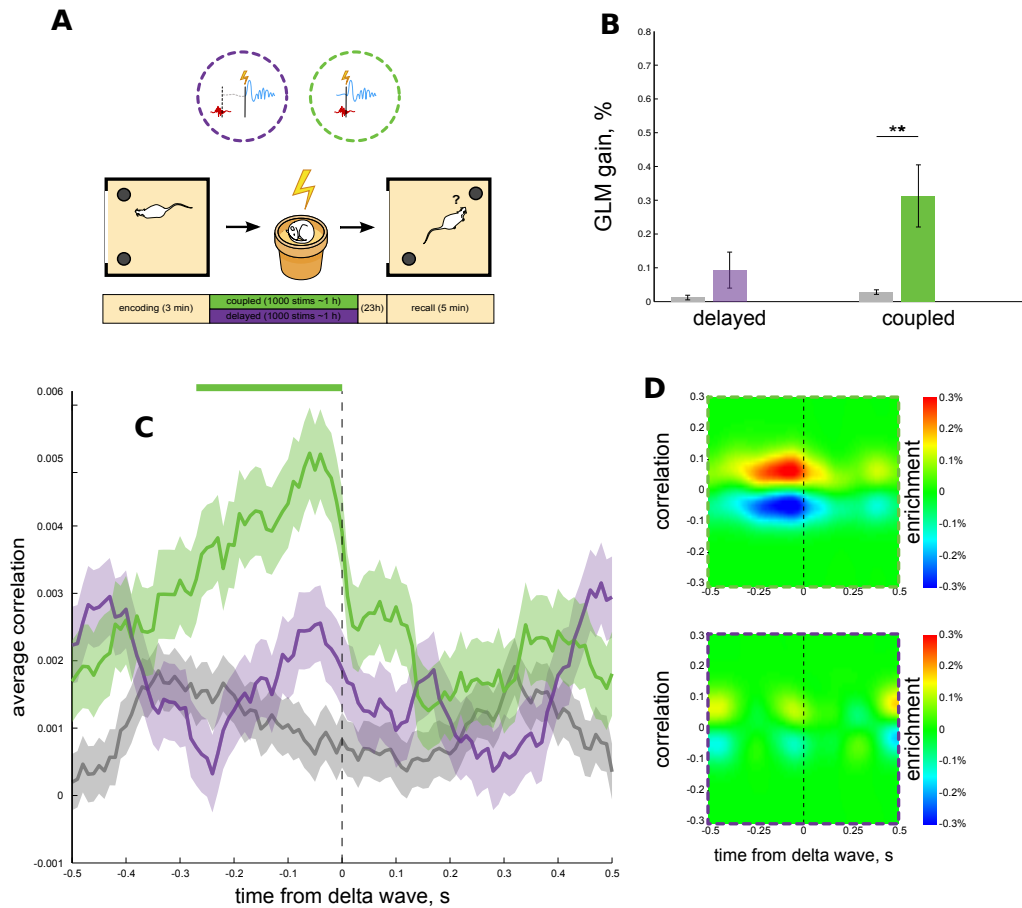


**Fig. 4. Ripple-delta coupling is instrumental to predicting delta spikes. (A)** Left: stimulation protocol. Ripple-triggered stimulation induced delta waves coupled to ripples (green) or delayed by 160–240 ms (purple) during sleep after rats explored two identical objects for 3 minutes. Right: Object discrimination index during the recall phase after each stimulation condition. Only coupled stimulation resulted in memory consolidation and enhanced task performance. **(B)** Performance of GLM trained to predict delta spikes in each of the stimulation conditions using the single unit (colored bars) or multiunit (grey bars) hippocampal activity in a 200 ms window preceding delta waves. Delta spikes during coupled ( $p=0.0030$ , Wilcoxon signed rank test), but not delayed ( $p=0.1301$ , Wilcoxon signed rank test) delta waves could be predicted by the preceding hippocampal activity. **(C)** Cross-correlation (shaded areas, mean  $\pm$  s.e.m.) of the hippocampal activity and delta spikes in the coupled (green) and delayed (purple) condition. The green line highlights the interval where the cross-correlation in the coupled condition are significantly ( $p<0.05$ , Wilcoxon rank sum test) greater than the shifted control (grey). **(D)** Enrichment plots for the distributions of the cross-correlation values for the coupled (top) and delayed (bottom) condition relative to the shifted control.

## Materials and Methods

### Animals

The analyses presented here were performed on data collected for a previous study by (5). Briefly, a total of 9 male Long Evans rats (René Janvier, Le Genest, St Isle, France; weight, 280–350 g) were maintained on a 12h:12h light-dark cycle (lights on at 07:00 a.m.). Training and experiments took place during the day. Rats were group-housed until one week before surgery. All experiments were in accord with institutional (CNRS Comité Opérationnel pour l'Éthique dans les Sciences de la Vie) and international (US National Institutes of Health guidelines) standards, legal regulations (Certificat no. B751756), and ethical requirements (Ethics Committee approval #2012-0048) regarding the use and care of animals.

### Surgery

The rats were deeply anesthetized (xylazine, 0.1 ml intramuscular; pentobarbital, 40 mg per kg of body weight, intraperitoneal; 0.1 ml pentobarbital supplemented every hour) and implanted with a custom-built microdrive with 16 individual tetrodes (groups of four twisted 12  $\mu\text{m}$  tungsten wires, gold-plated to 200 k $\Omega$ ), of which 8 targeted the prelimbic and infralimbic regions of the right mPFC (AP: +2.7 mm from bregma; ML: +1.5 mm, angled at 10° from the sagittal plane), and the other 8 targeted the CA1 subfield of the right hippocampus (AP: -3.5 to -5.5 mm; ML: +2.5 to +5 mm). A custom-built bipolar stimulation electrode consisting of two stainless steel wires (total length 1.5 mm, inter-wire interval 0.5 mm, wire diameter 70  $\mu\text{m}$ ) was implanted in the left neocortex (AP: +2 mm; ML: -2 mm; DV: -1.5 mm from the dura – motor area). Miniature stainless steel screws (reference and ground) were implanted above the cerebellum. During recovery from surgery (minimum 3 days), the rats received food and water ad libitum. The recording electrodes were then progressively lowered until they reached their targets and

then adjusted every day to optimize yield and stability.

## **Behavioral task**

During a 3-minute encoding phase rats explored a 70 cm  $\times$  50 cm arena with two identical objects placed in two adjacent corners. The rats were then placed in a flower pot for sleep sessions, which lasted until 1,000 stimulations had been delivered ( $\sim$ 4,000 s of SWS), then returned to their home cage. On the following day, during a 5-minute recall phase rats explored the same arena, in which one of the objects had been displaced to the opposite corner. The rats were then placed in a flower pot for uninterrupted sleep sessions without stimulation. After an interval of at least two days, each rat performed the task a second time with different objects. The order of the stimulation conditions (coupled-then-delayed versus delayed-then-coupled) was pseudo-randomly distributed among rats.

## **Stimulation protocol**

The stimulation protocol has been described previously (5). Briefly, threshold crossing on the ripple band-filtered hippocampal signal automatically triggered a monophasic single-pulse (0.1 ms) stimulation of the deep layers of the motor cortex, delivered by a constant current stimulator (SD9 square pulse stimulator, Grass Technologies). For each animal, the optimal stimulation voltage (the minimum voltage necessary to reliably induce propagating delta waves) was determined prior to training (range: 17.5–22.5 V). The number of stimulations was limited to one every two seconds, and the total number of stimulations was set to 1,000, yielding a stimulation period of  $\sim$ 4,000 s. For coupled stimulation, pulses were triggered 20 ms after SPW-R detection to emulate endogenous fine-tuned SPW-R-delta coordination. For delayed stimulation, an additional random delay (range: 160–240 ms) was introduced between SPW-R detection and stimulation onset.

## Data acquisition and processing

Brain signals were preamplified (unity-gain headstage, Noted Bt, Pécs, Hungary), amplified 500x (Neuralynx L8, Bozeman, MT, USA), acquired and digitized with two synchronized Power1401 systems (CED, Cambridge, UK). A red LED was used to track the instantaneous position of the animals (25 Hz). For off-line spike sorting, the wideband signals were converted, digitally high-pass filtered (nonlinear median-based filter) and thresholded, and waveforms were extracted and projected to a PCA subspace using NDManager (L. Hazan and M. Zugaro, <http://neurosuite.sourceforge.net> (23)). Spike sorting used a semi-automatic cluster cutting procedure combining KlustaKwik (K.D. Harris, <http://klustakwik.sourceforge.net> and Klusters (L. Hazan, <http://neurosuite.sourceforge.net> (23)). In the prefrontal cortex, excitatory and inhibitory cells were discriminated based on significant short-latency peaks and trough in cross-correlograms (24) that were validated by visual inspection. In the hippocampus, putative pyramidal cells were identified based on firing rate and bursting properties. Neurophysiological and behavioral data were explored using NeuroScope (L. Hazan, <http://neurosuite.sourceforge.net> (23)). LFPs were derived from wideband signals by downsampling all channels to 1,250 Hz.

At the end of the experiments, recording sites were marked with small electrolytic lesions. Rats were deeply anesthetized with a lethal dose of pentobarbital, and intracardially perfused with saline (0.9%) followed by paraformaldehyde (10%). Coronal slices (40  $\mu$ m) were stained with cresyl-violet.

## Data analysis and statistics

Data were analyzed in Matlab (MathWorks, Natick, MA), using Freely Moving Animal Toolbox (M.Zugaro, <http://fmatoolbox.sourceforge.net>) and custom written programs. Spectrograms were constructed using chronux (<http://www.chronux.org>).

### Object responsivity

To assess how cells in the medial prefrontal cortex responded to objects, the responsivity index  $R$  was defined as the mean firing rate  $r$  over the quadrants containing the objects, z-scored relative to distribution  $F$  of firing rates in the empty quadrants, i.e.  $R = (r - \mu) / \sigma$  where  $\mu$  and  $\sigma$  are the mean and standard deviation of  $F$ . Thus, the object responsivity index  $R$  measured by how much, relative to its baseline variability, a cell increased its firing rate around the objects.

### Sleep scoring

Sleep stages (SWS/REM) were determined by automatic K-means clustering of the theta/delta ratio extracted from the power spectrograms during the episodes where the animal was immobile (linear velocity  $< 3$  cm/s for at least 30 s, with brief movements  $< 0.5$  s).

### Ripple detection

To detect ripple events, we first detrended the LFP signal and used the Hilbert transform to compute its ripple band (100–250 Hz) amplitude. We then averaged the ripple amplitudes across the channels recorded in the CA1 pyramidal layer, yielding the average ripple amplitude  $A_{ripple}$ . To exclude events of high-spectral power non-specific to the ripple-band, we subtracted the average high-frequency (300–500 Hz) amplitude  $A_{noise}$  from  $A_{ripple}$ , and when  $A_{noise}$  was higher than  $A_{ripple}$ , we set  $A_{ripple}$  to 0. We then z-scored  $A_{ripple}$ , yielding a transformed signal  $R(t)$ . Ripples were defined as events where  $R(t)$  crossed the threshold of 3 s.d. and remained above 1 s.d. for 30 ms to 110 ms.

### Delta wave detection

Delta wave detection was based on combination of LFP signal and spiking information. The LFP recorded on each tetrode in the mPFC was filtered (0–6 Hz) and z-scored, yielding  $D(t)$ . We extracted sequences of local minima and maxima ( $t_{beginning}$ ,  $t_{peak}$ ,  $t_{end}$ ,

corresponding to the putative beginning, peak and end of delta waves, respectively) by detecting upward-downward-upward zero-crossings of  $D'(t)$ . Delta waves corresponded to epochs where  $D(t_{peak}) > 2$ , or  $D(t_{peak}) > 1$  and  $D(t_{end}) < -1.5$ . Detected events lasting less than 150 ms or more than 500 ms were discarded. Detected events in which the instantaneous smoothed (60 ms Gaussian window) mPFC multiunit activity decreased (relative to a 2-s period around each  $t_{peak}$ ) were defined as delta waves.

### Activity during delta waves

To quantify spiking during delta waves, we computed the distribution of delays between a delta wave peak and the nearest spike emitted by each neuron detected on the same tetrode as the delta wave. This yielded a bimodal distribution (Fig. 1B): while in the majority of cases, the nearest spike was 100-200 ms from the delta wave (i.e. in the upstate), we saw a fraction of delta waves in which a spike occurred within 15 ms of the delta wave peak. We used this window as a conservative estimate for the activity occurring during delta waves, and defined delta spikes as spikes emitted within 15 ms of the peak of a delta wave detected on the same tetrode as the active neuron.

We used independent component analysis (ICA) to detect significant cell assemblies (25). We computed a delta spike matrix  $M$ , where  $M(i, j)$  is the number of spikes emitted by neuron  $i$  within 15-ms of delta wave  $j$ . We z-scored  $M$  for each neuron and projected it onto its significant principle components – the first  $n$  components after principle component analysis (PCA), where  $n$  is equal to the number of eigenvalues exceeding the Marcenko-Pastur threshold  $\lambda_{max}$ . We then ran ICA (using the FastICA package for Matlab, <http://research.ics.aalto.fi/ica/fastica/>) on the projection matrix to obtain the weight vectors describing the assemblies.

To assess the activation of a given cell assembly  $k$ , we computed its projection operator  $P^k$  – the outer product of its weight vector – and set its diagonal to zero. Component

activation  $A$  was defined as  $A = M^T P^k M$ .

### Predicting delta spikes from hippocampal activity

**Cross-correlations** To compute the correlation of hippocampal ripple activity and delta spikes with a temporal delay  $k$  (between -500 ms and 500 ms with a step of 10 ms), we considered each cross-structural pair of neurons  $i$  and  $j$ , where  $i$  is a prefrontal neuron and  $j$  is a putative pyramidal neuron in the hippocampus. We first discarded delta waves which did not involve hippocampal activity within a 200 ms window centered on  $(t_{\text{delta}} + k)$ . We then counted the number of spikes emitted by neuron  $i$  within 15 ms of each remaining  $t_{\text{delta}}$ , producing the delta spike vector  $D_i$ . We also counted the number of spikes emitted by  $j$  in a 200-ms window centered on  $(t_{\text{delta}} + k)$ , yielding a spike vector  $H_{kj}$ . We computed the Spearman’s rank-order correlation between  $D_i$  and  $H_j^k$ , yielding  $\rho_{ijk}$ . To produce the plots in Figs. 3A and 4C, we took the average and s.e.m. of  $\rho_{ijk}$  over all the values of  $i$  and  $j$  for a given temporal distance  $k$ .

To compute the correlation of hippocampal ripple activity and the activation of a given component, we repeated the above procedure, replacing the delta spike count of the  $i$ th neuron  $D_i$  with the activation of the  $i$ th cell assembly  $A_i$ .

To assess the significance of the cross-correlation, we repeated the above procedure introducing a shift in the events, measuring the correlation between the hippocampal activity centered on  $(t_{\text{delta}} + k)$  and the delta spikes emitted during  $t_{\text{delta}+1}$ , producing the control correlations  $\rho_{ijk}^{\text{shifted}}$ . The advantage of this approach relative to shuffling all events randomly is that it only disrupts fine timescale correlations and preserves slow correlations, which may be due to other factors that cells are independently modulated by, such as sleep progression or depth.

To compute the enrichment plots in Figs. 3B and 4D, we computed the distribution of correlation values of  $\rho_{ijk}$  for a given  $k$ , and subtracted from it the distribution of

correlation values of shifted control data  $\rho_{ijk}^{shifted}$ .

**Generalized Linear Model (GLM)** To estimate the predictive power of hippocampal ripple activity, we used prediction gain defined by (22). Briefly, for each prefrontal neuron  $i$  we trained a Generalized Linear Model (GLM) to predict its binary delta spike vector  $D_i$ , using the matrix  $H$  containing the spike count of each hippocampal pyramidal neuron in the 200 ms window preceding the delta wave ( $H_{mj}$  is the number of spikes emitted by neuron  $j$  before the  $m$ th delta wave). For each prediction of the GLM, we performed multi-fold cross-validation, where we split the delta waves into  $n$  non-overlapping groups, where  $n$  is the number of delta waves in which neuron  $i$  fired, such that each of the partitions had the same number of silent and non-silent delta waves. When predicting the activity of a given partition to test the model, we used the other partitions to training the model. The quality of the prediction was estimated by comparing the average prediction error  $e$  to the average error  $e_{shuffled}$  given by shuffling the predictions relative to the real data  $D_i$  1,000 times. Prediction gain  $g$  was then  $g = e_{shuffled}/e$  (22).

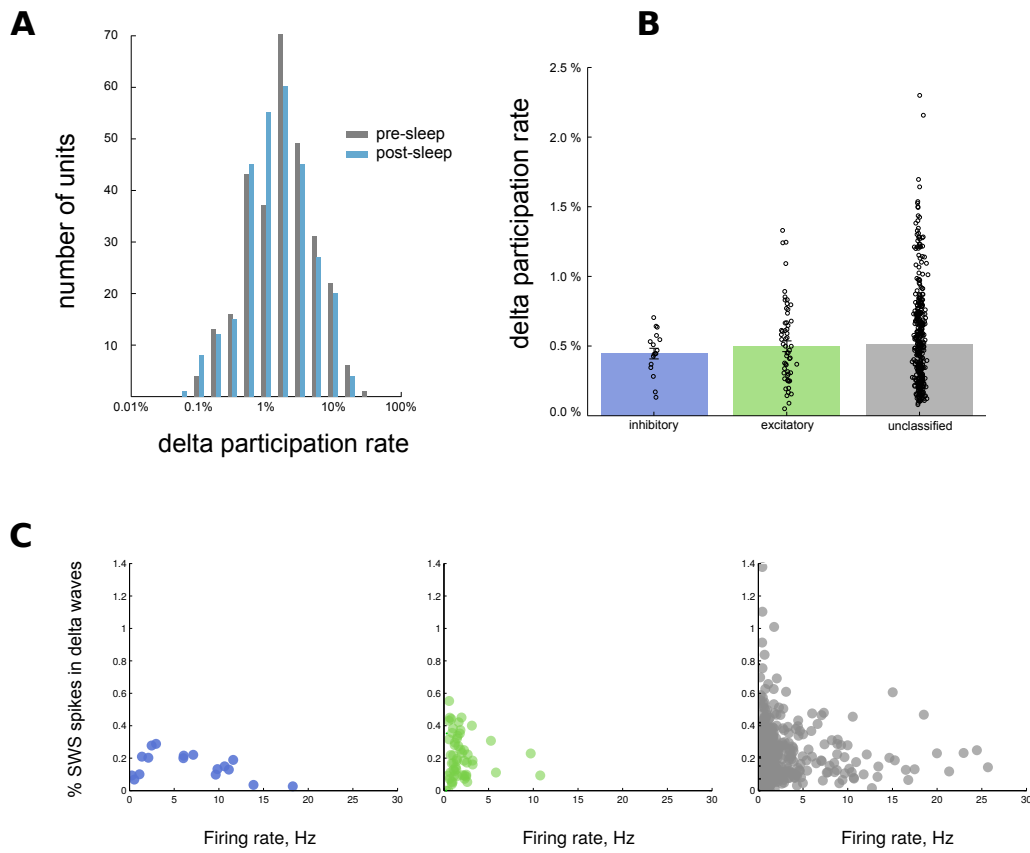


**Fig. S1.** Neuronal firing in delta waves. **A.** Distribution of the delta participation rate (the proportion of delta waves in which a neuron emitted a delta spikes) in sleep before and after a memory task. **B.** Delta participation rate for inhibitory ( $n=17$ ), excitatory ( $n=57$ ), and unclassified cells ( $n=360$ ), for which no local monosynaptic connections were found. There was no difference between the groups (Kruskal-Wallis test,  $p>0.05$ ). **C.** The proportion of slow-wave sleep spikes emitted in delta waves was not correlated with firing rate for inhibitory (left), excitatory (middle), or unclassified cells (right).

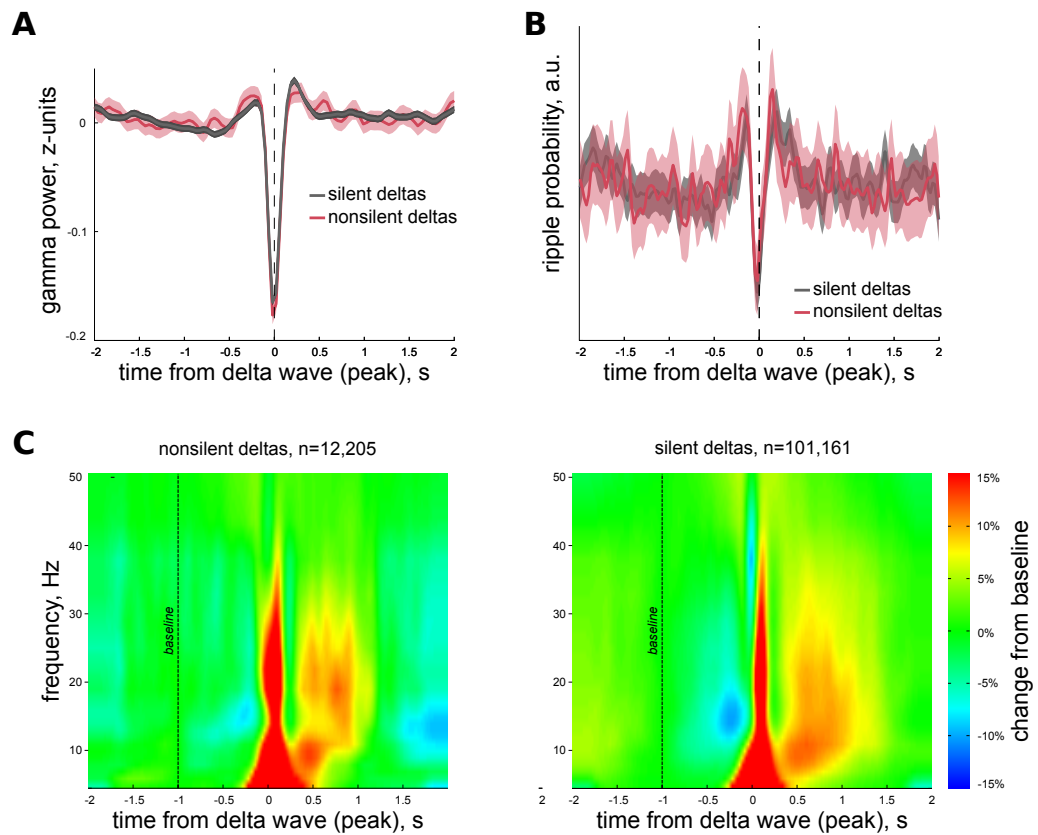


**Fig. S2.** Properties of delta waves with detected spikes in endogenous sleep. **A.** Gamma power (z-scored) around delta waves. Note that the gamma power decrease during delta waves was similar regardless of whether spikes were detected during the delta wave. **B.** Ripple coupling around delta waves. The prevalence of ripples preceding and following the delta wave did not depend on whether spikes were detected during the delta wave. **C.** Event-centered spectrograms centered on the delta wave peak. The signal in each frequency bin has been normalized by dividing it by the power for that frequency 1 s before the delta wave (baseline). Left: delta waves with detected spikes. Right: silent delta waves. Note the spindle following both non-silent and silent delta waves by 0.5–1 s.

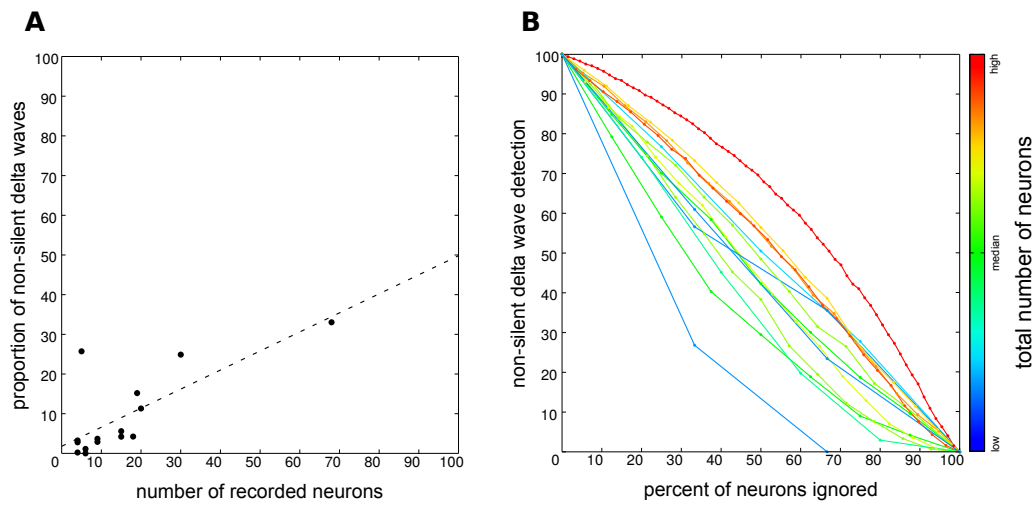


**Fig. S3.** Delta spike detection. **A.** The number of recorded neurons in each session and the proportion of delta waves in which spikes were detected. Note the correlation ( $r=0.7456$ ,  $p=0.0014$ , regression line shown). **B.** Detection of non-silent delta waves after limiting the number of recorded neurons. For each session, delta wave detection was repeated after ignoring a recorded neuron. This was repeated progressively until no neurons remained. Non-silent delta wave detection is computed as the proportion of non-silent delta waves in these limited datasets compared to baseline, where all recorded neurons were taken into account. Sessions are colour-coded based on the total number of neurons recorded in the session (range, 4–68). Note that the proportion of delta waves with detected delta spikes is greatly underestimated in limited datasets.

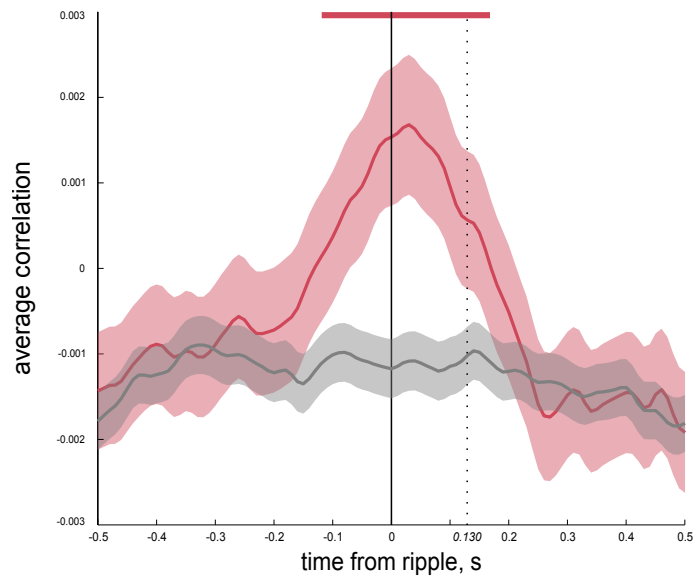


**Fig. S4.** Ripple prediction of prefrontal activity outside of delta-waves. Cross structural correlation (mean  $\pm$ s.e.m.) between hippocampal spikes during ripple activity (binned within a 100 ms window centered on the ripple peak at 0 s) and spikes in the prefrontal cortex (sliding window of 100 ms width). Real cross-correlations (red) were significantly different from a shifted control (grey) for cortical activity following ripples (red line, Monte-Carlo test,  $p < 0.05$ ). Analysis was restricted to ripples not followed by delta waves. Dotted line marks the timing of coupled delta waves relative to ripples.

## CHAPTER 6. ROLE OF DELTA SPIKES IN MEMORY CONSOLIDATION

---

The articles presented above have implications for systems memory consolidation through sleep rhythms and in particular for the role of delta waves. The following chapters present a discussion of those findings, accompanied by illustrations from our data where they relate to the subject at hand.

## **Part III**

# **Discussion**



# Chapter 7

## Delta waves

In the articles presented here, we have shown that delta waves following hippocampal ripples cause memory consolidation and reorganization of cortical networks, and that delta spikes, emitted while the rest of the network is silent, contain information about the preceding ripple. In this chapter, I discuss the implications of these findings on the role of delta waves in memory consolidation.

### 7.1 Ripple-delta coupling

In Maingret et al. (2016), we showed that boosting ripple-delta coupling by inducing delta waves upon ripple detection results in memory consolidation, but introducing a brief random delay ( $\sim 200$  ms) was introduced between ripples and triggered delta waves abolished this effect. These results indicate that the underlying mechanism was a remarkably fine temporal precision of ripple-delta coupling and that memory consolidation could not be accounted for by increased occurrences of delta waves, since the number of these events was unchanged between test and control conditions. This appears to be at odds with previous studies documenting a direct role for delta waves in memory consolidation (see section 4.1). One possibility that could explain this apparent discrepancy would be that in previous studies, boosting slow oscillations incidentally increased their coupling to hippocampal ripples, and that this coupling, rather than the reinforced slow oscillations *per se*, was instrumental in triggering improvements in memory performance.

The work presented in this thesis suggests the following sequence of events as a possible scenario for how a hippocampo-cortical dialogue involving ripple-delta coupling can lead to memory consolidation. Ripple-related activity facilitates the resurgence of cortical cell assemblies relevant to a given memory trace (Peyrache et al., 2009). This is followed by a delta wave, which isolates the cortical network from competing inputs. During the delta wave, information about the memory trace remains reflected in the activity of a minority of neurons that don't transition into a DOWN state with the rest of the network (chapter 6). This would bias the network towards information related to the memory trace at UP-state onset, which would lead to the selective reorganization of the network and memory consolidation (Maingret et al., 2016).

## 7.2 Delta spikes

While delta waves are characterized by silence, we observed neuronal activity persistent through some delta waves. It is possible that this only affects a minority of delta waves; however, we observed no differences between delta waves where we observed delta spikes (spikes from the same recording site as the delta wave was detected) and delta waves where we observed no activity. In addition to having the same waveform (see chapter 6, Fig. 1D) and the same relation with ripples, spindles, and gamma power (see chapter 6, Supp. Fig. 1) as silent delta waves, non-silent delta waves were also induced by cortical stimulation (Figure 7.1). Moreover, in one rat implanted in the thalamic reticular nucleus in addition to the prefrontal cortex, we observed the same thalamic notion that there is no inherent difference between apparently silent and non-silent delta waves apart from whether delta spikes happen to be recorded.

What is the mechanism for persistent firing during delta waves? The network hyperpolarisation at the UP-DOWN transition results from a reduction of synaptic excitation (Timofeev et al., 2001b; Bazhenov et al., 2002). Neurons particularly depolarized before the network transition might be less affected by the net decrease in synaptic, possibly enough to skip a population DOWN state. Indeed, a neuron's activity during delta waves was positively correlated with its firing before the delta wave (data not shown).

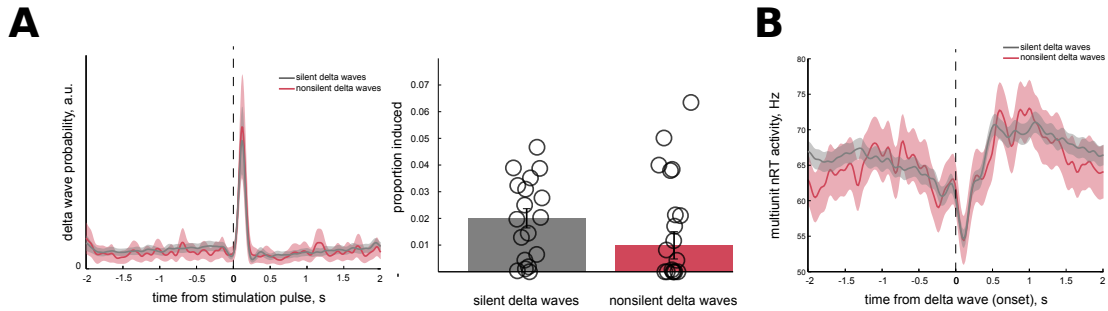


**Figure 7.1:** Non-silent delta waves. **A.** Non-silent delta waves were induced by cortical stimulation. Left: delta wave rate (mean  $\pm$  s.e.m., normalised by the total number of silent and non-silent delta waves, respectively) following cortical stimulation. Note that non-silent delta waves had the same Right: Bottom right: Proportion of delta waves (median  $\pm$  s.e.median) following stimulation pulses within 200 ms. The proportion of induced delta waves was not different between conditions (Wilcoxon signed rank test,  $p > 0.05$ ). Open circles represent individual sessions. **B.** Multiunit activity (mean  $\pm$  s.e.m.) from the thalamic reticular nucleus relative to the onset of delta waves recorded in the prefrontal cortex. Data is from a single session from one animal.

### 7.2.1 Influence on delta spikes

It is perhaps not surprising that delta spikes reflect cortical inputs. Past activity of an interconnected network influences future activity, and delta waves are often preceded by the substantial cortical response to hippocampal ripples. This can lead to the content of such ripples biasing the delta spikes emitted in the following delta waves. In this view, delta spikes may reflect the inputs arriving just before UP state termination. This often corresponds to strong inputs such as ripples, as they can trigger an UP-DOWN transition (see section 3.1.1).

In this manner, delta spikes may serve as a bridge between the activity at the end of one UP state (reflecting inputs at the UP state termination) and the onset of the following UP state, where plasticity takes place. According to this hypothesis, delta spikes during ripple-preceded delta waves should reflect hippocampal content, but delta spikes during other delta waves should reflect the activity of other partner areas beside the hippocampus. In a project with Céline Boucly and Virginie Oberto, we are investigating the interplay between the striatum and the prefrontal cortex in sleep, and preliminary analysis is in agreement with the possibility that delta spikes may also reflect striatum activity. This supports idea of delta spikes as an general mechanism for linking information between UP states involved in the communication with multiple cortical partner areas.

## 7.2.2 Influence of delta spikes

The scenario proposed in section 7.1 requires that delta spikes exert influence on the following UP state. In the coupled stimulation condition, delta spikes reflect the preceding hippocampal activity and cortical sequences at the DOWN-UP transition are modified, while in the delayed stimulation condition, delta spikes do not reflect the preceding hippocampal activity and cortical sequences at the DOWN-UP transition remain stable. Yet a direct link between the recorded delta spikes in a given delta wave and the spike sequence following that delta wave remains to be demonstrated. The method we employed to measure the stability of DOWN-UP sequences does not allow for the examination of sequences on the scale of single events. Investigating this question would therefore require the development of new data analysis tools.

What would be the impact of delta spikes on synaptic plasticity? Chauvette et al. (2012) showed that hyperpolarisation of the post-synaptic cell during DOWN states is required component for long-lasting synaptic plasticity. A synapse is thus more likely to be modified if the post-synaptic cell was hyperpolarized and therefore silent during a delta wave. Cells emitting spikes during a delta wave could participate in synaptic plasticity either as pre-synaptic cells or indirectly, by biasing network activity. Throughout the course of sleep, a cell would emit delta spikes during a minority of delta waves and undergo synaptic plasticity following delta waves in which it was silent.

Delta spikes represent an intriguing candidate mechanism for how hippocampal ripples preceding delta waves would affect the network beyond the silence. However, a causal role of delta spikes remains to be demonstrated. Electrophysiological studies in slices may elucidate how activity during delta waves may bias the following UP state, and research in in freely moving animals involving closed-loop experiments silencing cells during delta waves could demonstrate the impact of delta spikes on memory consolidation.

# Chapter 8

## Alternative mechanisms for the hippocampo-cortical dialogue

The proposed scenario for memory consolidation through ripple-delta coupling involves (1) ripples preceding delta waves stimulating relevant cortical ensembles, (2) delta waves isolating the network from competing inputs while persistent activity of small subpopulations of neurons bridges the information to the upcoming UP state, and (3) synaptic plasticity mechanisms taking place through neuronal sequences at the DOWN-UP transition as well as spindles following the delta wave. However, the hippocampo-cortical dialogue is not limited to ripple-delta-spindle coupling; notably, it includes ripples following delta waves (Isomura et al., 2006) and ripples embedded in spindles (Sirota et al., 2003). This chapter discusses these other modes of hippocampo-cortical communication as alternative mechanisms that could drive the memory consolidation effects brought about by ripple-delta coupling.

### 8.1 Delta-ripple coupling

While the information communicated to the cortex through a ripple preceding the delta wave needs to be retained within the network for the next UP state where synaptic plasticity occurs, this caveat does not apply to ripples following the delta wave. Ripples occurring immediately following delta waves and preceding spindles are well-timed to influence spindle-mediated synaptic plasticity. I therefore considered succeeding ripples as a possible mechanism driving the memory consolidation we observed in the coupled stimulation condition.

One hypothesis for how ripple-delta coupling results in memory consolidation was

that the ripple preceding the delta wave ('first ripple') serves simply to trigger a delta wave, initiating a window of communication during the subsequent UP state. In this view, the information content of the first ripple is irrelevant and need not be preserved during the delta wave to consolidated in the cortical network; rather, the first ripple increases the likelihood that the cortex would be in a more receptive state during a subsequent ripple ('second ripple'), which would follow the first ripple. In support of this hypothesis, ripple-preceded delta waves are more likely to be immediately followed by another ripple (Figure 8.1A). This may be accounted for by delta wave amplitude: ripple-preceded delta waves are more likely to be stronger (involving the synchronized DOWN state of a more extensive area around the recording site than lower-amplitude delta waves), and stronger delta waves are more likely to be immediately followed by hippocampal ripples (Figure 8.1C). This is in agreement with the hypothesis that the role of ripple-delta coupling is to ensure that delta-ripple-spindle sequences occur. However, delta waves induced by delayed stimulation were equally likely to be followed by a ripple as coupled delta waves (Figure 8.1B), and these delayed delta-ripple-spindle sequences were not sufficient to boost memory consolidation. Therefore the presence of delta-ripple-sequences cannot account for the effect of ripple-delta coupling on memory consolidation.

In an amended version of this hypothesis, the temporal proximity of the two ripples ( $\sim 250$ - $300$  ms for a ripple preceding and a ripple following the same delta waves) could affect the efficacy of the delta-ripple-spindle sequence. If recently active neurons remain more excitable in the hippocampal network, perhaps the second ripple ( $\sim 250$  ms following the first ripple) would be more likely to replay the same memory trace – restating the relevant information to the cortex (preventing the need for the cortex to retain the information during the delta wave), and also consolidating it in the hippocampus. To test this hypothesis, I directly compared the neurons active in such pairs of ripples<sup>1</sup>. Indeed, hippocampal neurons were more likely to fire in the second ripple if they had already fired in the first ripple (Figure 8.1D,E). However, this was true both in the coupled and the delayed stimulation conditions, leading me to reject the hypothesis that the second ripple is driving the effect of ripple-delta coupling on memory consolidation. The role of this second ripple in the hippocampo-cortical dialogue remains unknown.

---

<sup>1</sup>Correlations: for a given neuron, its firing rate within each ripple (100 ms window centered on the ripple peak) forms a firing rate vector  $V1$ . Each of these initial ripples is paired with the first ripple in a 200-ms temporal window fixed at a given delay  $d$  from the initial ripple. The neuron's firing rate within these partner ripples forms a firing vector  $V2$ . The correlation between  $V1$  and  $V2$  is shown for varying distances  $d$  in Figure 8.1D. Note that to avoid overlapping activity,  $d \geq 200$  ms. For computing control correlations, the partner ripples are shuffled.

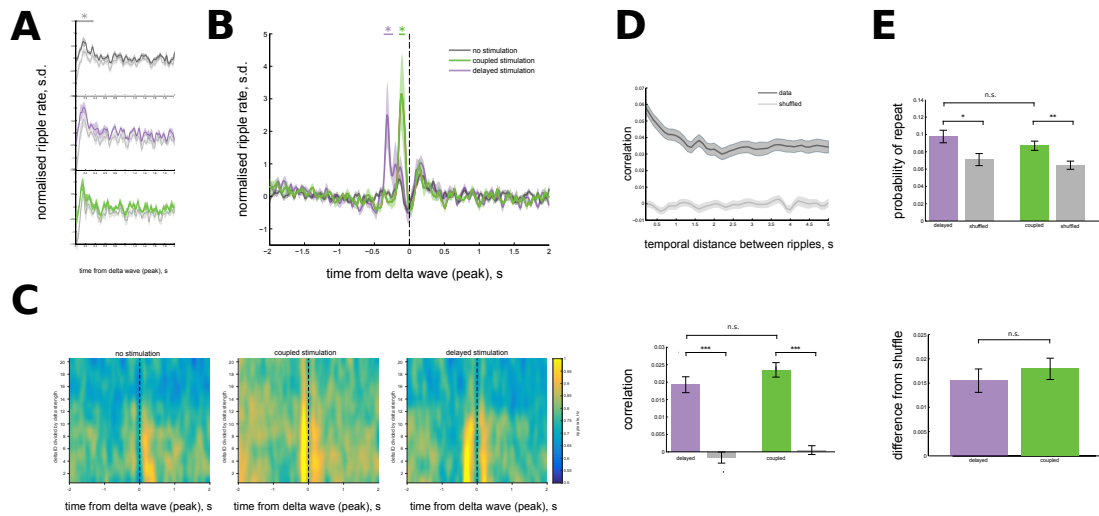


**Figure 8.1:** Ripples following ripple-coupled delta waves. **A.** Ripple rate (mean  $\pm$ s.e.m., z-scored with respect to the ripple rate 0.5–2 s away from delta waves) following delta waves preceded ( $<0.5$  s) by ripples (solid) or delta waves not preceded by ripples (pale grey). Top: non-stimulated sleep (test day in (Maingret et al., 2016)); middle: coupled stimulation; bottom: delayed stimulation. Ripple-preceded delta waves were more likely to be followed by ripples in all conditions (Monte-Carlo test, interval of significant ( $p < 0.05$ ) difference marked by line above). **B.** Ripple rate around delta waves. The two stimulation condition had more ripple-preceded delta waves than natural sleep (Monte-Carlo test, respective intervals of significant ( $p < 0.05$ ) difference marked by lines above), but the ripple rate following delta waves was the same in all conditions (Monte-Carlo test,  $p > 0.05$ ). **C.** Ripple rate depending on delta wave strength. Left: non-stimulated sleep; middle, coupled stimulation; right, delayed stimulation. In each session, delta waves have been divided in 20 quantiles depending on delta wave strength, defined as the difference in voltage between the peak and the trough. Note that ripples tend to precede and follow stronger delta waves (located at the bottom). **D.** Correlation between each hippocampal neuron's activity ( ) in pairs of ripples. Top: The correlation between the activity of each neuron in one ripple and another ripple as a function of the delay between the two ripples. Bottom: The correlation (median  $\pm$ s.e.median) between the activity of each neuron in the last ripples preceding (within 500 ms) delta waves and the first ripples following (within 500 ms) delta waves. Activity was correlated between these pairs of ripples in both stimulation conditions, but not different between conditions. Note that correlations are lower than expected for the temporal distances between the pairs ripples (see Top) possibly due to effects of the delta wave on hippocampal activity. **E.** For a given neuron active in a ripple preceding a delta wave, the probability that it will fire again in the ripple following the delta wave. Top: such repeating activity was significantly different from shuffled data (shuffled ripples following delta waves) in both conditions. Bottom: the improvement from shuffle was not different in the delayed and the coupled stimulation conditions. Shaded plots in **A**, **B** and **D** represent mean  $\pm$ s.e.m. Bars in **D** and **E** represent median  $\pm$ standard error of the median. Tests in **D** and **E** are Wilcoxon rank-sum tests, where \* $p < 0.05$ ; \*\* $p < 0.01$ , \*\*\*;  $p < 0.001$ .

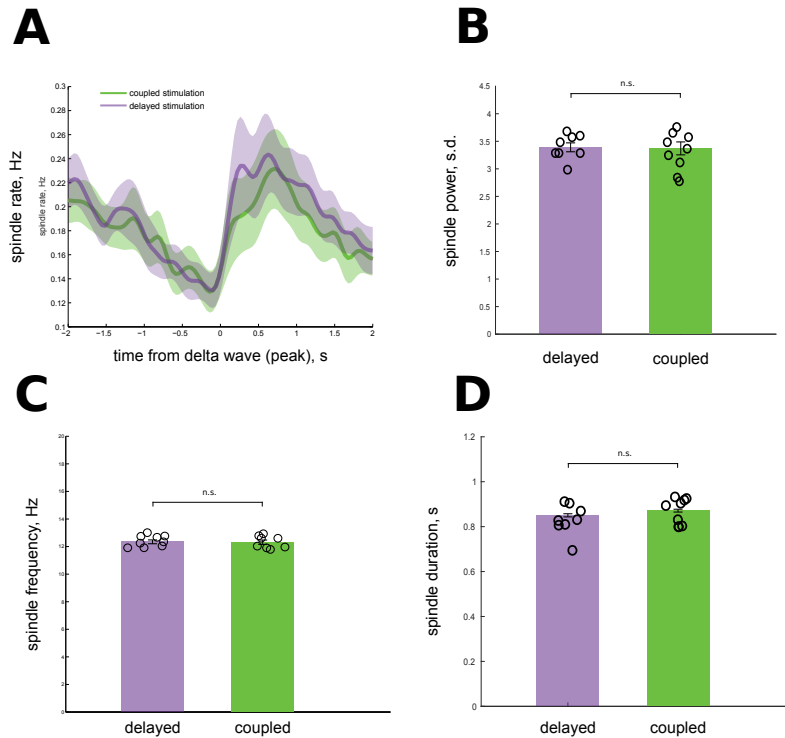


**Figure 8.2:** Spindle properties in the coupled and delayed delta stimulation conditions. **A.** Spindle rate centered on delta waves. **B.** Spindle power as detected at the spindle peak (z-scored over the whole recording session). **C.** Average spindle frequency (number of cycles divided by spindle duration). **D.** Spindle duration. Shaded plots in **A** represent mean  $\pm$  s.e.m. Bars in **B**, **C** and **D** represent median  $\pm$  standard error of the median. Tests in **B**, **C**, and **D** are Wilcoxon rank-sum tests,  $p > 0.05$  in all panels.

## 8.2 Ripple-spindle coupling

Sleep spindles, known to promote synaptic plasticity (Sejnowski and Destexhe 2000; Rosanova and Ulrich 2005, see section 3.2), are a candidate mechanism to drive the effect of ripple-delta coupling on memory consolidation. I therefore investigated how ripple-delta coupling affects spindles. Spindle rate, power, frequency, and duration were not different between the coupled and the delayed stimulation conditions (Figure 8.2), indicating the ripple-delta coupling does not affect spindle properties. It is therefore possible that synaptic plasticity takes place after coupled and delayed delta waves alike; however, the memory traces being strengthened could depend on the activity of the network around and during spindles.

It is possible that the activity immediately preceding spindles could bias neuronal activity and the synaptic plasticity processes taking place during spindles.

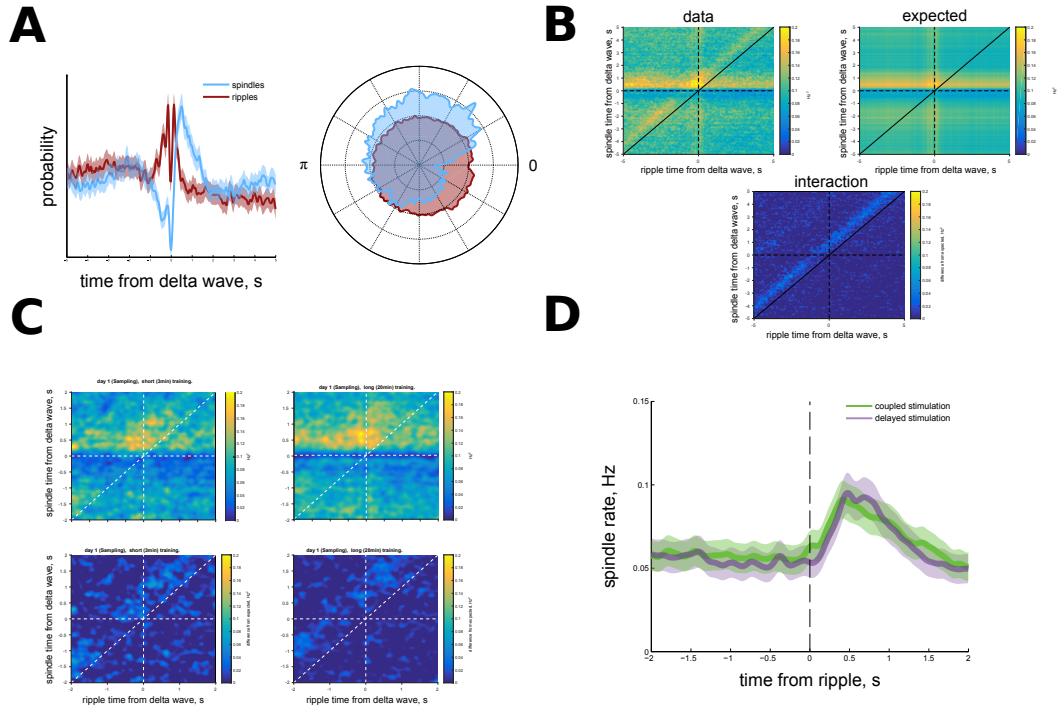


**Figure 8.3:** Spindles preceded by ripples. **A.** Ripple and spindle timing in the slow oscillation. Left: ripple and spindle occurrence relative to delta wave. Right: Probability of ripple and spindle occurrence within an UP state. Phases interpolated based on delta wave occurrence: 0 rad. corresponds to a delta wave peak and  $\pi$  rad. corresponds to the middle of the UP state duration. **B.** Left: ripple-spindle occurrence around delta waves as represented by a two-dimensional histogram, produced by multiplying  $S^T R$ , where  $S$  is a matrix of spindle occurrence and  $R$  is a matrix of ripple occurrence around delta waves (delta waves are rows in the matrix). Right: a control histogram for the expected distributions for independent ripple and spindle modulation around delta waves, produced by substituting each line of  $R$  and  $S$  by the mean ripple rate and spindle rate, respectively, removing any interactions before multiplying the matrices. Bottom: the difference between the two matrices represents the interaction between ripples and spindles. Note the diagonal representing ripple occurrence before spindles. **C.** Spindle tendency to follow ripples and memory consolidation in natural sleep following the spatial object recognition task. Top: two-dimensional histograms as described in B. Left: sleep following time-limited training on the task. Right: sleep following long training on the task. Note the increased rate of event occurrence. Bottom: interaction plots indicating the ripple-spindle relationship independent of delta waves is not stronger in sleep following long training which leads to memory consolidation. **D.** Spindle rate (mean  $\pm$  s.e.m.) centred on ripples in the stimulation and the control condition.

Spindles are preceded by the upsurge of cortical activity at the DOWN-UP transition and they may therefore potentiate synapses related to the memory trace which has been kept active possibly through delta spikes. In addition, spindles are also preceded by ripples (Siapas and Wilson 1998; Peyrache et al. 2009, see section 4.2). In part, this is orchestrated by delta waves, which are followed by both ripples and spindles, with spindles occurring later (Sirota and Buzsáki 2005, Figure 8.3A). However, ripple-spindle coupling is stronger than what would be expected if they were independently induced by delta waves (Figure 8.3B). It is possible that, like the cortical upsurge of activity at the DOWN-UP transition (Amzica and Steriade, 1997; Peyrache et al., 2011), the synchronous ripple activity may help induce sleep spindles. However, ripple-spindle coupling cannot account for the memory consolidation effects of ripple-delta coupling, because it was not different between the coupled and delayed stimulation conditions (Figure 8.3D).

One of the hallmarks of the hippocampo-cortical dialogue is the ripples nested in individual spindle cycles, which has been proposed to drive to memory consolidation (Latchoumane et al. 2017, see section 4.2). We considered the possibility that ripple-delta coupling might maximize the coordination between the hippocampal and the cortical networks following the delta wave and potentially enhance this phase-locking. However, we found no differences in ripple nesting in spindle cycles between the two conditions (Figure 8.4), indicating that coupled and delayed delta waves alike were followed by spindles with phase-locked ripples, and that the effects of ripple-delta coupling on memory consolidation cannot be accounted for by differences in this fine-tuned ripple-spindle coordination. Naturally, this does not exclude the possibility that this intact ripple-spindle phase-locking is necessary for the effects of the coupled stimulation on memory consolidation, but it was not sufficient.

### 8.3 Perspectives

While many of these alternative modes of hippocampo-cortical communications were unaffected by ripple-delta coupling, they are by no means irrelevant to the hippocampo-cortical dialogue. Successful memory consolidation might require the integration of all of these factors. Understanding the role of each phenomenon would require further investigation.

One promising line of inquiry would involve investigating the replay content taking into account the relative timing with respect to delta waves and spindles. Extended replay events spanning chains of ripples have been reported in awake animals (Davidson et al., 2009), but it is unknown whether ripples following

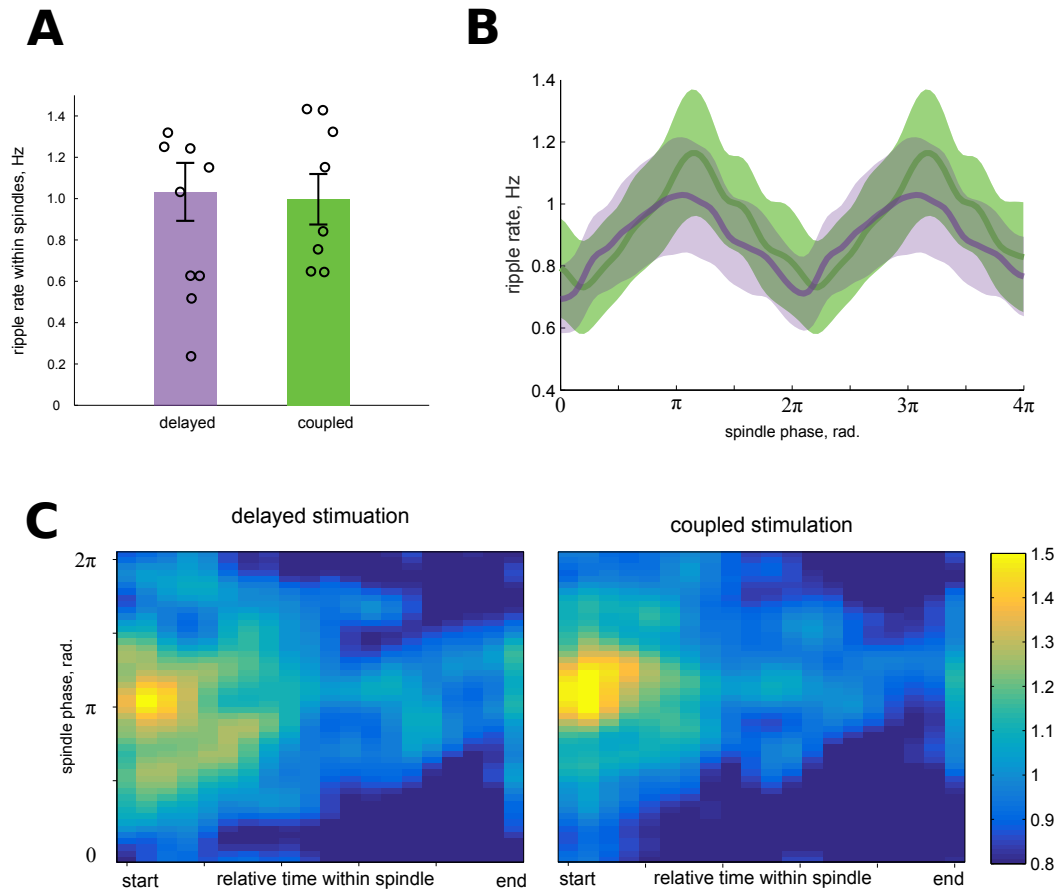


**Figure 8.4:** Ripples nested in spindles. **A.** Ripple rate (median $\pm$ s.e.median) within spindles was not affected by the coupling of the stimulation conditions (Wilcoxon rank-sum test,  $p > 0.05$ ). **B.** Ripple phase-locking to individual spindle cycles. Phases were estimated by the Hilbert transform of the filtered (9–17 Hz) signal. **C.** Ripple phase-locking throughout spindle. Each spindle was divided into 20 quantiles of equal duration, and the average ripple rate was computed for each phase bin ( $2\pi/50$ ) and each quantile across all spindles. Left: delayed stimulation condition; right: coupled stimulation condition. Note that in both conditions, ripple phase-locking peaks early within a spindle and persists throughout the spindle.

delta waves could provide additional information complementing the preceding ripple, and whether replay during sleep spindles is related. Moreover, only a small proportion of ripples have decodable replay events (it is not yet known if other ripples are noisy or have replay content we cannot decode), and it is possible that some of the relationships with cortical rhythms described here might affect these ripples disproportionately, possibly reflecting the direction of communication. Due to the nature of the task requiring a short duration of exploration, we were unable to decode replay trajectories to investigate these questions. However, new experiments in the lab are carried out by Nadia Benabdallah to collect the data that could answer these questions.

Future studies may also consider suppressing specific ripples based on their timing, in particular ripples following delta waves and ripples locked to thalamocortical spindles. Novel imaging techniques at the level of synaptic boutons, combined with field recordings, may shed light on how ripple timing affects synaptic plasticity during these events.

**Part IV**

**Appendix**



## Chapter 9

# Role of awake theta sequences in memory formation

In addition to the work on the hippocampo-cortical dialogue that has been the main focus of this thesis, I have taken part in a project testing the role of theta sequences on sleep replay.

When moving through an environment, a rat's trajectory is reflected by the place field activity on multiple timescales (Figure 9.1). On a behavioural timescale (seconds), firing fields of multiple place fields are crossed successively, reflecting the animal's trajectory. During exploration, the LFP is dominated by theta oscillations (7–14 Hz), and theta sequences reflect the trajectory on a compressed (5–10) timescale (Skaggs et al., 1996; Foster and Wilson, 2007). Theta sequences can emerge from the phase coding properties of individual place cells (Chadwick et al., 2015), although additional mechanisms may be at play (Feng et al., 2015; Middleton and McHugh, 2016).

When a rat is exploring a novel environment, NMDA receptor-dependent synaptic plasticity is required for the formation of trajectory sequences which can be later replayed during sleep ripples for memory consolidation (Silva et al., 2015). Multiple lines of evidence suggest that theta sequences are the mechanism for the initial trajectory encoding. First, the temporally compressed timescale of theta sequences is compatible with synaptic plasticity, making them a good candidate mechanism for memory formation (Skaggs et al., 1996; Wójtcowicz and Mozrzymas, 2015). Second, pharmacologically disrupting the theta oscillation impairs performance on spatial memory (Robbe and Buzsáki, 2009; Wang et al., 2015b). Incidentally, an alternative mechanism for sequence encoding has been ruled out – perturbing awake ripples has no effect on subsequent sleep replay sequences (Jadhav et al., 2012).

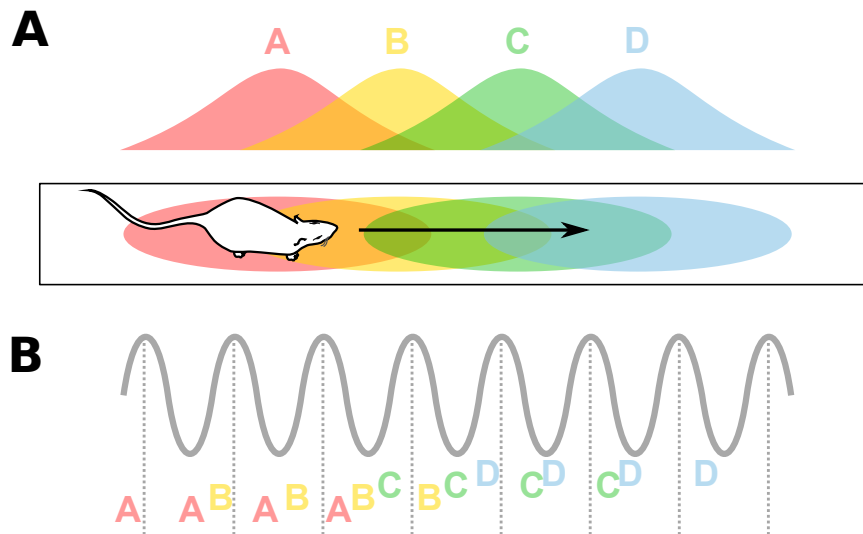


**Figure 9.1:** Hippocampal sequences during exploration. **A.** Behavioural sequences. Top: Firing rates of place cells (A,B,C, and D) on a linear track. Bottom: in a given lap, the rat crosses the place fields (ellipses) of the above place cells. **B.** Theta LFP and nested theta sequences. Within a theta cycle, place cells with overlapping place fields discharge in a sequence ( $\sim 120$  ms) reflecting the order of field traversal at a compressed time-scale.

While multiple lines of evidence suggest that theta sequences are the mechanism for the initial encoding of memory traces and trajectories that can be later replayed in sleep, this hypothesis has never been directly tested. Moreover, an alternative slow-timescale synaptic plasticity has been recently discovered, providing a possible mechanism for behavioural sequences to be encoded directly (Bittner et al., 2017).

To test the causality of theta sequences on trajectory encoding, we selectively disrupted theta sequences while preserving firing field sequences to determine if intact theta sequences were required for subsequent replay during sleep. We took advantage of the fact that passive transportation retains the spatial selectivity of place cells while perturbing their precise timing relative to theta (Terrazas et al., 2005), except if the animals actively run on an on-board treadmill (Cei et al., 2014). We thus transported rats on a model train with the on-board treadmill off ('Passive') or on ('Active'), to respectively perturb theta sequences or leave them intact. Critically, the rats were tested on a single day in an entirely novel environment (different from the training room), in order to avoid any network plasticity changes due to previous experience of the environment. We found that following selective disruption of theta sequences, sleep replay remained at baseline levels observed prior to experience, while intact theta sequences resulted in boosted replay during subsequent sleep. Our results show that theta sequences of hippocampal cell assemblies underlie subsequent replay during sleep, supporting

---

the view that theta sequences are the substrate of the initial formation of memory traces subsequently consolidated during sleep.

All the experiments were performed by Céline Drieu. My contribution to this project was with some of the data analyses; in particular, the implementation of the sequence scoring measure of Davidson et al. (2009) and its adaptation for circular data, correlations between individual sequences, the detection of LFP events (ripples and asymmetric theta cycles), and phase precession analyses.

# Nested Sequences of Hippocampal Assemblies During Behavior Support Subsequent Sleep Replay

Céline Drieu,<sup>1</sup> Ralitsa Todorova,<sup>1</sup> Michaël Zugaro,<sup>1\*</sup>

<sup>1</sup>Center for Interdisciplinary Research in Biology (CIRB),  
Collège de France, CNRS, INSERM, PSL Research University, Paris, France

\*Corresponding author. E-mail: michael.zugaro@college-de-france.fr

**Consolidation of spatial and episodic memories is thought to rely on replay of neuronal activity sequences during sleep. However, the network dynamics underlying the initial storage during wake have never been tested. While slow, behavioral timescale sequences have been claimed to sustain sequential memory formation, fast (‘theta’) timescale sequences, nested within slow sequences, could be instrumental. We found that during passive travel, place cells formed behavioral timescale sequences but theta sequences were degraded, resulting in impaired subsequent sleep replay. In contrast, when the rats actively ran during transportation, place cells generated clear theta sequences and accurate trajectory replay during sleep. Our results support the view that nested sequences underlie the initial formation of memory traces subsequently consolidated during sleep.**

The sequential activation of neuronal ensembles is a ubiquitous brain coding scheme possibly underlying numerous diverse behaviors (1–4). Sequential neuronal activity occurs at different timescales, ranging from slow (‘behavioral’) timescales, where the dynamics are constrained by stimulus or motor time constants, to fast (‘endogenous’) timescales mostly driven by intrinsic network properties. A prominent example is the hippocampus, where place cells code for an animal’s location (5). As the animal explores its environment, different place cell ensembles become successively active along the ongoing trajectory, yielding sequences of neuronal activity at the behavioral timescale. During subsequent slow wave sleep (SWS), the same sequences are endogenously replayed during sharp-wave ripple (SWR) complexes, at a highly accelerated (20x) timescale (6), mediating memory consolidation during sleep (7–10). How is the sequential organization of place cell assemblies maintained across these two timescales expressed at entirely disjoint moments in time and during different brain states?

Sequential information could be readily stored during exploration in the hippocampal network by the sequential activation of place cells at the behavioral timescale, via a recently uncovered form of behavioral timescale plasticity (11). An intriguing alternative is that sequential structure is stored via the remarkable property of the hippocampal network to generate nested sequences of cell assemblies, whereby both slow and fast neural sequences are intermingled in time. This occurs during spatial navigation: nested within behavioral timescale sequences, the hippocampal network also produces sequences at the ‘theta’ timescale (one sequence per theta cycle of  $\sim 150$  ms, (12–14)) allowing cell assemblies to fire within brief delays ( $\sim 25$  ms, (15)) compatible with classical Hebbian plasticity, such as spike-timing dependent plasticity (16). Are these nested sequences of hippocampal cell assemblies required for subsequent sleep replay (12, 13), or are they but a stunning epiphenomenon, deriving from preexisting connectivity within the hippocampal network (17–19)?

Contrasting these predictions requires a protocol that selectively disrupts fast, theta se-

quences, but preserves slow, behavioral sequences of place cell assemblies. Further crucial constraints are the necessity to target the entire hippocampal formation (both in terms of extent, to overcome information redundancy along the septo-temporal axis of the hippocampus, and in terms of fields, to overcome compensatory network mechanisms such as pattern completion in CA3 which could restore locally induced impairments), as well as the ability to trigger or release theta sequence disruption with temporal precision. During passive transportation in space, place cells remain spatially selective, but their precise timing relative to theta ('phase precession', (12)) is altered (20), except if the animals actively run on an onboard treadmill (21). We thus transported rats on a model train (Fig. S1A), and turned the onboard treadmill off (Passive) or on (Active), to respectively perturb nested sequences or leave them intact. The goal was to determine if intact nested sequences were required for subsequent replay during SWS. The rats were tested in an entirely novel environment, different from the training room. Hence, hippocampal activity was monitored as the animals learned a novel spatial context, which is known to induce the formation of a novel hippocampal map, increase network coordination, boost replay and enhance plasticity (22–25). Further, because the rats were tested on a single day, this avoided any confounding network changes that could have resulted from previous experience.

We recorded CA1 pyramidal units and local field potentials in five rats. Following a baseline sleep session, the rats underwent three travel sessions (Passive 1, Active, Passive 2) interspersed with sleep sessions (Fig. 1A). The train velocity, number of laps and recording duration were similar in all conditions for all rats (Fig. S1B-D). We first verified the presence of place cell sequences at the behavioral timescale in all three conditions. Pyramidal cells always coded for the location of the animal in space (Figs. 1B and S2). Their fields remained similar in terms of size (Figs. 1C and S3), and together covered the entire train track (Fig. S2C). However, peak firing rates and place cell count were somewhat reduced during passive travels (Figs. 1C and S2B; (20)); specific controls for these factors will be provided in ensuing analyses. Incidentally,

we also confirmed that place fields did not undergo random remapping (Figs. 1D and S2D). This further supported that hippocampal dynamics were virtually identical at the slow timescale in all travel sessions.

Clear theta oscillations with similar frequencies were observed in all conditions (Fig. 2A). However, during passive travel, power was slightly reduced at both the fundamental frequency and first harmonic, the latter resulting in decreased cycle asymmetry, indicative of a change in the internal structure of theta cycles (Fig. 2A-B). This was expected to alter the precise spike timing of active cell assemblies. Consistently, while place cells continued to oscillate slightly faster than theta ('phase precession') during active travel, this was reduced in passive travel (Figs. 2C-D and S4A-B), indicating an overall degradation of phase precession (Fig. 2E-F; in phase precessing neurons, phase range was similar in all conditions (26), Fig. S4C-E). This degradation was noteworthy, because phase precession is thought to be instrumental for the formation of nested sequences: because place cells normally oscillate slightly faster than theta, they emit spike bursts earlier and earlier in successive theta cycles; this (possibly combined with additional coordinating mechanisms (27, 28)) results in newly activated cells to fire after those that have started firing in earlier cycles, effectively resulting in temporal sequences of activity.

To directly assess how perturbation of phase precession affected theta sequences, we used a Bayesian reconstruction approach (21, 29, 30). Briefly, theta cycles were subdivided in 6 phase bins, and the sequential structure of reconstructed positions in these bins ('candidate events') was evaluated using two previously described complementary measures (30): trajectory scores (normalized to compare across animals and conditions, see Methods), which assess the quality (linearity) of the reconstructed events, i.e. whether the events represent spatially aligned positions vs mere series of random locations; and slopes, which estimate the speed at which reconstructed events are played and indicate whether the events do move through space vs remain merely stationary (absence of actual trajectories). Thus, clear theta sequences would be

characterized by both high scores and slopes, whereas static representations of current position would result in high scores but low or zero slopes, and random activity would be associated with low scores (but possibly spuriously high slopes). Clear sequential structure was readily visible in individual theta cycles during active, but not passive, travel (Fig. 3A). This was confirmed over all theta cycles for all rats (Figs. 3B and S5). While normalized trajectory scores were significantly better than chance in all conditions (Fig. 3C), slopes were significantly steeper during active travel (Figs. 3D and S5C-D). Joint analysis of trajectory scores and slopes revealed a much greater proportion of high-value pairs during active travel (Fig. 3E). To confirm and extend these results using an independent measure, we computed the quadrant score (27) of each candidate event, which assessed the overall direction of reconstructed trajectories without assuming constant velocity. Quadrant scores were significantly greater for active travel (clear trajectories), and remained very low for passive travel (degraded trajectories) (Figs. 3F and 5B).

Hence, theta sequences were degraded during passive travel. Note that reconstruction quality and quadrant scores were higher in Passive 2 than in Passive 1 (Fig. 3E-F). This argues that sequential structure was slightly less degraded in the second passive travel session (Fig. 3B). This is further supported by higher self-consistency of theta sequences (see Methods) in Passive 2 compared to Passive 1, while Active sequences were the most self-consistent (Figs. 3G and S6A).

We controlled that our results could not be accounted for by differences in the number of simultaneously recorded place cells (Fig. S7) and their firing rates (Fig. S8). We also controlled for decoding quality (see Methods and Fig. S9), ruling out a potential bias due to differences in spatial coding, both at the single cell and at the population level. Finally, because small variations in field locations between individual laps could have altered sequence detection, we also ruled out differences in firing variability between travel conditions (see Methods; Fig. S10).

Taken together, the above results show that place cell sequences at the behavioral timescale

were present in all three conditions, but theta sequences were disrupted during passive travel, when stationary network activity continued to reflect the ongoing position at the endogenous timescale. How did this impact subsequent activity during slow wave sleep? Candidate replay events were defined as transient surges in aggregate firing rate (30) during SWS epochs (Fig. S11C), which coincided with SPW-R events (Fig. S11F-G; results remained unchanged when candidate events were restricted to ripples, Fig. S12). The average SWS duration, number of candidate events and ripple occurrence rate were not significantly different across animals (Figs. S11A-F). To reconstruct replayed trajectories, the Bayesian decoder was first trained using place cell activity recorded during the preceding travel session, then tested during SWS on candidate events subdivided into 20 ms non-overlapping time windows (see Methods).

Candidate replay events were evaluated using the same method as theta sequences, whereby genuine sequences are characterized by both high trajectory scores and slopes. While candidate events with significant trajectory scores were present in all three sleep sessions, overall the reconstructed trajectories were notably sharper following active travel (Figs. 4A and S13A), and scores were significantly improved relative to baseline (see Methods) only in sleep sessions following Active and Passive 2 (Fig 4B). In addition, slopes were significantly steeper following Active (Figs. 4C and S13B). Joint analysis of trajectory scores and slopes confirmed a much greater proportion of high value pairs following active travel (Figs. 4D and S13C-D).

We next addressed the critical question of whether these trajectories did constitute genuine replay of awake behavior, or merely reflected preexisting connectivity patterns independent of experience. We compared the proportion of significant trajectories in each sleep session relative to baseline sleep, i.e. relative to the sleep session preceding any exploration of the environment (as pointed out above, recordings took place in an entirely novel environment). We did not observe replay during sleep following Passive 1 (Fig. 4E), when theta sequences had been selectively disrupted (Fig. 3). Trajectory replay was then boosted in sleep following Active

(Fig. 4E), when nested sequences had remained intact (Fig. 3). Finally, an intermediate but significant level of reactivation was observed following Passive 2 (Fig. 4E), when theta sequences had been perturbed to a lesser degree than during Passive 1 (Fig. 3). Interestingly, while forward and backward trajectories were found in equal proportions during sleep following passive travel, only active travel resulted in a greater proportion of forward replay actually reflecting awake experience (Fig. 4F). Finally, a direct comparison of theta and replay sequences (see Methods) highlighted a selective correlation between theta sequences in Active and candidate replay events in subsequent sleep (Figs. 4G and S6B-C).

Our results thus show that during sleep following selective disruption of theta sequences (Passive 1), the proportion of significant trajectories remained at baseline levels observed prior to experience. By contrast, intact nested sequences (Active) resulted in boosted replay during sleep, and trajectories in hippocampal space were preferentially replayed in the same direction as in physical space. In Passive 2, theta sequences were perturbed to a lesser degree than in Passive 1, yielding intermediate levels of trajectory replay during subsequent sleep. This has three implications. First, repeated experience alone cannot account for the improved replay following Active, because replay was degraded following Passive 2. Second, the improved theta sequences during Passive 2 compared to Passive 1 are consistent with the notion that replay following Active resulted in consolidation (7–10), possibly consisting of functional network changes (12, 13), that carried over to subsequent sessions. Third, during Passive 2, scrambled activation of place cells at the theta timescale appears to have interfered with previously formed and consolidated memory traces (during Active and subsequent sleep), resulting in degraded replay during sleep after Passive 2.

How would nested sequences be altered during passive travel? In the absence of active locomotor signals, spike bursts of pyramidal cells recurred at slightly longer time intervals, consistent with the fact that bursting frequency increases with running speed (12, 31). As predicted

by theoretical models (13, 14, 32, 33), this decrease in oscillation frequency resulted in impaired theta phase precession and prevented the formation of theta sequences. Theta sequences have been related to memory performance (34, 35), although the underlying mechanisms have remained unclear. Our results indicate a causal link between theta sequences and sleep replay for memory consolidation, and suggest that behavioral timescale sequences are insufficient to store sequential information for reactivation during subsequent sleep. Nested sequences, emerging from independently phase precessing place cells (13, 33), enabled hippocampal assemblies to fire dozens of milliseconds apart, which is optimal for classical plasticity mechanisms (16) and can reinforce synaptic connections (13, 14). This would effectively store sequential organization as network connectivity patterns, which can later be replayed during sleep for long term consolidation (7–10). Spatio-temporal spike patterns supporting nested sequences have also been reported in the striatum (36) and medial prefrontal cortex (37). This may represent a general neural mechanism to encode and store initial memory traces, and plan future actions (34, 38).

## References

1. A. J. Peters, S. X. Chen, T. Komiyama, *Nature* **510**, 263 (2014).
2. T. S. Okubo, E. L. Mackevicius, H. L. Payne, G. F. Lynch, M. S. Fee, *Nature* **528**, 352 (2015).
3. K. MacLeod, G. Laurent, *Science* **274**, 976 (1996).
4. E. Pastalkova, V. Itskov, A. Amarasingham, G. Buzsáki, *Science (New York, N.Y.)* **321**, 1322 (2008).
5. J. O'Keefe, L. Nadel, *The hippocampus as a cognitive map* (Clarendon Press, Oxford, 1978).
6. A. K. Lee, M. A. Wilson, *Neuron* **36**, 1183 (2002).
7. G. Buzsáki, *Neuroscience* **31**, 551 (1989).
8. G. Girardeau, K. Benchenane, S. I. Wiener, G. Buzsáki, M. B. Zugaro, *Nature Neuroscience* **12**, 1222 (2009).
9. V. Ego-Stengel, M. A. Wilson, *Hippocampus* **20**, 1 (2010).
10. N. Maingret, G. Girardeau, R. Todorova, M. Goutierre, M. Zugaro, *Nat. Neurosci.* **19**, 959 (2016).
11. K. C. Bittner, A. D. Milstein, C. Grienberger, S. Romani, J. C. Magee, *Science* **357**, 1033 (2017).
12. J. O'Keefe, M. L. Recce, *Hippocampus* **3**, 317 (1993).
13. W. E. Skaggs, B. L. McNaughton, M. A. Wilson, C. A. Barnes, *Hippocampus* **6**, 149 (1996).

14. G. Dragoi, G. Buzsáki, *Neuron* **50**, 145 (2006).
15. K. D. Harris, J. Csicsvari, H. Hirase, G. Dragoi, G. Buzsáki, *Nature* **424**, 552 (2003).
16. J. C. Magee, D. Johnston, *Science (New York, N.Y.)* **275**, 209 (1997).
17. M. V. Tsodyks, W. E. Skaggs, T. J. Sejnowski, B. L. McNaughton, *Hippocampus* **6**, 271 (1996).
18. G. Dragoi, S. Tonegawa, *Nature* **469**, 397 (2011).
19. A. D. Grosmark, G. Buzsáki, *Science* **351**, 1440 (2016).
20. A. Terrazas, *et al.*, *J Neurosci* **25**, 8085 (2005).
21. A. Cei, G. Girardeau, C. Drieu, K. E. Kanbi, M. Zugaro, *Nature Neuroscience* **17**, 719 (2014).
22. S. Leutgeb, J. K. Leutgeb, A. Treves, M. B. Moser, E. I. Moser, *Science* **305**, 1295 (2004).
23. S. Cheng, L. M. Frank, *Neuron* **57**, 303 (2008).
24. J. O'Neill, T. J. Senior, K. Allen, J. R. Huxter, J. Csicsvari, *Nature Neuroscience* **11**, 209 (2008).
25. S. Li, W. K. Cullen, R. Anwyl, M. J. Rowan, *Nature Neuroscience* **6**, 526 (2003).
26. A. P. Maurer, S. L. Cowen, S. N. Burke, C. A. Barnes, B. L. McNaughton, *Hippocampus* **16**, 785 (2006).
27. T. Feng, D. Silva, D. J. Foster, *J. Neurosci.* **35**, 4890 (2015).
28. S. J. Middleton, T. J. McHugh, *Nat. Neurosci.* **19**, 945 (2016).

29. K. Zhang, I. Ginzburg, B. L. McNaughton, T. J. Sejnowski, *J Neurophysiol* **79**, 1017 (1998).
30. T. J. Davidson, F. Kloosterman, M. A. Wilson, *Neuron* **63**, 497 (2009).
31. C. Geisler, *et al.*, *Proceedings of the National Academy of Sciences of the United States of America* **107**, 7957 (2010).
32. N. Burgess, M. Recce, J. O'Keefe, *Neural Networks* **7**, 1065 (1994).
33. A. Chadwick, M. C. W. van Rossum, M. F. Nolan, *ELife* **4** (2015).
34. D. Robbe, G. Buzsáki, *The Journal of Neuroscience : the Official Journal of the Society for Neuroscience* **29**, 12597 (2009).
35. Y. Wang, S. Romani, B. Lustig, A. Leonardo, E. Pastalkova, *Nat. Neurosci.* **18**, 282 (2015).
36. M. A. A. van der Meer, A. D. Redish, *J. Neurosci.* **31**, 2843 (2011).
37. M. W. Jones, M. A. Wilson, *PLoS Biol* **3**, e402 (2005).
38. A. M. Wikenheiser, A. D. Redish, *Nat. Neurosci.* **18**, 289 (2015).
39. L. Hazan, M. Zugaro, G. Buzsáki, *J Neurosci Methods* pp. 207–216 (2006).
40. N. Schmitzer-Torbert, J. Jackson, D. Henze, K. Harris, A. D. Redish, *Neuroscience* **131**, 1 (2005).
41. B. E. Pfeiffer, D. J. Foster, *Nature* **497**, 74 (2013).
42. M. A. Belluscio, K. Mizuseki, R. Schmidt, R. Kempster, G. Buzsáki, *The Journal of Neuroscience : the Official Journal of the Society for Neuroscience* **32**, 423 (2012).
43. R. Kempster, C. Leibold, G. Buzsáki, K. Diba, R. Schmidt, *Journal of Neuroscience Methods* **207**, 113 (2012).

44. Z. J. Roth, Ph.D. thesis, University of Nebraska (2015).

## Acknowledgments

We thank D. Robbe for comments on an earlier version of the manuscript, Y. Dupraz for technical support, and A.C. Segú for help in animal training. This work was supported by the Agence Nationale de la Recherche (ANR-15-CE16-0001-02), French Ministry of Research (C.D.), Collège de France (C.D.), and a joint grant from École des Neurosciences de Paris Île-de-France and LabEx MemoLife (ANR-10-LABX-54 MEMO LIFE, ANR-10-IDEX-0001-02 PSL\*) (R.T.). The authors declare no competing interests. C.D. and M.Z. designed the study. C.D. performed the experiments. C.D., R.T. and M.Z. designed the analyses. C.D. and R.T. performed the analyses. C.D. and M.Z. wrote the manuscript. Data of this study were stored and curated in servers of the Collège de France, Paris, France.

## Figure Legends

**Fig. 1. Maintenance of behavioral timescale properties.** (A) Behavioral protocol. In a novel environment, rats underwent three successive travel sessions (Passive 1–Active–Passive 2), interspersed with sleep recordings (see also Fig. S1). Passive travel was intended to selectively perturb spike timing at the theta, but not at the behavioral, timescale. (B) Linearized normalized firing curves of place cells recorded from one example rat across travel sessions, showing complete track coverage in all conditions. (C) Place field size was maintained across travel conditions (KW test,  $P > 0.05$ ). Peak firing rates were somewhat lower in Passive 1 than Active (KW test,  $*** P < 10^{-4}$ ). (D) Firing fields did not remap between Passive 1 and Active (left), nor between Active and Passive 2 (right). Left, mean unsigned proportional shifts  $\sigma$  (vertical grey lines; P1–A,  $**P < 0.01$ ; P2–A,  $***P \sim 0$ ) and  $\sigma$  distributions for  $n = 2,000$  bootstrapped remapping data sets (black histograms). Insets, circular distributions of angular differences between place field peak locations on the maze (P1–A, Rayleigh test,  $***P < 0.001$ , V-test against 0,  $***P < 10^{-4}$ ; A–P2, Rayleigh test,  $***P < 10^{-9}$ , V-test against 0,  $***P < 10^{-11}$ ). Right, spatial cross-correlograms of firing fields across successive travel sessions (x axis normalized to field size; black dots represent correlogram modes; top black histograms, mode distributions).

**Fig. 2. Perturbation of single-cell theta timescale properties.** (A) Theta maintenance across travel sessions. Top: example raw LFPs (duration, 1 s). Center: power spectrograms (arrow and black dashed line, time of LFP traces shown above; black calibration bar, 15 s). Bottom: normalized power spectra (mean  $\pm$  s.e.m.). (B) While theta frequency was unchanged across conditions (top; rmANOVA,  $P < 0.90$ ), theta power (middle; rmANOVA,  $***P < 10^{-6}$ ) and shape (bottom, theta asymmetry; KW test,  $P < 10^{-84}$ ) were altered during passive travel (frequency and power, mean  $\pm$  s.e.m.) (C–D) During passive travel, spike bursts recurred at lower rates, closer to baseline theta frequency. (C) Distributions of spectral modes of spike trains (measured relative to theta frequency, x axis trimmed at  $\pm 25\%$  around theta frequency). (D) Spectral modes ( $***P < 10^{-6}$ ,  $*P < 0.02$ ). (E–F) Theta phase precession was perturbed during passive travel. (E) Average normalized phase precession density plots for significantly phase-precessing cells (blue indicates minimum, and red maximum, spike density). (F) Distribution of phase precession slopes for all place cells (KS test,  $**P < 0.008$ ,  $*P < 0.04$ ; colored dashed vertical lines, medians).

**Fig. 3. Perturbation of theta sequences.** (A) Top: raw LFPs and place cell spikes in 6 example theta cycles (black dashed lines, theta peaks; place cells are ordered by their place field location on the track) in each travel condition (black calibration bars, 50 ms). Bottom: Bayesian reconstruction of position encoded in the ongoing activity of the hippocampal network (6 phase windows per theta cycle; white vertical lines, theta peaks; white dashed lines, actual position of the animal). (B) Average Bayesian reconstruction of position (relative to actual position of the animal) across theta subcycles for all rats. Trajectory score and slope are indicated above each reconstruction. Two cycles are shown for clarity. (C) Left: normalized score of theta sequences (KW test,  $***P < 10^{-23}$ ). Right: proportion of significant theta sequences (P1: 7.95%, A: 13.61%, P2: 9.05%; all proportions are significantly greater than shuffled control proportions, Monte-Carlo test,  $***P \sim 0$ ). (D) Distributions of significant theta sequence slopes (KS tests; left: P1–A,  $***P < 10^{-16}$ ; right: A–P2,  $***P < 10^{-18}$ ). Colored bands indicate significant differences. (E) Distribution of theta sequence quality assessed by joint trajectory score and slope (for all animals; color codes for proportion normalized relative to shuffled control data). (F) Quadrant score computed from individual theta cycles (KW test,  $***P < 10^{-24}$ ). (G) Sequences were stable only during active travel. Pairwise bias correlation between awake theta sequences (ordered according to time of occurrence). Note absence of correlation during P1, and progressive decay following A during P2.

**Fig. 4. Replay is degraded following perturbation of theta sequences.** (A) Examples of significant replay events in post sleep sessions (see Fig. S13 for more examples). (B) Scores of replay events relative to baseline sleep (KW test,  $***P < 10^{-17}$ ). (C) Absolute slopes of replay events (KW test,  $***P < 10^{-27}$ ). (D) Distribution of replay quality assessed by joint trajectory score and slope (for all animals; color codes for proportion normalized relative to shuffled control data). (E) Proportion of significant replay events relative to baseline sleep. Sleep replay was boosted following active travel, compared to passive travel. (F) Proportion of forward (darker colors) vs reverse (lighter colors) replay events. (G) Pairwise bias correlation between awake theta sequences and sleep replay (ordered according to time of occurrence).

## Supplementary materials

Materials and Methods

Supplementary Text

Figs. S1 to S13

References (39-44)

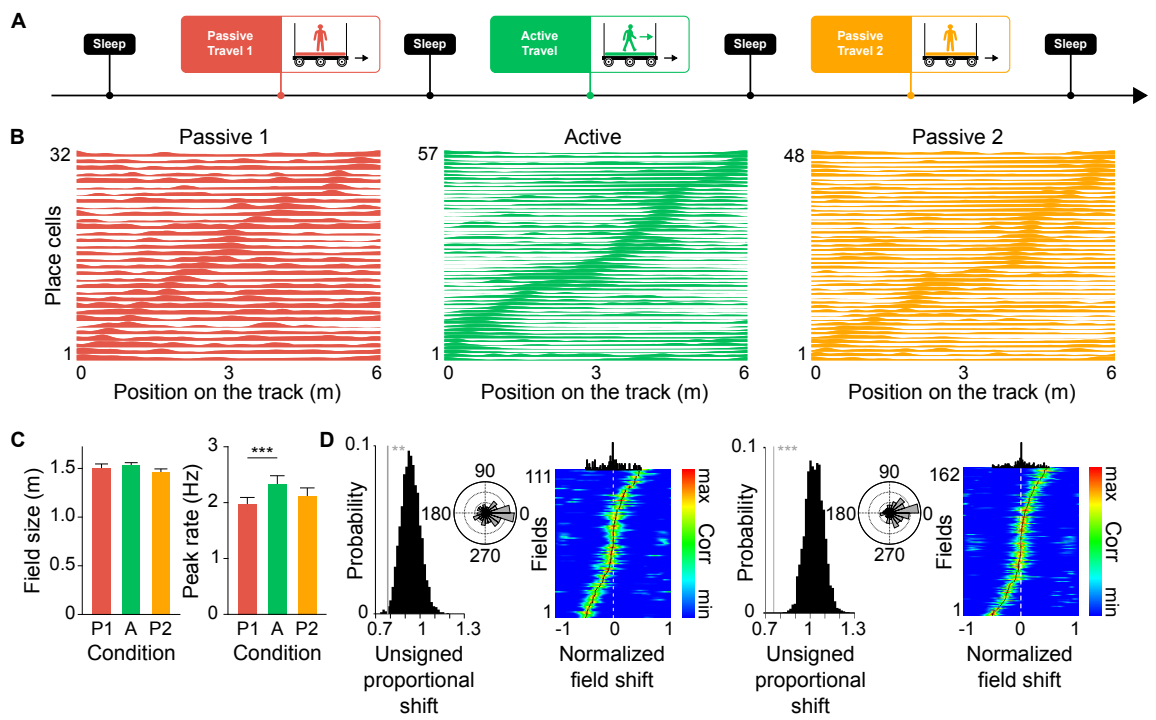


Figure 1

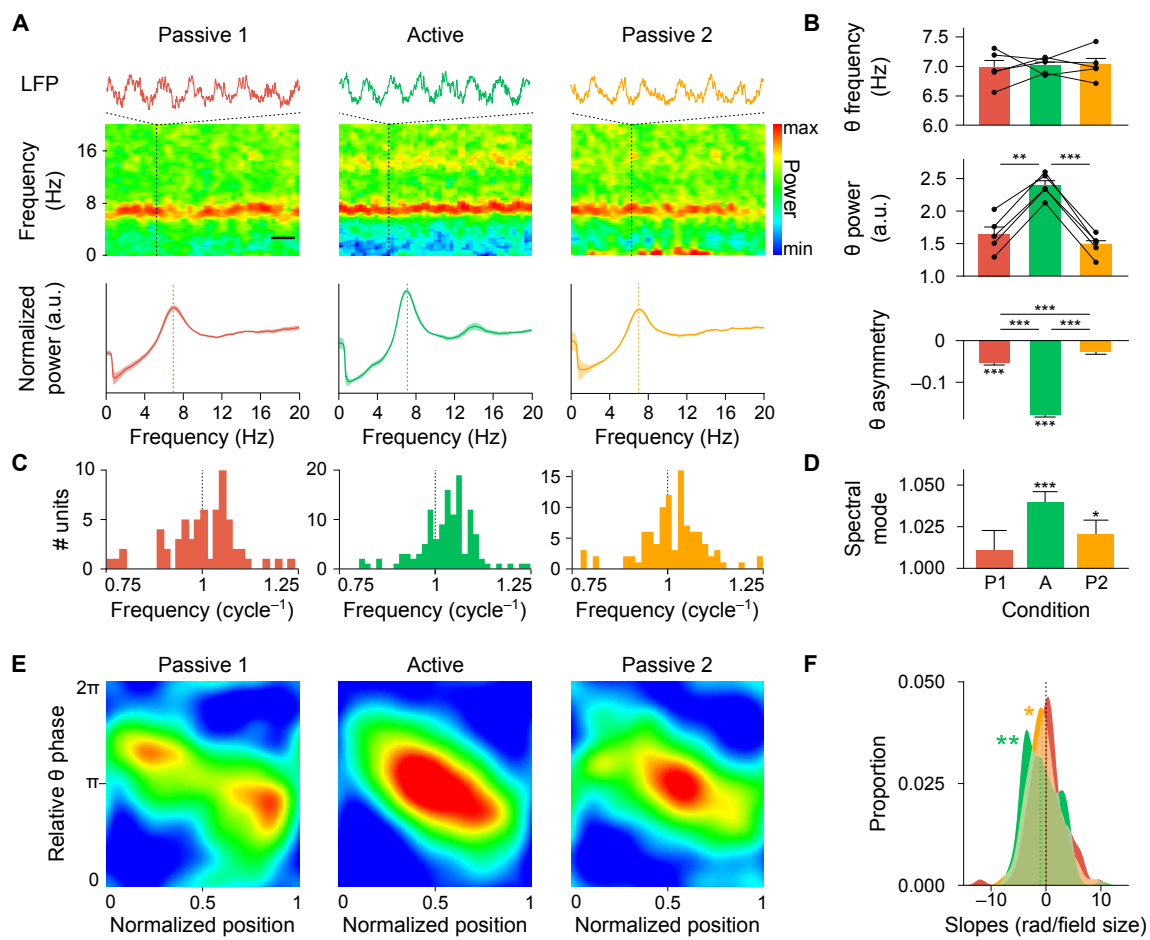


Figure 2

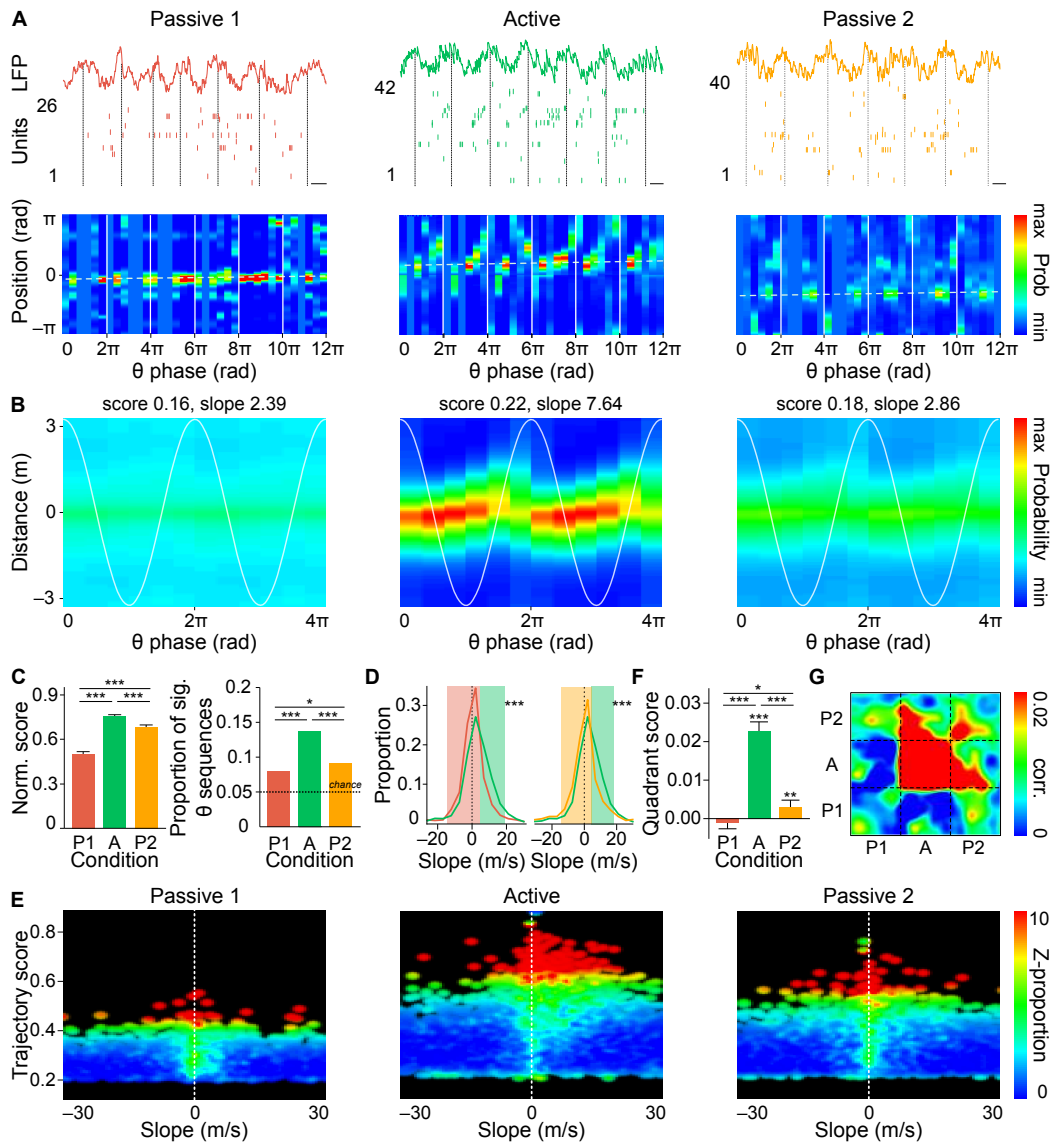


Figure 3

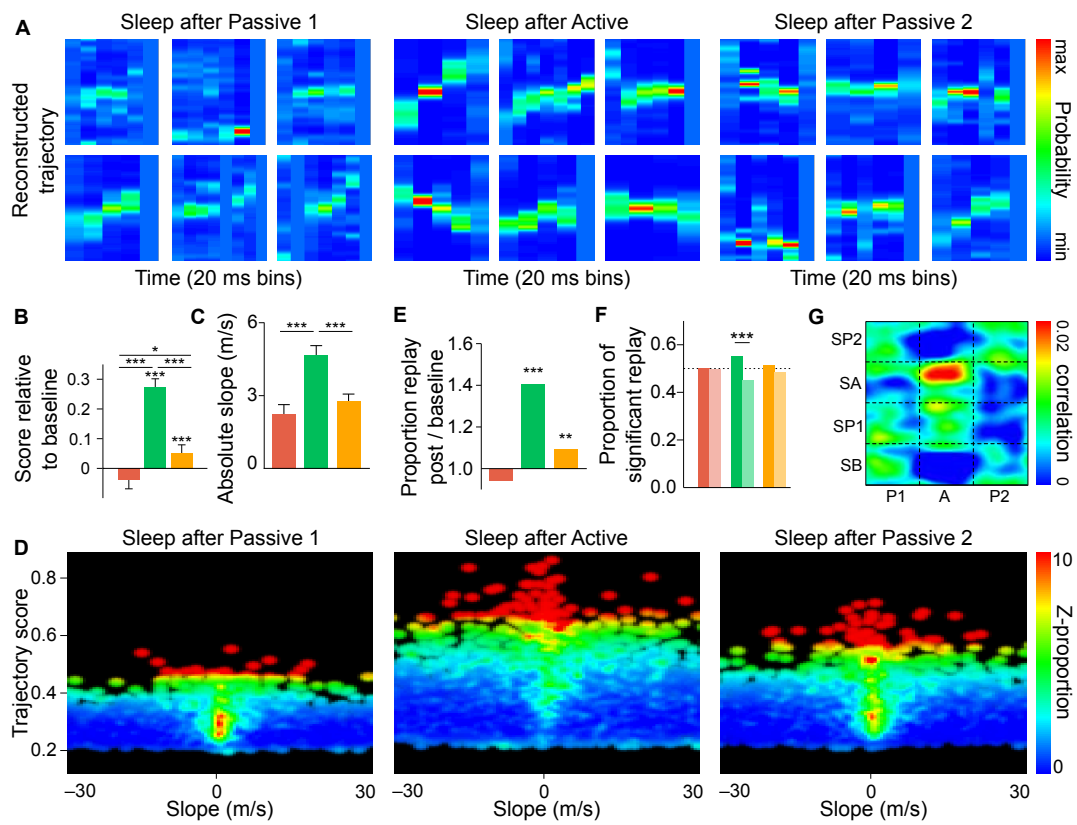


Figure 4

## Materials and Methods

### Animal training

Five adult male Long-Evans rats (René Janvier, Le Genest Saint Isle, France) weighing 350–400 g were used in this study. Two days after arrival, they were housed individually and maintained on a 12-hour light/dark cycle. Rats were kept on a mild water restriction diet (>85% of normal body weight) throughout the training and experiment phases. Critically, training took place in a dedicated room, separate from that where experiments were subsequently carried out. Following one week of daily handling, the rats were first trained to run on a regular treadmill. The speed of the treadmill and the running duration were increased daily over 3–5 days. In parallel, in order to familiarize the rats with the model train (LGB, Germany), they were placed in the immobile car for 10–15 min sessions. Subsequently, the rats learned to run on the miniature treadmill located inside the (immobile) car, as well as to be passively transported by the train (treadmill off), before they finally learned to run on the miniature treadmill while being transported by the train (~3 weeks; Fig. S1A). The rats were always transported in the forward direction at constant speed (~45–50 cm.s<sup>-1</sup>, Fig. S1B) on the 2.20 m × 1.30 m obround-shaped track. The treadmill and the train velocity were controlled by the same generator. The rats received sucrose water rewards (1.25% saccharine), delivered by a solenoid valve in a fountain placed at the front of the car (Fig. S1A, right) whenever the car arrived at one of two different reward locations on the track. The entire experimental setup was remotely controlled in order to avoid interference with experimenters. All procedures were in accordance with national (Comite d’Ethique #2011-0008) and international (US National Institutes of Health guidelines) standards and legal regulations (Certificat d’Autorisation d’Expérimentation #A75-1756) regarding the use and care of animals. Training and experiments took place during the day.

### Surgical implantation and electrode adjustment

The rats had free access to water for at least two days before surgery. They were deeply anesthetized (xylazine, 0.12 ml intramuscular; pentobarbital, 40 mg per kg of body weight, intraperitoneal; 0.1 ml pentobarbital supplemented every hour). Sixteen independently movable tetrodes or octrodes (groups of four or eight twisted 13 μm tungsten wires, gold-plated to

$\sim 150$  k $\Omega$ ) were bilaterally implanted above the dorsal hippocampus (3.5 mm or 4 mm AP,  $\pm 2.5$  mm ML relative to bregma). Two screws attached to the skull above the cerebellum served as ground and reference, respectively. After a one-week recovery period, the rats were placed back on the mild water restriction diet and retrained in the dedicated training room. The electrodes were progressively lowered into the CA1 pyramidal layer, identified based on both neural firing patterns (e.g. complex spikes) and local field potential (LFP) characteristics (especially sharp wave-ripple complexes).

### **Behavioural task**

The experiments took place in a separate, novel room. Following a baseline sleep recording session, the rats underwent three transportation sessions: passive (treadmill off), then active (treadmill on), then passive again (Fig. 1A). Each travel condition consisted of  $2 \times \sim 15$  laps (Fig. S1C). During the interval period, the rats stayed for less than 2 min in a flower pot while the experimenter unrolled the recording tethers. Each travel session was followed by a sleep epoch in the flower pot. Each sleep epoch, including baseline sleep, lasted for  $\sim 90$  minutes.

### **Data acquisition and preprocessing**

For the three rats implanted with sixteen tetrodes, brain signals were preamplified using two 32-channel unity-gain preamplifiers (Noted Bt, Pecs, Hungary) and acquired at 32,552.083 Hz (Digital Lynx, Neuralynx, Bozeman, MO). The head-stages were connected to the recording setup via two custom-made tethers (New England Wire, Lisbon, NH). For the three rats implanted with sixteen octrodes, brain activity was recorded using a 128-channel digital data acquisition system (KJE-1001, Amplipex, Szeged, Hungary). The signals were digitized using two 64-channel preamplifiers (Amplipex HS2) and sampled at 20,000 Hz. In both setups, one LED (red) or two LEDs (red and green) were used to track the head of the animal using an overhead video camera (sampling rate 30 Hz, resampled at 39.0625 Hz).

Data were pre-processed and visualized using NeuroSuite (<http://neurosuite.sourceforge.net>, (1)). Briefly, to extract spiking activity, wide-band signals were high-pass filtered (nonlinear median-based filter) and thresholded using NDManager (L. Hazan and M. Zugaro, <http://neurosuite.sourceforge.net>). Extracted spike waveforms were sorted via a semi-automatic

cluster cutting procedure using KlustaKwik (K.D. Harris, <http://klustakwik.sourceforge.net>) and Klusters (L. Hazan, <http://neurosuite.sourceforge.net>). Neurophysiological and behavioral data were explored using NeuroScope (L. Hazan, <http://neurosuite.sourceforge.net>). Units were classified as putative interneurons or pyramidal cells using k-means clustering based on waveform width, waveform trough-to-peak duration, and firing rate. Cluster isolation quality was assessed using the  $L_{ratio}$  (2, 3). Briefly, the  $L_{ratio}$  of cluster  $C$  is:

$$L_{ratio} = \frac{1}{n_s} \sum_{i \notin C} \{1 - CDF_{\chi_{df}^2}(D_{i,C}^2)\}$$

where  $n_s$  is the total number of spikes recorded on the tetrode throughout the recording epoch,  $i \notin C$  is the set of spikes that are not members of cluster  $C$ ,  $D_{i,C}^2$  is the Mahalanobis distance of spike  $i$  from cluster  $C$ , and  $CDF_{\chi_{df}^2}$  is the cumulative distribution function of the  $\chi^2$  distribution with  $df = \text{number of channels of the electrode} \times \text{number of features}$ . Only well-isolated clusters with an  $L_{ratio} < 0.05$  were included in the analyses. LFPs were derived from wideband signals by downsampling all channels to 1,250 Hz.

### Recording site verification

Upon completion of the experiments, recording sites were marked with small electrolytic lesions. Two days later, rats were deeply anesthetized with a lethal dose of pentobarbital, and intracardially perfused with saline (0.9%) followed by paraformaldehyde (10%). The desiccated brains were post-fixed and conserved in PFA (4%) at 4°C until the histology (50  $\mu\text{m}$  coronal slices, Cresyl violet staining).

### Data analysis and statistics

All analyses were performed in Matlab (MathWorks, Natick, MA), using the Freely Moving Animal toolbox (FMAToolbox, M. Zugaro, <http://fmatoolbox.sourceforge.net>) and additional custom programs.

Descriptive statistics are reported as mean  $\pm$  standard error of the mean when the underlying distribution is Gaussian-shaped (Jarque-Bera test) or median  $\pm$  standard error of the median otherwise. Unless indicated otherwise, bars represent median  $\pm$  standard error of the median. Repeated measures ANOVA was used for multiple comparisons of paired Gaussian distributions,

and differences between groups were assessed using paired Student’s t-test with Bonferroni correction for post-hoc analysis. For non-Gaussian distributions of independent (non-paired) data, multiple comparisons were made using Kruskal-Wallis (KW) and differences between groups were assessed using Wilcoxon rank sum test with Bonferroni-correction for post-hoc analysis. For paired data following a non-Gaussian distribution, Friedman test was employed, with signed rank tests with Bonferroni-correction for post-hoc analyses for assessing differences between groups.

Proportions were compared using the binomial proportion test. Medians (of non-Gaussian distributions) were compared to single values with Wilcoxon signed rank tests. Distributions were compared using the Kolmogorov-Smirnov test. No statistical methods were used to pre-determine sample sizes, but our sample sizes are similar to those generally employed in the field. Data collection and analysis were not performed blind to the conditions of the experiments. All statistical tests were two-tailed.

## Firing fields

All analyses of spike trains emitted during the awake state were restricted to epochs in which the linear velocity of the rat was greater than 5 cm.s<sup>-1</sup>. Firing maps and linearized firing curves were computed using a kernel-based method (bin size: 2.4 cm). The firing rate was estimated at each point  $x$  as:

$$f(x) = \sum n_t \times w(|x - x_t|) / \sum dt \times w(|x - x_t|)$$

where, in a given time bin  $t$ ,  $n_t$  is the number of action potentials emitted,  $x_t$  is the position of the rat, and  $dt$  is the time bin size. The kernel  $w$  was a Gaussian of width 4.5 cm. Firing fields were defined as the set of contiguous bins containing the location of maximal firing rate (min 1 Hz for Active and 0.7 Hz for Passive), for which the firing rates exceeded 30% of the peak firing rate. Pyramidal cells with at least one firing field were defined as place cells.

The stability of firing fields between conditions was assessed using two complementary methods (Figs. 1D and S2D). We first tested for random remapping using the method described in (4). Briefly, we measured the unsigned proportional field shifts of all the recorded place cells and compared their average to a null distribution constructed by shuffling ( $n = 2,000$ ) the identity

of the cells to simulate a random rearrangement of the fields. Second, for each place cell, the location of the peak firing rate was measured as an angle on the obround-shaped track, and peak shifts were measured as angular deviations between two conditions. After testing distribution uniformity (Rayleigh test), the mean direction of the shift distribution was compared to zero using a V test.

### **Theta power, frequency and cycles**

Power spectra and spectrograms were computed from the detrended LFP signal using multitaper estimation methods (<http://chronux.org>). Power spectra were normalized for each rat as  $(S_{ij} - \mu_j)/\sigma_j$ , where  $S_{ij}$  is the power spectrum for a given condition  $i$  of rat  $j$ , and  $\mu_j$  and  $\sigma_j$  are the mean and the standard deviation of the power spectra for all of the conditions for rat  $j$ . Theta power was measured as the maximum power in the theta band (6–10 Hz) of the normalized power spectrum, and frequency was measured as the mode located in the same range (Fig. 2A-B). Theta cycles started at the peak of the LFP filtered in the theta band. Cycles shorter than 80 ms or longer than 200 ms were discarded, and only periods containing at least three contiguous cycles were selected for further analysis.

### **Theta asymmetry and phase precession**

To preserve the asymmetrical shape of the theta oscillation, precise peak and trough times were detected on the LFP filtered between 1 and 40 Hz. This was used to assess theta asymmetry and spike phase precession. Theta asymmetry was measured as  $\log(\Delta t_2/\Delta t_1)$ , where  $\Delta t_1$  is the duration between cycle start and trough, and  $\Delta t_2$  the duration between trough and cycle end (5). Hence, a positive value indicates a shorter descending phase, a negative value indicates a shorter ascending phase, and zero indicates symmetrical cycles (Fig. 2B).

To analyze theta phase precession, in-field spike theta phases were plotted against linearized positions on the track. Slopes and significance were determined by linear-circular regression (6). Average phase precession density plots were constructed by normalizing the position in the firing field and shifting the mean spike theta phase to  $180^\circ$ , then normalizing by the total number of spikes, and averaging over cells (Fig. 2E).

## Theta burst frequency

Spike times were converted to unwrapped theta phases and divided by  $2\pi$ , yielding units of theta cycles. Spectrograms computed on the resulting spike trains measured frequencies relative to theta, compensating for moment-to-moment variations in theta frequency over the course of a given experiment (Figs. 2C,D and S4A).

## Candidate replay events

Candidate replay events were detected using place cell ensemble activity during slow wave sleep (SWS). SWS periods were first determined by k-means clustering of the theta (6–10 Hz) / delta (1–4 Hz) ratio computed from spectrograms during sleep sessions (min duration of SWS epoch >120 s, permitting brief discontinuities <1 s; Fig. S11A). The method was validated by comparing the outcome to episodes where the animal was immobile (linear velocity <0.05 cm/s for at least 120 s, with brief movements <1 s) and by visual examination of the video recordings. Candidate replay events were defined as epochs of elevated place cell spiking activity (7), i.e. when the instantaneous firing rate (1-ms bins, smoothed using a Gaussian kernel of s.d.= 10 ms) reached a peak >3 s.d. and remained greater than the mean (Fig. S11C). Candidate events lasting >500 ms were excluded.

## Bayesian trajectory decoding

To decode potential trajectories from place cell ensemble activity during both travel and sleep conditions, we used a previously described Bayesian position reconstruction approach (8). Briefly, in the training step, we estimated the probability  $P(x)$  that the rat visited location  $x$  as the normalized occupancy curve, and the average firing rate probability  $\lambda_i(x)$  for each place cell  $i$  at position  $x$  as the normalized firing curve of the cell. Then in the test step, given the instantaneous firing rate vector  $n$  in each phase or time window  $\tau$  ( $\tau = \pi/3$  for theta sequences,  $\tau = 20$  ms for replay events), we estimated the probability  $P(x|n)$  (Figs. 3A and 4A):

$$P(x|n) = \frac{P(n|x).P(x)}{P(n)}$$

where

$$P(n|x) = \prod_{i=1}^N \frac{(\lambda_i(x) \cdot \tau)^{n_i}}{n_i!} e^{-\lambda_i(x) \cdot \tau}$$

assuming that the  $N$  cells fired as independent Poisson processes. We only considered trajectory events involving at least three units in candidate events lasting  $>60$  ms.

To compute the average reconstructed trajectory over a given condition, reconstructions from individual theta subcycles (i.e. phase windows) were centered on the current position of the animal and averaged over successive cycles (4). This yielded an average estimate of theta sequences (Figs. 3B, S5A, S7A, S8A, S9A, S10A).

To allow comparison of trajectories across conditions, the Bayesian decoding algorithm was independently trained on each of the travel sessions (e.g. firing fields in Passive 1) and applied to the same travel session (theta sequences in Passive 1) and subsequent sleep session (replay events in sleep following Passive 1). One caveat was therefore that differences in training conditions could bias the comparisons of reconstruction quality. To control for this possibility, we used four different controls: (i) Control for cell count (Fig. S7). Passive 1 typically included fewer cells. To control for this, analyses were restricted to matching random subsets of place cells in Active and Passive 2. This was repeated 30 times in order to obtain a representative data set, and up to 300 theta cycles were reconstructed for a given cell subset. (ii) Control for spike count (Fig. S8). Firing rates in Passive 1 were somewhat lower than in Active. For each rat, we randomly downsampled the spike trains of the most active place cells in Active and Passive 2 to match the median of the firing rate distribution in Passive 1. (iii) Control for decoding quality (Fig. S9). To match decoding quality across conditions, reconstruction errors were first computed in 500-ms time bins for each travel condition. For Passive 1 and Passive 2, bins with a high decoding error were progressively excluded, until the median of the error distribution was smaller than the median of the error distribution in Active. Finally, positions were decoded using only theta cycles falling in these low error bins. Note that this also controlled for potential alterations in spatial coding, both at the single cell and at the population level (i.e. including higher order alterations that would not be manifested at the single cell level). (iv) Control for field variability (Fig. S10). To rule out a possible effect of firing variability between successive laps

(e.g. small changes in field locations), analyses were repeated on a lap-by-lap basis, whereby the Bayesian decoding algorithm was retrained on each individual lap before sequences were assessed. Together, these four controls ruled out the possibility that our main conclusions based on direct comparisons could be accounted for by differences in training conditions.

### **Assessing trajectories: trajectory scores and slopes, quadrant scores**

To identify trajectories, we measured the previously defined trajectory score and slope (7) of each candidate event. These assess whether events consist of linearly aligned positions, i.e. whether the successive reconstructed positions are tightly arranged (high score) along an oblique line (high slope). Briefly, each candidate trajectory consisted of reconstructed positions  $P(x|n)$  during  $m$  successive time or phase intervals  $\Delta\xi$  ( $\Delta\xi = \pi/3$  for theta sequences,  $\Delta\xi = 20$  ms for replay events). For a given candidate trajectory, the average likelihood  $R$  that the rat is located within a distance  $d$  of a linear trajectory defined by its velocity  $v$  and starting location  $\rho$  is:

$$R(v, \rho) = \frac{1}{m} \sum_{k=0}^{m-1} P(|pos - (\rho + v.k.\Delta\xi)| \leq d)$$

where the value of  $d$  was set to 45 cm to allow for small local variations in velocity (i.e. 1/3 of the mean field size, consistent with previous studies). Because in the present experiments the track was obround, for those time bins  $k$  when a trajectory would specify a location beyond the end of the linearized track, the trajectory was wrapped around and continued from the start. To find the best fit line (i.e. maximize  $R$ ), we evaluated all possible combinations of  $v$  and  $\rho$  that yielded a total distance less than the track length (6 m).

Thus, genuine trajectories would yield both high scores and slopes ( $R \gg 0$ ,  $|v| \gg 0$ ), whereas static representations of current position would result in high scores but low or zero slopes ( $R \gg 0$ ,  $v \sim 0$ ), and random activity would be associated with low scores ( $R \sim 0$ ), but possibly spuriously high slopes.

In order to assess the significance of trajectory scores, we used a shuffling procedure developed by (7). Briefly, we generated  $n = 5,000$  shuffled candidates by shifting each reconstructed position  $P(x|n)$  by a random distance, yielding a null distribution of scores. Note that this selectively scrambled the linear arrangement of reconstructed positions, while preserving the spatial coherence of positions represented by individual cell assemblies (contrary to e.g. independent

shuffling of individual spike trains). In other words, shuffling was applied at the level of cell assemblies rather than single neurons.

More precisely, shuffles were generated by circularly shifting the decoded probabilities within each phase or time window by a random number of bins. The Monte Carlo  $p$ -value was calculated as the proportion of scores in the shuffled distribution greater than the score of the candidate trajectory. Candidate trajectories with a  $p$ -value  $\leq 0.05$  were considered significant. In addition, in order to compare trajectory events from different rats recorded in different conditions (i.e. with differences in number of neurons, decoding quality, etc.), trajectory scores were normalized by computing a non-parametric equivalent of a z-score, i.e. by subtracting the mean and dividing by the standard deviation of the distribution of shuffled scores (Figs. 3C, S7C, S8C, S9C, S10C). In Figure 4B, to assess changes in sleep activity induced by preceding awake behavior, for each rat, we evaluated each score in post-sleep relative to baseline sleep by computing a non-parametric equivalent of a z-score, i.e. by subtracting the median score in baseline sleep, and dividing by the difference between the first and third quartiles of the distribution of scores in baseline sleep. These scores relative to baseline were then pooled across rats and compared between conditions. Candidate replay events during baseline sleep were decoded using the Bayesian algorithm trained on the same travel condition as the post sleep session.

To compute the proportion of significant theta sequences (Fig. 3C), only events with significant score and positive slope were counted (the same conclusion was reached without the slope restriction: 14.66% in Passive 1, 20.20% in Active, 16.37% in Passive 2; all proportions were significantly greater than shuffled control proportions and all proportions were different between one another; data not shown).

To confirm the above trajectory assessment using an independent measure, we used the quadrant score first described in (9). Similar to the trajectory score and slope method, each candidate trajectory was first described by a probability matrix consisting of successive reconstructed positions  $P(x|n)$ . The central zone of this probability matrix was defined as  $\pm 1.5$  m from the current position of the animal and  $\pm 2/3$  theta cycle around the cycle trough. This was divided equally into four quadrants. The summed decoded probabilities in the top left and bot-

tom right quadrants (opposite to the current running direction of the animal) were subtracted from the sum in the bottom left and top right quadrants (along the current running direction), then normalized by the sum of all four quadrants (Figs. 3F, S7D, S8D, S9D, S10D). Hence, positive differences would correspond to theta sequences sweeping in the running direction of the animal, whereas differences close to zero would indicate a lack of sequential structure in the decoded probabilities.

### Assessing trajectories: Z-proportions and proportion ratios

In order to simultaneously visualize the distribution of trajectory scores and slopes across candidate trajectories and contrast them between behavioral conditions, events were first sorted according to their trajectory scores and slopes. Each cell of the resulting score-slope matrix contains the number of events within that specific range of scores and slopes divided by the total number of events. To assess the statistical significance of these proportions, we created  $n = 5,000$  surrogate score-slope matrices using shuffled data as described in the previous section. We then z-scored the proportion in each cell of the observed matrix (data) relative to the mean and standard deviation of the 5,000 proportions located in the same cell of the surrogate matrices (z-proportion; Figs. 3E, 4D, S7E, S8E, S9E, S10E, S12F, S13C).

A complementary approach was used in Figure S13D, where the color code indicates the proportion ratio  $r$  defined as:

$$r_c = \frac{1}{m} \sum_{i=1}^m \frac{n_{data}}{n_{data} + n_{shuffle_i}}$$

where  $m$  is the number of shuffles,  $n_{data}$  the number of events in cell  $c$  of the score-slope matrix, and  $n_{shuffle_i}$  the number of events in cell  $c$  for the  $i$ -th shuffle. Thus, a ratio of 0.5 indicates that the cell contains the same proportion of observed and shuffled data, ratios above 0.5 indicate that scores and slopes in cell  $c$  are enriched in the data relative to the shuffle (up to a maximum ratio of 1 indicating that events with the corresponding score and slope were observed in the data but in none of the 5,000 shuffle iterations), and ratios below 0.5 indicate that the scores and slopes in  $c$  are depleted in the data relative to the shuffle (down to a minimum ratio of 0 indicating that events with the corresponding score and slope occurred in the shuffle but not in the original data).

## Pairwise bias correlations

In order to directly compare the order between any two spike sequences, we used the pairwise bias correlation method developed by (10). Briefly, we computed a bias matrix  $B_k$  for each sequence  $k$ :

$$B_k(i, j) = \frac{n_k(i, j) - n_k(j, i)}{n_k(i) \cdot n_k(j)}$$

where  $n_k(i)$  is the number of spikes emitted by neuron  $i$  in the  $k$ -th sequence, and  $n_k(i, j)$  is the number of times neuron  $i$  spiked before neuron  $j$  in the  $k$ -th sequence.  $B_k(i, j)$  therefore reflects the bias of  $i$  to spike before  $j$  in the  $k$ -th sequence, taking values between -1 ( $i$  never precedes  $j$ ) and 1 ( $i$  always precedes  $j$ ), with 0 representing no bias ( $i$  precedes  $j$  half of the time).

The correlation between two sequences  $k$  and  $l$  is  $\rho(k, l) = \cos \theta$ , where  $\theta$  is the angle between the directions of  $B_k$  and  $B_l$ , when  $B_k$  and  $B_l$  are considered as vectors. Therefore

$$\rho(k, l) = \frac{\sum_{i,j} B_k(i, j) \cdot B_l(i, j)}{\sqrt{\sum_{i,j} B_k(i, j)^2} \cdot \sqrt{\sum_{i,j} B_l(i, j)^2}}$$

where  $i$  and  $j$  are neurons that fired in both sequences  $k$  and  $l$ .

Comparisons within and between theta sequences and replay events were restricted to sequences including three or more (common) neurons. Autocorrelations ( $k = l$ ) were discarded from the analysis.

To assess significance for the correlation of a given pair  $(k, l)$  of sequences, we constructed a surrogate distribution of pairwise bias correlations by shuffling the spike order in sequence  $l$ . The observed pairwise bias correlation  $\rho(k, l)$  was deemed significant if it exceeded 95% of the shuffled distribution.

In Figures 3G and 4G, each condition (baseline sleep, Passive 1, etc.) was subdivided into 20 temporal bins. To represent the similarity between two given temporal bins, we first computed for each recording session the median correlation between individual sequences within these bins, then took the median across all sessions.

## Ripple detection

LFPs from all channels located in or close to the pyramidal layer were detrended and filtered between 100 and 250 Hz, then averaged. In order to prevent spurious detection due to high

frequency noise contamination, the detrended signal from the selected channels was also filtered between 300 and 500 Hz, then averaged and subtracted from the mean filtered signal. Negative values, reflecting high frequency noise periods, were discarded while all positive values were z-scored, and ripples were defined as epochs during which the values remained above 1 s.d. with a peak greater than 3 s.d. Excessively brief ( $\leq 20$  ms) or long ( $\geq 110$  ms) epochs were excluded from subsequent analyses.

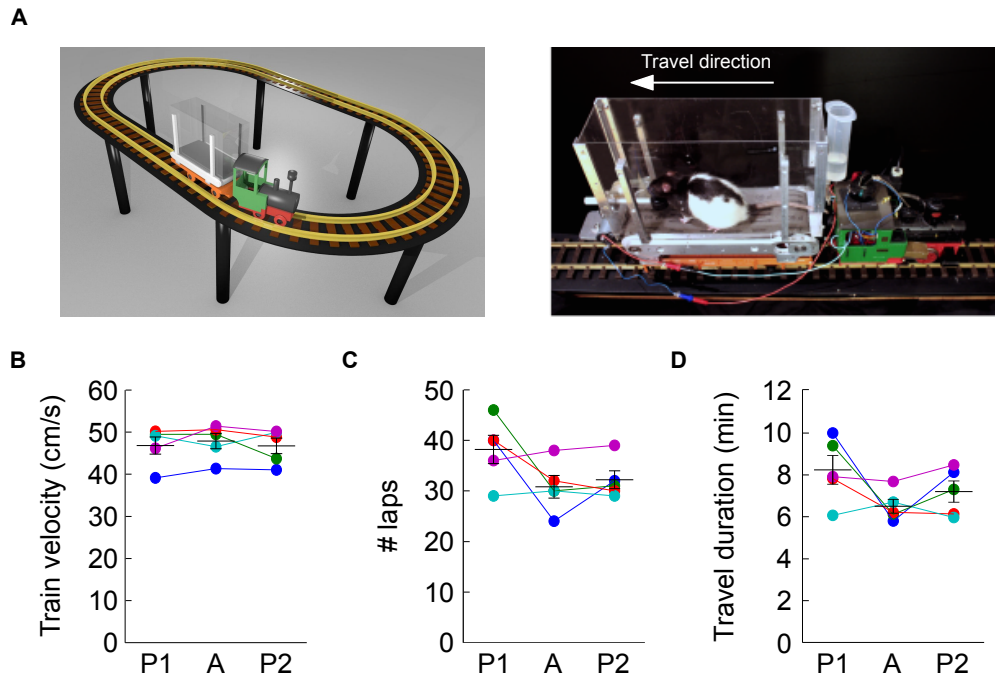


**Fig. S1. Behavioral task.** (A) Left, 3D representation of the experimental setup. Right, rats were transported on a miniature treadmill in a model train. Rats were displaced in the forward direction at all times. The locomotive was placed at the rear of the wagon in order to avoid obstruction of the visual field of the animal. Rats traveled in the novel environment while either running on the treadmill (Active travel) or standing still (Passive travel). (B) Train velocity in each condition for each rat ( $n = 5$  rats, mean  $\pm$  s.e.m., P1:  $46.80 \pm 2.04$  cm.s<sup>-1</sup>, A:  $47.87 \pm 1.83$  cm.s<sup>-1</sup>, P2:  $46.73 \pm 1.85$  cm.s<sup>-1</sup>; repeated measures ANOVA,  $P > 0.05$ ). (C) Number of laps traveled by each rat in each condition ( $n = 5$  rats, mean  $\pm$  s.e.m., P1:  $38.2 \pm 2.8$  laps, A:  $30.8 \pm 2.24$  laps, P2:  $32.2 \pm 1.77$  laps; repeated measures ANOVA,  $P > 0.05$ ). (D) Travel duration for each rat in each condition ( $n = 5$  rats, mean  $\pm$  s.e.m., P1:  $8.24 \pm 0.69$  min, A:  $6.50 \pm 0.33$  min, P2:  $7.20 \pm 0.51$  min; repeated measures ANOVA,  $P > 0.05$ ).

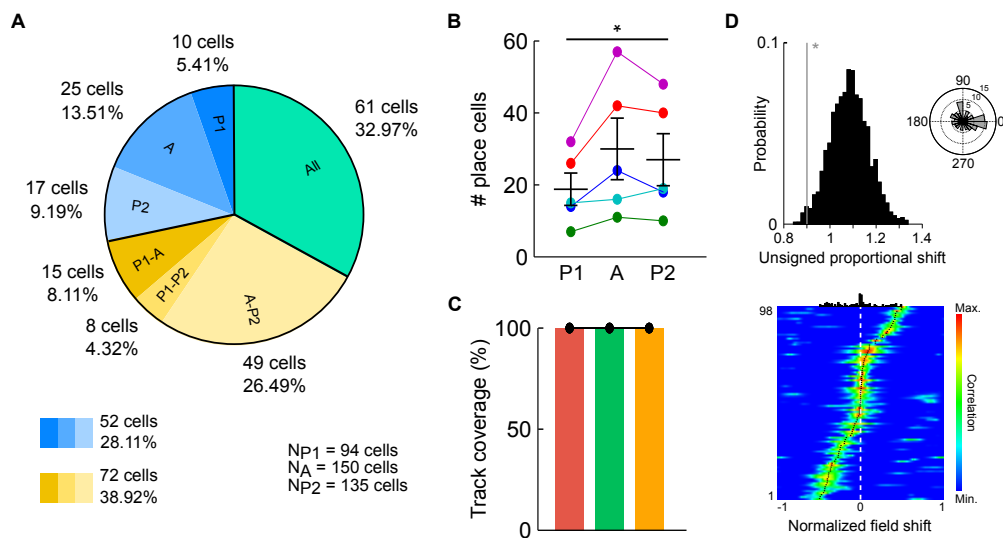


**Fig. S2. Place cell activity during travels.** (A) Number of individual place cells recorded in one or more travel sessions. Place cells recorded in only one or two conditions are represented in blue and yellow, respectively. (B) Total number of place cells recorded in each travel condition (repeated measures ANOVA,  $*P < 0.05$ ). (C) Percentage of the track covered by place fields in each travel condition. (D) Stability of place fields between Passive 1 and Passive 2. Top, mean unsigned proportional shift  $\sigma$  ( $*P < 0.02$ ). Histogram represents the distribution of  $\sigma$  for  $n = 2,000$  bootstrap random remapping data sets. Inset, circular distribution of angular differences between in-field peak firing rates (Rayleigh test,  $P > 0.05$ , V-test against 0,  $*P < 0.05$ ). Bottom, spatial cross-correlograms of firing fields. Black dots represent correlogram modes. Top black histogram, mode distribution.

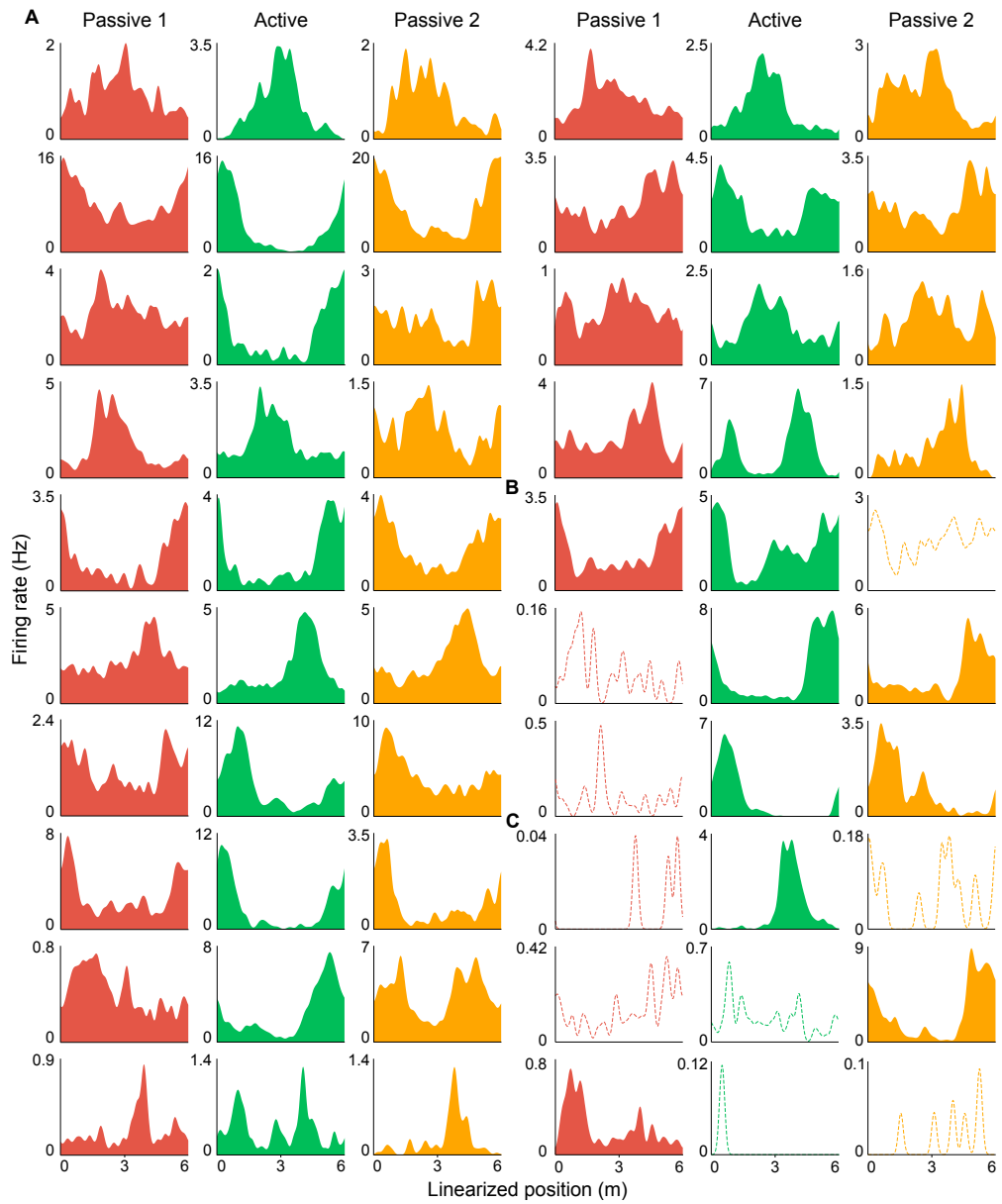


**Fig. S3. Example firing fields recorded in the three travel conditions.** (A–C) Firing curves of putative pyramidal cells defined as place cells (see Methods) in all three travel conditions (A), in two travel conditions (B), or in one travel condition (C). Dotted lines, firing curves of cells lacking an identified place field.

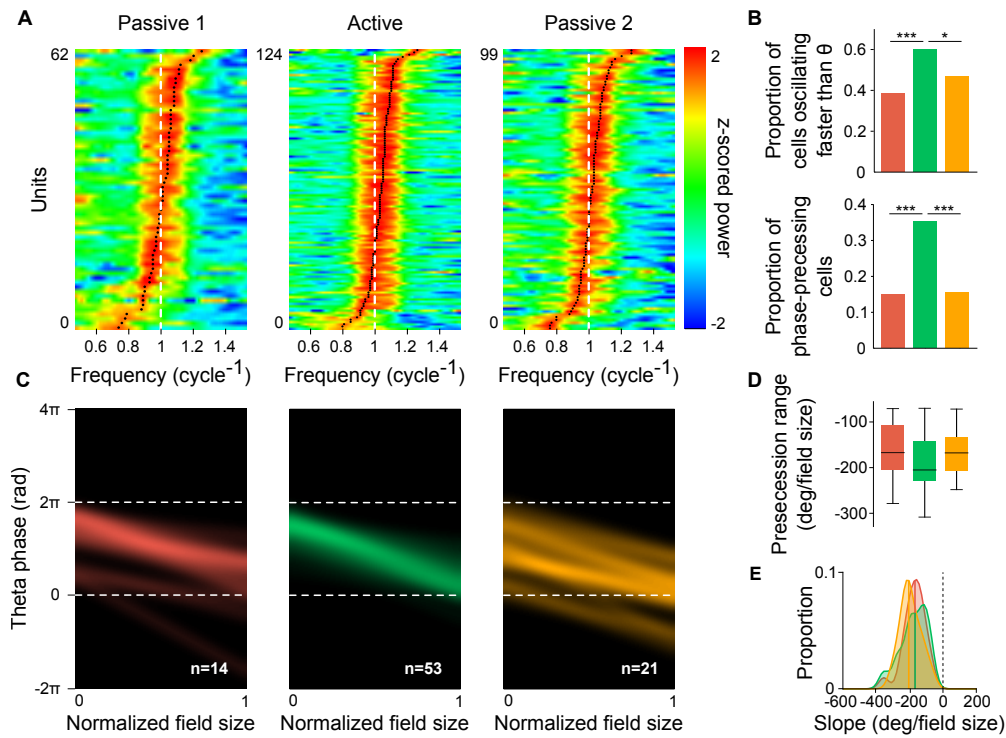


**Fig. S4. Phase precession is altered during passive travel.** (A) Power spectra of unit spike trains measured relative to theta (dashed white line indicates theta frequency). Only place cells with a peak around  $\pm 25\%$  of theta frequency are shown. Black dots indicate spectral modes. (B) Proportion of place cells oscillating faster than theta frequency (top, Passive 1: 36/94, Active: 90/150, Passive 2: 63/135) and proportion of significant phase-precessing cells (bottom, Passive 1: 14/94, Active: 53/150, Passive 2: 21/135). (C) Density of phase precession slopes for significant cells. (D) Range of phase precession for significant cells. Passive and Active travels were not significantly different (KW test,  $P > 0.05$ ). (E) Distributions of significant phase precession slopes (KS test,  $P > 0.05$ ). Solid lines represent medians (KW test,  $P > 0.05$ ).

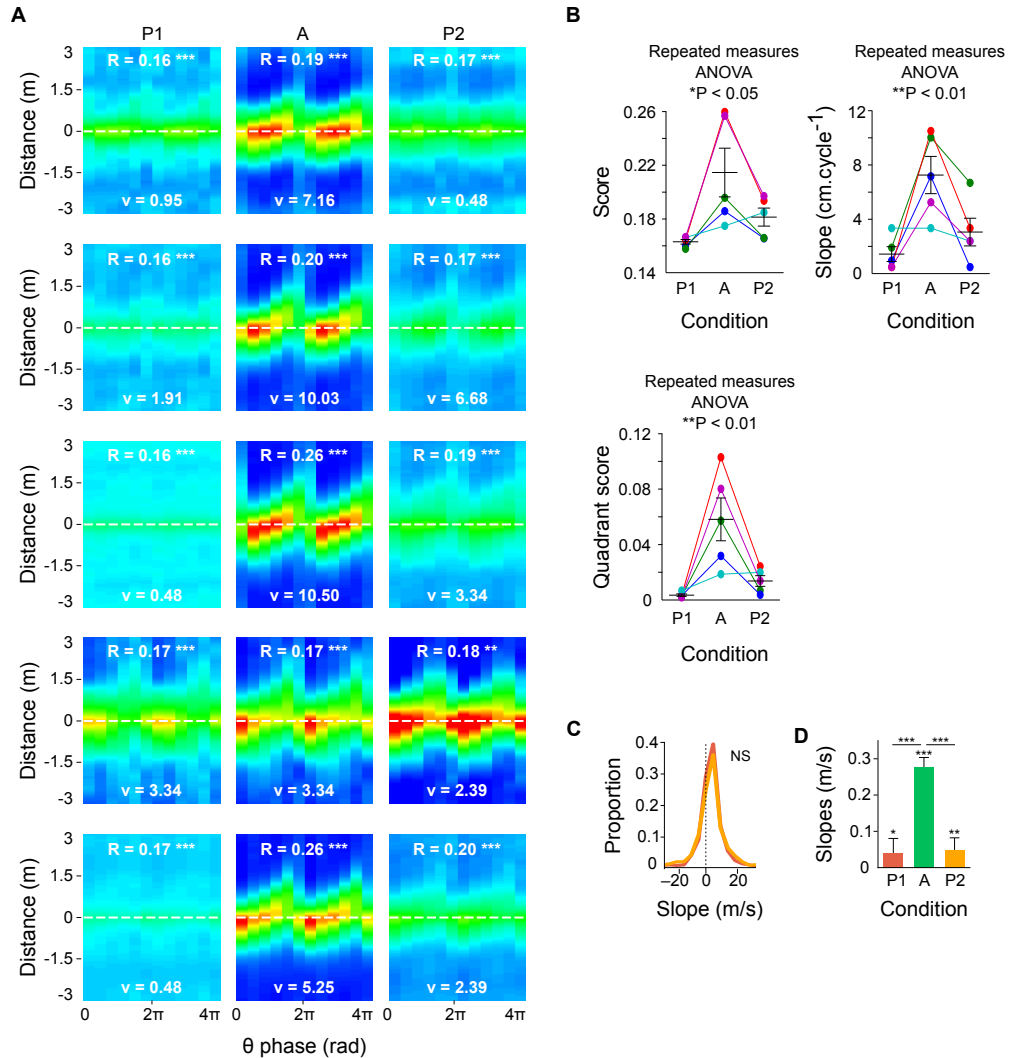


**Fig. S5. Position decoding from theta-scale place cell activity for each rat.** (A) Average reconstruction of rat position estimated across theta cycles for the 5 rats used in the study (dashed white line, actual animal position). Trajectory score  $R$  and slope  $v$  are indicated above each reconstruction. For each rat, the same scale was applied to the three reconstructions. (B) Trajectory scores, slopes and quadrant scores of reconstructions shown in (A) (mean  $\pm$  s.e.m.). (C) Distributions of significant theta sequence slopes in Passive 1 and Passive 2 (KS tests, P1–P2,  $P > 0.05$ ). (D) Significant theta sequence slopes (KW test, \*\*\* $P < 10^{-20}$ ).

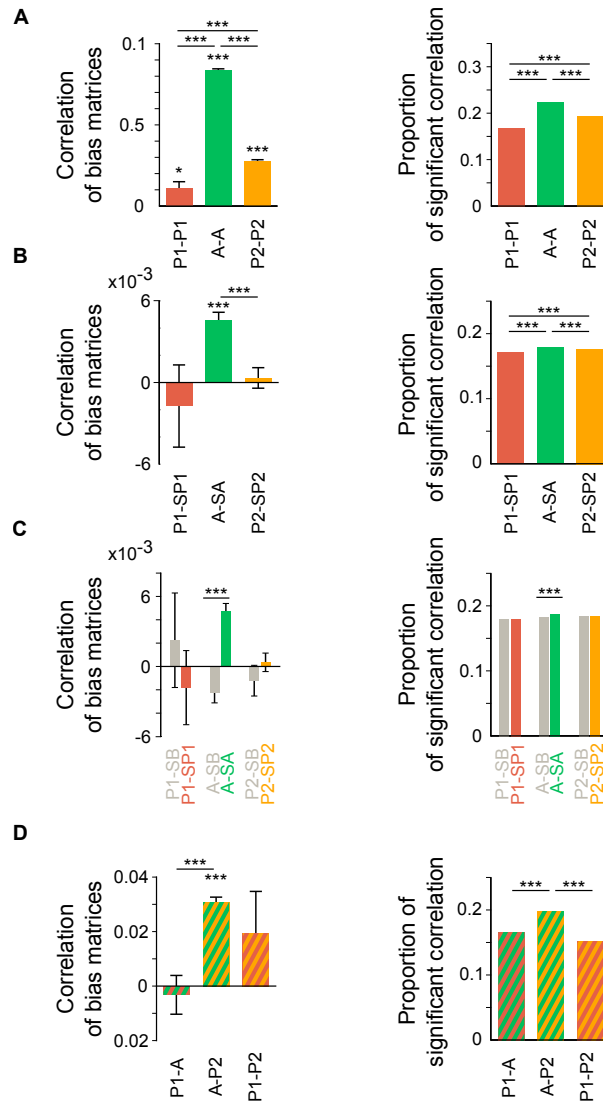


**Fig. S6. Direct measure of correlations between sequences within and across conditions. (A–D)** Left, average correlation between sequence biases (KW test). Right, proportion of significantly correlated pairs of sequences (binomial proportion test,  $***P < 0.001$ ). **(A)** Self-consistency within travel conditions (correlation between theta sequences within the same condition). **(B)** Similarity between awake (theta sequences) and respective post-sleep (candidate replay events). **(C)** Comparison of the similarity in (B) with the similarity between awake (theta sequences) and baseline sleep (grey). **(D)** Similarity of theta sequences between travel conditions.

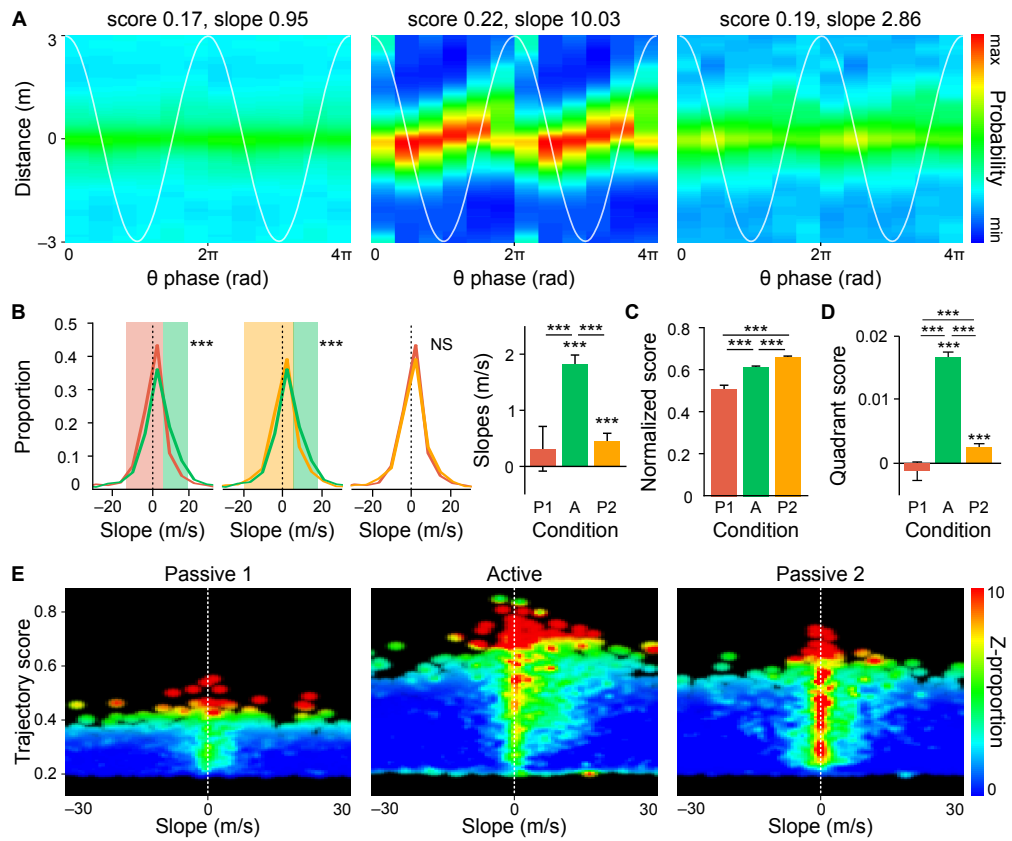


**Fig. S7. Reduced cell count does not account for theta sequence degradation during passive travel.** For each rat, subsets of place cells were selected in Active and Passive 2 to match the number of place cells recorded in Passive 1, and used to decode position in space. This downsampling procedure was repeated 30 times. **(A)** Rat position was then estimated across individual theta subcycles and averaged across all rats (same as in Fig. 3B). Trajectory scores and slopes are indicated above each reconstruction. **(B)** Distributions of significant theta sequence slopes (KS tests; left: P1-A,  $***P < 10^{-13}$ ; center: A-P2,  $***P < 10^{-43}$ ; right: P1-P2,  $P > 0.05$ ). Colored bands indicate significant differences. Right, slopes of significant theta sequences (KW test,  $***P < 10^{-39}$ ). **(C)** Normalized score of theta sequences (KW test,  $***P < 10^{-9}$ ). **(D)** Quadrant score computed from individual theta cycles (KW test,  $***P < 10^{-75}$ ). **(E)** Distribution of theta sequence quality assessed by joint trajectory score and slope (color codes for proportion relative to shuffled control data).

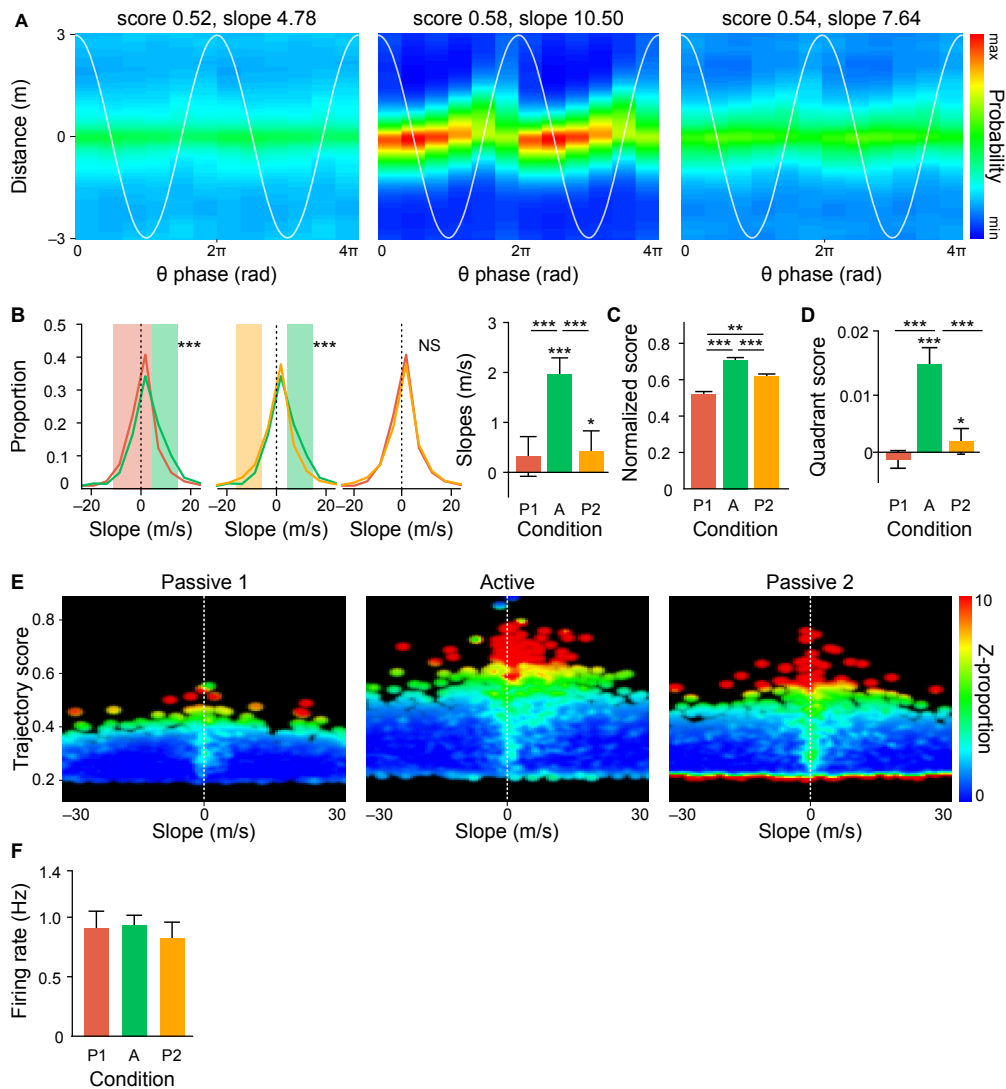


**Fig. S8. Reduced firing rate does not account for theta sequence degradation during passive travel.** For each rat, random spikes of place cells in Active and Passive 2 were progressively removed until the median firing rate of place cells in Active and Passive 2 was smaller than the median firing rate of Passive 1 place cells. **(A)** Rat position was then estimated across individual theta subcycles and averaged across all rats (same as in Fig. 2B; dashed white line, actual location of the animal). Trajectory score and slope are indicated above each reconstruction. **(B)** Distributions of significant theta sequence slopes (KS tests; left: P1–A,  $***P < 10^{-9}$ ; center: A–P2,  $***P < 10^{-9}$ ; right: P1–P2,  $P > 0.1$ ). Colored bands indicate significant differences. Right, slopes of significant theta sequences (KW test,  $***P < 10^{-11}$ ). **(C)** Normalized score of theta sequences (KW test,  $***P < 10^{-10}$ ). **(D)** Quadrant score computed from individual theta cycles (KW test,  $***P < 10^{-7}$ ). **(E)** Distribution of theta sequence quality assessed by joint trajectory score and slope (color codes for proportion relative to shuffled control data). **(F)** Resulting place cell firing rates following spike downsampling (P1:  $0.905 \pm 0.145$  Hz, A:  $0.933 \pm 0.083$  Hz, P2:  $0.829 \pm 0.130$  Hz; KW test,  $P > 0.90$ ).

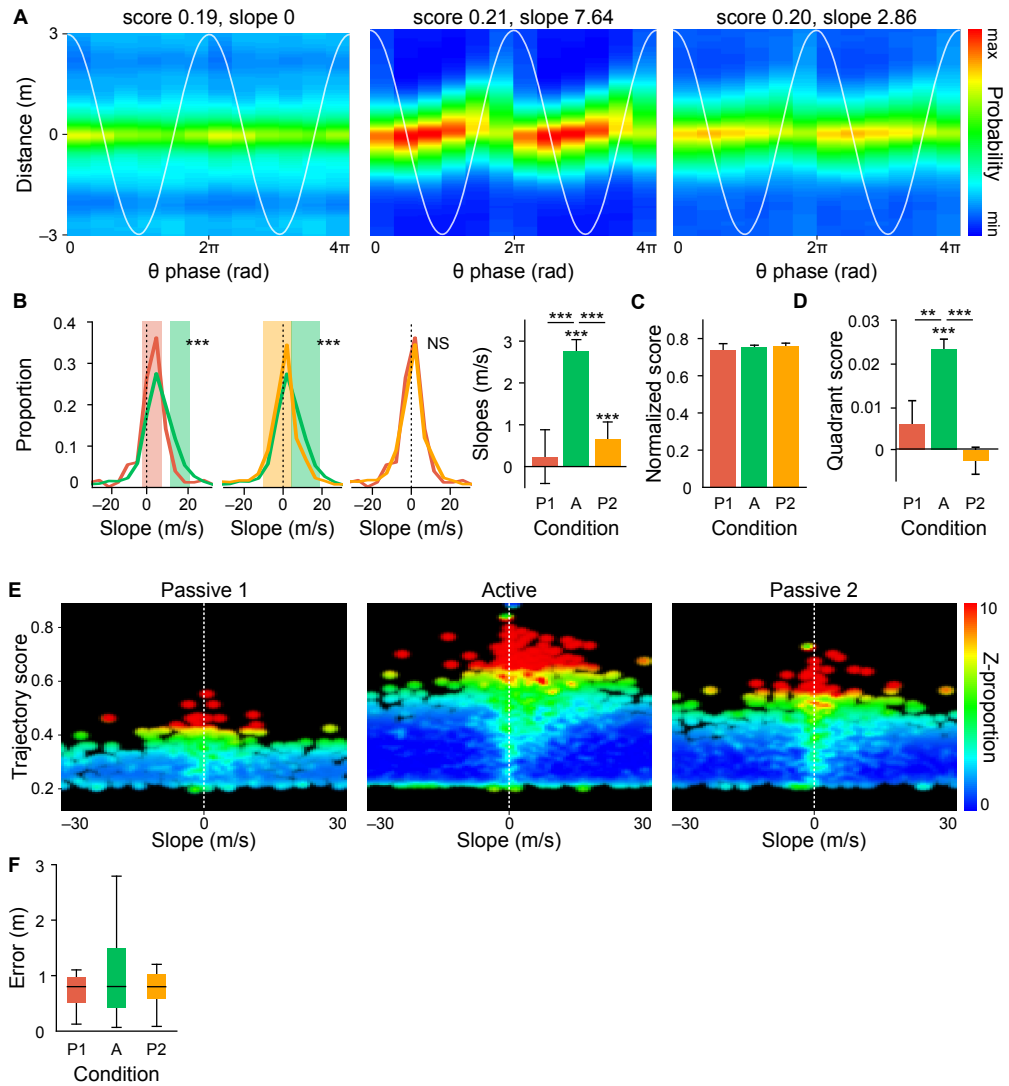


**Fig. S9. Reduced decoding quality cannot account for theta sequence degradation during passive travel.** In order to control for reduced decoding quality in passive travel sessions, the present analyses were restricted to theta cycles in Passive 1 and Passive 2 where decoding error (estimated in 500 ms time bins) was low, i.e. close to the error median in Active (see Methods). **(A)** Average Bayesian reconstruction of position (relative to actual position of the animal) across theta subcycles for all rats (as in Fig. 3B). Trajectory scores and slopes are indicated above each reconstruction. **(B)** Distributions of significant theta sequence slopes (KS tests; left: P1–A,  $***P < 10^{-9}$ ; center: A–P2,  $***P < 10^{-16}$ ; right: P1–P2,  $P > 0.05$ ). Colored bands indicate significant differences. Right, slopes of significant theta sequences (KW test,  $***P < 10^{-15}$ ). **(C)** Normalized score of theta sequences (KW test,  $P > 0.05$ ). **(D)** Quadrant score computed from individual theta cycles (KW test,  $***P < 10^{-16}$ ). **(E)** Distribution of theta sequence quality assessed by joint trajectory score and slope (color codes for proportion relative to shuffled control data). **(F)** Decoding errors were similar in all travel conditions following the restriction procedure described here (P1:  $0.802 \pm 0.018$ , A:  $0.80 \pm 0.023$ , P2:  $0.802 \pm 0.014$ ).

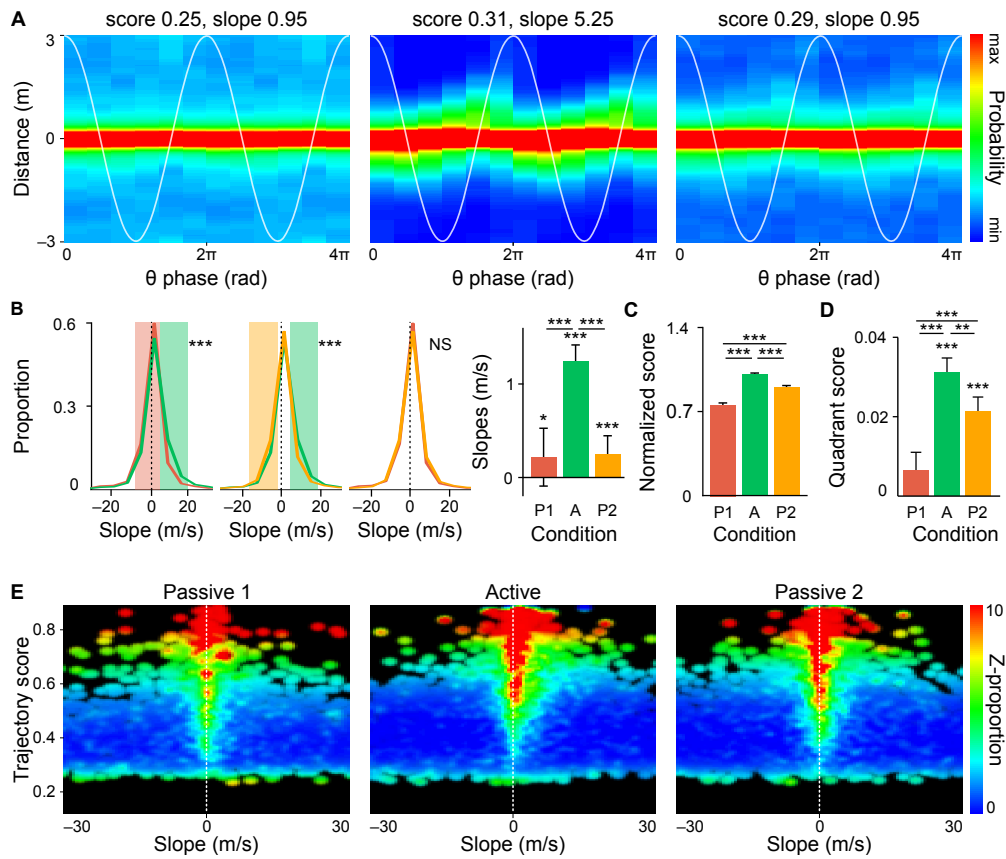


**Fig. S10. Trial-to-trial field variability does not account for theta sequence degradation during passive travel.** In order to control for firing variability across laps, the Bayesian decoding algorithm was retrained on each individual lap before sequences were assessed. **(A)** Rat position was estimated across individual theta subcycles and averaged across all rats (same as in Fig. 3B). Trajectory scores and slopes are indicated above each reconstruction. **(B)** Distributions of significant theta sequence slopes (KS tests; left: P1–A,  $***P < 10^{-12}$ ; center: A–P2,  $***P < 10^{-13}$ ; right: P1–P2,  $P > 0.05$ ). Colored bands indicate significant differences. Right, slopes of significant theta sequences (KW test,  $***P < 10^{-18}$ ). **(C)** Normalized score of theta sequences (KW test,  $***P < 10^{-27}$ ). **(D)** Quadrant score computed from individual theta cycles (KW test,  $***P < 10^{-9}$ ). **(E)** Distribution of theta sequence quality assessed by joint trajectory score and slope (color codes for proportion relative to shuffled control data).

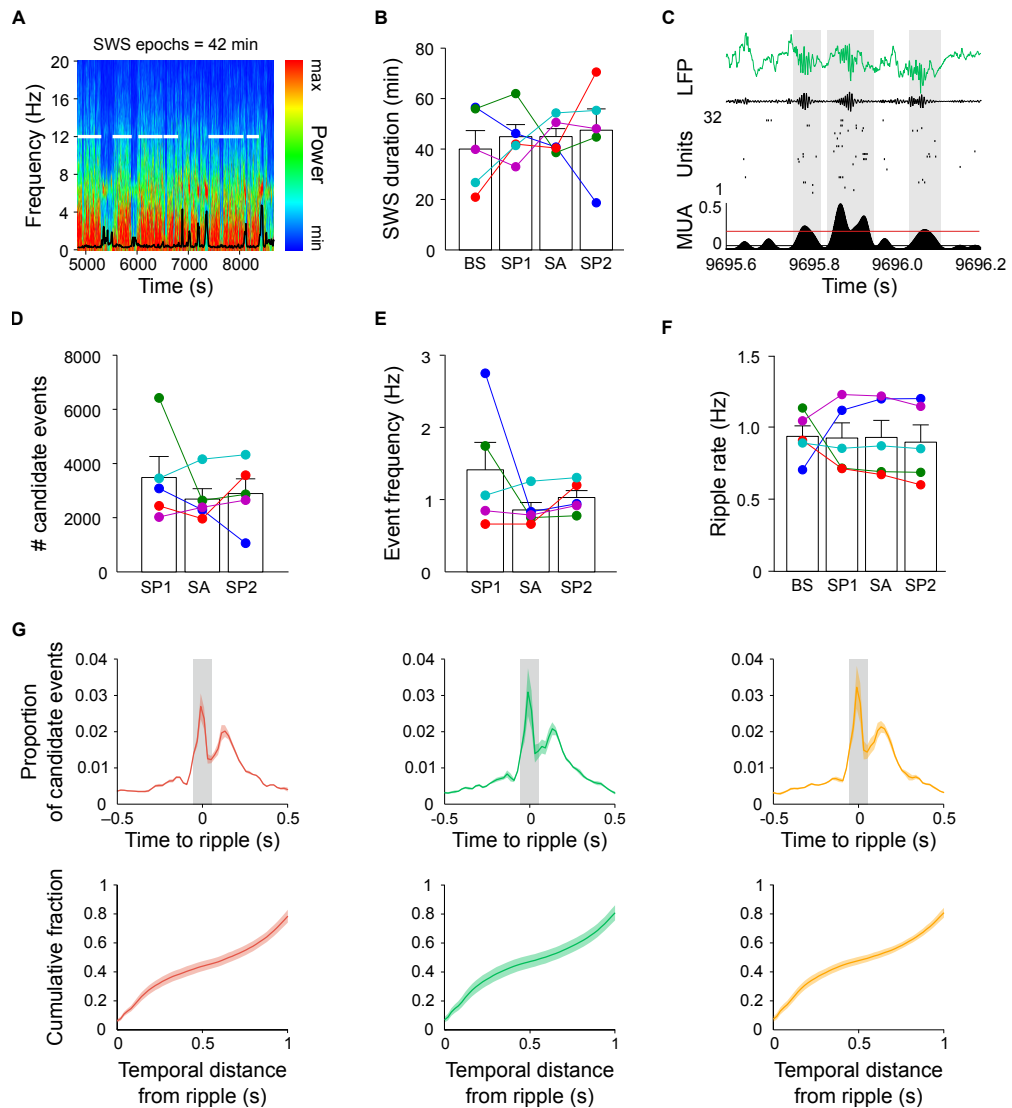


**Fig. S11. Candidate replay events during SWS.** (A) During sleep recordings, SWS periods were isolated based on the theta/delta ratio (black curve on power spectrogram). K-means clustering identified epochs with the smallest ratio (min duration 120 s, brief interruptions  $<1$  s). (B) SWS duration was not significantly different between sleep conditions (repeated measures ANOVA,  $P > 0.05$ ). (C) Detection of candidate events for an example SWS period. Top traces, raw (green) and ripple-band filtered (black) LFP. Middle, place cell activity. Cells are ordered according to the location of their place field on the track. Bottom, multi-unit activity (MUA) of place cells (time bin, 1 ms; black line, mean of the smoothed histogram, used to define the beginning and end of selected candidates; red line, 3 s.d. above the mean, used as a threshold for the peak). Note that candidate events coincide with ripples. (D–F) The number of candidate events (D), their frequency (E), and ripple rates (F) were not significantly different between sleep conditions (repeated measures ANOVA,  $P > 0.05$ ). (G) Top, peri-event time histograms of candidate replay events relative to peak ripple power. Grey area indicates the beginning and end of ripples and 0 the time of the peak ripple power (KS test,  $P > 0.05$  between all condition pairs). Bottom, cumulative distribution of replay events in  $\pm 1$  s time windows centered on ripple peak.

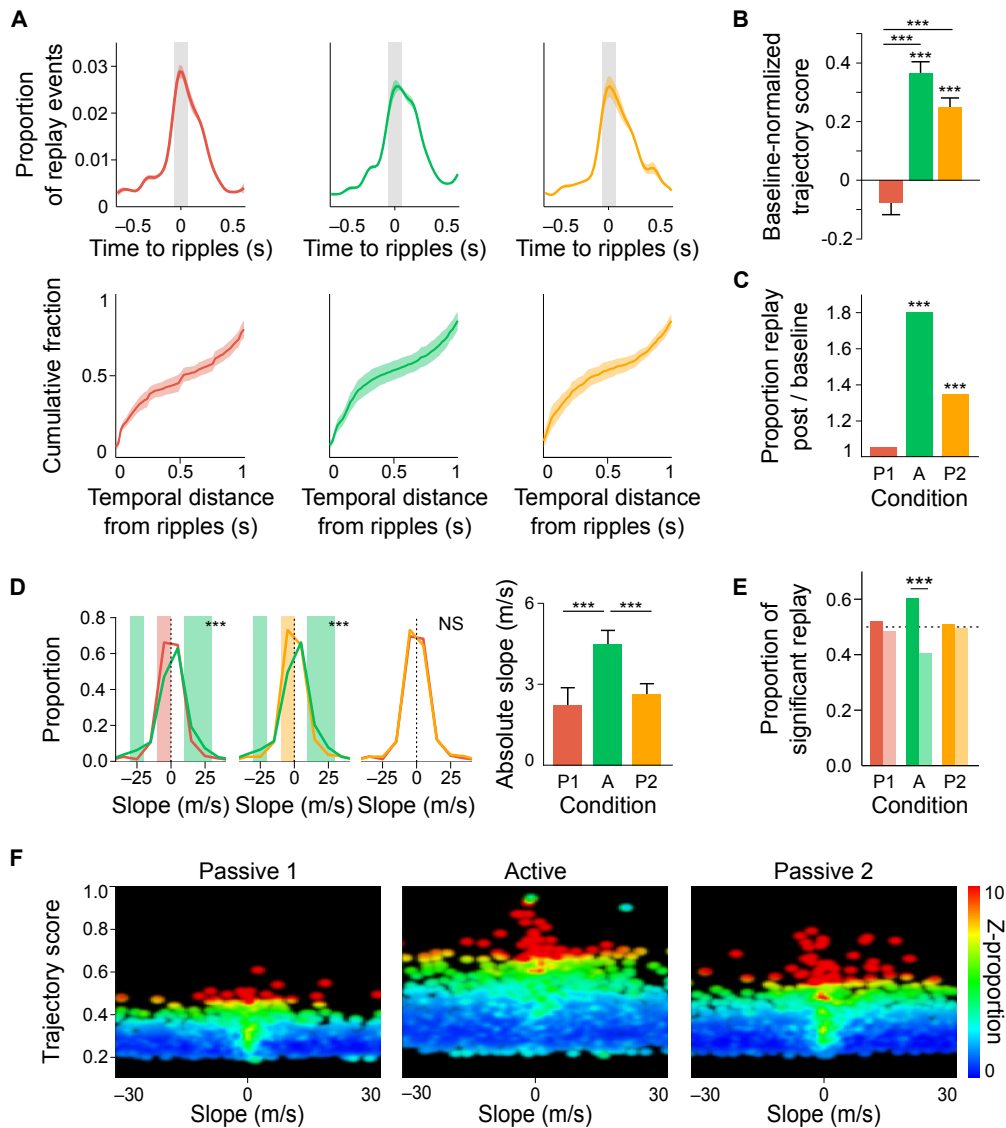


**Fig. S12. Restricting analyses to ripple epochs does not alter the results.** (A) Top, peri-event time histograms of candidate replay events relative to peak ripple power. Dashed lines indicates the beginning and end of ripples and 0 the time of peak ripple power (KS test,  $P > 0.05$  between all condition pairs). Bottom, cumulative distribution of replay events in  $\pm 1$  s time windows centered on ripple peak. (B–F) The analyses in Fig. 4 were replicated on candidate events restricted to ripple epochs. (B) Scores of replay events relative to baseline sleep (KW test,  $***P < 10^{-15}$ ). (C) Proportion of significant replay events relative to baseline sleep. Sleep replay was boosted following active travel, compared to passive travel. (D) Distributions of replay slopes (KS test; left: SP1–SA,  $***P < 10^{-5}$ ; center: SA–SP2,  $***P < 10^{-5}$ ; right: SP1–SP2,  $P > 0.05$ ). Colored bands indicate significant differences (binomial proportion test). Right, absolute slopes of replay events (KW test,  $***P < 10^{-27}$ ). (E) Proportion of forward (darker colors) vs reverse (lighter colors) replay events. Only in sleep following active travel was replay biased to reflect actual wake experience. (F) Distribution of replay quality assessed by joint trajectory score and slope (color codes for proportion relative to shuffled control data).

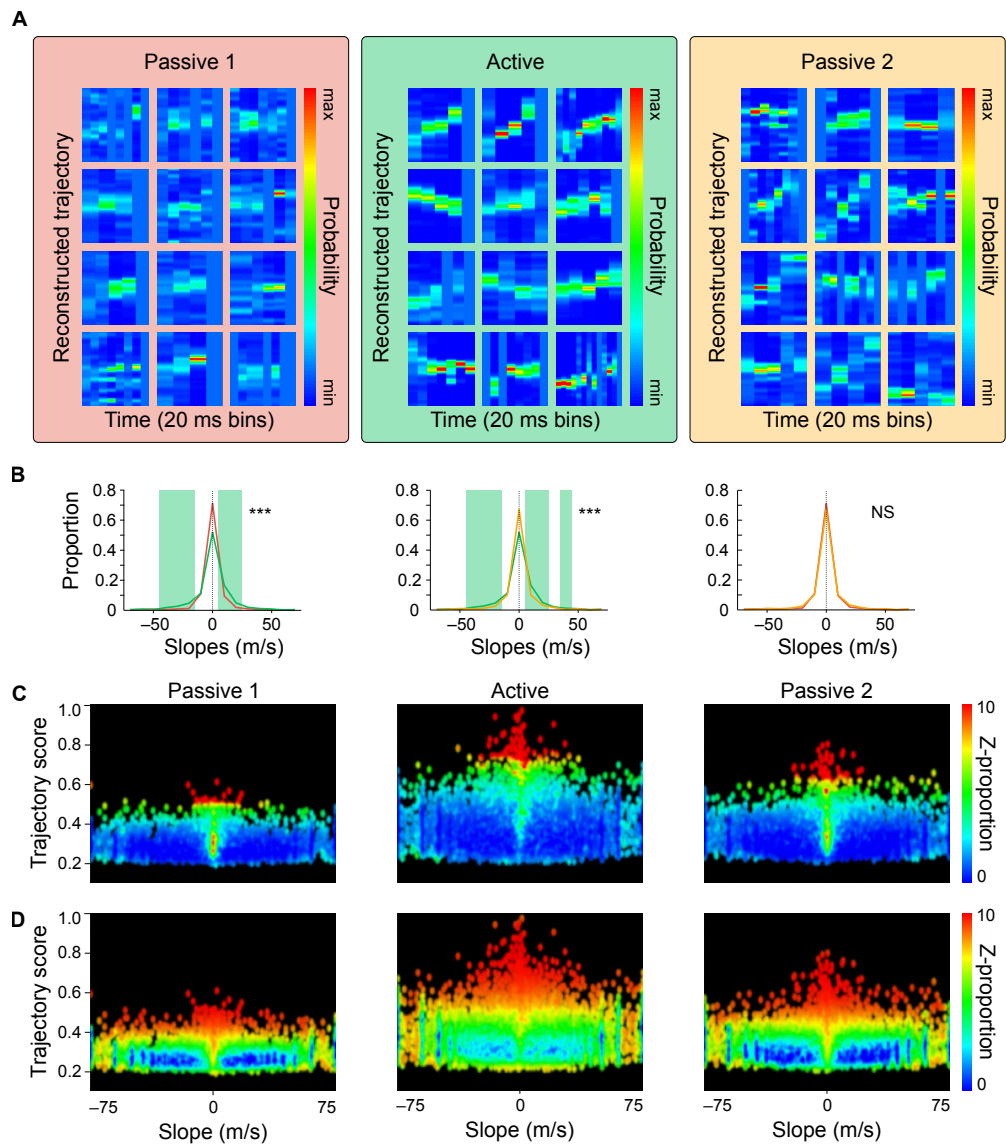


**Fig. S13. Replay is degraded following passive travel.** (A) Example significant replay events in post-sleep sessions. (B) Distributions of replay slopes (KS tests; left: SP1-SA,  $***P < 10^{-8}$ ; center: SA-SP2,  $***P < 10^{-6}$ ; right: SP1-SP2,  $P > 0.05$ ). Colored bands indicate significant differences. (C-D) Distribution of replay quality assessed by joint trajectory score and slope. (C) Color codes for proportion relative to shuffled control data (same as Fig. 4D). (D) Color codes for ratio of observed replay events relative to shuffled control data.

CHAPTER 9. ROLE OF AWAKE THETA SEQUENCES IN MEMORY  
FORMATION

---

# Bibliography

- Ambrose, R. E., Pfeiffer, B. E., Foster, D. J., 2016. Reverse replay of hippocampal place cells is uniquely modulated by changing reward. *Neuron* 91 (5), 1124–1136.
- Amzica, F., Steriade, M., 1997. Cellular substrates and laminar profile of sleep K-complex. *Neuroscience* 82 (3), 671–686.
- Ballarini, F., Moncada, D., Martinez, M. C., Alen, N., Viola, H., 2009. Behavioral tagging is a general mechanism of long-term memory formation. *Proceedings of the National Academy of Sciences* 106 (34), 14599–14604.
- Barker, G. R. I., Warburton, E. C., 2011. When is the hippocampus involved in recognition memory? *Journal of Neuroscience* 31 (29), 10721–10731.
- Battaglia, F. P., Sutherland, G. R., McNaughton, B. L., 2004. Hippocampal sharp wave bursts coincide with neocortical "up-state" transitions. *Learning & Memory* 11 (6), 697–704.
- Bazhenov, M., Timofeev, I., Steriade, M., Sejnowski, T. J., 2002. Model of thalamocortical slow-wave sleep oscillations and transitions to activated States. *Journal of Neuroscience* 22 (19), 8691–8704.
- Behrens, C. J., van den Boom, L. P., de Hoz, L., Friedman, A., Heinemann, U., 2005. Induction of sharp wave-ripple complexes in vitro and reorganization of hippocampal networks. *Nature Neuroscience* 8 (11), 1560–1567.
- Bendor, D., Wilson, M. A., 2012. Biasing the content of hippocampal replay during sleep. *Nature Neuroscience* 15 (10), 1439–1444.
- Berger, H., 1933. Über das Elektrenkephalogramm des Menschen. *Archiv für Psychiatrie und Nervenkrankheiten* 98 (1), 231–254.
- Binder, S., Berg, K., Gasca, F., Lafon, B., Parra, L. C., Born, J., Marshall, L., 2014. Transcranial slow oscillation stimulation during sleep enhances memory consolidation in rats. *Brain Stimulation* 7 (4), 508–515.

## BIBLIOGRAPHY

---

- Bittner, K. C., Milstein, A. D., Grienberger, C., Romani, S., Magee, J. C., 2017. Behavioral time scale synaptic plasticity underlies CA1 place fields. *Science* 357 (6355), 1033–1036.
- Brzosko, Z., Schultz, W., Paulsen, O., 2015. Retroactive modulation of spike timing-dependent plasticity by dopamine. *eLife* 4, e09685.
- Buzsáki, G., 1984. Long-term changes of hippocampal sharp-waves following high frequency afferent activation. *Brain Research* 300 (1), 179–182.
- Buzsáki, G., 1986. Hippocampal sharp waves: Their origin and significance. *Brain Research* 398 (2), 242–252.
- Buzsáki, G., 1989. Two-stage model of memory trace formation: A role for “noisy” brain states. *Neuroscience* 31 (3), 551–570.
- Buzsáki, G., 2006. Rhythms of the Brain. Oxford University Press.
- Buzsáki, G., Haas, H. L., Anderson, E. G., 1987. Long-term potentiation induced by physiologically relevant stimulus patterns. *Brain Research* 435 (1), 331–333.
- Buzsáki, G., Horváth, Z., Urioste, R., Hetke, J., Wise, K., 1992. High-frequency network oscillation in the hippocampus. *Science* 256 (5059), 1025–1027.
- Buzsáki, G., Lai-Wo S., L., Vanderwolf, C. H., 1983. Cellular bases of hippocampal EEG in the behaving rat. *Brain Research Reviews* 6 (2), 139–171.
- Carr, M. F., Jadhav, S. P., Frank, L. M., 2011. Hippocampal replay in the awake state: a potential physiological substrate of memory consolidation and retrieval. *Nature Neuroscience* 14 (2), 147–153.
- Cei, A., Girardeau, G., Drieu, C., Kanbi, K. E., Zugaro, M., 2014. Reversed theta sequences of hippocampal cell assemblies during backward travel. *Nature Neuroscience* 17 (5), 719–24.
- Cenquizca, L. A., Swanson, L. W., 2007. Spatial organization of direct hippocampal field CA1 axonal projections to the rest of the cerebral cortex. *Brain Research Reviews* 56 (1), 1–26.
- Chadwick, A., Rossum, M. C. W. v., Nolan, M. F., 2015. Independent theta phase coding accounts for CA1 population sequences and enables flexible remapping. *eLife* 4.
- Chauvette, S., Crochet, S., Volgushev, M., Timofeev, I., 2011. Properties of slow oscillation during slow-wave sleep and anesthesia in cats. *Journal of Neuroscience* 31 (42), 14998–15008.

- Chauvette, S., Seigneur, J., Timofeev, I., 2012. Sleep oscillations in the thalamocortical system induce long-term neuronal plasticity. *Neuron* 75 (6), 1105–1113.
- Chen, J.-Y., Chauvette, S., Skorheim, S., Timofeev, I., Bazhenov, M., 2012. Interneuron-mediated inhibition synchronizes neuronal activity during slow oscillation. *Journal of Physiology* 590 (16), 3987–4010.
- Chrobak, J. J., Buzsáki, G., 1994. Selective activation of deep layer (V-VI) retrohippocampal cortical neurons during hippocampal sharp waves in the behaving rat. *Journal of Neuroscience* 14 (10), 6160–6170.
- Chrobak, J. J., Buzsáki, G., 1996. High-frequency oscillations in the output networks of the hippocampal–entorhinal axis of the freely behaving rat. *Journal of Neuroscience* 16 (9), 3056–3066.
- Clemens, Z., Mölle, M., Eross, L., Jakus, R., Rásonyi, G., Halász, P., Born, J., 2011. Fine-tuned coupling between human parahippocampal ripples and sleep spindles. *European Journal of Neuroscience* 33 (3), 511–520.
- Compte, A., Sanchez-Vives, M. V., McCormick, D. A., Wang, X.-J., 2003. Cellular and network mechanisms of slow oscillatory activity (<1 Hz) and wave propagations in a cortical network model. *Journal of Neurophysiology* 89 (5), 2707–2725.
- Contreras, D., Destexhe, A., Sejnowski, T. J., Steriade, M., 1996. Control of spatiotemporal coherence of a thalamic oscillation by corticothalamic feedback. *Science* 274 (5288), 771–774.
- Contreras, D., Destexhe, A., Steriade, M., 1997. Intracellular and computational characterization of the intracortical inhibitory control of synchronized thalamic inputs in vivo. *Journal of Neurophysiology* 78 (1), 335–350.
- Contreras, D., Steriade, M., 1995. Cellular basis of EEG slow rhythms: a study of dynamic corticothalamic relationships. *Journal of Neuroscience* 15 (1 Pt 2), 604–622.
- Csicsvari, J., Henze, D. A., Jamieson, B., Harris, K. D., Sirota, A., Barthó, P., Wise, K. D., Buzsáki, G., 2003. Massively parallel recording of unit and local field potentials with silicon-based electrodes. *Journal of Neurophysiology* 90 (2), 1314–1323.
- Csicsvari, J., Hirase, H., Mamiya, A., Buzsáki, G., 2000. Ensemble patterns of hippocampal CA3-CA1 neurons during sharp wave–associated population events. *Neuron* 28 (2), 585–594.

## BIBLIOGRAPHY

---

- Csicsvari, J., O'Neill, J., Allen, K., Senior, T., 2007. Place-selective firing contributes to the reverse-order reactivation of CA1 pyramidal cells during sharp waves in open-field exploration. *European Journal of Neuroscience* 26 (3), 704–716.
- Davidson, T. J., Kloosterman, F., Wilson, M. A., 2009. Hippocampal replay of extended experience. *Neuron* 63 (4), 497–507.
- de la Rocha, J., Doiron, B., Shea-Brown, E., Josić, K., Reyes, A., 2007. Correlation between neural spike trains increases with firing rate. *Nature* 448 (7155), 802–806.
- de Lavilléon, G., Lacroix, M. M., Rondi-Reig, L., Benchenane, K., 2015. Explicit memory creation during sleep demonstrates a causal role of place cells in navigation. *Nature Neuroscience* 18 (4), 493–495.
- Destexhe, A., Contreras, D., Steriade, M., 1998. Mechanisms underlying the synchronizing action of corticothalamic feedback through inhibition of thalamic relay cells. *Journal of Neurophysiology* 79 (2), 999–1016.
- Destexhe, A., Contreras, D., Steriade, M., 1999. Spatiotemporal analysis of local field potentials and unit discharges in cat cerebral cortex during natural wake and sleep states. *Journal of Neuroscience* 19 (11), 4595–4608.
- Destexhe, A., Hughes, S. W., Rudolph, M., Crunelli, V., 2007. Are corticothalamic ‘up’ states fragments of wakefulness? *Trends in Neurosciences* 30 (7), 334–342.
- Diba, K., Buzsáki, G., 2007. Forward and reverse hippocampal place-cell sequences during ripples. *Nature Neuroscience* 10 (10), 1241.
- Diekelmann, S., Born, J., 2010. The memory function of sleep. *Nature Reviews Neuroscience* 11 (2), 114–126.
- Dragoi, G., Forooq, Usman, Sibille, Jérémie, Liu, Kefei, 2017. Preconfigured, plastic networks: Unified view on integration of Hebbian and homeostatic processes during learning. 523.18 / UU50.
- Dragoi, G., Harris, K. D., Buzsáki, G., 2003. Place representation within hippocampal networks is modified by long-term potentiation. *Neuron* 39 (5), 843–853.
- Dragoi, G., Tonegawa, S., 2011. Preplay of future place cell sequences by hippocampal cellular assemblies. *Nature* 469 (7330), 397–401.

- Dragoi, G., Tonegawa, S., 2013. Distinct preplay of multiple novel spatial experiences in the rat. *Proceedings of the National Academy of Sciences* 110 (22), 9100–9105.
- Dupret, D., O’Neill, J., Pleydell-Bouverie, B., Csicsvari, J., 2010. The reorganization and reactivation of hippocampal maps predict spatial memory performance. *Nature Neuroscience* 13 (8), 995–1002.
- Eggert, T., Dorn, H., Sauter, C., Nitsche, M. A., Bajbouj, M., Danker-Hopfe, H., 2013. No effects of slow oscillatory transcranial direct current stimulation (tDCS) on sleep-dependent memory consolidation in healthy elderly subjects. *Brain Stimulation* 6 (6), 938–945.
- Ego-Stengel, V., Wilson, M. A., 2010. Disruption of ripple-associated hippocampal activity during rest impairs spatial learning in the rat. *Hippocampus* 20 (1), 1–10.
- El Boustani, S., Yger, P., Frégnac, Y., Destexhe, A., 2012. Stable learning in stochastic network states. *Journal of Neuroscience* 32 (1), 194–214.
- Ellender, T. J., Nissen, W., Colgin, L. L., Mann, E. O., Paulsen, O., 2010. Priming of hippocampal population bursts by individual perisomatic-targeting interneurons. *Journal of Neuroscience* 30 (17), 5979–5991.
- Eschenko, O., Mölle, M., Born, J., Sara, S. J., 2006. Elevated sleep spindle density after learning or after retrieval in rats. *Journal of Neuroscience* 26 (50), 12914–12920.
- Eschenko, O., Ramadan, W., Mölle, M., Born, J., Sara, S. J., 2008. Sustained increase in hippocampal sharp-wave ripple activity during slow-wave sleep after learning. *Learning & Memory* 15 (4), 222–228.
- Euston, D. R., Tatsuno, M., McNaughton, B. L., 2007. Fast-forward playback of recent memory sequences in prefrontal cortex during sleep. *Science* 318 (5853), 1147–1150.
- Feng, T., Silva, D., Foster, D. J., 2015. Dissociation between the experience-dependent development of hippocampal theta sequences and single-trial phase precession. *Journal of Neuroscience* 35 (12), 4890–4902.
- Foster, D. J., Wilson, M. A., 2006. Reverse replay of behavioural sequences in hippocampal place cells during the awake state. *Nature* 440 (7084), 680–683.
- Foster, D. J., Wilson, M. A., 2007. Hippocampal theta sequences. *Hippocampus* 17 (11), 1093–9.

## BIBLIOGRAPHY

---

- Frankland, P. W., Bontempi, B., 2005. The organization of recent and remote memories. *Nature Reviews Neuroscience* 6 (2), 119–130.
- Froemke, R. C., Dan, Y., 2002. Spike-timing-dependent synaptic modification induced by natural spike trains. *Nature* 416 (6879), 433.
- Gais, S., Mölle, M., Helms, K., Born, J., 2002. Learning-dependent increases in sleep spindle density. *Journal of Neuroscience* 22 (15), 6830–6834.
- Gardner, R. J., Hughes, S. W., Jones, M. W., 2013. Differential spike timing and phase dynamics of reticular thalamic and prefrontal cortical neuronal populations during sleep spindles. *Journal of Neuroscience* 33 (47), 18469–18480.
- Gelinas, J. N., Khodagholy, D., Thesen, T., Devinsky, O., Buzsáki, G., 2016. Interictal epileptiform discharges induce hippocampal-cortical coupling in temporal lobe epilepsy. *Nature Medicine* 22 (6), 641–648.
- Girardeau, G., Benchenane, K., Wiener, S. I., Buzsáki, G., Zugaro, M. B., 2009. Selective suppression of hippocampal ripples impairs spatial memory. *Nature Neuroscience* 12 (10), 1222–1223.
- Girardeau, G., Cei, A., Zugaro, M., 2014. Learning-induced plasticity regulates hippocampal sharp wave-ripple drive. *Journal of Neuroscience* 34 (15), 5176–5183.
- Girardeau, G., Inema, I., Buzsáki, G., 2017. Reactivations of emotional memory in the hippocampus–amygdala system during sleep. *Nature Neuroscience* 20 (11), 1634.
- Gomperts, S. N., Kloosterman, F., Wilson, M. A., 2015. VTA neurons coordinate with the hippocampal reactivation of spatial experience. *eLife* 4, e05360.
- Grosmark, A. D., Buzsáki, G., 2016. Diversity in neural firing dynamics supports both rigid and learned hippocampal sequences. *Science* 351 (6280), 1440–1443.
- Gupta, A. S., van der Meer, M. A. A., Touretzky, D. S., Redish, A. D., 2010. Hippocampal replay is not a simple function of experience. *Neuron* 65 (5), 695–705.
- Hahn, T. T. G., McFarland, J. M., Berberich, S., Sakmann, B., Mehta, M. R., 2012. Spontaneous persistent activity in entorhinal cortex modulates cortico-hippocampal interaction in vivo. *Nature Neuroscience* 15 (11), 1531–1538.

- Heib, D. P. J., Hoedlmoser, K., Anderer, P., Zeitlhofer, J., Gruber, G., Klimesch, W., Schabus, M., 2013. Slow oscillation amplitudes and Up-state lengths relate to memory improvement. *PLoS ONE* 8 (12).
- Hirase, H., Leinekugel, X., Czurkó, A., Csicsvari, J., Buzsáki, G., 2001. Firing rates of hippocampal neurons are preserved during subsequent sleep episodes and modified by novel awake experience. *Proceedings of the National Academy of Sciences* 98 (16), 9386–9390.
- Huber, R., Ghilardi, M. F., Massimini, M., Tononi, G., 2004. Local sleep and learning. *Nature* 430 (6995), 78–81.
- Hunt, D. L., Linaro, D., Si, B., Romani, S., Spruston, N., 2018. A novel pyramidal cell type promotes sharp-wave synchronization in the hippocampus. *Nature Neuroscience* 21 (7), 985–995.
- Isomura, Y., Sirota, A., Özen, S., Montgomery, S., Mizuseki, K., Henze, D. A., Buzsáki, G., 2006. Integration and segregation of activity in entorhinal-hippocampal subregions by neocortical slow oscillations. *Neuron* 52 (5), 871–882.
- Jadhav, S. P., Kemere, C., German, P. W., Frank, L. M., 2012. Awake hippocampal sharp-wave ripples support spatial memory. *Science* 336 (6087), 1454–1458.
- Jadhav, S. P., Rothschild, G., Roumis, D. K., Frank, L. M., 2016. Coordinated excitation and inhibition of prefrontal ensembles during awake hippocampal sharp-wave ripple events. *Neuron* 90 (1), 113–127.
- Jarrard, L. E., 1995. What does the hippocampus really do? *Behavioural Brain Research* 71 (1), 1–10.
- Jercog, D., Roxin, A., Barthó, P., Luczak, A., Compte, A., Rocha, J. d. l., 2017. UP-DOWN cortical dynamics reflect state transitions in a bistable network. *eLife* 6, e22425.
- Ji, D., Wilson, M. A., 2007. Coordinated memory replay in the visual cortex and hippocampus during sleep. *Nature neuroscience* 10 (1), 100–107.
- Johnson, L., Euston, D., Tatsuno, M., McNaughton, B., 2010. Stored-trace reactivation in rat prefrontal cortex is correlated with down-to-up state fluctuation density. *Journal of Neuroscience* 30 (7), 2650–2661.
- Karlsson, M. P., Frank, L. M., 2009. Awake replay of remote experiences in the hippocampus. *Nature Neuroscience* 12 (7), 913–918.

## BIBLIOGRAPHY

---

- Khodagholy, D., Gelinas, J. N., Buzsáki, G., 2017. Learning-enhanced coupling between ripple oscillations in association cortices and hippocampus. *Science* 358 (6361), 369–372.
- King, C., Henze, D. A., Leinekugel, X., Buzsáki, G., 1999. Hebbian modification of a hippocampal population pattern in the rat. *Journal of Physiology* 521 (Pt 1), 159–167.
- Kovács, K. A., O'Neill, J., Schoenenberger, P., Penttonen, M., Ranguel Guerrero, D. K., Csicsvari, J., 2016. Optogenetically blocking sharp wave ripple events in sleep does not interfere with the formation of stable spatial representation in the CA1 area of the hippocampus. *PLOS ONE* 11 (10), e0164675.
- Kruskal, P. B., Li, L., MacLean, J. N., 2013. Circuit reactivation dynamically regulates synaptic plasticity in neocortex. *Nature Communications* 4, 2574.
- Kudrimoti, H. S., Barnes, C. A., McNaughton, B. L., 1999. Reactivation of hippocampal cell assemblies: effects of behavioral state, experience, and EEG dynamics. *Journal of Neuroscience* 19 (10), 4090–4101.
- Lafon, B., Henin, S., Huang, Y., Friedman, D., Melloni, L., Thesen, T., Doyle, W., Buzsáki, G., Devinsky, O., Parra, L. C., Liu, A., 2017. Low frequency transcranial electrical stimulation does not entrain sleep rhythms measured by human intracranial recordings. *Nature Communications* 8 (1), 1199.
- Lansink, C. S., Goltstein, P. M., Lankelma, J. V., McNaughton, B. L., Pennartz, C. M. A., 2009. Hippocampus leads ventral striatum in replay of place-reward information. *PLOS Biology* 7 (8), e1000173.
- Laroche, S., Jay, T. M., Thierry, A.-M., 1990. Long-term potentiation in the prefrontal cortex following stimulation of the hippocampal CA1/subicular region. *Neuroscience Letters* 114 (2), 184–190.
- Latchoumane, C.-F. V., Ngo, H.-V. V., Born, J., Shin, H.-S., 2017. Thalamic spindles promote memory formation during sleep through triple phase-locking of cortical, thalamic, and hippocampal rhythms. *Neuron* 95 (2), 424–435.e6.
- Lee, A. K., Wilson, M. A., 2002. Memory of sequential experience in the hippocampus during slow wave sleep. *Neuron* 36 (6), 1183–1194.
- Lemieux, M., Chauvette, S., Timofeev, I., 2015. Neocortical inhibitory activities and long-range afferents contribute to the synchronous onset of silent states of the neocortical slow oscillation. *Journal of Neurophysiology* 113 (3), 768–779.
- Levenstein, D., Watson, B. O., Rinzal, J., Buzsáki, G., 2017. Sleep regulation of the distribution of cortical firing rates. *Current Opinion in Neurobiology* 44, 34–42.

- Li, S., Cullen, W. K., Anwyl, R., Rowan, M. J., 2003. Dopamine-dependent facilitation of LTP induction in hippocampal CA1 by exposure to spatial novelty. *Nature Neuroscience* 6 (5), 526–531.
- Lin, Y.-W., Min, M.-Y., Chiu, T.-H., Yang, H.-W., 2003. Enhancement of associative long-term potentiation by activation of  $\alpha$ -adrenergic receptors at CA1 synapses in rat hippocampal slices. *Journal of Neuroscience* 23 (10), 4173–4181.
- Lubenov, E. V., Siapas, A. G., 2008. Decoupling through synchrony in neuronal circuits with propagation delays. *Neuron* 58 (1), 118–131.
- Luczak, A., Barthó, P., Marguet, S. L., Buzsáki, G., Harris, K. D., 2007. Sequential structure of neocortical spontaneous activity in vivo. *Proceedings of the National Academy of Sciences of the United States of America* 104 (1), 347–352.
- MacLean, J. N., Watson, B. O., Aaron, G. B., Yuste, R., 2005. Internal dynamics determine the cortical response to thalamic stimulation. *Neuron* 48 (5), 811–823.
- Magee, J. C., Johnston, D., 1997. A synaptically controlled, associative signal for Hebbian plasticity in hippocampal neurons. *Science* 275 (5297), 209–213.
- Maingret, N., Girardeau, G., Todorova, R., Goutierre, M., Zugaro, M., 2016. Hippocampo-cortical coupling mediates memory consolidation during sleep. *Nature Neuroscience* 19 (7), 959–964.
- Mao, D., Kandler, S., McNaughton, B. L., Bonin, V., 2017. Sparse orthogonal population representation of spatial context in the retrosplenial cortex. *Nature Communications* 8.
- Markram, H., Lübke, J., Frotscher, M., Sakmann, B., 1997. Regulation of synaptic efficacy by coincidence of postsynaptic APs and EPSPs. *Science* 275 (5297), 213–215.
- Marr, D., 1971. Simple memory: a theory for archicortex. *Philosophical Transactions of the Royal Society B: Biological Sciences* 262 (841), 23–81.
- Marshall, L., Helgadottir, H., Molle, M., Born, J., 2006. Boosting slow oscillations during sleep potentiates memory. *Nature* 444 (7119), 610–610.
- Massimini, M., Huber, R., Ferrarelli, F., Hill, S., Tononi, G., 2004. The sleep slow oscillation as a traveling wave. *Journal of Neuroscience* 24 (31), 6862–6870.

## BIBLIOGRAPHY

---

- McNamara, C. G., Tejero-Cantero, A., Trouche, S., Campo-Urriza, N., Dupret, D., 2014. Dopaminergic neurons promote hippocampal reactivation and spatial memory persistence. *Nature Neuroscience* 17 (12), 1658–1660.
- Mednick, S. C., McDevitt, E. A., Walsh, J. K., Wamsley, E., Paulus, M., Kanady, J. C., Drummond, S. P. A., 2013. The critical role of sleep spindles in hippocampal-dependent memory: a pharmacology study. *Journal of Neuroscience* 33 (10), 4494–4504.
- Mena-Segovia, J., Sims, H. M., Magill, P. J., Bolam, J. P., 2008. Cholinergic brainstem neurons modulate cortical gamma activity during slow oscillations. *Journal of Physiology* 586 (12), 2947–2960.
- Middleton, S. J., McHugh, T. J., 2016. Silencing CA3 disrupts temporal coding in the CA1 ensemble. *Nature Neuroscience* 19 (7), 945–951.
- Miyawaki, T., Norimoto, H., Ishikawa, T., Watanabe, Y., Matsuki, N., Ikegaya, Y., 2014. Dopamine receptor activation reorganizes neuronal ensembles during hippocampal sharp waves in vitro. *PLOS ONE* 9 (8), e104438.
- Morris, R. G., Garrud, P., Rawlins, J. N., O’Keefe, J., 1982. Place navigation impaired in rats with hippocampal lesions. *Nature* 297 (5868), 681–683.
- Mukovski, M., Chauvette, S., Timofeev, I., Volgushev, M., 2007. Detection of active and silent states in neocortical neurons from the field potential signal during slow-wave sleep. *Cerebral Cortex* 17 (2), 400–414.
- Mölle, M., Yeshenko, O., Marshall, L., Sara, S. J., Born, J., 2006. Hippocampal sharp wave-ripples linked to slow oscillations in rat slow-wave sleep. *Journal of Neurophysiology* 96 (1), 62–70.
- Nadel, L., Moscovitch, M., 1997. Memory consolidation, retrograde amnesia and the hippocampal complex. *Current Opinion in Neurobiology* 7 (2), 217–227.
- Ngo, H.-V. V., Martinetz, T., Born, J., Mölle, M., 2013. Auditory closed-loop stimulation of the sleep slow oscillation enhances memory. *Neuron* 78 (3), 545–553.
- Norimoto, H., Makino, K., Gao, M., Shikano, Y., Okamoto, K., Ishikawa, T., Sasaki, T., Hioki, H., Fujisawa, S., Ikegaya, Y., 2018. Hippocampal ripples down-regulate synapses. *Science* 359 (6383), 1524–1527.
- Novitskaya, Y., Sara, S. J., Logothetis, N. K., Eschenko, O., 2016. Ripple-triggered stimulation of the locus coeruleus during post-learning sleep disrupts ripple/spindle coupling and impairs memory consolidation. *Learning & Memory* 23 (5), 238–248.

- Nádasdy, Z., Hirase, H., Czurkó, A., Csicsvari, J., Buzsáki, G., 1999. Replay and time compression of recurring spike sequences in the hippocampus. *Journal of Neuroscience* 19 (21), 9497–9507.
- O’Keefe, J., Dostrovsky, J., 1971. The hippocampus as a spatial map. Preliminary evidence from unit activity in the freely-moving rat. *Brain Research* 34 (1), 171–175.
- O’Keefe, J., Nadel, L., 1978. The hippocampus as a cognitive map. Oxford: Clarendon Press.
- Oliva, A., Fernández-Ruiz, A., Buzsáki, G., Berényi, A., 2016. Role of hippocampal CA2 region in triggering sharp-wave ripples. *Neuron* 91 (6), 1342–1355.
- O’Mara, S. M., Commins, S., Anderson, M., 2000. Synaptic plasticity in the hippocampal area CA1-subiculum projection: Implications for theories of memory. *Hippocampus* 10 (4), 447–456.
- O’Neill, J., Boccara, C. N., Stella, F., Schoenenberger, P., Csicsvari, J., 2017. Superficial layers of the medial entorhinal cortex replay independently of the hippocampus. *Science* 355 (6321), 184–188.
- O’Neill, J., Senior, T., Csicsvari, J., 2006. Place-selective firing of CA1 pyramidal cells during sharp wave/ripple network patterns in exploratory behavior. *Neuron* 49 (1), 143–155.
- O’Neill, J., Senior, T. J., Allen, K., Huxter, J. R., Csicsvari, J., 2008. Reactivation of experience-dependent cell assembly patterns in the hippocampus. *Nature Neuroscience* 11 (2), 209–215.
- Papale, A. E., Zielinski, M. C., Frank, L. M., Jadhav, S. P., Redish, A. D., 2016. Interplay between hippocampal sharp-wave-ripple events and vicarious trial and error behaviors in decision making. *Neuron* 92 (5), 975–982.
- Patel, J., Schomburg, E. W., Berényi, A., Fujisawa, S., Buzsáki, G., 2013. Local generation and propagation of ripples along the septotemporal axis of the hippocampus. *Journal of Neuroscience* 33 (43), 17029–17041.
- Pavlidis, C., Winson, J., 1989. Influences of hippocampal place cell firing in the awake state on the activity of these cells during subsequent sleep episodes. *Journal of Neuroscience* 9 (8), 2907–2918.
- Pennartz, C. M. A., Lee, E., Verheul, J., Lipa, P., Barnes, C. A., McNaughton, B. L., 2004. The ventral striatum in off-line processing: ensemble reactivation during sleep and modulation by hippocampal ripples. *Journal of Neuroscience* 24 (29), 6446–6456.

## BIBLIOGRAPHY

---

- Peyrache, A., Battaglia, F. P., Destexhe, A., 2011. Inhibition recruitment in prefrontal cortex during sleep spindles and gating of hippocampal inputs. *Proceedings of the National Academy of Sciences* 108 (41), 17207–17212.
- Peyrache, A., Khamassi, M., Benchenane, K., Wiener, S. I., Battaglia, F. P., 2009. Replay of rule-learning related neural patterns in the prefrontal cortex during sleep. *Nature Neuroscience* 12 (7), 919–926.
- Pfeiffer, B. E., Foster, D. J., 2013. Hippocampal place-cell sequences depict future paths to remembered goals. *Nature* 497 (7447), 74–79.
- Phillips, K. G., Bartsch, U., McCarthy, A. P., Edgar, D. M., Tricklebank, M. D., Wafford, K. A., Jones, M. W., 2012. Decoupling of sleep-dependent cortical and hippocampal interactions in a neurodevelopmental model of schizophrenia. *Neuron* 76 (3), 526–533.
- Ramadan, W., Eschenko, O., Sara, S. J., 2009. Hippocampal sharp wave/ripples during sleep for consolidation of associative memory. *PLOS ONE* 4 (8), e6697.
- Rasch, B., Büchel, C., Gais, S., Born, J., 2007. Odor cues during slow-wave sleep prompt declarative memory consolidation. *Science* 315 (5817), 1426–1429.
- Rigas, P., Castro-Alamancos, M. A., 2007. Thalamocortical Up states: differential effects of intrinsic and extrinsic cortical inputs on persistent activity. *Journal of Neuroscience* 27 (16), 4261–4272.
- Robbe, D., Buzsáki, G., 2009. Alteration of theta timescale dynamics of hippocampal place cells by a cannabinoid is associated with memory impairment. *Journal of Neuroscience* 29 (40), 12597–605.
- Rosanova, M., Ulrich, D., 2005. Pattern-specific associative long-term potentiation induced by a sleep spindle-related spike train. *Journal of Neuroscience* 25 (41), 9398–9405.
- Rothschild, G., Eban, E., Frank, L. M., 2017. A cortical-hippocampal-cortical loop of information processing during memory consolidation. *Nature Neuroscience* 20 (2), 251–259.
- Roumis, D. K., Frank, L. M., 2015. Hippocampal sharp-wave ripples in waking and sleeping states. *Current Opinion in Neurobiology* 35 (Supplement C), 6–12.
- Roux, L., Hu, B., Eichler, R., Stark, E., Buzsáki, G., 2017. Sharp wave ripples during learning stabilize the hippocampal spatial map. *Nature Neuroscience* 20 (6), 845–853.

- Rudoy, J. D., Voss, J. L., Westerberg, C. E., Paller, K. A., 2009. Strengthening individual memories by reactivating them during sleep. *Science* 326 (5956), 1079–1079.
- Sadowski, J. H. L. P., Jones, M. W., Mellor, J. R., 2016. Sharp-wave ripples orchestrate the induction of synaptic plasticity during reactivation of place cell firing patterns in the hippocampus. *Cell Reports* 14 (8), 1916–1929.
- Sahlem, G. L., Badran, B. W., Halford, J. J., Williams, N. R., Korte, J. E., Leslie, K., Strachan, M., Breedlove, J. L., Runion, J., Bachman, D. L., Uhde, T. W., Borckardt, J. J., George, M. S., 2015. Oscillating square wave transcranial direct current stimulation (tDCS) delivered during slow wave sleep does not improve declarative memory more than sham: A randomized sham controlled crossover study. *Brain stimulation* 8 (3), 528–534.
- Sanchez-Vives, M. V., McCormick, D. A., 2000. Cellular and network mechanisms of rhythmic recurrent activity in neocortex. *Nature Neuroscience* 3 (10), 1027–1034.
- Scoville, W. B., Milner, B., 1957. Loss of recent memory after bilateral hippocampal lesions. *Journal of Neurology, Neurosurgery, and Psychiatry* 20 (1), 11–21.
- Seibt, J., Richard, C. J., Sigl-Glöckner, J., Takahashi, N., Kaplan, D. I., Doron, G., Limoges, D., Bocklisch, C., Larkum, M. E., 2017. Cortical dendritic activity correlates with spindle-rich oscillations during sleep in rodents. *Nature Communications* 8 (1), 684.
- Sejnowski, T. J., Destexhe, A., 2000. Why do we sleep? *Brain Research* 886 (1), 208–223.
- Shu, Y., Hasenstaub, A., McCormick, D. A., 2003. Turning on and off recurrent balanced cortical activity. *Nature* 423 (6937), 288–293.
- Siapas, A. G., Wilson, M. A., 1998. Coordinated interactions between hippocampal ripples and cortical spindles during slow-wave sleep. *Neuron* 21 (5), 1123–1128.
- Silva, D., Feng, T., Foster, D. J., 2015. Trajectory events across hippocampal place cells require previous experience. *Nature Neuroscience* 18 (12), 1772–1779.
- Singer, A. C., Carr, M. F., Karlsson, M. P., Frank, L. M., 2013. Hippocampal SWR activity predicts correct decisions during the initial learning of an alternation task. *Neuron* 77 (6), 1163–1173.

## BIBLIOGRAPHY

---

- Singer, A. C., Frank, L. M., 2009. Rewarded outcomes enhance reactivation of experience in the hippocampus. *Neuron* 64 (6), 910–921.
- Sirota, A., Buzsáki, G., 2005. Interaction between neocortical and hippocampal networks via slow oscillations. *Thalamus and Related Systems* 3 (4), 245–259.
- Sirota, A., Csicsvari, J., Buhl, D., Buzsáki, G., 2003. Communication between neocortex and hippocampus during sleep in rodents. *Proceedings of the National Academy of Sciences* 100 (4), 2065–2069.
- Skaggs, W. E., McNaughton, B. L., 1996. Replay of neuronal firing sequences in rat hippocampus during sleep following spatial experience. *Science* 271 (5257), 1870–1873.
- Skaggs, W. E., McNaughton, B. L., Wilson, M. A., Barnes, C. A., 1996. Theta phase precession in hippocampal neuronal populations and the compression of temporal sequences. *Hippocampus* 6 (2), 149–172.
- Sosa, M., Joo, Hannah, Frank, Loren, 2017. Reactivation of nucleus accumbens neurons during awake dorsal and ventral hippocampal sharp-wave ripples. 84.07 / SS6.
- Squire, L. R., Alvarez, P., 1995. Retrograde amnesia and memory consolidation: a neurobiological perspective. *Current Opinion in Neurobiology* 5 (2), 169–177.
- Stark, E., Roux, L., Eichler, R., Buzsáki, G., 2015. Local generation of multineuronal spike sequences in the hippocampal CA1 region. *Proceedings of the National Academy of Sciences* 112 (33), 10521–10526.
- Steriade, M., Amzica, F., Nuñez, A., 1993a. Cholinergic and noradrenergic modulation of the slow (approximately 0.3 Hz) oscillation in neocortical cells. *Journal of Neurophysiology* 70 (4), 1385–1400.
- Steriade, M., McCormick, D. A., Sejnowski, T. J., 1993b. Thalamocortical oscillations in the sleeping and aroused brain. *Science* 262 (5134), 679–685.
- Steriade, M., Nunez, A., Amzica, F., 1993c. A novel slow (<1 Hz) oscillation of neocortical neurons in vivo: depolarizing and hyperpolarizing components. *Journal of Neuroscience* 13 (8), 3252–3265.
- Steriade, M., Timofeev, I., 2003. Neuronal plasticity in thalamocortical networks during sleep and waking oscillations. *Neuron* 37 (4), 563–576.
- Steriade, M., Timofeev, I., Grenier, F., 2001. Natural waking and sleep states: a view from inside neocortical neurons. *Journal of Neurophysiology* 85 (5), 1969–1985.

- Sullivan, D., Csicsvari, J., Mizuseki, K., Montgomery, S., Diba, K., Buzsáki, G., 2011. Relationships between hippocampal sharp waves, ripples and fast gamma oscillation: influence of dentate and entorhinal cortical activity. *Journal of Neuroscience* 31 (23), 8605–8616.
- Sullivan, D., Mizuseki, K., Sorgi, A., Buzsáki, G., 2014. Comparison of sleep spindles and theta oscillations in the hippocampus. *Journal of Neuroscience* 34 (2), 662–674.
- Takeuchi, T., Duzskiewicz, A. J., Sonneborn, A., Spooner, P. A., Yamasaki, M., Watanabe, M., Smith, C. C., Fernández, G., Deisseroth, K., Greene, R. W., Morris, R. G. M., 2016. Locus coeruleus and dopaminergic consolidation of everyday memory. *Nature* 537 (7620), 357–362.
- Tang, W., Shin, J. D., Frank, L. M., Jadhav, S. P., 2017. Hippocampal-prefrontal reactivation during learning is stronger in awake as compared to sleep states. *Journal of Neuroscience*, 2291–17.
- Terrazas, A., Krause, M., Lipa, P., Gothard, K. M., Barnes, C. A., McNaughton, B. L., 2005. Self-motion and the hippocampal spatial metric. *Journal of Neuroscience* 25 (35), 8085–8096.
- Tierney, P. L., Dégenétais, E., Thierry, A.-M., Glowinski, J., Gioanni, Y., 2004. Influence of the hippocampus on interneurons of the rat prefrontal cortex. *European Journal of Neuroscience* 20 (2), 514–524.
- Timofeev, I., Bazhenov, M., 2005. Mechanisms and biological role of thalamocortical oscillations. *Trends in chronobiology research*, 1–47.
- Timofeev, I., Bazhenov, M., Sejnowski, T. J., Steriade, M., 2001a. Contribution of intrinsic and synaptic factors in the desynchronization of thalamic oscillatory activity. *Thalamus & Related Systems* 1 (1), 53–69.
- Timofeev, I., Contreras, D., Steriade, M., 1996. Synaptic responsiveness of cortical and thalamic neurones during various phases of slow sleep oscillation in cat. *Journal of Physiology* 494 (Pt 1), 265–278.
- Timofeev, I., Grenier, F., Bazhenov, M., Sejnowski, T. J., Steriade, M., 2000. Origin of slow cortical oscillations in deafferented cortical slabs. *Cerebral Cortex* 10 (12), 1185–1199.
- Timofeev, I., Grenier, F., Steriade, M., 2001b. Disfacilitation and active inhibition in the neocortex during the natural sleep-wake cycle: an intracellular study. *Proceedings of the National Academy of Sciences of the United States of America* 98 (4), 1924–1929.

## BIBLIOGRAPHY

---

- Timofeev, I., Steriade, M., 1996. Low-frequency rhythms in the thalamus of intact-cortex and decorticated cats. *Journal of Neurophysiology* 76 (6), 4152–4168.
- Todorova, R., Zugaro, M., 2018. Hippocampal ripples as a mode of communication with cortical and subcortical areas. *Hippocampus*.
- Tolman, E. C., 1938. The determiners of behavior at a choice point. *Psychological Review* 45 (1), 1–41.
- Tse, D., Langston, R. F., Kakeyama, M., Bethus, I., Spooner, P. A., Wood, E. R., Witter, M. P., Morris, R. G. M., 2007. Schemas and Memory Consolidation. *Science* 316 (5821), 76–82.
- Ul Haq, R., Liotta, A., Kovacs, R., Rösler, A., Jarosch, M. J., Heinemann, U., Behrens, C. J., 2012. Adrenergic modulation of sharp wave-ripple activity in rat hippocampal slices. *Hippocampus* 22 (3), 516–533.
- Valdés, J. L., McNaughton, B. L., Fellous, J.-M., 2015. Offline reactivation of experience-dependent neuronal firing patterns in the rat ventral tegmental area. *Journal of Neurophysiology* 114 (2), 1183–1195.
- van de Ven, G. M., Trouche, S., McNamara, C. G., Allen, K., Dupret, D., 2016. Hippocampal offline reactivation consolidates recently formed cell assembly patterns during sharp wave-ripples. *Neuron* 92 (5), 968–974.
- Vandecasteele, M., Varga, V., Berényi, A., Papp, E., Barthó, P., Venance, L., Freund, T. F., Buzsáki, G., 2014. Optogenetic activation of septal cholinergic neurons suppresses sharp wave ripples and enhances theta oscillations in the hippocampus. *Proceedings of the National Academy of Sciences* 111 (37), 13535–13540.
- Varela, C., Kumar, S., Yang, J. Y., Wilson, M. A., 2014. Anatomical substrates for direct interactions between hippocampus, medial prefrontal cortex, and the thalamic nucleus reuniens. *Brain Structure and Function* 219 (3), 911–929.
- Volgushev, M., Chauvette, S., Mukovski, M., Timofeev, I., 2006. Precise long-range synchronization of activity and silence in neocortical neurons during slow-wave oscillations [corrected]. *Journal of Neuroscience* 26 (21), 5665–5672.
- Vyazovskiy, V. V., Faraguna, U., Cirelli, C., Tononi, G., 2009. Triggering slow waves during NREM sleep in the rat by intracortical electrical stimulation: effects of sleep/wake history and background activity. *Journal of Neurophysiology* 101 (4), 1921–1931.

- Wang, D. V., Yau, H.-J., Broker, C. J., Tsou, J.-H., Bonci, A., Ikemoto, S., 2015a. Mesopontine median raphe regulates hippocampal ripple oscillation and memory consolidation. *Nature Neuroscience* 18 (5), 728–735.
- Wang, Y., Romani, S., Lustig, B., Leonardo, A., Pastalkova, E., 2015b. Theta sequences are essential for internally generated hippocampal firing fields. *Nature Neuroscience* 18 (2), 282 – 288.
- Wang, Y., Roth, Z., Pastalkova, E., 2016. Synchronized excitability in a network enables generation of internal neuronal sequences. *eLife* 5, e20697.
- Wierzynski, C. M., Lubenov, E. V., Gu, M., Siapas, A. G., 2009. State-dependent spike-timing relationships between hippocampal and prefrontal circuits during sleep. *Neuron* 61 (4), 587–596.
- Wilber, A. A., Skelin, I., Wu, W., McNaughton, B. L., 2017. Laminar organization of encoding and memory reactivation in the parietal cortex. *Neuron* 95 (6), 1406–1419.e5.
- Wilson, M. A., McNaughton, B. L., 1994. Reactivation of hippocampal ensemble memories during sleep. *Science* 265 (5172), 676–679.
- Winocur, G., Moscovitch, M., Bontempi, B., 2010. Memory formation and long-term retention in humans and animals: Convergence towards a transformation account of hippocampal–neocortical interactions. *Neuropsychologia* 48 (8), 2339–2356.
- Wittenberg, G. M., Wang, S. S.-H., 2006. Malleability of spike-timing-dependent plasticity at the CA3–CA1 synapse. *Journal of Neuroscience* 26 (24), 6610–6617.
- Wu, C.-T., Haggerty, D., Kemere, C., Ji, D., 2017. Hippocampal awake replay in fear memory retrieval. *Nature Neuroscience* 20 (4), 571–580.
- Wójtowicz, T., Mozrzymas, J. W., 2015. Diverse impact of neuronal activity at frequency on hippocampal long-term plasticity. *Journal of Neuroscience Research* 93 (9), 1330–1344.
- Zhang, J.-C., Lau, P.-M., Bi, G.-Q., 2009. Gain in sensitivity and loss in temporal contrast of STDP by dopaminergic modulation at hippocampal synapses. *Proceedings of the National Academy of Sciences* 106 (31), 13028–13033.
- Ólafsdóttir, H. F., Barry, C., Saleem, A. B., Hassabis, D., Spiers, H. J., 2015. Hippocampal place cells construct reward related sequences through unexplored space. *eLife* 4, e06063.

## BIBLIOGRAPHY

---

- Ólafsdóttir, H. F., Carpenter, F., Barry, C., 2016. Coordinated grid and place cell replay during rest. *Nature Neuroscience* 19 (6), 792–794.
- Ólafsdóttir, H. F., Carpenter, F., Barry, C., 2017. Task demands predict a dynamic switch in the content of awake hippocampal replay. *Neuron* 96 (4), 925–935.e6.

## Résumé

Le stockage à long terme des souvenirs épisodiques requiert la formation de la mémoire pendant l'expérience d'éveil ainsi que la consolidation de la mémoire, un processus de renforcement de la mémoire qui a lieu pendant le sommeil. L'encodage rapide des traces mnésiques a lieu dans l'hippocampe pendant l'éveil. Pendant le sommeil, les traces mnésiques de l'hippocampe sont « rejouées » pendant les ondulations -- de brefs motifs oscillatoires hippocampiques (50-150 ms) à haute fréquence associés à une activité synchrone élevée. Les bouffées d'activité synchrone des neurones de l'hippocampe pendant les ondulations font d'eux des acteurs clés dans la consolidation de la mémoire des systèmes -- le processus de communication des mémoires vers le néocortex pour un stockage à long terme.

L'activité corticale dans le sommeil est dominée par l'oscillation lente -- l'alternance synchrone des neurones corticaux entre un état dépolarisé (état HAUT) associé à des niveaux élevés d'activité endogène, et un état bref (~200ms) hyperpolarisé (état BAS) lorsque les neurones restent silencieux. Les états BAS sont accompagnés de grandes déviations du potentiel de champ local -- ondes delta, tandis que les états HAUTS sont associés à une activité élevée et des fuseaux thalamocorticaux, deux processus pouvant entraîner une plasticité synaptique. On pense que la consolidation de la mémoire des systèmes implique une coordination entre les rythmes hippocampiques et corticaux -- notamment, les ondulations hippocampiques précèdent (~130ms) les ondes delta corticales, qui sont ensuite suivies par des fuseaux thalamocorticaux.

Pour vérifier si ce couplage temporel entraîne une consolidation de la mémoire, nous avons déclenché des ondes delta corticales suite à des ondulations hippocampiques afin d'améliorer la cooccurrence d'événements ondulation-delta couplés. Cela a augmenté la consolidation de la mémoire et la performance du rat sur une tâche de mémoire spatiale, et a entraîné une réorganisation des réseaux corticaux préfrontaux suite à des ondes delta induites ainsi qu'une réponse accrue du cortex préfrontal à la tâche le lendemain. De manière cruciale, ces améliorations n'ont pas été observées lorsqu'un retard (160-240 ms) a été introduit en plus du couplage endogène, indiquant que la stabilisation des traces mnésiques nécessite une interaction très fine entre les ondulations et les ondes delta.

Comment l'interruption de l'activité corticale par des périodes de silence généralisées pendant les ondes delta peut-elle sous-tendre la consolidation de la mémoire lorsqu'elle se produit précisément entre le transfert d'informations (réactivation hippocampique) et la plasticité du réseau (état HAUT) ? Contrairement à un principe généralement accepté, nous avons constaté que les ondes delta ne sont pas des périodes de silence complet, et que l'activité résiduelle n'est pas un simple bruit neuronal. Au lieu de cela, nous avons montré que les cellules corticales émettent des « delta spikes » pendant les ondes delta en réponse à la réactivation transitoire d'ensembles hippocampiques pendant les ondulations, et que cela se produit sélectivement pendant la consolidation endogène ou induite de la mémoire. Ces résultats suggèrent un nouveau rôle pour les ondes delta, à savoir que le silence synchronisé de la grande majorité des cellules isole le réseau des entrées concurrentes, tandis qu'une sous-population sélectionnée de neurones reste active en réponse aux réactivations de l'hippocampe, faisant le pont entre les états HAUTS et coordonnant la consolidation de la mémoire.

## Mots Clés

Mémoire, consolidation, hippocampe, électrophysiologie

## Abstract

Long term storage of episodic memories requires memory formation during awake experience as well as memory consolidation, a process strengthening the memory taking place during sleep. The rapid encoding of memory traces takes place in the hippocampus during awake behaviour. In sleep, hippocampal memory traces are 'replayed' during sharp wave-ripples -- brief (50-150 ms) high-frequency oscillatory patterns of high synchronous activity. The synchronous bursting of hippocampal neurons during ripples makes them a key player in systems memory consolidation -- the process of communicating memories to the neocortex for long-term storage.

Cortical activity in sleep is dominated by the slow oscillation -- the synchronous alternation of cortical neurons between a depolarised (UP) state associated with high levels of endogenous activity, and a brief (~200 ms) hyperpolarized (DOWN) state when neurons remain silent. DOWN states are accompanied by large deflections of the local field potential -- delta waves, while UP states bring elevated activity and thalamocortical spindles, both of which can drive synaptic plasticity. Systems memory consolidation is thought to involve the coordination between hippocampal and cortical rhythms -- notably, hippocampal ripples precede (~130 ms) cortical delta waves, which are then followed by thalamocortical spindles.

To test if this temporal coupling drives memory consolidation, we triggered cortical delta waves following ripples to enhance the co-occurrence of coupled ripple-delta events. This boosted memory consolidation and rat performance on a spatial memory task, and resulted in a reorganisation of prefrontal cortical networks following induced delta waves as well as increased prefrontal responsivity to the task on the next day. Crucially, these enhancements were not observed when a small delay (160-240 ms) was introduced in addition to the endogenous coupling, indicating the stabilization of memory traces requires a very fine-tuned interaction between ripples and delta waves.

How can the 'interruption' of cortical activity by generalised periods of silence during delta waves underlie memory consolidation when it occurs precisely between information transfer (hippocampal replay) and network plasticity (UP state)? Contrary to a generally accepted tenet, we found that delta waves are not periods of complete silence, and that the residual activity is not mere neuronal noise. Instead, cortical cells fired 'delta spikes' during delta waves in response to transient reactivation of hippocampal ensembles during ripples, and this occurred selectively during endogenous or induced memory consolidation. This suggests a new role for delta waves -- namely, that the synchronised silence of the large majority of cells isolates the network from competing inputs, while a select subpopulation of neurons remain active in response to hippocampal replay, bridging information between UP states and coordinating memory consolidation.

## Keywords

Memory, consolidation, hippocampus, electrophysiology